BIOMETAL CATALYZED RING-OPENING POLYMERIZATION OF CYCLIC ESTERS: LIGAND DESIGN, CATALYST STEREOSELECTIVITY, AND COPOLYMER PRODUCTION

A Dissertation

by

OSIT KARROONNIRUN

Submitted to the Office of Graduate Studies of
Texas A&M University
in partial fulfillment of the requirements for the degree of

DOCTOR OF PHILOSOPHY

May 2011

Major Subject: Chemistry

BIOMETAL CATALYZED RING-OPENING POLYMERIZATION OF CYCLIC ESTERS: LIGAND DESIGN, CATALYST STEREOSELECTIVITY, AND COPOLYMER PRODUCTION

A Dissertation

by

OSIT KARROONNIRUN

Submitted to the Office of Graduate Studies of
Texas A&M University
in partial fulfillment of the requirements for the degree of

DOCTOR OF PHILOSOPHY

Approved by:

Chair of Committee,	Donald J. Darensbourg
Committee Members,	Abraham Clearfield
	Timothy R. Hughbanks
	Jean-Philippe Pellois
Head of Department,	David H. Russell

May 2011

Major Subject: Chemistry

ABSTRACT

Biometal Catalyzed Ring-Opening Polymerization of Cyclic Esters:

Ligand Design, Catalyst Stereoselectivity, and Copolymer Production. (May 2011)

Osit Karroonnirun, B.S., Mahidol University

Chair of Advisory Committee: Dr. Donald J. Darensbourg

Biodegradable polyesters represent a class of extremely useful polymeric materials for many applications. Among these polyesters, the biodegradable and biocompatible, polylactide is very promising for many applications in both medical and industrial areas. Other biodegradable polymers such as polytrimethylene carbonate, polybutyrolactone, polyvalerolactone, and polycaprolactone can be blended or copolymerized with polylactide to fine tune the properties to fit the needs for their applications. The properties of these polymers and copolymers depend upon the tacticity of the polymers which can be directly controlled by the catalysts used for polymer production. Therefore, it has been of great interest to develop new selective catalytic systems for the ring-opening polymerization of lactide and other cyclic monomers. This dissertation focuses on developing new zinc and aluminum complexes and studying their selectivity and reactivity of these complexes for the ring-opening polymerization of lactide and other cyclic monomers, *i.e.* trimethylene carbonate, β-butyrolactone, δ-valerolactone, and ε-caprolactone.

Herein, aspects of the ring-opening polymerization of lactide and other cyclic monomers utilizing novel zinc and aluminum complexes will be discussed in detail. In the process for the ring-opening polymerization of lactide, chiral zinc half-salen complexes derived from natural amino acids have shown to be very active catalysts for producing polymers with high molecular weight and narrow polydispersities at ambient temperature. The chiral zinc complexes were found to catalyze *rac*-lactide to heterotactic polylactides with P_r values ranging from 0.68-0.89, depending on the catalyst and reaction temperature employed during the polymerization process. The reactivities of the various catalysts were greatly affected by substituents on the Schiff base ligands, with sterically bulky substituents being rate-enhancing. Furthermore, a series of both chiral and achiral aluminium half-salen complexes have been synthesized and characterized. These aluminum complexes all showed moderate selectivity to the ring-opening polymerization of *rac*-lactide to produce isotactic polylactide with P_m value up to 0.82 in toluene at 70 ^oC. Moreover, some of the studied aluminum complexes displayed epimerization of *rac*-lactide to *meso*-lactide during the polymerization process. Kinetic studies for the ring-opening polymerization of lactide utilizing these zinc and aluminum complexes are included in this dissertation. Along with these studies, the copolymerization of lactide with ε-caprolactone and δ-valerolactone will also be presented.

DEDICATION

I dedicate this dissertation to my parents, Sumate and Wilawan, my brother, Kavit, and my sister, Kornnika. Thank you Mom and Dad for the love you have given me and supporting me in everything I do. Without your constant encouragement and the belief you have in me, I would never have succeeded in my life the way that I have. Thanks to my siblings for always being such good friends to me. I love you all so much.

ACKNOWLEDGEMENTS

I have always heard that being in a graduate school can either be the most valuable or difficult time in one's life. To me, it has been delightful. This would have not happened without my graduate advisor, Dr. Donald J. Darensbourg. I can only say that having Don as a graduate advisor is one of the best decisions that I have ever made in my life. Thank you, Don, for being patient and putting up with me during my graduate career. Don has given me the scientific freedom in the lab which has allowed me to grow as a scientist, and I am so grateful for that. I would like to also thank my undergraduate research advisor, Dr. Tienthong Thongpanchang, for being so enthusiastic about chemistry and encouraging me to continue on to graduate school. Dr. Abraham Clearfield, Dr. Jean-Philippe Pellois, Dr. Marcetta Y. Darensbourg, and Dr. Timothy R. Hughbanks are to be thanked for being involved in my education, for their guidance and assistance when needed, and for serving as my committee members. I would like to also express my appreciation to Dr. Nattamai Bhuvanesh and Dr. Joseph Reibenspies for their time and guidance for X-ray crystallography during my tenure here at A&M.

I would like to thank all the former and present members of the DJD group not only for their advice but also for the beautiful friendships they have given me. I would especially like to thank to my very good friend Dr. Adriana I. Moncada for being so supportive and encouraging during the time I spent here in DJD group. I thank Dr. Wonsook Choi for advising me when I first arrived here, Dr. Eric B. Frantz for his time teaching me on X-ray crystallography, and Dr. Shawn B. Fitch and Dr. Jeremy R.

Andreatta for their assistance when I needed it. I would like to also thank Ross Poland, Sheng-Hsuan Wei, Stephanie J. Wilson, Andrew Yeung, Samuel John Rajkumar, and Wan-Chun Chung, as well as the MYD research group for their friendships and their help in many different ways while I have been here at A&M. Stephanie is probably helping me correcting my thesis right now, and just for your information she is so good at everything she does, so please ask her for help. They have been some really awesome people to work with, and I am very thankful for that opportunity. Susan Winters and Ethel Mejia are to be thanked for their help with paperwork and miscellaneous questions. I have truly enjoyed my time here, and this is due to the wonderful people I have met and worked with while at A&M. Thank you, guys.

Finally, thanks to my mother and father for their encouragement and to my brother and sister for their love and support.

TABLE OF CONTENTS

Page

ABSTRACT iii

DEDICATION v

ACKNOWLEDGEMENTS vi

TABLE OF CONTENTS viii

LIST OF FIGURES x

LIST OF TABLES xvi

CHAPTER

I INTRODUCTION 1

Petroleum-Based Polymers and Bio-Based Polymers: An Overview 1
Polylactides as an Alternative Bio-Based Polymer 2
Tacticity and Thermal Properties of Polylactide 5
Strategies to Control Tacticity of Polylactide 7
Catalyst Development: A Brief Introduction to Sn, Al, and Zn Complexes for the ROP of Lactide 9
Copolymers 13

II RING-OPENING POLYMERIZATION OF LACTIDE CATALYZED BY NATURAL AMINO-ACID BASED ZINC CATALYSTS 16

Introduction 16
Experimental Section 19
Results and Discussion 29
Summary Remarks 49

CHAPTER Page

III RING-OPENING POLYMERIZATION OF L-LACTIDE AND ε-CAPROLACTONE UTILIZING BIOCOMPATIBLE ZINC CATALYSTS: RANDOM COPOLYMERIZATION OF L-LACTIDE AND ε-CAPROLACTONE 50

Introduction 50
Experimental Section 51
Results and Discussion 54
Summary Remarks 68

IV STEREOSELECTIVE RING-OPENING POLYMERIZATION OF *RAC*-LACTIDES CATALYZED BY CHIRAL AND ACHIRAL ALUMINUM HALF-SALEN COMPLEXES 69

Introduction 69
Experimental Section 71
Results and Discussion 83
Summary Remarks 93

V RING-OPENING POLYMERIZATION OF CYCLIC ESTERS AND TRIMETHYLENE CARBONATE CATALYZED BY ALUMINUM HALF-SALEN COMPLEXES 95

Introduction 95
Experimental Section 96
Results and Discussion 99
Summary Remarks 129

VI SUMMARY AND CONCLUSIONS 131

REFERENCES 138

APPENDIX A 148

APPENDIX B 149

VITA 234

LIST OF FIGURES

FIGURE		Page
I-1	Polylactide microstructure from the stereocontrolled ROP of lactide	6
I-2	Coordination-insertion polymerization of lactide by metal-based catalysts	8
I-3	Stereoselective aluminum complexes for the ROP of *rac*-lactide	11
I-4	General structure of zinc complexes prepared from the β-diketiminate ligand by Coates and cowerkers	13
I-5	Solvated magnesium, calcium, and zinc complexes of the β-diketiminate ligand by Chisholm and coworkers	13
I-6	Various monomers for the copolymerization with lactide	15
II-1	X-ray crystal structures of (a) **II6a**, (b) **II6b**, (c) **II6c**, and (d) **II6d**. Thermal ellipsoids represent the 50% probability surfaces. Hydrogen atoms are omitted for the sake of clarity	33
II-2	X-ray crystal structure of complex **II6e**. Thermal ellipsoids represent the 50% probability surfaces. Hydrogen atoms are omitted for the sake of clarity. Selected bond lengths (Å) and angles (deg): Zn2-N3 : 2.050 (6), Zn2-N4 : 2.301 (5), Zn2-O2 : 2.080 (4), Zn2-O3 : 2.016 (5), Zn2-O4 : 1.977 (4), O4-Zn2-O3 : 106.69 (17), O4-Zn2-N3 : 89.61 (18), O3-Zn2-N3 : 126.78 (19), O4-Zn2-O2 : 95.69 (16), O3-Zn2-O2 : 80.79 (16), N3-Zn2-O2 : 148.99 (18), O4-Zn2-N4 : 161.08 (19), O3-Zn2-N4 : 92.24 (18), N3-Zn2-N4 : 78.79 (19), O2-Zn2-N4 : 87.10 (17)	34
II-3	$\ln([La]_0/[La]_t)$ *vs* time plots for the ROP of D-lactide(●) or L-lactide(▲) catalyzed by various zinc complexes at ambient temperature. (a) complex **II6a**, (b) complex **II6b, (c)** complex **II6c**, and (d) complex **II6d**.	36
II-4	$\ln([LA]_0/[LA]_t)$ *vs* time plot for the ROP of L-lactide by the dimeric complex **II6e** at ambient temperature	37

FIGURE Page

II-5 Independence of the rate constant for the ROP of L-lactide on the THF concentration in C_6D_6 at ambient temperature. (a) Complex **II6a** as catalyst, (b) complex **II6d** as catalyst 37

II-6 ^{1}H NMR spectrum in C_6D_6 during the ROP of L-lactide in the presence of complex **II6d** at ambient temperature. Mething proton of *meso*-lactide observed at 4.15 ppm 38

II-7 ^{1}H NMR spectra of polylactide in $CDCl_3$ prepared from L-lactide. (a) In the presence of complex **II6d**, with **1**→ **2** illustrating expanded methine region before and after homonuclear decoupling. (b) In the presence of complex **II6a**, with **3**→ **4** illustrating expanded methine region before and after homonuclear decoupling 40

II-8 Linear relationship observed between M_n and monomer/initiator ratio of polylactide produced from *rac*-lactide catalyzed by complex **II6a** at ambient temperature in $CHCl_3$ 42

II-9 Homonuclear decoupled ^{1}H NMR ($CDCl_3$, 500 MH_3) spectra of the methine region of polylactide produced from *rac*-lactide with catalyst (a) **II6a**, (b) **II6b**, (c) **II6c**, and (d) **II6d**. **A.** Polymerization temperature ambient. **B.** Polymerization temperature -30 ^{o}C 43

II-10 ^{1}H NMR spectrum (C_6D_6, rt) of **II6d** before addition of 2-methylcyclohexanone (bottom) and 15 min after addition of 6 equiv of 2-methylcyclohexanone (top) 45

II-11 ^{1}H NMR spectrum (C_6D_6, rt) of **II6d** before addition of THF (bottom) and 15 min after addition of 10 equiv of THF (top) 46

III-1 Plot of $\ln([M]_0/[M]_t$ vs time for ROP of L-lactide (red solid circles) or ε-caprolactone (blue solid triangles) catalyzed by the specified zinc complex at ambient temperature. Each reaction was performed in C_6D_6 at ambient temperature. Monomer and catalyst concentrations were held constant at 0.34 and 0.0069 M, respectively. (**A**) Complex **III1a**: the rate constants were determined by the slope of the plots and were found to be 0.110 ± 0.005 $M^{-1}sec^{-1}$ with $R^2 = 0.999$ for ROP of L-lactide and $(2.17 \pm 0.10) \times 10^{-3}$ $M^{-1}sec^{-1}$ with $R^2 = 0.994$ for ROP of ε-caprolactone. (**B**) Complex **III1b**: the rate constants were determined by the slope of the plots and were

FIGURE Page

found to be (8.90 ± 0.12) x 10^{-3} $M^{-1}sec^{-1}$with R^2 = 0.998 for ROP of L-lactide and (2.90 ± 0.10) x 10^{-3} $M^{-1}sec^{-1}$with R^2 = 0.998 for ROP of ε-caprolactone 56

III-2 (a) X-ray crystal structure of complex **III1a**. (b) Stick drawings of complexes **III1a** (red) and **III1b** (blue) obtained for X-ray determined structures 58

III-3 (a) Linear relationship observed between M_n and monomer/initiator ratio of polylactide from *rac*-lactide catalyzed by complex **III1a** at ambient temperature in $CHCl_3$. (b) Linear relationship observed between M_n and monomer/initiator ratio of polycaprolactone from ε-caprolactone in bulk at 110 ^oC..... 60

III-4 Linear relationship observed between M_n and monomer/initiator ratio of copolymer from L-lactide and ε-caprolactone catalyzed by complex **III1a** in the melt at 110 ^oC 63

III-5 ^1H NMR spectra of the copolymer in $CDCl_3$ at ambient temperature showing the ε- and α-methylene ranges in the copolymers of entry 1 (a), entry 2 (b), entry 3(c), entry 4 (d) from Table III-4..... 64

III-6 ^{13}C NMR spectra of the copolymer in $CDCl_3$ at ambient temperature of the mixture of polylactide and polycaprolactone (a), entry 2 (b), entry 3(c), entry 4 (d) from Table III-4 65

III-7 DSC curves (second heating run) of polymers from table III-5, entries 1-10 from top to bottom..... 66

III-8 Plots of the dependence of T_g (**a**), T_c (**b**), and T_m (**c**) of copolymers on the molar % lactide in copolymers..... 67

IV-1 ^1H NMR spectrum ($CDCl_3$, rt) of the reaction mixtures during the ROP of L-lactide in the presence of complex **IV2a** (A), **IV2e** (B), **IV2g** (C) (entries 3, 10, 12; Table IV-1, respectively). The polymerization reactions were performed in toluene at 70 ^oC for 15 h. Methyl proton of *meso*-lactide, L-lactide, and polylactide were observed at 1.70 (a), 1.66 (b), and 1.57 (c) respectively 86

FIGURE Page

IV-2 DSC curves (second heating run) of polylactide from *rac*-lactide catalyzed by complex **IV2i** 88

IV-3 X-ray crystal structures of (a) **IV2f** (*cis*-), (b) **IV2f** (*trans*-). Thermal ellipsoids represent the 50% probability surfaces. Hydrogen atoms are omitted for the sake of clarity 89

IV-4 Variable-temperature ^{1}H NMR spectrum (500 MHz) of complex **IV2f** in deuterated toluene taken sequentially at different temperatures. (**A**) room temperature, (**B**) 40 ^{o}C, (**C**) 70 ^{o}C, (**D**) 100 ^{o}C, (**E**) sample cooled down from 100 ^{o}C to room temperature, spectrum taken two days later 90

IV-5 Variable-temperature ^{1}H NMR spectrum (500 MHz) of complex **IV2g** in deuterated toluene taken sequentially at different temperatures. (**A**) room temperature, (**B**) 40 ^{o}C, (**C**) 70 ^{o}C, (**D**) 100 ^{o}C, (**E**) sample cooled down from 100 ^{o}C to room temperature, spectrum taken two days later 92

V-1 X-ray crystal structures of (a) complex **V2a**, (b) complex **V2d**, and (c) complex **V3b**. Thermal ellipsoids represent the 50% probability levels with hydrogen atoms omitted for the sake of clarity 102

V-2 X-ray crystal structures of (a) **V2g** (*trans*-), (b) **V2f** (*cis*), and (c) **V2f** (*trans*-). Thermal ellipsoids represent the 50% probability surfaces. Hydrogen atoms are omitted for the sake of clarity 104

V-3 X-ray crystal structure of complex **V3e**. Thermal ellipsoids represent the 50% probability surfaces. Hydrogen atoms and 2[$B(C_6H_3(CF_3)_2)_4]^-$ are omitted for the sake of clarity. Selected bond lengths (Å) and angles (deg): Al1-N1: 1.944 (4), Al1-O1: 1.779 (4), Al1-O2: 1.873 (4), Al1-O4: 1.862 (3), Al2-N2: 1.959 (4), Al2-O3: 1.765 (4), Al2-O4: 1.876 (4), Al2-O5: 1.817 (4), N1-Al1-O1: 92.06 (18), N1-Al1-O2: 82.50 (17), O1-Al1-O4: 96.97 (16), O2-Al1-O4: 76.15 (15), N1-Al1-O4: 150.00 (19), O1-Al1-O2: 152.03 (17), N2-Al2-O3: 91.67 (19), N2-Al2-O4: 81.80 (17), O2-Al2-O4: 76.79 (15), O2-Al2-O3: 97. 18 (17), N2-Al2-O2: 150.29 (19), O3-Al2-O4: 151.12 (18), O3-Al2-O5: 105.53 (18)..... 109

V-4 X-ray crystal structure of complex **V4e**. Thermal ellipsoids represent the 50% probability surfaces. Hydrogen atoms and 2[$B(C_6H_3(CF_3)_2)_4]^-$ are omitted for the sake of clarity. Selected bond lengths (Å)

FIGURE Page

and angles (deg): Al1-N1: 1.948 (8), Al1-O1: 1.756 (7), Al1-O2: 1.886 (6), Al1-O4: 1.839 (6), Al1-O9: 1.805 (6), O11-H9D: 1.876 (8), N1-Al1-O1: 92.4 (3), N1-Al1-O2: 81.7 (3), O2-Al1-O4: 76.5 (3), O1-Al1-O4: 96.7 (3), N1-Al1-O4: 149.7 (3), O1-Al1-O2: 151.4 (3), O1-Al1-O9: 104.6 (3), Al1-O9-Al3: 139.2 (3)..... 110

V-5 (a) Linear relationship observed between M_n and monomer/initiator ratio of polylactide from *rac*-lactide catalyzed by complex **V2g** at 70 ^oC in toluene. (b) Linear relationship observed between M_n and monomer/initiator ratio of poly-β-butyrolactone from *rac*-β-butyrolactone catalyzed by complex **V2g** at 70 ^oC in toluene. 113

V-6 $\ln([rac\text{-LA}]_0/[rac\text{-LA}]_t)$ *vs* time plot depicting a reaction order of unity with respect to monomer concentration ($R^2 = 0.999$)..... 115

V-7 (a) Plot of k_{obsd} *vs* [Al] with slope = 0.011 and $R^2 = 0.984$. (b) Plot of ln k_{obsd} *vs* ln[Al] with slope = 0.86 and $R^2 = 0.984$ 116

V-8 Eyring plot of ROP of *rac*-lactide in the presence of catalyst **V2g** in toluene-d_8. Slope = -7.180 with $R^2 = 0.995$..... 117

V-9 $\ln([M]_0/[M]_t)$ *vs* time plot depicting a reaction order of unity with respect to a) [TMC] ($R^2 = 0.987$), b) [*rac*-β-BL] ($R^2 = 0.996$), c) [δ-VL] ($R^2 = 0.997$), and d) [ε-CL] ($R^2 = 0.995$). 118

V-10 Plot of ln k_{obsd} *vs* ln[Al] from the ROP of a) TMC (slope = 0.73, $R^2 = 0.997$), b) *rac*-β-BL (slope = 0.85, $R^2 = 0.994$), c) δ-VL (slope = 0.48, $R^2 = 0.954$), and d) ε-CL (slope = 0.54, $R^2 = 0.994$)..... 119

V-11 Eyring plot of ROP of a) TMC (Slope = -5.193 with $R^2 = 0.994$), b) *rac*-β-BL (Slope = -11.285 with $R^2 = 0.990$), c) δ-VL (Slope = -6.500 with $R^2 = 0.992$), and d) ε-CL (Slope = -6.645 with $R^2 = 0.991$) in the presence of catalyst **V2g** in toluene-d_8.. 121

V-12 Plot of $(f\text{-}1)/F$ vs f/F^2 with slope = 2.78 and and $R^2 = 0.98$, the interception = 0.14..... 124

V-13 $\ln([M]_0/[M]_t)$ *vs* time plot depicting a reaction order of unity with respect to *rac*-lactide (red solid circles) and ε-VL (green solid squares) concentration ($R^2 = 0.993$ for polylactide and $R^2 = 0.991$

FIGURE Page

for poly-δ-VL). 125

V-14 (a) Plot of k_{obsd} *vs* [Al] with slope = 0.016 for *rac*-lactide (red solid circles ,R^2 = 0.996) and slope = 0.038 for δ-VL(green solid squares, R^2 = 0.995). (b) Plot of ln k_{obsd} vs ln[Al] with slope = 0.92 for *rac*-lactide (red solid circles ,R^2 = 0.997) and slope = 1.20 for δ-VL(green solid squares, R^2 = 0.999). 126

LIST OF TABLES

TABLE		Page
I-1	Mechanical Properties of Poly(L-Lactide), Polystyrene, and Polyethylene Terepthalate (PET). Reproduced from Reference 7	4
II-1	Selected Bond Lengths (Å) and Angles (deg) for Zn Complexes **II6a-d**	34
II-2	Rate Constants for the ROP of D- or L-Lactide in the Presence of Zinc Complexes. [a]	37
II-3	Polylactides Produced from the ROP of *Rac*-lactide in Chloroform at Ambient Temperature	41
II-4	P_r Values of Poly(*Rac*-Lactide) at Different Temperature. [a,b]	44
II-5	Physical and Thermal Properties of Polylactides	47
II-6	Crystallographic Data for Complexes **II6a-b**	48
II-7	Crystallographic Data for Complexes **II6c-e**	48
III-1	Rate Constants for the ROP of L-Lactide or ε-Caprolactone in The Presence of Zinc Complexes. [a]	55
III-2	Polylactides Produced from the ROP of *Rac*-Lactide in Chloroform at Ambient Temperature	59
III-3	Polycaprolactone Produced from the ROP of ε-caprolactone in the melt at 110 ^{o}C	61
III-4	Copolymerization of L-Lactide and ε-Caprolactone with Complex **III1a**.[a]	61
III-5	Molecular Weight of Copolymer Depending on M/I. [a]	62
III-6	Thermal Properties of Copolymers of Polylactide and Polycaprolactone.	65

TABLE Page

IV-1 Reactivity and Selectivity of Aluminum Complexes **IV2a-j** for the ROP of *Rac*-Lactide.[a] 85

IV-2 The ROP of *rac*- and L-Lactide Using Aluminum Complexes **2IVe-g**, **2IVi-j**.[a] 87

IV-3 Crystallographic Data for Complexes **IV2f** (*cis*-) and **IV2f** (*trans*-). 93

V-1 Selected Bond Lengths (Å) and Angles (deg) for Al Complexes **V2a**, **V2b**, **V2d**, **V2f** (*cis*-), **V2f** (*trans*-), and **V2g** (*trans*-). 103

V-2 Reactivity and Selectivity of Aluminum Complexes **V2a-k** for the ROP of *Rac*-Lactide.[a] 105

V-3 Reactivity of Aluminum Complex **V2g** for the ROP of Cyclic Monomers.[a] 111

V-4 Polylactide Produced from the ROP of *Rac*-Lactide in Toluene at 70 ^{o}C . 112

V-5 Poly-β-Butyrolactone Producted from the ROP of *Rac*-Lactide in Toluene at 70 ^{o}C. 112

V-6 Rate Constants Dependence on the Concentration of the Catalyst (**V2g)** and Temperature for the Ring-Opening Polymerization of *Rac*-Lactide.[a] 116

V-7 Rate Constants Dependence on the Concentration of the Catalyst (**V2g**) and Temperature in the ROP of Cyclic Monomers.[a] 119

V-8 Activation Parameter in Homopolymerization..... 121

V-9 The Data Set of Mole Fraction of the Fineman-Ross Plot.[a]..... 123

V-10 Rate Constants Dependence on the Concentration of the Catalyst (**V2g)** and Temperature in Copolymerization of *Rac*-Lactide and δ-Velerolactone.[a] 126

V-11 Comparison of Rates and Activation Parameters in Homopolymerization and of Copolymerization of *Rac*-Lactide and δ-VL Catalyzed by Complex **V2g**.. 127

V-12 Crystallographic Data for Complexes **V2a,** V**3b,** and V**2d**. 127

TABLE Page

V-13 Crystallographic Data for Complexes **V2f** (*cis*-), **V2f** (*trans*-), and **V2g** (*trans*-). 128

V-14 Crystallographic Data for Complexes **V3e** and **V4e** 128

CHAPTER I

INTRODUCTION

Petroleum-Based Polymers and Bio-Based Polymers: An Overview

Petroleum-based synthetic polymers, such as polyethylene, polypropylene, and polyamide are very useful materials in industry due to their numerous applications in our daily life. Despite their many benefits, these polymers seem inappropriate for applications in which plastics are used for short time periods and then disposed. Accumulations of the resulting waste from petroleum-based plastics have become an environmental concern. Since these synthetic polymers have been around in nature for only a short period of time, and microorganisms have not yet developed new enzyme structures to consume them.[1] As a result, they often end their life cycles either buried in landfill sites or being burned, generating harmful gaseous emissions to the atmosphere. In addition, since they are derived from petrochemical resources, there are concerns over the long-term availability of these petrochemical feedstocks.[2] Bio-based plastics have been receiving much recent attention from scientific community. They are not only biodegradable in the ecosystem by the enzyme action of microorganisms such as bacteria, fungi, and algae, but the polymer chains may also be shorten by nonenzymatic processes such as chemical hydrolysis and photolysis. Biodegradation of these

---

This dissertation follows the style of *Inorganic Chemistry*.

bio-based plastics transforms them to natural substances, such as carbon dioxide, methane, water, biomass, and humus that can be reused for photosynthesis by plants. The raw materials for bio-based plastics are generally available from the fermentation of sugar (beet or cane) or starch (corn, wheat, potatoes, or manioc). Therefore, bio-plastics are considered to be renewable and will eliminate concerns of long-term uses of these renewable materials. Currently, bio-based plastics can be found in various every day products (*i.e.* trash bags, wrappings, loose-fill, food container, film wrapping, laminated pater), hygiene products (*i.e.* diaper, bed sheets, cotton swabs), consumer goods, (*i.e.* fast-food tableware, containers, egg cartons, razor handles, toys), and agricultural tools (*i.e.* mulch films, planters).[2b] The worldwide consumption of biodegradable polymers has increased from 14 million kg in 1996 to 326 million kg in 2007 and is expected to grow to 2,113 million kg in 2020.[2b, 3] Although bio-plastics have found their ways in many applications in our society, the price of producing these plastics are still expensive compared with commodity petroleum-based plastics. Furthermore, some of the physical and mechanical properties of bio-based plastics have not yet met the necessary requirements for many different applications. As a result, there are numerous researchers have been focusing on finding effective and cheaper ways to make and process these biodegradable polymers as well as improve the physical and mechanical properties of the polymers to fit the needs of the global market.

Polylactides as an Alternative Bio-Based Polymer

Polylactide or polylactic acid (PLA) is an aliphatic polyester produced via direct condensation from lactic acid, direct coupling by isocyanate[4], or by ring-opening

polymerization (ROP) of lactide (the cyclic dimer of lactic acid, Scheme I-1). Polylactide is highly biocompatible, being resorbed via the Krebs cycle in human body.[5] The life cycle of polylactide is shown in Scheme I-2. The original application of polylactide was found in biomedical and pharmaceutical industries, including but not limited to biodegradable sutures, slow release drug delivery, and tissue engineering.[6] An example of first resorbable sutures was a copolyester, composed of 8% L-lactide and 92% glycolide, developed in 1962 by American Cyanamide Co. under the trade name of Dexon.[5] Although, polylactide was originally used in the biomedical field, it has many attractive properties comparable to those of synthetic thermoplastics such as polystyrene and poly(ethylene terephthalate) (Table I-1)[7], *i.e.* mechanical strength, elastic recovery, and heat sealability. Polylactide also has other properties similar to bio-based polymers, such as biodegradability, barrier characteristics, and dyeability.[8] Nature Works and PURAC have agreed on the potential of polylactide in partially replacement of low density polyethylene (LDPE), high density polyethylene (HDPE), polypropylene (PP), polyamide (PA), polyethylene terephthalate (PET), and polymethylmethacrylate (PMMA). Although polylactide has been widely used in textile and packaging industry, its market is expected to grow and extend to transportation as well as electronic and electrical equipment.[3]

Scheme I-1. Formation of Lactide from Lactic Acids.

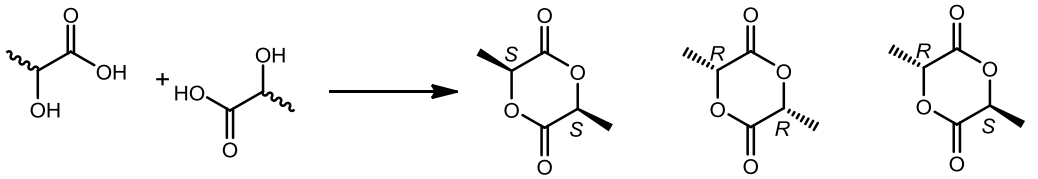

Scheme I-2. Life Cycle of Polylactide.[8] Adapted from Reference 8.

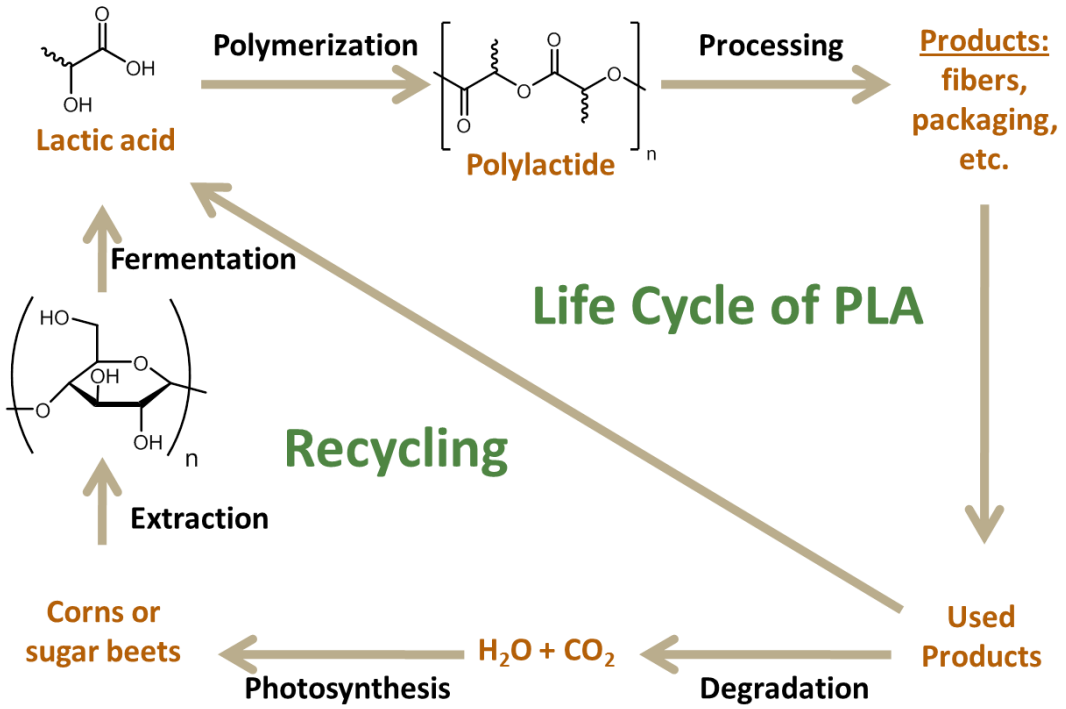

Table I-1. Mechanical Properties of Poly(L-Lactide), Polystyrene, and Polyethylene Terepthalate (PET). Reproduced from Reference 7.

Polymer	Density ($kg.m^{-3}$)	Tensile strength (MPa)	Elastic modulas (GPa)	Elongation at break (%)	Notched Izod ($J.m^{-1}$)	Heat deflection (^oC)
PLLA[a]	1.26	59	3.8	4-7	26	55
PS	1.05	45	3.2	3	21	75
PET	1.40	57	2.8-4.1	300	59	67

[a] PLA properties are highly dependent on a range of molecular parameters such as molecular weight, architecture, and stereochemistry as well as several processing parameters that can have a dramatic effect on some or all of these properties.

Tacticity and Thermal Properties of Polylactide

As previously mentioned, there are three possible methods to synthesize polylactide. This work will focus on the ring-opening polymerization (ROP) of lactide (the cyclic dimer of lactic acid). The ROP of lactide offers a great degree of control over the polymerization process. In comparison with direct condensation, the ROP of cyclic monomers uses milder reaction conditions and avoids the formation of small molecule byproducts. In addition, the relief of lactide's ring strain is the thermodynamic driving force for the ROP processes.[9] The resulting polylactide obtained from this method typically has lower polydispersities, higher molecular weight, and high levels of end-group reliability in contrast to direct condensation from lactic acids.

Since lactic acid is a chiral molecule, there are three possible isomers of lactide formed during the dimerization, *i.e.* L-, D- and *meso*-lactide as shown in Scheme I-1. A *rac*-lactide is defined as a mixture of 50% L- and 50% D-lactide. The stereocontrolled ROP of *rac*- and *meso*-lactide will result in polylactide with different microstructures (Figure I-1). Stereocontrolled ROP of *meso*-lactide can possibly yield either syndiotactic polylactide (polylactide with alternating of *S* and *R* stereocenters in the polymer chain *i.e.* -*SRSRSR*-) or heterotactic polylactide (having the stereocenters doubly alternate *i.e.* –*SSRRSSRR*-) throughout the polymer chain. Heterotactic polylactide can possibly be obtained from stereocontrolled ROP of *rac*-lactide when each L- and D-lactide are alternatively ring-opened resulting in a doubly alternating sequence in polymer chain. Isotactic polylactide, obtained from either L-, D-, or *rac*-lactide, has a pure enantiomeric enrichment in the polymer chain, *i.e.* -*SSSSSSSS*- or *RRRRRRRR*-.

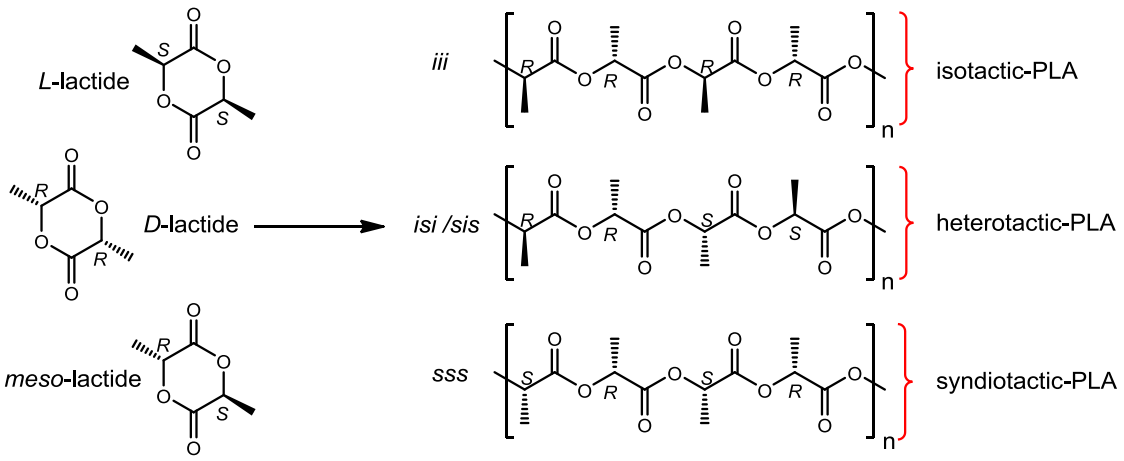

Figure I-1. Polylactide microstructure from the stereocontrolled ROP of lactide.

The tacticity of polylactide was initially determined by the optical activity of the polymer compared to isotactic polylactide (M_n > 6000, a^{22}_D remains constant at 142°).[10] However, ^{13}C NMR and homonuclear decoupled ^{1}H NMR studies of polylactide reported by Munson and coworkers showed that the tacticity of polylactide can be determined.[11] The degree of stereoselectivity is shown as the probability of *racemic* or *meso* enrichment, that is, the probability of forming a new *racemic* (syndiotactic) or *meso* (isotactic) diad), P_r and P_m, respectively. P_r or P_m values are calculated based on the ratio of the (area of *racemic* or *meso*)/(total area in methine proton region) from the homonuclear decoupled ^{1}H NMR spectra. If P_r or P_m is equal to 0.50 for polylactide obtained from the ROP of either *rac*- or *meso*-lactide, this indicates a completely atactic polymer. In the case of the ROP of *rac*-lactide, a P_r or P_m equals to 1 means that the resulting polymer is completely heterotactic or isotactic, respectively. When *meso*-lactide is ring-opened and P_r = 1 or P_m = 1, this describes a perfect syndiotactic or heterotactic polymer being formed during the polymerization process, respectively.

Interestingly, thermal properties of polylactides highly depend upon the microstructure of the polymer. Differences in tacticity of the polymer have shown to cause different in crystallization temperature (T_c), melting temperature (T_m), and glass transition temperature (T_g) of the polymer. For example, there is no T_m observed in heterotactic polylactide, while isotactic polylactide is more crystalline and displays a T_m of 180 ^oC. Both isotactic and heterotactic polylactide show a T_g ranging from 55-60 ^oC, while syndiotactic polylactide displays a T_g around 45-50 ^oC. Isotactic polylactide possesses a T_c of 90 ^oC, in contrast, there is no T_c observed in heterotactic or syndiotactic polylactide. In addition, when poly-L-lactide and poly-D-lactide are mixed together in a 1:1 ratio, a polymer with significantly high in melting temperature (T_m = 230 ^oC) is formed. This dramatic change in T_m is due to the formation of a stereocomplex from cocrystallization of the two opposite chains of poly-L-lactide and poly-D-lactide, leading to polymer with much more stable structure than both pure enantiomeric chains.

Strategies to Control Tacticity of Polylactide

There are several catalytic processes for the ring-opening polymerization of lactide, including anionic, cationic, organocatalytic, and coordination-insertation polymerizations (Figure I-2). The coordination-insertation has proven to be an effective method to control the stereoselectivity of PLA through the coordination of the carbonyl oxygen from the lactide monomer to the metal center during the polymerization process. Binding of the carbonyl oxygen to the metal center will activate the carbonyl carbon and allow the lactide monomer to be ring-opened by the metal. The combination of the ligand architecture and the growing polymer chain play crucial role in stereocontrol

during the polymerization process. From a mechanistic point of view, there are two different mechanisms for the stereoselective ROP of lactide.[12] When a chiral catalyst is employed for the ROP of lactide that results in a stereocontrolled polymerization process, an enantiomorphic site-control mechanism is applied for such process. If the stereocontrol, however, is observed utilizing an achiral catalytic system, a chain-end controlled mechanism is accounted for the stereoselectivity.[13]

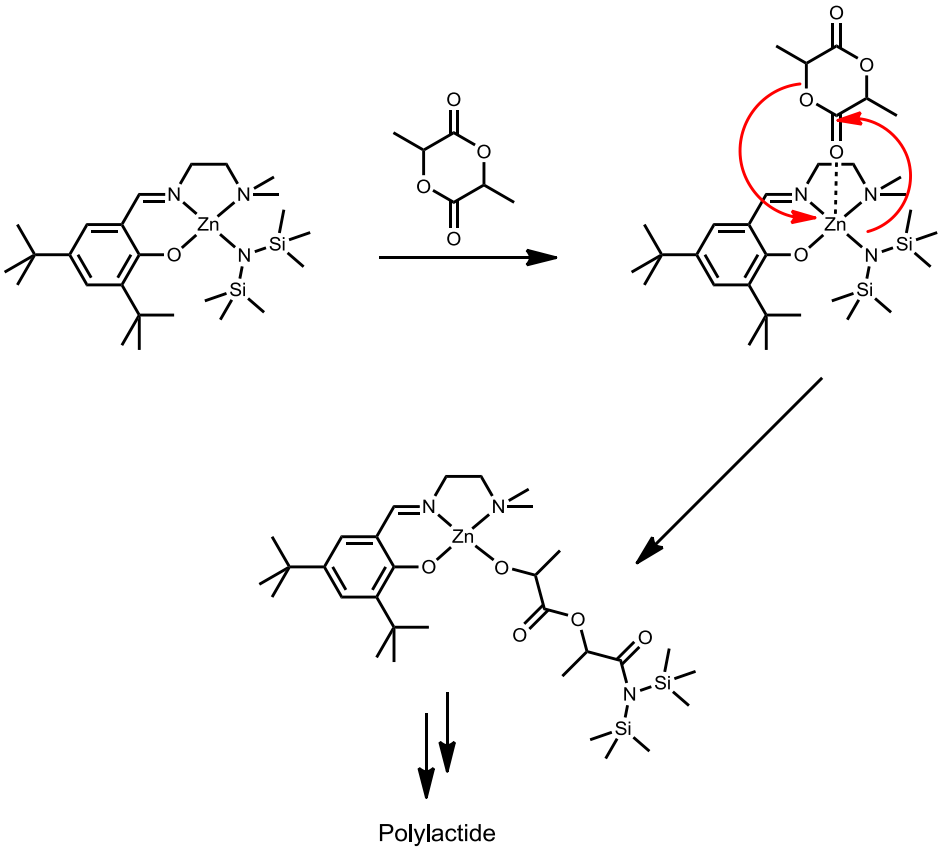

Figure I-2. Coordination-insertation polymerization of lactide by metal-based catalysts.

Catalyst Development: A Brief Introduction to Sn, Al, and Zn Complexes for the ROP of Lactide

A large number of simple metal salts and coordination compounds have been reported as effective catalysts for the ROP of lactide. Among these catalytic systems, tin (II) 2-ethylhexanoate (stannous octanoate, $SnOct_2$) is the most commonly used catalyst for the ROP of lactide. It is easy to handle and is well soluble in most common organic solvents.[5] Although tin(II) 2-ethylhexanoate is approved by the Food and Drug Administration (FDA), it has been reported that this tin compound cannot be removed completely by a purification method including precipitation and dissolution. In addition, it has been reported by Schwach and coworkers that a residue of 306 ppm of tin compound remained in the purified polymer.[14] This has raised concerns for the use of polylactide in biomedical and pharmaceutical applications due to the trace amount of toxic tin compound in the purified polymer.

Even though stannous otanoate and several tin compounds have shown moderate to good activity for the ring-opening polymerization of lactide, there is no evidence of stereocontrolled polymerizations utilizing these catalytic systems. Aluminum complexes on the other hand show excellent stereoselectivity toward the ROP of lactide. In 1996, Spassky and coworkers were the first group to have success in the stereocontrolled polymerization of *rac*-lactide utilizing an aluminum methoxide complex bearing a binaphthyl Schiff-base ligand (Figure I-3, 1).[15] They reported the kinetic resolution polymerization of *rac*-lactide by aluminum complex **1**. The chiral binaphthyl Schiff-base ligand led to the highly selective ring-opening polymerization of D-lactide from *rac*-

lactide to give isotactic polylactide via an enantiomorphic site-control mechanism. L-lactide was left largely unreacted in the polymerization media. In 2002, Feijen and coworkers reported another chiral base aluminum complex **2** derived from (*R*, *R*)-cyclohexanediamine Schiff base ligand stereoselectively catalyzed L-lactide over D-lactide.[16] Although aluminum complexes bearing chiral ligands by Spassky and coworkers and Feijen and coworkers have shown excellent stereoselectivity for the ROP of lactide, Nomura and coworkers reported the first achiral aluminum based catalyst **3** that can polymerize *rac*-lactide to a highly stereoblock polylactide (T_m = 230 ^oC) via a chain-end control mechanism.[13a] Similar results were observed by Gibson and coworkers when achiral aluminum complexes **4a** and **4b** with tetradentate *N*,*N*'-disubstituted bis(amino-phenoxide) was used for the polymerization process. In this instance, an isotactic stereoblock of polylactide with a P_m value up to 0.79 was produced.[17] It was also shown by the work of Gibson and coworkers that the tacticity is dramatically influenced by the substituents R^1 attached to the nitrogen atoms. In this manner, the larger substituent found in complex **4b** results in higher isotacticity (P_m = 0.79) compared with the resulting polylactide from the smaller substituent on complex **4a** (P_m = 0.68). It has also been shown that the ligand chirality, polymer chain end, and even the solvent can effect in the stereocontrol of the ROP of lactide.[18] Although these aluminum complexes have shown excellent stereoselectivity toward for the ROP of lactide, the reaction temperature for the polymerization (70-100 ^oC) is rather high, yet the rate for the ROP of lactide is slow compared to other catalytic systems.

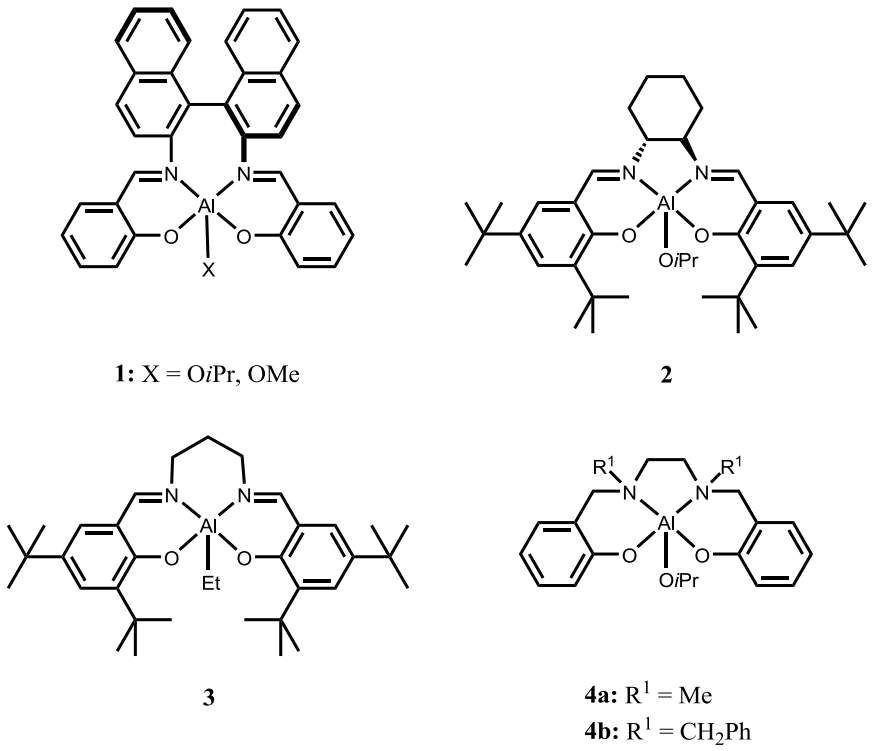

Figure I-3. Stereoselective aluminum complexes for the ROP of *rac*-lactide.

Zinc-based catalysts are considered to be less toxic to humans because zinc is an essential trace element for humans. It is also important for many biological functions, and about 2-3 grams of zinc cam be found in an adult body.[19] There are many zinc catalysts have been reported in the literature for the ring-opening polymerization of lactide.[20] Among these complexes, (*β*-diketiminate)zinc isopropoxide species **5** (Figure I-4) reported by Coates and coworkers polymerized *rac*-lactide to highly heterotactic polylactide with a P_m value of 0.94 at room temperature with monomer/initiator ratio = 200. The zinc complex **6** with alkoxide generated by reaction of **5** with isopropanol

yielded controlled polymers with narrow PDI at 20 ^{o}C. Variation of the initiators in the dimer bridge (β-diketiminate)zinc complex **7**, **8**, and **9** still resulted in active species for the ROP of lactide. Utilizing of a methyl lactate initiator **7** resulted in little changes in activity, whereas, amide **5** and alkyl **8** were dramatically less reactive compared to **6**, and acetate **9** was the worst performer among these initiators. They proposed that the stereocontrol of the ROP of lactide by these catalytic system occurred via a chain-end control mechanism.[21] These zinc complexes were the first Group 12 metal complexes to catalyze lactide polymerization with high stereochemical control. β-diiminate systems have since been investigated with great enthusiasm. Chisholm and coworkers[22] also showed that an analogous series of (β-diketiminate) complexes with one THF molecule coordinated to metal center are monomeric rather than dimeric compared to complexes reported by Coates and coworkers (Figure I-5). The experimental results revealed that all the complexes were reactive for the ROP of lactide and had the similar trends to those reported by Coates and coworkers. When the zinc metal center was changed to magnesium **11**, the polymerization reaction went significantly faster than complex **10**, however the results showed that there was no stereocontrolled polymerization observed when **11** was employed. Chisholm also discovered that solvent could significantly affect the stereoselectiviy. When complex **11** was employed in THF rather than in methylene chloride, 90% hetereotactic polylactide was observed from *rac*-lactide. In addition, they also showed that calcium complex **12** was also active for the ROP of *rac*-lactide, affording atactic polylactide.[23]

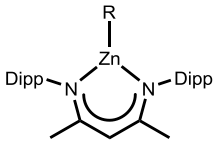

5: R = $N(SiMe_3)_2$
6: R = O*i*Pr
7: R = $OCHMeCO_2Me$
8: R = Et
9: R = OAc

Figure I-4. General structure of zinc complexes prepared from the β-diketiminate ligand by Coates and cowerkers.[21]

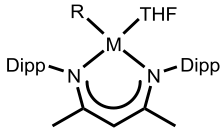

10: M = Zn, R = $OSiPh_3$
11: M = Mg, R = O^{t}Bu
12: M = Ca, R = $N(SiMe_3)_2$

Figure I-5. Solvated magnesium, calcium, and zinc complexes of the β-diketiminate ligand by Chisholm and coworkers.[22]

Copolymers

Synthetic biodegradable polymers are advantageous over natural based polymers for many reasons. They can be fine-tuned to meet specific needs, for example, hydrophobicity, crystallinity, degradability, solubility, glass transition temperature, and melting temperature by either copolymerization with different monomers or using different synthesis conditions. Polylactide is possibly the most important biodegradable polymer in pharmaceutical and medical applications due to its properties, such as high strength, degradability, and biocompatibility.[5, 24] Polylactide is often used to copolymerize with some other monomers, for example, trimethylene carbonate (TMC), β-butyrolactone, δ-valerolactone, and ε-caprolactone as shown in Figure I-6 to tune for desired polymeric properties. Polytrimethylene carbonate (poly(TMC)) is an amorphous elastomer with a glass transition temperature at about -15 ^{o}C. It displays good mechanical properties, including high flexibility and high tensile strength. In addition,

the byproduct from degradation of poly(TMC) is not acidic and therefore is not harmful to the living cells.[25] The hydrolytic degradation rate in vitro for poly(TMC) is rather slow and is dependent on initial molecular weights and the ionic strength of the conditioning medium.[26] Polyhydroxybutyrate (PHB or PBL) on the other hand is naturally produced from renewable resources by microorganisms. The level of PBL in bacteria can be as high as 95% of the cellular dry weight.[2b] Isotactic PBL has a glass transition temperature at about 5 ^{o}C and melting temperature (180 ^{o}C) comparable to isotactic polylactide. A atactic PBL on the other hand has a glass transition temperature of -2 ^{o}C. Poly-δ-valerolactone (PVL) and poly-ε-caprolactone (PCL) can be derived from the ROP of cyclic esters, *i.e.* δ-valerolactone and ε-caprolactone, respectively. Both PVL and PCL are semicrystalline polymers with glass transition temperatures of about -63 and -60 ^{o}C, respectively. They both also melt at similar temperatures around 60 ^{o}C for PVL and 65 ^{o}C for PCL.[27] Copolymerization of polyesters (PBL, PVL, and PCL) and poly(TMC) with polylactide is often used to adjust the degradation rate as well as mechanical properties.[28] Copolymers can be engineered to adjust the degradation rate suitable for various applications. For example in orthopedic fixation devices, the rate of the degradation should be slow enough to allow the healing bone to recover and be able to carry sufficient load during the healing process.

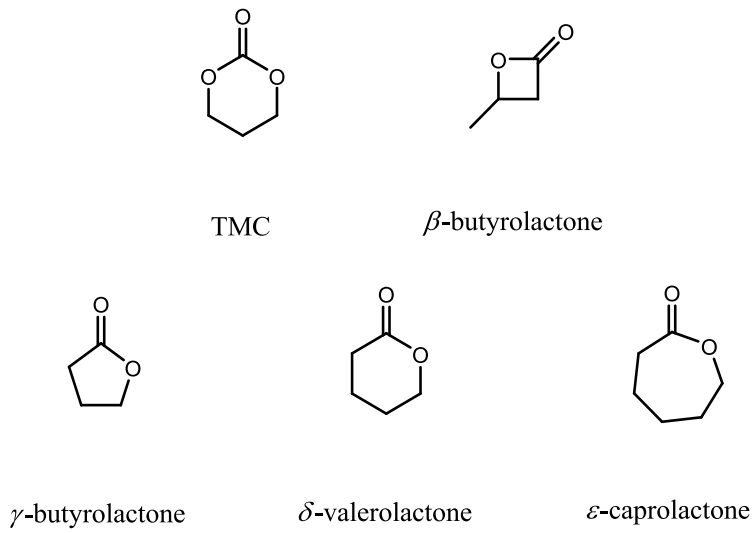

Figure I-6. Various monomers for the copolymerization with lactide.

Within the remainder of this dissertation, a new series of well-characterized zinc and aluminum complexes for the stereosective ring-opening polymeration of lactide will be deliberated. The topic discussed will range from ligand synthesis, complex characterization, comparison of selectivity and reactivity of each catalyst for the ROP of *rac*-lactide as well as kinetic investigation unique to this system. The copolymerization of lacitde with different monomers as well as detail kinetic studies for the copolymerization of lactide and δ-valerolactone will be presented.

CHAPTER II

RING-OPENING POLYMERIZATION OF LACTIDE CATALYZED BY NATURAL AMINO-ACID BASED ZINC CATALYSTS*

Introduction

Presently there is considerable interest in synthesizing useful polymeric materials wholly or in part from renewable resources.[29] For example, major efforts are underway for industrially preparing the most widely used polymers worldwide, polyethylene and poly(ethylene terephthalate), from renewable resources, that is, ethanol-based ethylene[30] and ethylene glycol derived from sugar and molasses.[31] Polyesters represent another class of polymers that can serve as alternative materials for petrochemical-based polymers and are derived from 100% renewable resources. That is, polylactides are aliphatic polyesters obtained by polymerizing lactic acid which is available from the fermentation of sugar (beet or cane) or starch (corn, wheat, potatoes, or manioc). Of importance, these polymers have the highly desirable properties of biocompatibility and biodegradability. As a consequence, polymers such as polylactides have been widely used in medical applications, such as, biodegradable sutures, slow release drug delivery, and tissue engineering.[6]

The use of metal-based catalysts for the ring-opening polymerization (ROP) of cyclic esters has been the subject of several reviews.[6c, 32] Included in these studies are metal complexes of Sn,[33] Ge,[34] Y,[35] Fe,[36] Ti/Zr,[33e, 37] Mg,[38] Al,[10a, 12-13, 17, 39] Ca,[38o, 40] Na,[41] Li,[42]Zn,[21b, 22b, 38a-c, 38e, 38l, 38n, 38o, 39q, 43] and In.[44] Although a large variety of metal derivatives effectively catalyzes the ROP of lactide, it is preferable to use biocompatible metals since polylactides are widely utilized in food packaging and biomedical applications. Because the lactide monomer consists of two stereocenters, it exists as three possible stereoisomers, L-lactide, D-lactide, and *meso*-lactide. The extent of stereocontrol exhibited by a catalytic system is very important because the physical and degradation properties of the polylactide depend upon the tacticity of the polymer. Isotactic L- or D-polylactides can easily be obtained from enantiomerically pure L- or D-lactide, respectively. However, upon polymerizing *rac*- or *meso*-lactide, selective catalysts greatly influence the tacticity of the resulting polymeric material. For example, utilizing a catalyst system with stereocontrol syndiotactic polylactide and heterotactic polylactide can be synthesized from *meso*- or *rac*-lactide, respectively. These processes are depicted in eqs 1 and 2.

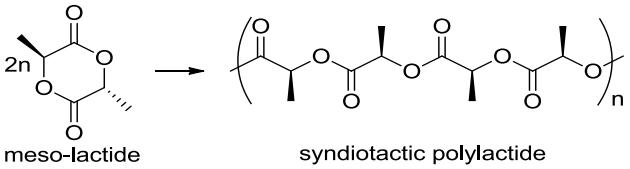

(1)

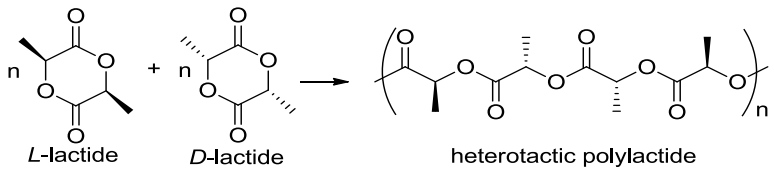

(2)

In addition, stereocomplexed polylactides can be produced from a blend of poly-L-lactide acid (PLLA) and poly-D-lactide acid (PDLA) which have a T_m value of 230 °C,[45] while homocrystallized polylactides have melting temperatures in the range of 170−180 °C.[46] An increase in T_m coupled with different physical and mechanical properties relative to the parent homopolymers makes the stereocomplexed polylactide an attractive polymer (eq 3). Because the properties of polylactide are so highly dependent on the polymer's tacticity,[32b, 47] research studies employing chiral catalysts for the ROP of lactides where enantiomorphic site control is possible are of much current interest.

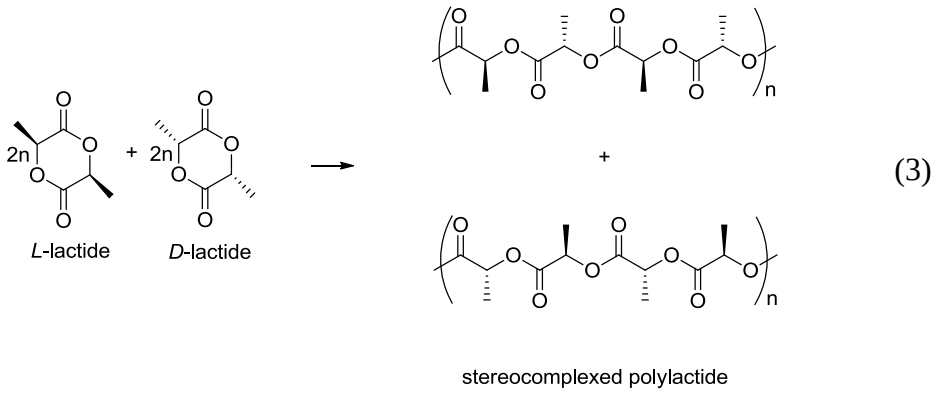

(3)

Herein we wish to describe the synthesis of chiral Schiff base ligands derived from the natural amino acids, L-phenylalanine, L-leucine, and L-methionine and their complexes with the biocompatible metal, zinc. These metal derivatives have been fully characterized and all shown to be highly active catalysts for the ROP of lactides. Included in these studies is the selectivity of these chiral zinc catalysts for the ROP of L- and D-lactide, as well as the effect of the substituents on the Schiff base ligands on the tacticity of the polylactide afforded from *rac*-lactide.

Experimental Section

Method and Materials. All manipulations were carried out using a double manifold Schlenk vacuum line under an argon atmosphere or an argon filled glovebox unless otherwise stated. Toluene and THF were freshly distilled from sodium/benzophenone before use. Methanol and dichloromethane were purified by an MBraun Manual Solvent Purification System packed with Alcoa F200 activated alumina desiccant. Pentane was freshly distilled from CaH_2. Deuterated chloroform and deuterated benzene from Cambridge Isotope Laboratories Inc. were stored in the glovebox and used as received. L- and D-lactide were gifts from PURAC America Inc., and *rac*-lactide was purchased from Aldrich. These lactides were recrystallized from toluene, dried under vacuum at 40 °C overnight, and stored in the glovebox. Sodium *bis*(trimethylsilyl)amide and *p*-fluophenol were purchased from Alfa Aesar, zinc chloride anhydrous was purchased from Strem Chemicals, and all were stored in the glovebox. *N*-Boc-L-phenylalanine, *N*-Boc-L-methionine, and *N*-Boc-L-leucine were purchased from Chem-Impex international and used as received. *N*,*N*-dimethylethylendiamine was purchased from Acros and used as received. 3,5-Di-*tert*-butyl-2-hydroxybenzaldehyde and zinc(bis-trimethylsilyl amide)$_2$ were prepared according to published procedure.[40c, 40d, 48] All other compounds and reagents were obtained from Aldrich and were used without further purification. Analytical elemental analysis was provided by Canadian Microanalytical Services Ltd.

Measurements. ^{1}H NMR spectra were recorded on Unity+ 300 MHz and VXR 300 MHz superconducting NMR spectrometers. Molecular weight determinations were

carried out with Viscotek Modular GPC apparatus equipped with ViscoGEL I-series columns (H + L) and Model 270 dual detector composed of refractive index and light scattering detectors. TGA measurements were performed with TGA 1000 Thermogravimetric Analyzer by Instrument Specialists Incorporated. The samples were scanned from room temperature to the desired temperature under argon atmosphere with a heating rate of 5 °C/min. DSC measurements were performed with a Polymer DSC by Mettler Toledo. The samples were scanned from -100 to 200 °C under nitrogen atmosphere. The glass transition temperature (T_g), the crystallization temperature (T_c), and the melting temperature (T_m) of polylactides were determined from the second heating at a heating rate of 5 °C/min. X-ray crystallography was done on a Bruker Smart 1000 diffractometer equipped with a CCD detector in a nitrogen cold stream maintained at 110 K. Crystal data and details of the data collection for complexes **II6a**-**6e** are provided in Tables on page 48.

General Procedure for Synthesis of Chiral Diamines II4a-c. The chiral diamines **II4a-c** were prepared according to the reported literature[49] with some modifications. To *N*-Boc-L-phenylalanine (75 mmol) in CH_2Cl_2 (200 mL) was added DCC (83 mmol) followed by HOBt (83 mmol) at ambient temperature. The dimethylamine (83 mmol, 40% aq solution) was added after 2 h. The reaction mixture was stirred overnight, and the solvent was removed under reduced pressure to obtain a white precipitate. The white precipitate was removed by filtration, and the filtrate was washed with 10% citric acid solution followed by washing with a saturated $NaHCO_3$ solution. The organic layer was separated, dried over $NaSO_4$, and concentrated to

dryness under reduced pressure to afford the crude amides **II2a-c** which were used in the next step without further purification.

The *N*-Boc-protected amines were then deprotected with TFA. To a solution of *N*-Boc-protected amines **II2a-c** (55 mmol) in anhydrous CH_2Cl_2 (15 mL), TFA (165 mmol) was added and stirred for overnight at room temperature. Excess TFA and solvent were removed under reduced pressure. The resulting yellowish oil was neutralized with sat. $NaHCO_3$, extracted with CH_2Cl_2 (10 × 30 mL), dried over Na_2SO_4, and evaporated to dryness. The crude amides **II3a-c** were used for the next step without purification.

The amides **II3a-c** (45 mmol) were dissolved in THF (30 mL) and cannulated into a suspension of $LiAlH_4$ (180 mmol) in THF (60 mL) cooled in an ice bath. The reaction mixture was heated to reflux overnight. The mixture was placed in an ice bath, and EtOAc (100 mL) was slowly added to the mixture, followed by saturated Na_2SO_4 (100 mL). The resulting white solid was washed with EtOAc (3× 50 mL). The combined organic layers were dried over Na_2SO_4, and the solvent was removed under reduced pressure to afford slightly yellow oils **II4a-c**. The crude products **II4a-c** were purified by vacuum distillation in a short-path apparatus.

(*S*)-*N′*,*N′*-dimethyl-3-phenylpropane-1,2-diamine II4a Following the general procedure for synthesis of chiral diamines, the title compound **II4a** was purified by vacuum distillation (0.5−0.7 mmHg) in a short-path apparatus at 121 °C; 4.36 g of yellowish liquid was collected (61% yield). $[\alpha]_D$ = +12.64 (*c* = 1.1, $CHCl_3$); ^{1}H NMR (300 MHz, $CDCl_3$) δ = 1.20−1.80 (br s, 2H), 2.13−2.19 (m, 1H), 2.23 (s, 6H), 2.27−2.31

(m, 1H), 2.47 (dd, *J* = 13.46, 8.8 Hz, 1H), 2.74 (dd, *J* = 13.25, 4.5 Hz, 1H), 3.09−3.18 (m, 1H), 7.19−7.25 (m, 3H), 7.26−7.32 (m, 2H); ^{13}C NMR (300 MHz, $CDCl_3$) δ = 49.25, 52.05, 53.35, 68.46, 116.28, 118.08, 118.78, 126.78. Anal. Calcd for $C_{11}H_{18}N_2$: C, 74.11; H, 10.18; N, 15.71. Found: C, 71.98; H, 10.26; N, 14.56. HRMS (ESI), *m*/*z*, 179.1591 [M+H$^+$], calcd for $C_{11}H_{18}N_2$, 179.15.

(*S*)-*N′*,*N′*,4-trimethylpentane-1,2-diamine II4b. Following the general procedure for synthesis of chiral diamines, the title compound **II4b** was purified by vacuum distillation (0.5−0.7 mmHg) in a short-path apparatus at 110 °C; 3.75 g of product was collected (59% yield). $[\alpha]_D^{20}$ = +27.77 (*c* = 1.8, $CHCl_3$); ^{1}H NMR (300 MHz, $CDCl_3$) δ = 0.89 (d, *J* = 7.0 Hz, 3H), 0.91 (d, *J* = 6.9 Hz, 3H), 1.11−1.24 (m, 2H), 1.69−1.80 (m, 1H), 2.06 (dd, *J* = 12.0, 3.8 Hz, 1H), 2.12−2.19 (m, 1H), 2.15 (br s, 2H), 2.22 (s, 6H), 2.90−2.98 (m, 1H); ^{13} C NMR (300 MHz, $CDCl_3$) δ = 22.00, 23.52, 24.60, 45.09, 45.81, 45.99, 67.43. Anal. Calcd for $C_8H_{20}N_2$: C, 66.61; H, 13.97; N, 19.42. Found: C, 61.97; H, 13.34; N, 16.53. HRMS (ESI), *m*/*z*, 144.1523 [M+H$^+$], calcd for $C_8H_{20}N_2$, 144.15.

(*S*)-*N′*,*N′*-dimethyl-4-(methylthio)butane-1,2-diamine II4c. Following the general procedure for synthesis of chiral diamines, the title compound **II4c** was purified by vacuum distillation (1.2 mmHg) in a short-path apparatus at 125 °C; 4.22 g of product was collected (40% yield). $[\alpha]_D^{21}$ = +12.22 (*c* = 1.14, $CHCl_3$); ^{1}H NMR (300 MHz, $CDCl_3$) δ = 1.29−1.43 (m, 2H), 1.76−1.86 (m, 2H), 1.88 (s, 3H), 2.00 (s, 6H), 2.30−2.46 (m, 2H), 2.71−2.81 (m, 2H); ^{13}C NMR (300 MHz, $CDCl_3$) δ = 15.39, 30.74, 35.04, 45.49, 47.33, 66.68. Anal. Calcd for $C_7H_{18}N_2S$: C, 51,80; H, 11.18; N, 17.26; S, 19.76

Found: C, 51.51; H, 10.97; N, 15.11; S, 17.09. HRMS (ESI), *m*/*z*, 163.1309 [M+H^+], calcd for $C_7H_{18}N_2S$, 163.13.

General Procedure for Synthesis of Tridentate Schiff Base Ligands. 3,5-Di-*tert*-butyl-2-hydroxybenzaldehyde[40c, 40d, 48b] (1.0 equiv) in MeOH (30 mL) was added to **II4a-d**, (1.0 equiv). The solution mixture was heated to reflux overnight and dried over Na_2SO_4 followed by filtration. The volatile component was removed in vacuo to obtain tridentate Schiff base ligands **II5a-d** in 88% to quantitative yield.

(*S*,*E*)-2,4-di-*tert*-butyl-6-((1-(dimethylamino)-3-phenylpropan-2-ylimino) methyl)phenol (L^1-H) II5a. Following the general procedure for synthesis of tridentate Schiff base ligands, 3,5-di-*tert*-butyl-2-hydroxybenzaldehyde (1.26 g, 5.38 mmol) in MeOH (30 mL) was added to **II4a** (0.958 g, 5.38 mmol). The solution mixture was heated to reflux overnight and dried over Na_2SO_4 followed by filtration. The volatile component was removed in vacuo to obtain **II5a** in 95% yield. $[\alpha]_D^{20} = -154.54$ (*c* = 1.1, $CHCl_3$); ^{1}H NMR (300 MHz, $CDCl_3$) δ = 1.37 (s, 9H, C(C*H*$_3$)$_3$), 1.55 (s, 9H), 2.35 (s, 6H), 2.55−2.68 (m, 2H), 2.95 (dd, *J* = 13.39, 8.33 Hz, 1H), 3.13 (dd, *J* = 13.39, 4.16 Hz, 1H), 3.54−3.63 (m, 1H), 7.03 (d, 7.03 (d, *J* = 2.87 Hz, 1H), 7.23−7.32 (m, 5H, Ph*H*), 7.44 (d, *J* = 2.65 Hz,1H), 8.13 (s, 1H), 13.89 (s, 1H, O*H*); ^{13}C NMR (300 MHz, $CDCl_3$) δ = 29.58, 31.62, 34.21, 35.13, 41.14, 46.34, 65.14, 69.86, 117.90, 126.10, 126.28, 126.83, 128.41, 129.74, 136.54, 138.89, 139.83, 158.25, 165.63. Anal. Calcd for $C_{26}H_{38}N_2O$: C, 79.14; H, 9.71; N, 7.10. Found: C, 78.56; H, 9.69; N, 6.93. HRMS (ESI), *m*/*z*, 395.3184 [M+H^+], calcd for $C_{26}H_{38}N_2O$, 395.31.

(*S*,*E*)-2,4-di-*tert*-butyl-6-((1-(dimethylamino)-4-methylpentan-2-ylimino) methyl)phenol (L^2-H) II5b. Following the general procedure for synthesis of tridentate Schiff base ligands, 3,5-di-*tert*-butyl-2-hydroxybenzaldehyde (1.30 g, 5.54 mmol) in MeOH (30 mL) was added to **II4a** (0.799 g, 5.54 mmol). The solution mixture was heated to reflux overnight and dried over Na_2SO_4 followed by filtration. The volatile component was removed in vacuo to obtain **II5b** in 96% yield. $[\alpha]_D^{21} = -18.72$ (*c* = 1.17, $CHCl_3$); ^{1}H NMR (300 MHz, $CDCl_3$) δ = 0.87 (dd, *J* = 10.37, 5.88 Hz, 6H), 1.32 (s, 9H), 1.46 (s, 9H), 1.43−1.46 (m, 1H), 1.55−1.65 (m, 1H), 2.25 (s, 6H), 2.42−2.46 (m, 2H), 3.34−3.43 (m, 1H), 7.11 (d, *J* = 2.60 Hz, 1H), 7.38 (d, *J* = 2.60 Hz, 1H), 8.34 (s, 1H), 13.89 (s, 1H, O*H*); ^{13}C NMR δ = (300 MHz, $CDCl_3$) δ = 21.46, 23.89, 24.44, 29.59, 33.66, 34.26, 35.13, 43.36, 46.40, 65.14, 117.96, 126.06, 126.79, 136.65, 139.90, 158.37, 165.02. Anal. Calcd for $C_{23}H_{40}N_2O$: C, 76.61; H, 11.18; N, 7.77. Found: C, 76.19; H, 11.05; N, 7.36. HRMS (ESI), *m*/*z*, 361.3292 [$M+H^+$], calcd for $C_{23}H_{40}N_2O$, 361.31.

(*S*,*E*)-2,4-di-*tert*-butyl-6-((1-(dimethylamino)-4-(methylthio)butan-2-ylimino) methyl)phenol (L^3-H) II5c. Following the general procedure for synthesis of tridentate Schiff base ligands, 3,5-di-*tert*-butyl-2-hydroxybenzaldehyde (1.03 g, 4.41 mmol) in MeOH (30 mL) was added to **II4a** (0.72 g, 4.41 mmol). The solution mixture was heated to reflux overnight and dried over Na_2SO_4 followed by filtration. The volatile component was removed in vacuo to obtain **II5c** in 88% yield. $[\alpha]_D^{21} = -62.80$ (*c* = 1.21, $CHCl_3$); ^{1}H NMR (300 MHz, $CDCl_3$) δ = 1.33 (s, 9H), 1.46 (s, 9H), 1.84−2.08 (m, 2H), 2.10 (s, 3H), 2.26 (s, 6H), 2.38−2.65 (m, 4H), 3.44−3.56 (m, 1H), 7.12 (d, *J* = 2.63 Hz, 1H), 7.39

(d, *J* = 2.63 Hz, 1H), 8.39(s, 1H), 13.70 (s, 1H,O*H*); ^{13}C NMR (300 MHz, $CDCl_3$) δ = 15.57, 29.73, 31.11, 33.27, 34.26, 35.24, 46.45, 65.54, 66.52, 177.87, 126.32, 127.11, 136.75, 140.10, 158.39, 166.26. Anal. Calcd for $C_{22}H_{38}N_2OS$: C, 69.79; H, 10.12; N, 7.40; S, 8.47 Found: C, 69.88; H, 10.16; N, 7.17; S, 8.27. HRMS (ESI), *m*/*z*, 379.2673 [M+H$^+$], calcd for $C_{22}H_{38}N_2OS$, 379.27.

(*E*)-2,4-di-*tert*-butyl-6-((2-(dimethylamino)ethylimino)methyl)phenol (L^4-H) II5d[50]. Following the general procedure for synthesis of tridentate Schiff base ligands, 3,5-di-*tert*-butyl-2-hydroxybenzaldehyde (2.00 g, 8.53 mmol) in MeOH (30 mL) was added to **II4d** (*N*′,*N*′-dimethylethane-1,2-diamine) (0.75 g, 8.53 mmol). The solution mixture was heated to reflux overnight and dried over Na_2SO_4 followed by filtration. The volatile component was removed in vacuo to obtain **II5d** in 92% yield. ^{1}H NMR (300 MHz, $CDCl_3$) δ = 1.32 (s, 9H), 1.65 (s, 9H), 2.02 (s, 6H), 2.28 (t, *J* = 7.03, 2H), 3.31 (t, *J* = 7.03, 2H), 6.98 (d, *J* = 2.52, 1H), 7.56 (d, *J* = 2.52, 1H), 7.84 (s, 1H), 14.26 (s, 1H, O*H*); ^{13}C NMR (300 MHz, $CDCl_3$) δ = 29.8, 31.7, 34.3, 35.4, 45.7, 57.8, 60.1, 118.7, 126.3, 126.7, 137.1, 140.0, 158.9, 166.8. Anal. Calcd for $C_{19}H_{32}N_2O$: C, 74.95; H, 10.59; N, 9.20. Found: C, 74.94; H, 10.61; N, 9.02. HRMS (ESI), *m*/*z*, 305.2620 [M+H$^+$], calcd for $C_{19}H_{32}N_2O$, 305.25.

General Procedure for Synthesis of Tridentate Schiff Base Zinc Complexes ($L^{1–4}$-H) II6a−d. A Tridentate Schiff base ligand (1 equiv) was dissolved in pentane and was cannulated to a solution of $Zn[N(SiMe_3)_2]_2$ (1.0 equiv) in pentane. The reaction mixture was stirred until a yellow precipitate was formed and allowed to stir at room temperature for an additional 3 h. The resulting yellow precipitate was then washed with

cold pentane (3× 2 mL). The volatile component was removed under reduced pressure to obtain light yellow solid **II6a-d**.

Synthesis of [L^1ZnN(SiMe$_3$)$_2$] II6a. A Tridentate Schiff base ligand **II5a** (1.06 g, 2.68 mmol) was dissolved in pentane (3 mL) and was cannulated to a solution of Zn[N(SiMe$_3$)$_2$]$_2$ (1.04 g, 2.68 mmol) in pentane (1 mL). The reaction mixture was stirred until a yellow precipitate was formed and allowed to stir at room temperature for an additional 3 h. The resulting yellow precipitate was then washed with cold pentane (3× 2 mL). The volatile component was removed under reduced pressure to obtain light yellow solid **II6a** in 51% yield. $[\alpha]_D^{21}$ = +67.50 (*c* = 1.02, C_6D_6); ^{1}H NMR (300 MHz, C_6D_6) δ = 0.43 (s, 18H), 1.36 (s, 9H), 1.57−1.66 (m, 1H), 1.76 (s, 9H), 1.82 (s, 6H), 2.35−2.47 (m, 2H), 2.67−2.74 (m, 1H), 3.14−3.24 (m, 1H), 6.75 (d, *J* = 2.95 Hz, 1H), 6.93 (d, 1H), 6.96 (d, 1H), 7.09−7.18 (m, 3H), 7.45 (s, 1H), 7.63 (d, *J* = 2.53, 1H); ^{13}C NMR (300 MHz, C_6D_6) δ = 6.20, 30.04, 31.69, 34.02, 36.11, 39.91, 45.41, 61.89, 63.28, 118.24, 127.25, 128.33, 129.09, 129.63, 129.85, 137.17, 142.05, 168.56, 170.82, 165.63; Anal. Calcd for $C_{32}H_{55}N_3OSi_2Zn$: C, 62.05; H, 8.95; N, 6.78. Found: C, 62.48; H, 8.55; N, 6.07.

Synthesis of [L^2ZnN(SiMe$_3$)$_2$] II6b. A Tridentate Schiff base ligand **II5b** (1.08 g, 2.97 mmol) was dissolved in pentane (3 mL) and was cannulated to a solution of Zn[N(SiMe$_3$)$_2$]$_2$ (1.15 g, 2.97 mmol) in pentane (1 mL). The reaction mixture was stirred until a yellow precipitate was formed and allowed to stir at room temperature for an additional 3 h. The resulting yellow precipitate was then washed with cold pentane (3× 2 mL). The volatile component was removed under reduced pressure to obtain light yellow

solid **II6b** in 50% yield. $[\alpha]_D^{21}$ = +89.82 (*c* = 1.00, C_6D_6); ^{1}H NMR (300 MHz, $CDCl_3$) δ = 0.4 (s, 18H), 0.72 (dd, *J* = 11.25, 5.62 Hz, 6H), 1.38 (s, 9H), 1.78 (s, 9H), 1.82 (bs, 2H), 1.94 (s, 6H), 2.16 (m, 2H), 2.42 (bs, 1H), 3.13−3.27 (m, 1H), 7.03 (d, *J* = 3.03 Hz, 1H), 7.66 (d, *J* = 3.03 Hz, 1H), 7.86 (s, 1H); ^{13}C NMR (300 MHz,C_6D_6) δ = 2.78, 6.19, 22.20, 23.26, 24.54, 30.09, 31.80, 34.15, 36.28, 41.83, 46.10, 58.26, 64.88, 118.66, 129.97, 135.09, 142.35, 168.59; Anal. Calcd for $C_{29}H_{57}N_3OSi_2Zn$: C, 59.50; H, 9.81; N, 7.18. Found: C, 59.63; H, 9.63; N, 6.66.

Synthesis of [L^{3}ZnN(SiMe$_3$)$_2$] II6c. A Tridentate Schiff base ligand **II5c** (1.03 g, 2.73 mmol) was dissolved in pentane (3 mL) and was cannulated to a solution of $Zn[N(SiMe_3)_2]_2$ (1.05 g, 2.73 mmol) in pentane (1 mL). The reaction mixture was stirred until a yellow precipitate was formed and allowed to stir at room temperature for an additional 3 h. The resulting yellow precipitate was then washed with cold pentane (3× 2 mL). The volatile component was removed under reduced pressure to obtain light yellow solid **II6c** in 55% yield. $[\alpha]_D^{21}$ = +115.70 (*c* = 1.21, C_6D_6); ^{1}H NMR (300 MHz, $CDCl_3$) δ = 0.39 (s, 18H), 1.36 (s, 9H), 1.40−1.51 (m, 2H), 1.70 (s, 3H), 1.75 (s, 9H), 1.90 (s, 6H), 2.04−2.27 (m, 4H), 3.11−3.24 (m, 1H), 6.98 (d, *J* = 2.73 Hz, 1H), 7.64 (d, *J* = 2.73 Hz, 1H), 7.87 (s, 1H) ^{13}C NMR (300 MHz, $CDCl_3$) δ = 6.14, 15.23, 30.06, 30.26, 31.78, 32.50, 34.11, 36.18, 45.78, 59.33, 63.64, 118.46, 128.49, 129.99, 135.10, 142.14, 168.65, 170.03; Anal. Calcd for $C_{28}H_{55}N_3OSSi_2Zn$: C, 55.73; H, 9.91; N, 6.69; S, 5.31. Found: C, 55.68; H, 8.89; N, 6.05; S, 5.28.

Synthesis of [L^{4}ZnN(SiMe$_3$)$_2$] II6d. A Tridentate Schiff base ligand **II5d** (1.00 g, 3.28 mmol) was dissolved in pentane (3 mL) and was cannulated to a solution of

$Zn[N(SiMe_3)_2]_2$ (1.27 g, 3.28 mmol) in pentane. The reaction mixture was stirred until a yellow precipitate was formed and allowed to stir at room temperature for an additional 3 h. The resulting yellow precipitate was then washed with cold pentane (3× 2 mL). The volatile component was removed under reduced pressure to obtain light yellow solid **II6d** in 52% yield. $[\alpha]_D^{21}$ = 0.00 (*c* = 1.05, C_6D_6); ^{1}H NMR (300 MHz, $CDCl_3$) δ = 0.37 (s, 18H), 1.38 (s, 9H), 1.75 (s, 9H), 1.90 (s, 6H), 2.78 (t, *J* = 6.01 Hz, 2H), 3.11 (t, *J* = 6.01 Hz, 2H), 6.85 (d, *J* = 2.7 Hz, 1H), 7.40 (s, 1H), 7.63 (d, *J* = 2.7 Hz, 1H); ^{13}C NMR (300 MHz, $CDCl_3$) δ = 6.10, 30.06, 31.84, 34.06, 36.29, 45.64, 52.99, 57.22, 59.67, 60.33, 118.66, 129.79, 135.14, 142.26, 169.87. Anal. Calcd for $C_{25}H_{49}N_3OSi_2Zn$: C, 56.73; H, 9.33; N, 7.94. Found: C, 57.91; H, 8.61; N, 7.18.

Synthesis of [L^{1}ZnOPh] 6e. A Tridentate Schiff base ligand **II5a** (0.55 g, 1.82 mmol) and *p*-fluorophenol (0.24 g, 1.82 mmol) were dissolved in pentane (3 mL) and was cannulated to a solution of $Zn[N(SiMe_3)_2]_2$ (0.74 g, 1.82 mmol) in pentane (1 mL). The reaction mixture was stirred until a yellow precipitate was formed and allowed to stir at room temperature for an additional 3 h. The resulting yellow precipitate was then washed with cold pentane (3× 2 mL). The volatile component was removed under reduced pressure to obtain light yellow solid **II6e** in 55% yield. ^{1}H NMR (300 MHz, $CDCl_3$) δ = 1.39 (s, 9H), 1.76 (s, 9H), 1.99 (s, 6H), 2.80 (t, *J* = 5.72 Hz, 2H), 3.11 (t, *J* = 5.72 Hz, 2H), 6.70 (t, *J* = 8.78 Hz, 2H), 6.91 (bs, 2H), 7.02 (d, *J* = 2.72 Hz, 1H), 7.77 (m, 2H); ^{13}C NMR (300 MHz, $CDCl_3$) δ = 30.10, 30.36, 31.77, 34.12, 36.05, 45.50, 46.31, 54.44, 57.17, 59.57, 115.75, 116.04, 118.10, 119.50, 129.82, 135.49, 141.75,

169.67, 171.81, Anal. Calcd for $C_{25}H_{35}FN_2O_2Zn$: C, 62.56; H, 7.35; N, 5.84; F, 3.96. Found: C, 62.83; H, 7.54; N, 5.89; F, 3.84.

Polymerization Procedure. In a typical experiment (Table on page 41, entry 1), in the glovebox, a Schlenk flask was charged with a solution of complex **II6a** (8.58 mg, 13.87 μmol) in $CHCl_3$ (2 mL). To this solution was added *rac*-lactide (100 mg, 0.69 mmol, 50 equiv). The mixture was stirred at room temperature for 60 min. After a small sample of the crude solution was removed with a syringe to be characterized by ^{1}H NMR spectroscopy, the product was isolated and purified by precipitation from dichloromethane by the addition of 5% hydrochloric acid in methanol. The polymer was collected and dried under vacuum to constant weight.

Kinetic Studies. Polymerizations of L- or D-lactide using complexes **II6a-d** were monitored by ^{1}H NMR spectroscopy. Each monomer and corresponding zinc complex were dissolved in C_6D_6, and the % conversion was investigated from the integration of polymer and monomer signals. The chemical shifts of polylactide are 5.01 (q, H) and 1.32 (d, CH_3), and the chemical shifts of lactide monomer are 3.79 (q, H) and 1.16 (d, CH_3).

Results and Discussion

Synthesis and Characterization of Proligands and Their Zinc Complexes. The synthesis of chiral diamines **II4a-c** is based on the reported literature[49] using different *N*-Boc-L-protected amino acids with modification as shown in Scheme II-1. Condensation reactions of these diamines **II4a-d** with 3,5-di-*tert*-butyl-2-hydroxybenzaldehyde at reflux in methanol yielded the analogous compounds **II5a-d**,

where R = benzyl, isobutyl, 2-(methylthio)ethyl, and hydrogen, respectively (Scheme II-2). The reactions of these chiral ligands with zinc(*bis*-trimethylsilyl amide)$_2$, Zn[N(SiMe$_3$)$_2$]$_2$ in dry pentane resulted in straightforward formation of the yellow zinc complexes **II6a-d**. In an analogous manner, the reaction of **II5d** with Zn[N(SiMe$_3$)$_2$]$_2$ in the presence of *p*-fluorophenol yielded complex **II6e** as shown in (Scheme II-3). The complexes were characterized by ^{1}H and ^{13}C NMR spectroscopy, as well as, elemental analysis. The molecular structures of the complexes were determined by X-ray crystallography.

Scheme II-1

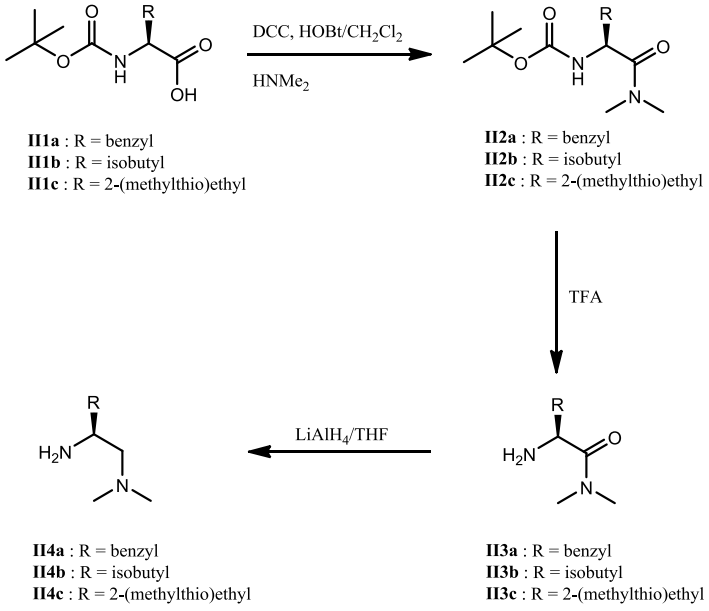

Suitable single crystals of complexes **II6a-e** were obtained from recrystallization in dry pentane, and their molecular structures were determined by single X-ray

crystallography. Complexes **II6a-d** are very similar to each other. The solid-state structures of complexes **II6a-d** have shown that two nitrogen atoms and one oxygen atom of the ligands coordinate to a metal center in a tridentate coordination mode along with one amido group. The geometry of the zinc complexes is a distorted tetrahedron with zinc at the center. The complexes are shown in Figure II-1, with atomic labeling for non-hydrogen atoms. Selected bond distances and angles are listed in Table II-1. On the other hand, if the amido group is replaced by *p*-fluorophenolate to give complex **II6e**, the solid-state structure is shown to be dimeric with a Zn(1)/O(2)/Zn(2)/O(3) planar core bridged by the two oxygen atoms of *p*-fluorophenol as illustrated in Figure II-2. The dimeric structure shows that one zinc center adopts a distorted tetrahedral geometry, in comparison with the other zinc center which possesses distorted trigonal bipyramidal geometry.

Scheme II-2

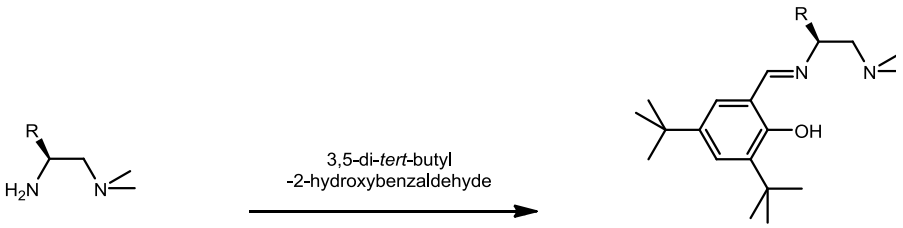

II4a : R = benzyl
II4b : R = isobutyl
II4c : R = 2-(methylthio)ethyl
II4d : R = H

II5a : R = benzyl
II5b : R = isobutyl
II5c : R = 2-(methylthio)ethy
II5d : R = H

Scheme II-3

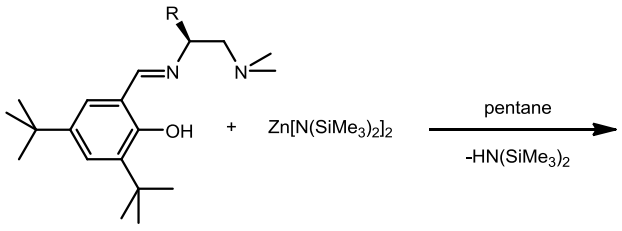

II5a : R = benzyl
II5b : R = isobutyl
II5c : R = 2-(methylthio)ethyl
II5d : R = H

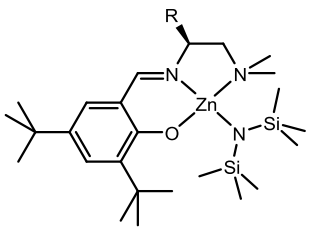

II6a : R = benzyl
II6b : R = isobutyl
II6c : R = 2-(methylthio)ethyl
II6d : R = H

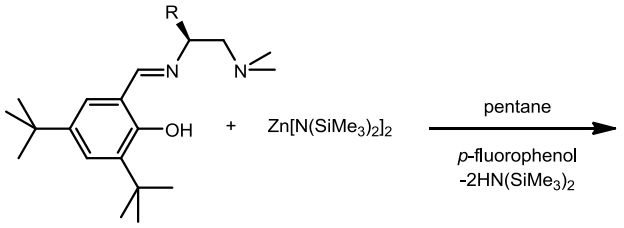

II5d : R = H

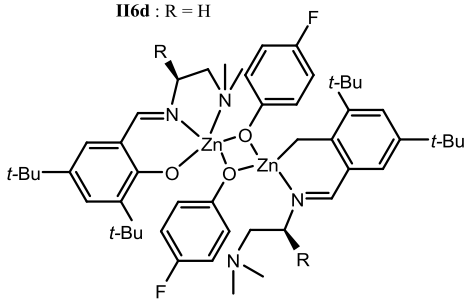

II6e : R = H

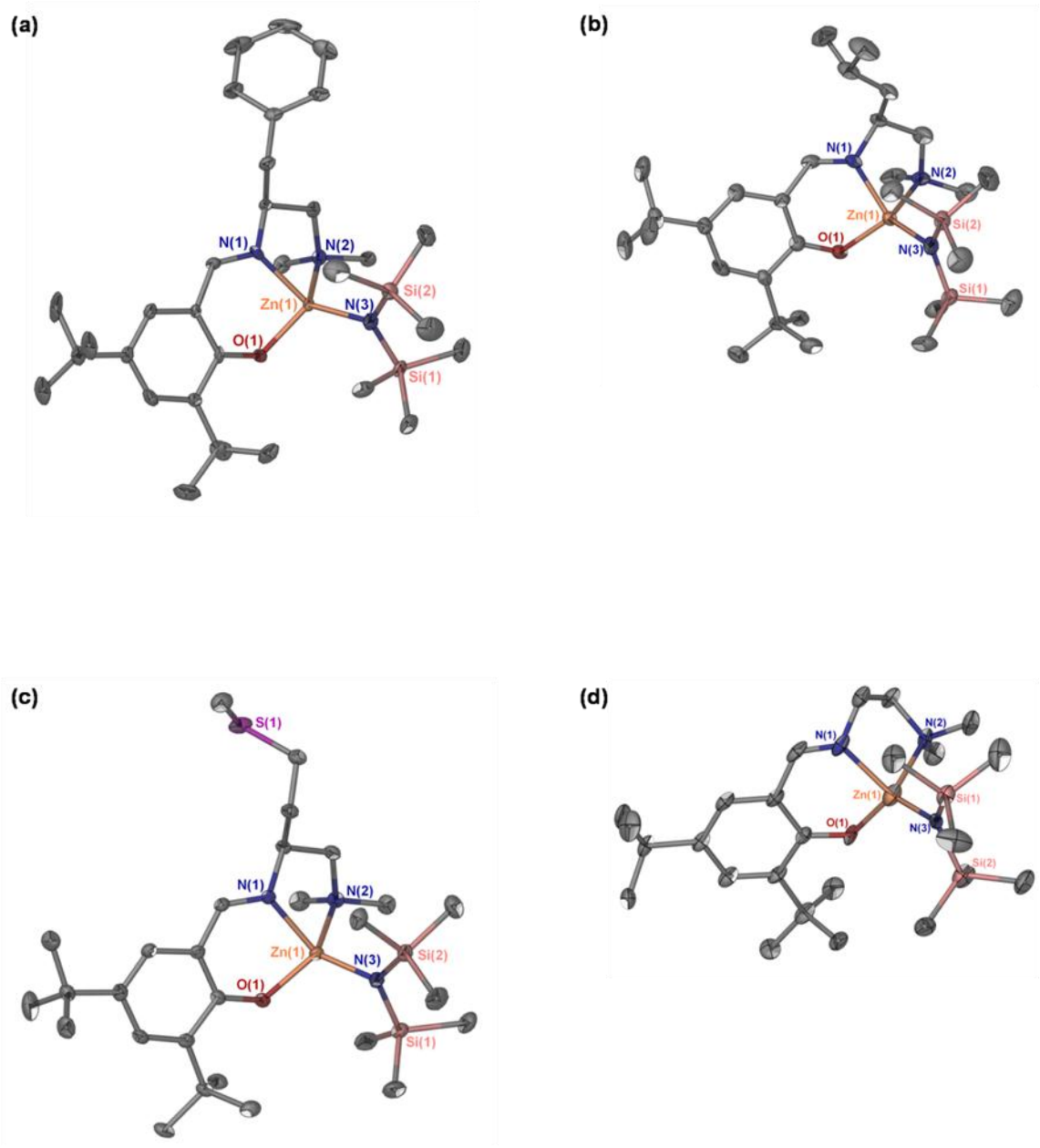

Figure II-1. X-ray crystal structures of (a) **II6a**, (b) **II6b**, (c) **II6c**, and (d) **II6d**. Thermal ellipsoids represent the 50% probability surfaces. Hydrogen atoms are omitted for the sake of clarity.

Table II-1. Selected Bond Lengths (Å) and Angles (deg) for Zn Complexes **II6a-d**.

	II6a	**II6b**	**II6c**	**II6d**
		Bond lengths		
Zn1-N1	2.017 (4)	2.030 (4)	2.022 (2)	2.010 (5)
Zn1-N2	2.198 (3)	2.193 (4)	2.211 (2)	2.211 (6)
Zn1-N3	1.920 (4)	1.921 (4)	1.913 (2)	1.917 (5)
Zn1-O1	1.933 (3)	1.930 (3)	1.9406 (18)	1.930 (4)
		Bond angles		
N3-Zn1-O1	115.60 (14)	119.64 (15)	116.01 (9)	122.2 (2)
N3-Zn1-N1	136.85 (16)	133.83 (15)	138.63 (9)	132.3 (2)
O1-Zn1-N1	91.24 (13)	92.20 (13)	91.58 (8)	90.6 (2)
N3-Zn1-N2	110.14 (14)	114.20 (16)	108.68 (9)	112.0 (2)
O1-Zn1-N2	121.26 (14)	112.07 (14)	120.65 (8)	110.9 (2)
N1-Zn1-N2	78.64 (14)	77.40 (14)	78.21 (8)	81.4 (2)

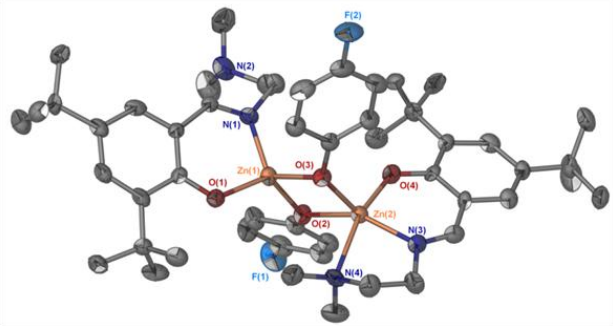

Figure II-2. X-ray crystal structure of complex **II6e**. Thermal ellipsoids represent the 50% probability surfaces. Hydrogen atoms are omitted for the sake of clarity. Selected bond lengths (Å) and angles (deg): Zn2-N3 : 2.050 (6), Zn2-N4 : 2.301 (5), Zn2-O2 : 2.080 (4), Zn2-O3 : 2.016 (5), Zn2-O4 : 1.977 (4), O4-Zn2-O3 : 106.69 (17), O4-Zn2-N3 : 89.61 (18), O3-Zn2-N3 : 126.78 (19), O4-Zn2-O2 : 95.69 (16), O3-Zn2-O2 : 80.79 (16), N3-Zn2-O2 : 148.99 (18), O4-Zn2-N4 : 161.08 (19), O3-Zn2-N4 : 92.24 (18), N3-Zn2-N4 : 78.79 (19), O2-Zn2-N4 : 87.10 (17).

Polymerization Studies. Ring-Opening of Lactides. There are two different mechanisms for the stereoselective ROP of *rac*-lactide,[13c] that is, a chain-end control[12] and an enantiomorphic site-control mechanism.[13a, 13b] To examine this latter mechanism we have synthesized enantiomerically pure zinc complexes **II6a-c**, and these plus the achiral complex **II6d** were tested for the ROP of L- and D-lactide under the same reaction conditions to compare their selectivity and reactivity for this polymerization process. All reactions were carried out in C_6D_6 at ambient temperature and were monitored by ^{1}H NMR spectroscopy. The experimental observations reveal all zinc complexes to be active for the ROP of D- and L-lactide, and the resulting polymers were obtained with the expected molecular weights and with low polydispersity indices. To quantitatively compare the selectivity of each complex for the ROP of D- and L-lactide, the rates of the reactions were investigated. The polymerization reactions were found to be first-order in monomer as illustrated in Figure II-3 for several catalytic systems. Table II-2 summarizes the rate constants (k_{obsd}) for these various processes. As evident in Figure II-3 and Table II-2 the ratio of $k_{d(obsd)}$ over $k_{l(obsd)}$ is close to unity for reactions catalyzed by complexes **II6a-c**, indicative of a lack of preferences of the enantiomerically pure complexes for L- or D-lactide. Complex **II6a** was found to be the most active of the zinc complexes. The ROP of L-lactide utilizing the dimeric complex **II6e** began slowly for the first 5 h, followed by a rate consistent with the more active monomeric catalyst **II6d** (Figure II-4). This is presumably due to dimeric disruption leading to a more active monomeric species as previously illustrated by Lin and co-workers.[43l]

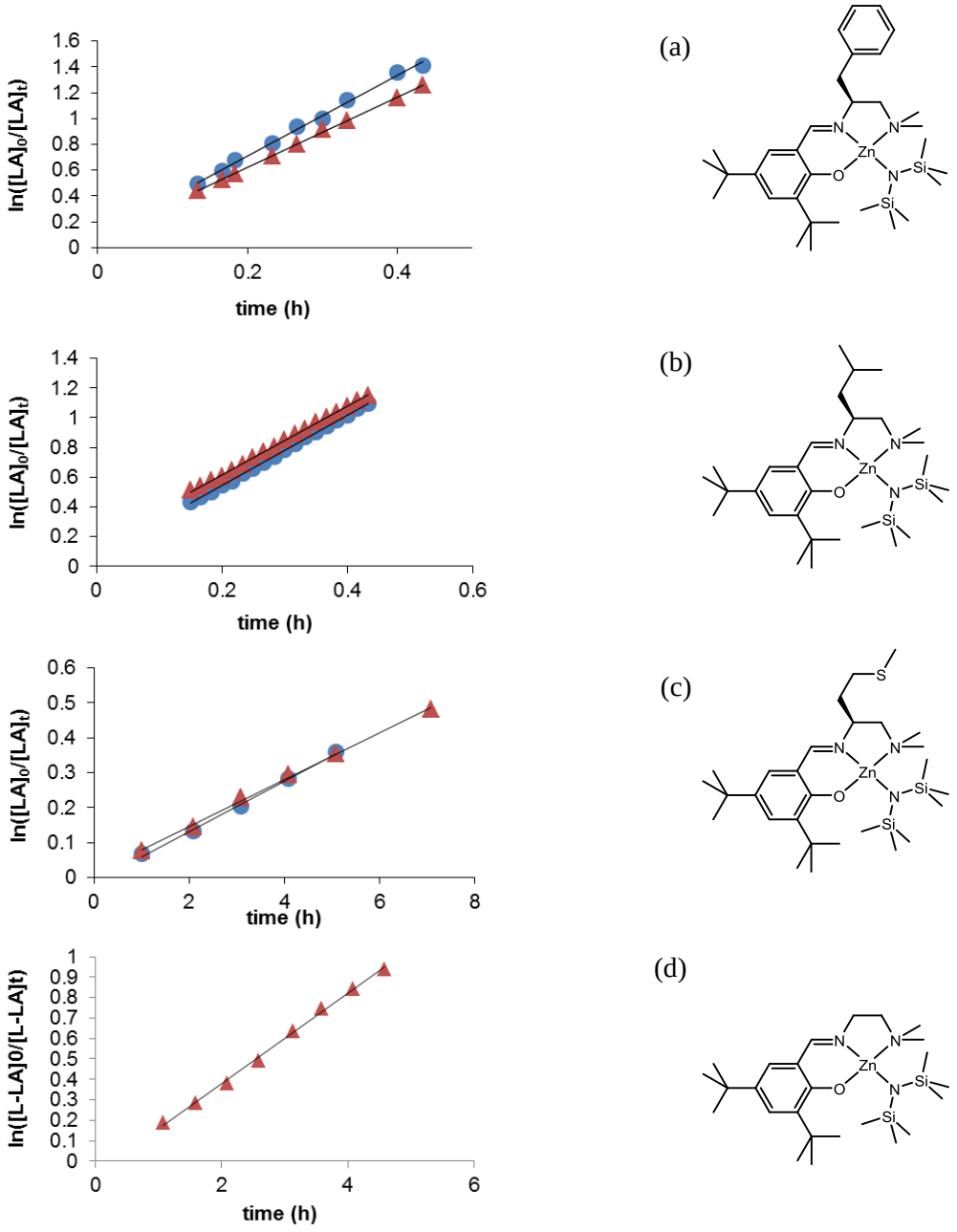

Figure II-3. $\ln([La]_0/[La]_t)$ *vs* time plots for the ROP of D-lactide(●) or L-lactide(▲) catalyzed by various zinc complexes at ambient temperature. (a) complex **II6a**, (b) complex **II6b, (c)** complex **II6c**, and (d) complex **II6d**.

Table II-2. Rate Constants for the ROP of D- or L-Lactide in the Presence of Zinc Complexes.[a]

entry	M	$k_{D(obsd)}$ h^{-1})	$k_{L(obsd)}$ (h^{-1})	k_D / k_L
1	**II6a**	3.13	2.73	1.14
2	**II6b**	2.38	2.30	1.03
3	**II6c**	0.07	0.06	1.16
4	**II6d**		0.22	
5	**II6e**		0.20[b]	

[a] Each reaction was performed in C_6D_6 at ambient temperature. Monomer and catalyst concentration were held constant at 0.34 M and 0.0069 M respectively. The k_{obsd} values were determined by the slope of the plots of $\ln([LA]_0/[LA]_t)$ *vs* time. [b] Linear portion of plot which occurs after 5 hours.

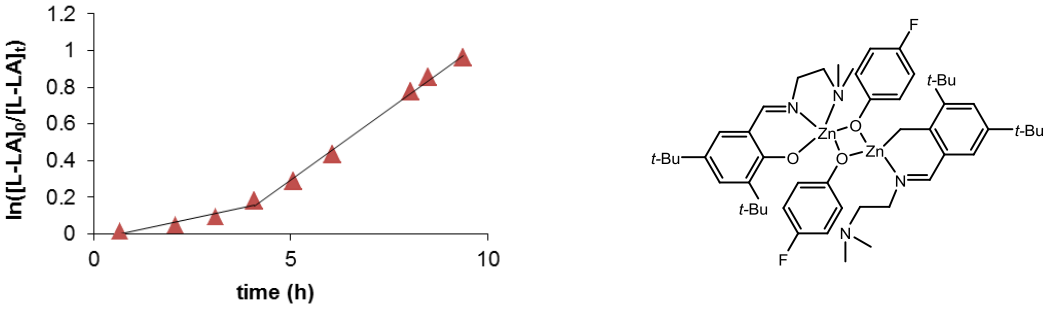

Figure II-4. $\ln([LA]_0/[LA]_t)$ *vs* time plot for the ROP of L-lactide by the dimeric complex **II6e** at ambient temperature.

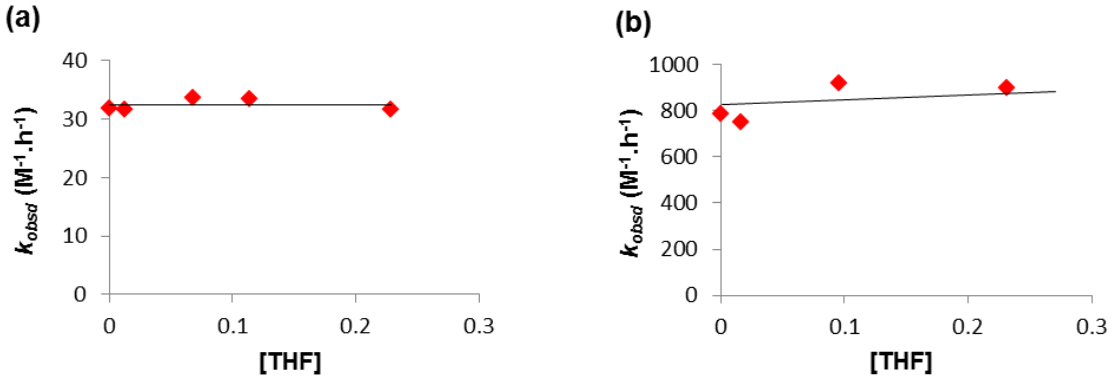

Figure II-5. Independence of the rate constant for the ROP of L-lactide on the THF concentration in C_6D_6 at ambient temperature. (a) Complex **II6a** as catalyst, (b) complex **II6d** as catalyst.

The rates of ROP of L-lactide in the presence of complex **II6a** or **II6d** were found to be independent of the addition of tetrahydrofuran (THF) to the benzene solvent. Figure II-5 illustrates the lack of influence of significant concentrations of THF on k_{obsd} at ambient temperature for either of the catalyst systems. This is to be contrasted with comparable calcium complexes which were shown to be more active upon addition of the coordinating THF solvent.[40d] That is, in this instance the larger calcium center is better able to expand its coordination number, thereby enhancing the nucleophilicity of the propagating chain end.

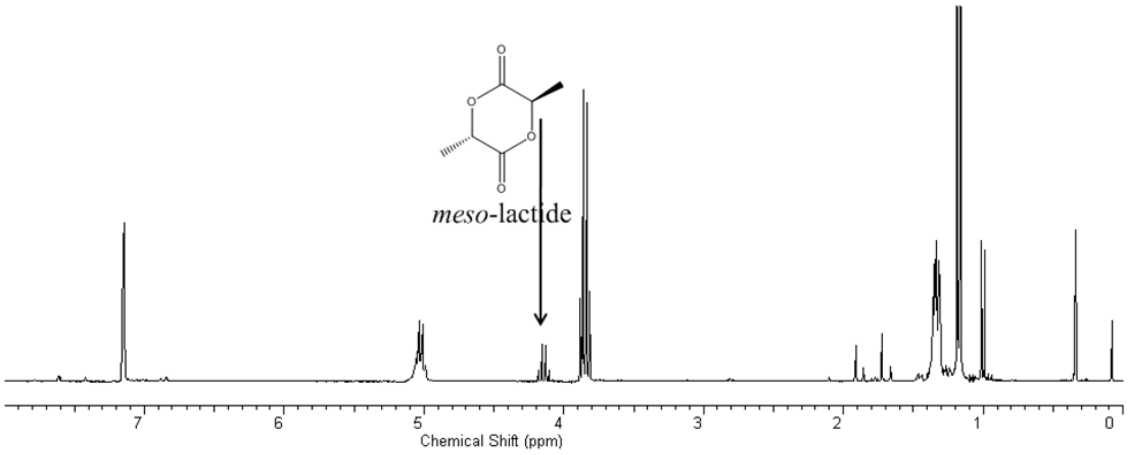

Figure II-6. ^{1}H NMR spectrum in C_6D_6 during the ROP of L-lactide in the presence of complex **II6d** at ambient temperature. Methine proton of *meso*-lactide observed at 4.15 ppm.

As noted in Table II-2 and Figure II-3d, the rate of ROP of L-lactide for complex **II6d** is slower than its more sterically hindered analogues, complexes **II6a** and **II6b**.

Another differentiating feature noted for the ROP of L-lactide in the presence of complex **II6d** is seen in the ^{1}H NMR spectra in C_6D_6 (Figure II-6) during the catalytic reaction. That is, a methine proton resonance at 4.15 ppm is observed which corresponds to a *meso*-lactide, indicating that epimerization of the lactide monomer occurs during the polymerization process. This is further seen in the ROP of L-lactide catalyzed by complex **II6d** where the anticipated isotactically pure polylactide exhibits small defects in microstructure as shown in Figure II-7a. With the other closely related, but sterically more encumbered catalysts, complexes **II6a-c**, this isomerization process is not observed as illustrated by the ^{1}H NMR spectrum of the polylactide in Figure II-7b. In the case of complex **II6c**, the sulfur atom from the amine backbone possibly coordinates to the zinc center following dissociation of the dimethylamine arm resulting in the slowest rate of catalysis for all the complexes (*vide infra*).

The ROP of *rac*-lactide catalyzed by complexes **II6a-d** was performed in chloroform at ambient temperature. The resulting polylactides were isolated and purified by precipitation from CH_2Cl_2 with 5% HCl in methanol followed by drying in vacuo. The molecular weights and polydispersity indices of the purified polymers were determined by gel permeation chromatography (dual RI and light scattering detectors) in THF using polystyrene as a standard. These experimental findings indicate that the polymerization process is well-controlled (Table II-3). The living character of the process can be noted by the low polydispersites over the range of 1.05−1.07, and the linear relationship between M_n and the monomer/initiator ratio as depicted in Figure II-8.

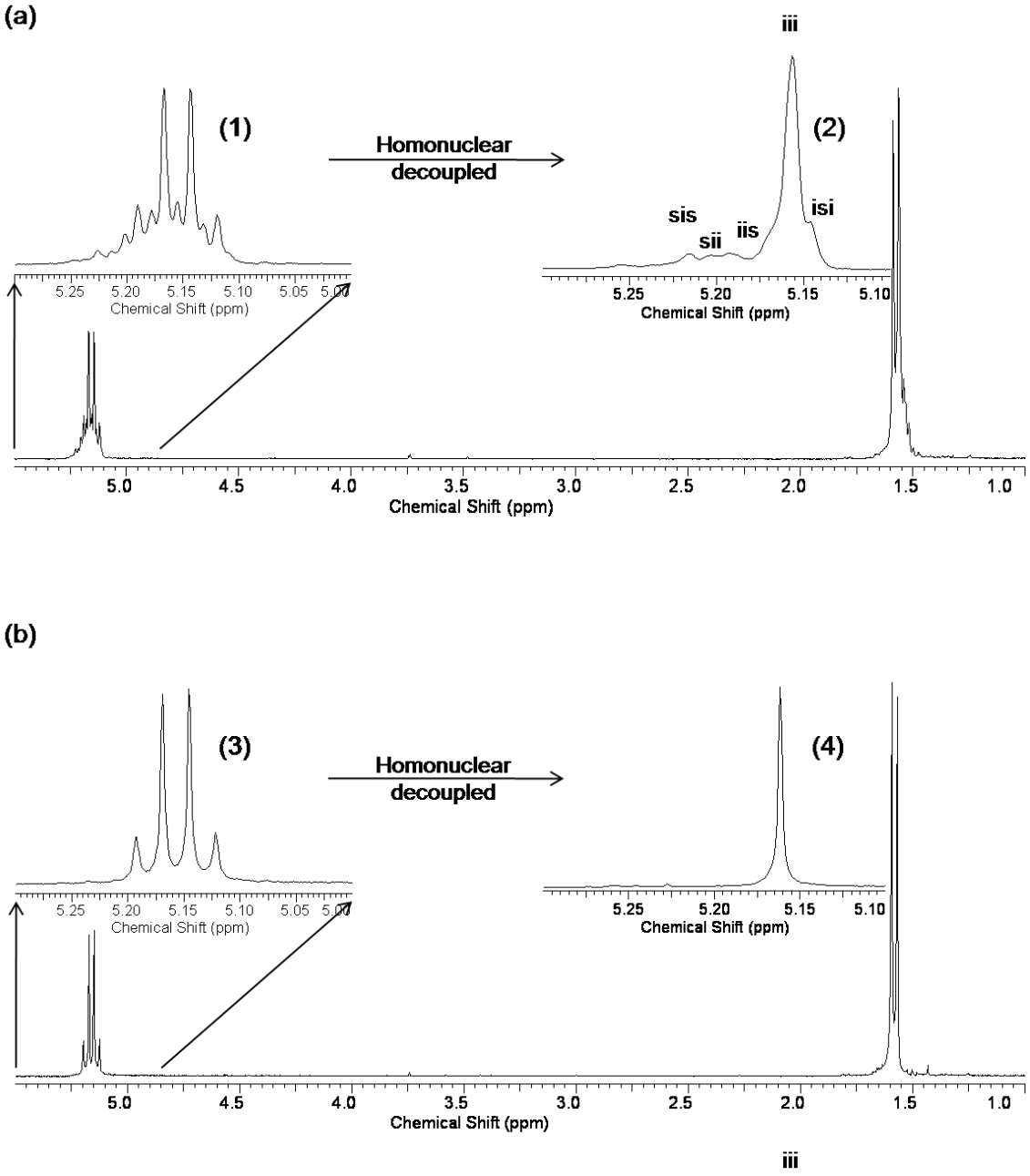

Figure II-7. ^{1}H NMR spectra of polylactide in $CDCl_3$ prepared from L-lactide. (a) In the presence of complex **II6d**, with **1→2** illustrating expanded methine region before and after homonuclear decoupling. (b) In the presence of complex **II6a**, with **3→4** illustrating expanded methine region before and after homonuclear decoupling.

Table II-3. Polylactides Produced from the ROP of *Rac*-lactide in Chloroform at Ambient Temperature.

entry	Complex	M/I	Conversion (%)[a]	M_n Theoretical[b]	M_n GPC	M_n $0.58M_{n,GPC}$[c]	PDI
1	**II6a**	50	97	6 990	8 630	5 000	1.08
2	**II6a**	300	96	41 509	96 191	55 790	1.05
3	**II6a**	700	96	96 855	181 730	105 400	1.08
4	**II6a**	1000	96	138 782	285 108	165 360	1.05
5	**II6a**	2000	96	279 612	530 141	307 480	1.07
6	**II6b**	50	98	7 062	8 161	4 730	1.31
7	**II6c**	50	95	6 846	8 757	5 080	1.31
8	**II6d**	50	98	7 062	8 171	4 740	1.13
9	**II6e**	50	97	6 990	8 056	4 672	1.07

[a] Obtained from ^{1}H NMR spectroscopy. For entries 1 and 6 the reaction times were 2 hours, all other reactions were carried out for 24 hours. [b] Theoretical M_n = (M/I) x (% conversion) x (mol. wt. of lactide). [c] M_n values corrected by the equation: $M_n = 0.58M_{n,GPC}$.[51]

As previously mentioned the physical and degradation properties of polylactides are intimately dependent on the tacticity of the polymer. Herein we have examined the tacticity of the polymers resulting from the ROP of *rac*-lactide as catalyzed by the series of zinc derivatives, since the ligand's architecture is expected to play a major role in stereoselectivity.[36g, 52] Complexes **II6a-d** were evaluated for the ROP of *rac*-lactide in $CHCl_3$ at various temperatures, and the afforded polymers' tacticities were assigned using the methine proton regions with homonuclear decoupling as described by Hillmyer and co-workers.[11]

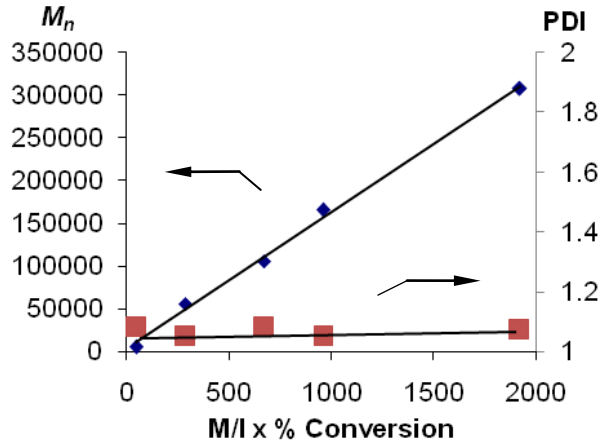

Figure II-8. Linear relationship observed between M_n and monomer/initiator ratio of polylactide produced from *rac*-lactide catalyzed by complex **II6a** at ambient temperature in $CHCl_3$.

P_r values were calculated from the ratio of the (area of isi and sis)/(total area in methine proton region) from the decoupled ^{1}H NMR spectra shown in Figure II-9. As illustrated in Figures II-9 and Table II-4, complex **II6c** produced the highest degree of heterotacticity in the polylactide produced from *rac*-lactide with a P_r = 0.83 at ambient temperature which increases to 0.89 at −30 °C. By way of contrast, the least sterically hindered zinc derivative, complex **II6d**, provided polylactide with the lowest degree of heterotacticity (P_r = 0.68 at ambient temperature). In this latter instance, decreasing the polymerization temperature to −30 °C provided a P_r value of 0.87. Since the chiral center in complexes **6a-c** did not exhibit any selectivity in the ROP of L- or D-lactide, we suggest that the stereoselectivity in the polymerization of *rac*-lactide occurs via a chain-end mechanism.[39t] Because the steric bulk of the ligands in complexes **II6a** and **II6b** is rather remote relative to the metal center, this rate effect may be due to a more facile dissociation of the dimethylamine arm during the polymerization process

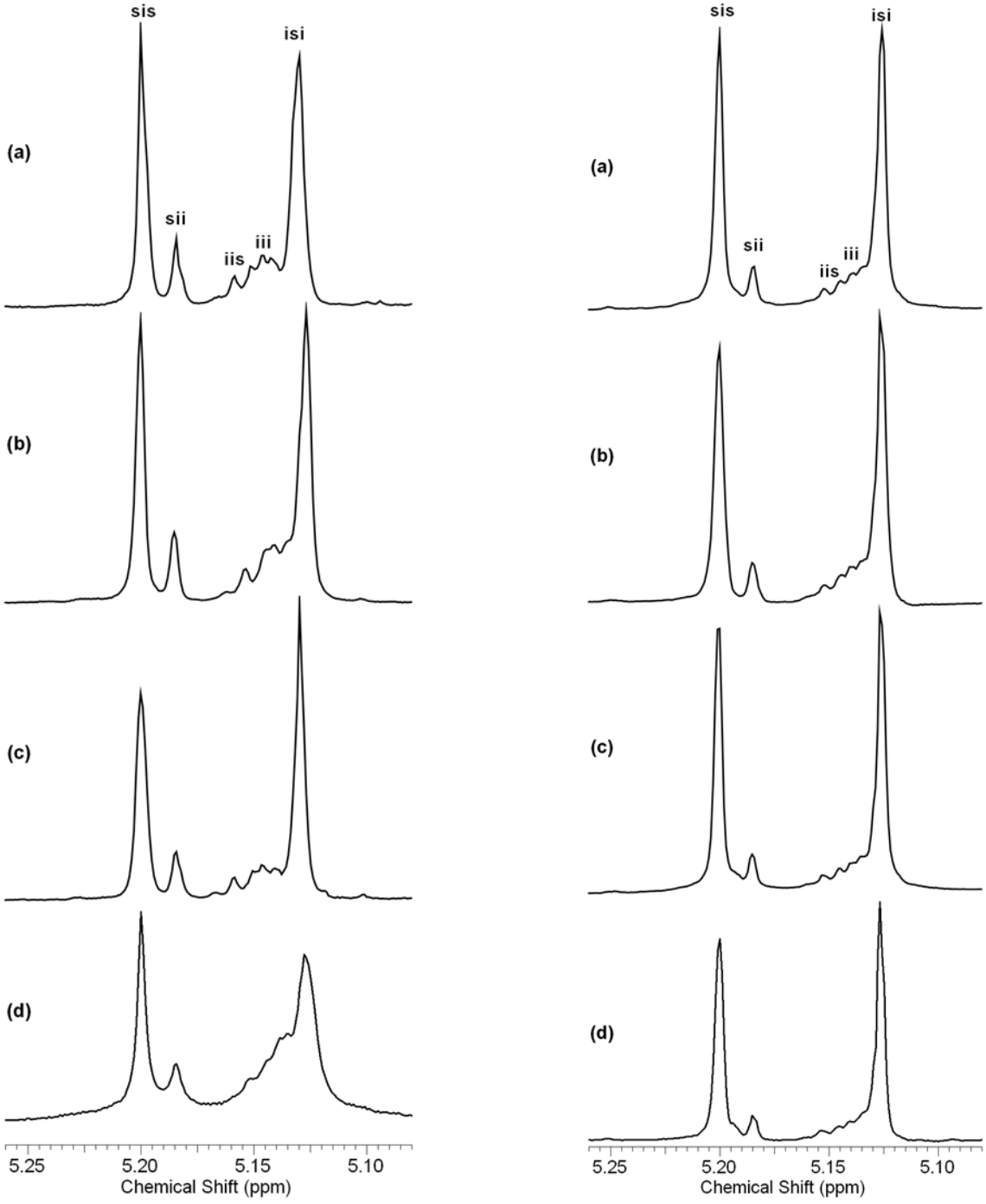

Figure II-9. Homonuclear decoupled ^{1}H NMR ($CDCl_3$, 500 MH_3) spectra of the methine region of polylactide produced from *rac*-lactide with catalyst (a) **II6a**, (b) **II6b**, (c) **II6c**, and (d) **II6d**. **A.** Polymerization temperature ambient. **B.** Polymerization temperature -30 ^{o}C.

involving these catalysts. Indeed, Mehrkhodavandi and co-workers have shown in related diamino-phenol zinc complexes that the dimethylamine arm of the ligand is hemilabile.[43s] To examine this possibility, we carried out an experiment where 6 equiv of 2-methylcyclohexanone were added to complex **II6d** in C_6D_6. As seen in Figure II-10, ^{1}H NMR spectroscopy reveals a significant portion of the complex showed the dimethylamine arm free with presumably concomitant binding of the ketone to the metal center via the oxygen donor. This binding would closely mimic the coordination of the lactide monomer to the zinc center. This reaction pathway would also account for the greatly reduced activity and highest heterotacticity exhibited by complex **II6c** which contains the methylthio group. Nevertheless, inconsistent with an amine dissociation mechanism and lactide ROP reactivity is the observation that complex **II6d** in the presence of excess THF exhibited a similar amine lability (Figure II-11). However, as noted in Figure II-5 the addition of THF did not inhibit the ROP of L-lactide.

Table II-4. P_r Values of Poly(*Rac*-Lactide) at Different Temperature.[a,b]

Complex	P_r at -30 ^{o}C	P_r at 0 ^{o}C	P_r at 22 ^{o}C
II6a	88	81	76
II6b	85	80	76
II6c	89	86	83
II6d	87	79	68

[a] Each reaction was performed in $CHCl_3$ at different temperatures. [b] P_r values were calculated from the ratio of the (area of isi and sis)/(total area in methine proton region).

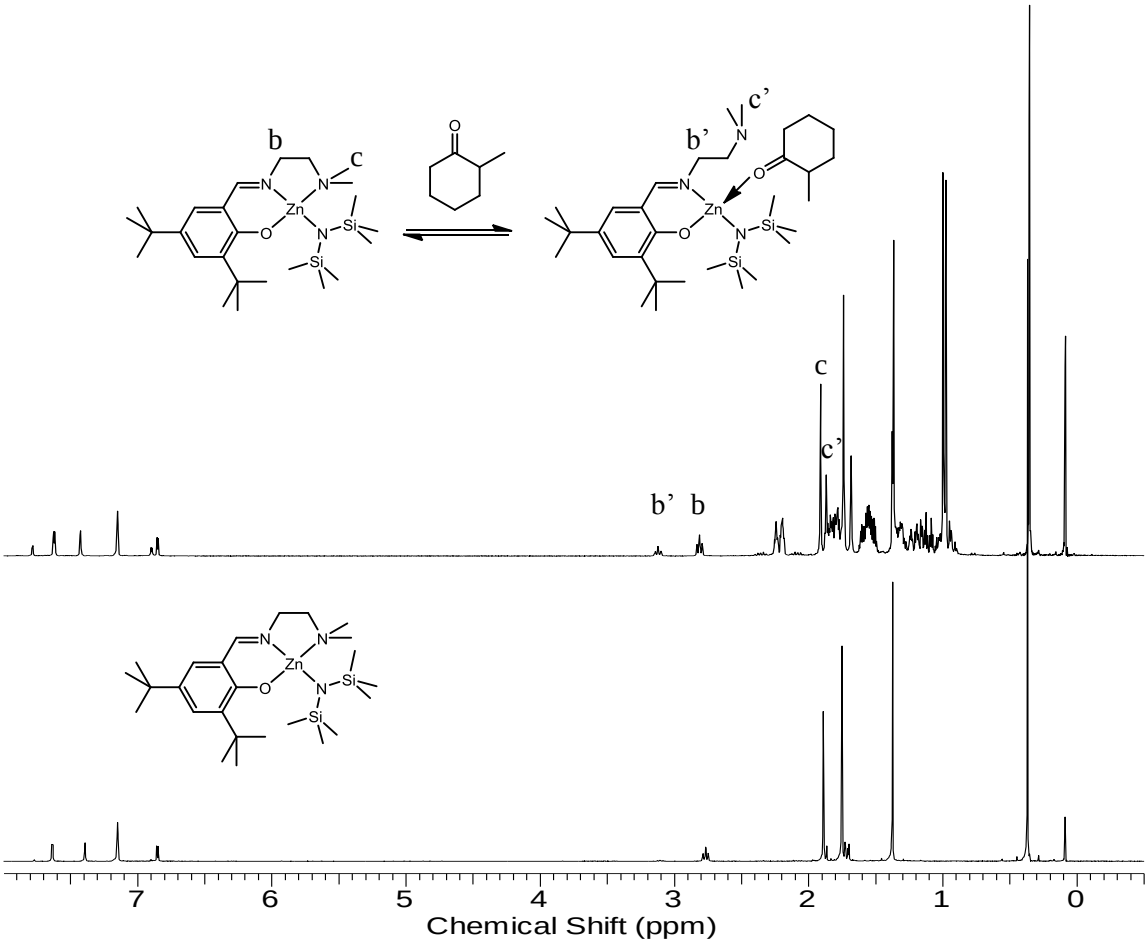

Figure II-10. ^{1}H NMR spectrum (C_6D_6, rt) of **II6d** before addition of 2-methylcyclohexanone (bottom) and 15 min after addition of 6 equiv of 2-methylcyclohexanone (top).

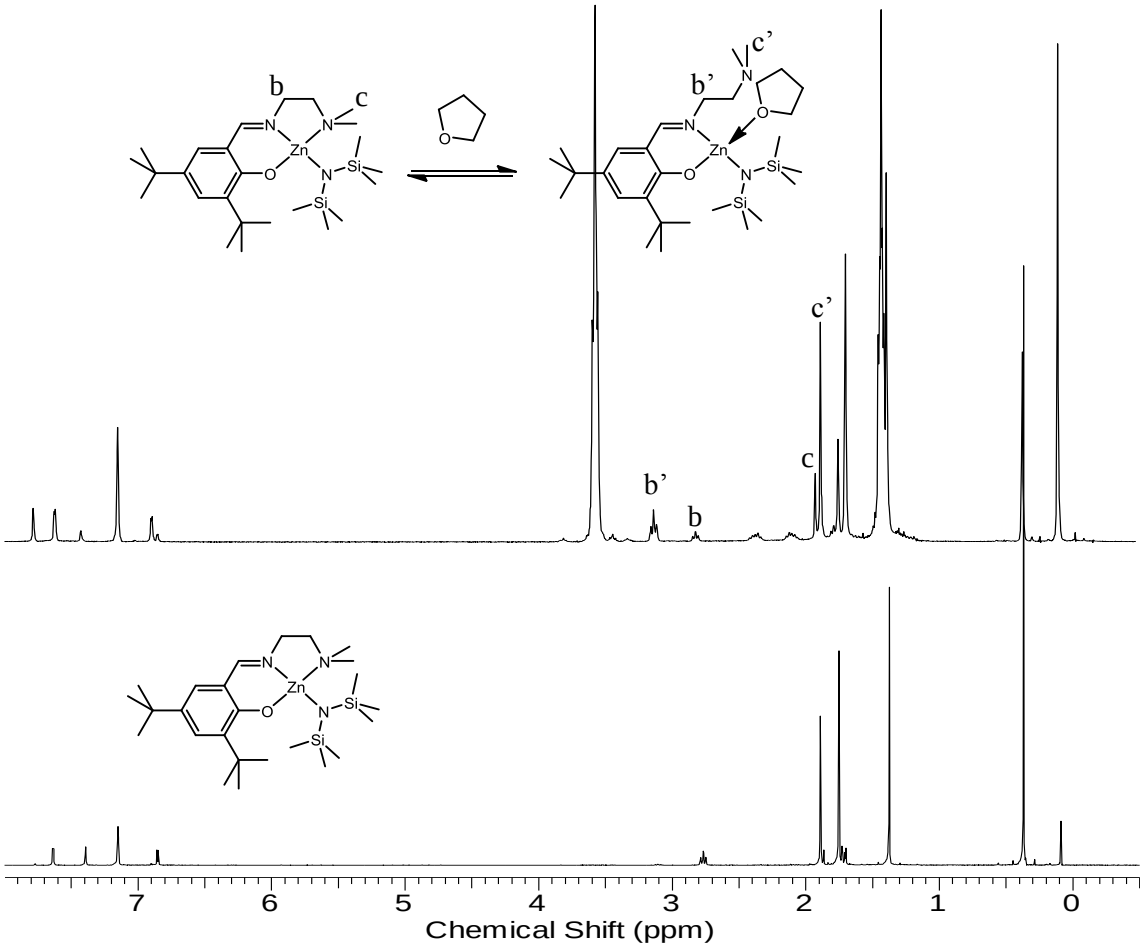

Figure II-11. ^{1}H NMR spectrum (C_6D_6, rt) of **II6d** before addition of THF (bottom) and 15 min after addition of 10 equiv of THF (top).

A point worthwhile noting regarding the measurement of P_r values from ^{1}H NMR peak areas is that the relative peak areas presented in Table II-4 were measured multiple times with a planimeter.[53] In general, we have observed this method provides lower P_r values than those routinely determined by programs provided for deconvolutions by NMR software providers. For example, complex **II6c** gave a P_r value of 0.89 at −30 °C for the polylactide produced from *rac*-lactide, whereas the FIT

deconvolution program provided by Varian Instruments yielded a value of 0.98. Hence, we conclude that P_r values determined by this latter technique overestimate the heterotacticity of the thus formed polylactide.

The dependence of the thermal properties on the tacticity of the polylactides synthesized can be readily gleamed from the DSC measurements listed in Table II-5. As is readily seen in Table II-5, the isotactically pure polylactide afforded from the ROP of L-lactide by complex **II6a** is highly crystalline and possesses a T_g value of 60 °C, with T_c and T_m values of 90 and 178 °C, respectively. On the other hand, the heterotactically enriched polymers provided by complexes **II6a** and **II6c** from the ROP of *rac*-lactide exhibited T_g parameters which increased with increasing P_r values. That is, complex **II6a** which gave a polymer with a P_r value of 0.76 has a T_g of 39 °C, and complex **II6c** which provided a polymer with a P_r of 0.89 has a T_g of 50 °C. Crystal data and details of the data collection for complexes **II6a**-**6e** are provided in Table II-6 and Table II-7.

Table II-5. Physical and Thermal Properties of Polylactides.

Complex	M/I	Lactide	Tacticity	M_n	Decomposition Temp. (^{o}C)	T_g[a] (^{o}C)	T_c[a] (^{o}C)	T_m[a] (^{o}C)
II6a	50	L-lactide	Isotactic	N/A[b]	300	60	90	178
II6a	50	*rac*-lactide	Hetero(P_r=0.76)	8630	300	39	-	-
II6c	50	*rac*-lactide	Hetero(P_r=0.89)	8760	300	50	-	-

[a]Determined from second heating run. [b]Molecular weight was not measured because of polymer's insolubility in THF due to its high crystallinity.

Table II-6. Crystallographic Data for Complexes **II6a-b**.

	II6a	**II6b**
empirical formula	$C_{32}H_{55}N_3OSi_2Zn$	$C_{58}H_{114}N_6O_2Si_4Zn_2$
fw	619.34	1170.65
temperature (K)	150(2) K	110(2) K
crystal system	orthorhombic	monoclinic
space group	P(2)1(2)1(2)1	P2(1)
a(Å)	8.719(4)	10.616(3)
b(Å)	16.535(8)	18.225(4)
c(Å)	24.901(12)	17.992(4)
α(deg)	90	90
β(deg)	90	91.995(13)
γ(deg)	90	90
V(A^o)	3590(3)	3478.7(14)
D_c(Mg/m^3)	1.146	1.118
Z	4	2
abs coeff(mm^{-1})	0.777	1.805
reflections collected	32055	27837
independent reflections	7063 [*R*(int) = 0.1231]	9520 [*R*(int) = 0.0627]
data/restrains/parameters	7063/4/373	9520/4/694
GOF on F^2	1.014	1.077
final *R* indices	R_1 = 0.0539	R_1 = 0.0402
[$I > 2\sigma(I)$]	R_w = 0.1190	R_w = 0.0963
final *R* indices	R_1 = 0.0779	R_1 = 0.0515
(all data)	R_w = 0.1299	R_w = 0.1030

Table II-7. Crystallographic Data for Complexes **II6c-e**.

	II6c	**II6d**	**II6e**
empirical formula	$C_{33}H_{67}N_3OSSi_2Zn$	$C_{55}H_{108}N_6O_2Si_4Zn_2$	$C_{50}H_{70}F_2N_4O_4Zn_2$
fw	675.51	1128.57	959.84
temperature (K)	110(2) K	110(2) K	110(2) K
crystal system	monoclinic	monoclinic	monoclinic
space group	P2(1)	P2(1)/c	P2(1)/n
a(Å)	15.315(7)	13.530(5)	12.128(12)
b(Å)	10.089(5)	23.298(5)	21.45(2)
c(Å)	26.190(13)	10.488(5)	20.25(2)
α(deg)	90	90.000(5)	90
β(deg)	104.946(6)	99.190(5)	105.529(12)
γ(deg)	90	90.000(5)	90
V(A^o)	3910(3)	3264(2)	5074(9)
D_c(Mg/m^3)	1.148	1.148	1.257
Z	4	2	4
abs coeff(mm^{-1})	0.770	0.848	0.997
reflections collected	44430	22528	48125
independent reflections	17705 [*R*(int) = 0.0242]	4681 [*R*(int) = 0.1202]	11309 [*R*(int) = 0.0242]
data/restrains/parameters	17705/44/818	4681/2/337	11309/0/575
GOF on F^2	1.032	0.965	1.036
final *R* indices	R_1 = 0.0347	R_1 = 0.0756	R_1 = 0.0932
[$I > 2\sigma(I)$]	R_w = 0.0899	R_w = 0.1935	R_w = 0.2505
final *R* indices	R_1 = 0.0408	R_1 = 0.1165	R_1 = 0.1435
(all data)	R_w = 0.0927	R_w = 0.2405	R_w = 0.3180

Summary Remarks

Herein we have reported a new series of well-characterized chiral tridentate Schiff base ligands and their zinc complexes. The complexes are shown to be active toward the ROP of lactide. The polymerization processes appear to be living systems as depicted by a linear relationship between M_n and % conversion, as well as, a low polydispersity index. Experimental results revealed that enantiomeric pure complexes did not preferably polymerize one enantiomer over the other as is evident from the ratios of $k_{d(obsd)}/k_{l(obsd)}$ being close to 1 for all catalysts investigated. However, the substituent of the chiral tridentate Schiff base ligands played a major role in producing heterotactic polylactide from *rac*-lactide, and it was shown that complex **II6c** produced the highest degree of heterotactic polylactide with P_r values of 0.83 and 0.89 at ambient and −30 °C, respectively. As might be anticipated, the T_g of the heterotactic polylactides increased significantly as the degree of heterotacticity increased.

CHAPTER III

RING-OPENING POLYMERIZATION OF L-LACTIDE AND ε-CAPROLACTONE UTILIZING BIOCOMPATIBLE ZINC CATALYSTS: RANDOM COPOLYMERIZATION OF L-LACTIDE AND ε-CAPROLACTONE*

Introduction

Polylactide, poly(ε-caprolactone), and their copolymers are among the most widely used polymeric materials in medical and pharmaceutical applications due to their physical properties and nontoxicity to humans. Biodegradable sutures, artificial skin, resorbable prostheses, and controlled drug release[54] are examples of the applications of these polymeric materials, since these copolymers can be metabolized and remove from the body via normal metabolic pathways.[54c, 55] It has been shown that polylactides from *rac*-lactide have shorter half-life (a few weeks) *in vivo* than that of polycaprolactone (one year);[56] in addition, the permeability to drugs of polycaprolactone is higher than polylactide.[54c] The permeability to drugs and biodegradability[2a, 54a, 57] of copolymers of these two monomers can be fine-tuned by the copolymer composition, monomer sequencing, and polymer's molecular weight.[28] Therefore, a number of reports have been focused on producing both random[39u, 56b, 58] and block[39u, 54b, 59] copolymers from

---

* Reproduced in part with permission from Darensbourg, D. J.; Karroonnirun, O. *Macromolecules* **2010**, *43*, 8880-8886. Copyright 2010 American Chemical Society.

lactide and ε-caprolactone to provide copolymers with desirable properties.

While a large variety of metal complexes successfully catalyzes the ring-opening polymerization (ROP) of lactide and ε-caprolactone, it is desirable to use biocompatible metals since polylactides, ε-caprolactone, and their copolymers are widely utilized in biomedical applications. In Chapter II, we have reported the effective use of zinc complexes derived from natural amino acids (Scheme 1) for the ROP of lactides that produces heterotactic polylactide with P_r value up to 0.89.[60] Since ε-caprolactone is expected to undergo the ring-opening polymerization in the same manner as lactide, we have investigated these zinc complexes for the ROP of ε-caprolactone. Our results show that these zinc complexes are active catalysts for the ring-opening polymerization of ε-caprolactone. Included in these studies is the production of copolymers from L-lactide and ε-caprolactone as well as the effect of the monomer composition on the thermal properties of produced polymers.

Experimental Section

Methods and Materials. All manipulations were carried out using a double manifold Schlenk vacuum line under an argon atmosphere or an argon-filled glovebox unless otherwise stated. Toluene was freshly distilled from sodium/benzophenone before use. Methanol and dichloromethane were purified by an MBraun Manual Solvent Purification System packed with Alcoa F200 activated alumina desiccant. Pentane was freshly distilled from CaH_2. Deuterated chloroform and deuterated benzene from Cambridge Isotope Laboratories Inc. were stored in the glovebox and used as received. L-Lactide and *rac*-lactide were gifts from PURAC America Inc. These lactides were

recrystallized from toluene, dried under vacuum at 40 °C overnight, and stored in the glovebox. ε-Caprolactone was distilled under vacuum from CaH_2 and strored on 4A molecular sieves in the glovebox. The zinc complexes **III1a** and **III1b** were synthesized according to our previously reported procedure.[60]

Measurement. ^{1}H NMR spectra were recorded on Unity+ 300 MHz and VXR 300 MHz superconducting NMR spectrometers. Molecular weight determinations were carried out with a Viscotek Modular GPC apparatus equipped with ViscoGEL I-series columns (H + L) and Model 270 dual detector comprised of refractive index and light scattering detectors. DSC measurements were performed with a Polymer DSC by Mettler Toledo. The samples were scanned from -100 to 200 °C under a nitrogen atmosphere. The glass transition temperature (T_g), the crystallization temperature (T_c), and the melting temperature (T_m) of polymers were determined from the second heating at heating rate of 5 °C/min. For these DSC measurements, samples were first heated to 200 °C at a rate of 10 °C/min and cooled to 20 °C for two cycles. The samples were then cooled to -100 °C by liquid nitrogen, followed by heating to 200 °C at a heating rate of 5 °C/min to determine their thermal properties (T_g, T_c, and T_m).

Lactide Polymerization Procedure. In a typical experiment (Table III-1, entry 1), in a glovebox, a Schlenk flask was charged with a solution of complex **III1a** (8.58 mg, 13.87 μmol) in $CHCl_3$ (2 mL) equipped with a magnetic stirring bar. To this solution was added *rac*-lactide (100 mg, 0.69 mmol, 50 equiv). The mixture was stirred at room temperature for 60 min. After a small sample of the crude solution was removed with a syringe to be characterized by ^{1}H NMR spectroscopy, the product was isolated and

purified by precipitation from dichloromethane by the addition of 5% hydrochloric acid in methanol. The polymer was collected and dried under vacuum to constant weight.

Caprolactone Polymerization Procedure. In a typical experiment (Table III-2, entry 1), in a glovebox, a glass ampule equipped with a magnetic stirring bar was charged with complex **III1a** (23.80 mg, 38.48 μmol) and ε-caprolactone (219.65 mg, 1.92 mmol, 50 equiv). The ampule was sealed under vacuum. The reaction mixture was stirred at 110 °C for 60 min. After the reaction mixture was allowed to cool to room temperature, 1 mL of $CDCl_3$ was added to the reaction mixture, and the reaction mixture was analyzed by ^1H NMR spectroscopy. The product was isolated and purified by precipitation from dichloromethane by the addition of 5% hydrochloric acid in methanol. The polymer was collected and dried under vacuum to constant weight.

Copolymerization of L-Lactide and ε-Caprolactone. In a typical experiment (Table on page 53, entry 2), in a glovebox, a glass ampule equipped with a magnetic stirring bar was charged with complex **III1a** (8.58 mg, 13.87 μmol), ε-caprolactone (285.06 mg, 2.49 mmol, 180 equiv), and L-lactide (40 mg, 0.27 mmol, 20 equiv). The ampule was sealed under vacuum. The reaction mixture was stirred at 110 °C for 30 min. After the reaction mixture was allowed to cool to room temperature, 1 mL of $CDCl_3$ was added, and the solution was analyzed by ^1H NMR spectroscopy. The product was isolated and purified by precipitation from dichloromethane by the addition of 5% hydrochloric acid in methanol. The polymer was collected and dried under vacuum to constant weight.

Kinetic Studies. Polymerizations of L-lactide and *ε*-caprolactone using complexes **III1a** and **III1b** were monitored by ^{1}H NMR spectroscopy. L-Lactide or *ε*-caprolactone and the corresponding zinc complex were dissolved in C_6D_6, and the % conversion was investigated from the integration of polymer and monomer signals. The chemical shifts of polylactide are 5.01 (q, H) and 1.32 (d, CH_3), and the chemical shifts of lactide monomer are 3.79 (q, H) and 1.16 (d, CH_3). The chemical shifts of polycaprolactone are 3.94 (2*H*, t, −O−C*H*$_2$−CH$_2$−), 2.09 (2*H*, t, −CH$_2$−C*H*$_2$−C═O), 1.47 (2*H*, m, −C*H*$_2$−), and 1.13 (4*H*, m, −C*H*$_2$−). The chemincal shifts of *ε*-caprolactone are 3.46 (2*H*, t, −O−C*H*$_2$−CH$_2$−), 2.09 (2*H*, t, −CH$_2$−C*H*$_2$−C═O), 1.12 (2*H*, m, −C*H*$_2$−), and 0.98 (4*H*, m, −C*H*$_2$−).

Results and Discussion

Polymerization of L-Lactide and *ε*-Caprolactone. As mentioned earlier, the zinc complexes indicated in Scheme III-1 were shown to be very effective catalysts for the controlled ring-opening polymerization (ROP) of lactides. Since lactides and lactones undergo similar ROP processes via a coordination-insertion mechanism,[43g, 43p, 61] it is of interest to examine the efficiency of these zinc derivatives to catalyze the ROP of *ε*-caprolactone. First, we determined the catalytic activity of complexes **III1a** and **III1b** for the ROP of L-lactide and *ε*-caprolactone under identical reaction conditions. This was achieved by monitoring the polymerization reactions in C_6D_6 at ambient temperature by ^{1}H NMR spectroscopy. Both complexes were found to be active catalysts for the ROP of L-lactide and *ε*-caprolactone, providing polymers with the expected molecular weights and with low polydispersity indices. The polymerization processes

were shown to be first-order in monomer concentrations as depicted in Figure III-1, affording the rate constants summarized in Table III-1. A zinc analogue complex containing a N,N,O ligand where the nitrogen atom is saturated was found to catalyze the ROP of lactide at 25 °C ~20 times faster than complex **1a**, 2.2 $M^{-1}s^{-1}$ *vs* 0.11 $M^{-1}s^{-1}$.[43g]

Scheme III-1

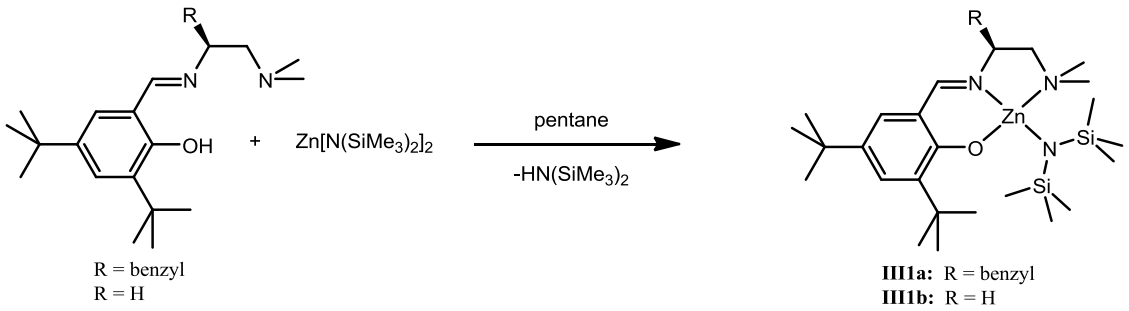

Table III-1. Rate Constants for the ROP of L-Lactide or ε-Caprolactone in the Presence of Zinc Complexes.[a]

entry	M	$k_{\text{L-lactide}}$ ($M^{-1}s^{-1}$)	$k_{\varepsilon\text{-capro}}$ M^{-1}-s^{-1}	$k_{\text{L-lactide}}$ / $k_{\varepsilon\text{-capro}}$
1	**III1a**	0.110 ± 0.005	2.17 ± 0.10 x 10^{-3}	51
2	**III1b**	(8.90 ± 0.12) x 10^{-3}	(2.90 ± 0.10) x 10^{-3}	3

[a] Each reaction was performed in C_6D_6 at ambient temperature. Monomer and catalyst concentrations were held constant at 0.34 M and 0.0069 M respectively. The rate constants were determined from the slope of the plots of $\ln([LA]_0/[LA]_t)$ *vs* time divided by [catalyst].

A

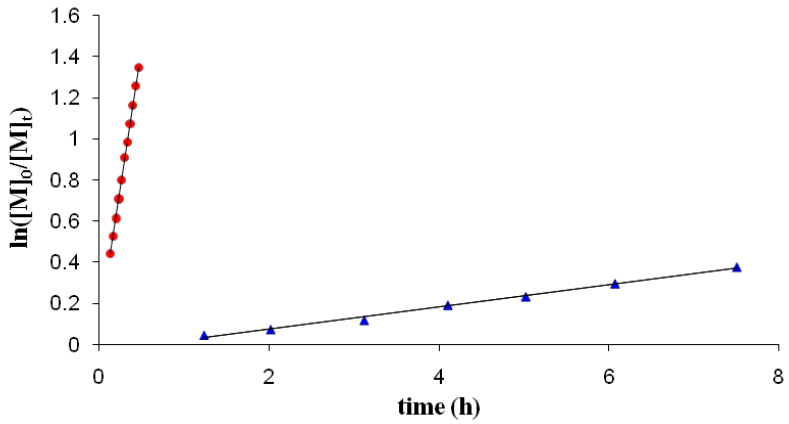

B

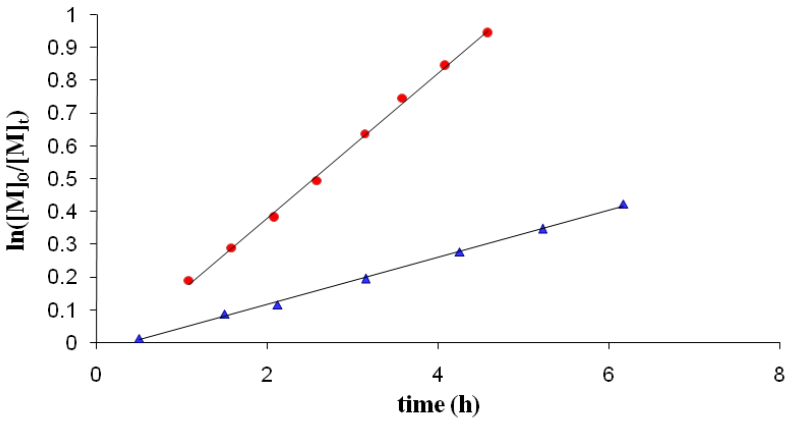

Figure III-1. Plot of $\ln([M]_0/[M]_t$ *vs* time for ROP of L-lactide (red solid circles) or ε-caprolactone (blue solid triangles) catalyzed by the specified zinc complex at ambient temperature. Each reaction was performed in C_6D_6 at ambient temperature. Monomer and catalyst concentrations were held constant at 0.34 and 0.0069 M, respectively. (**A**) Complex **III1a**: the rate constants were determined by the slope of the plots and were found to be 0.110 ± 0.005 $M^{-1}sec^{-1}$ with R^2 = 0.999 for ROP of L-lactide and (2.17 ± 0.10) x 10^{-3} $M^{-1}sec^{-1}$ with R^2 = 0.994 for ROP of ε-caprolactone. (**B)** Complex **III1b**: the rate constants were determined by the slope of the plots and were found to be (8.90 ± 0.12) x 10^{-3} $M^{-1}sec^{-1}$with R^2 = 0.998 for ROP of L-lactide and (2.90 ± 0.10) x 10^{-3} $M^{-1}sec^{-1}$with R^2 = 0.998 for ROP of ε-caprolactone.

As is evident from Figure III-1 as well as Table III-1, complex **III1a** catalyzes the polymerization of L-lactide significantly faster than complex **III1b**, with the ratio of k_{obsd} values determined to be 12.4 at ambient temperature. This behavior has previously been noted for a slightly different set of reaction conditions and was ascribed to sterically bulky substituents on the Schiff base ligands being rate enhancing.[60] However, as depicted in Figure III-2 for overlapping stick structures for the two catalysts as defined by X-ray crystallography, in the solid state the steric impact of the benzyl group appears to be minimal. Hence, the rate enhancement observed may at least in part be due to the electron-donating effect of the benzyl substituent. By way of contrast, the rate constants for the ROP of ε-caprolactone catalyzed by the two zinc complexes were quite similar at 2.17×10^{-3} and 2.90×10^{-3} $M^{-1}s^{-1}$ at ambient temperature. This difference in rates of polymerization of the two monomers may reflect the difference in Lewis basicity of lactides *vs* caprolactone. Even if the Lewis basicities are similar, lactides have two carboxyl groups for potential coordination at the metal center. Another consideration is that the alkoxide resulting from the ring-opening of a caprolactone monomer is a primary alkoxide which should bind to zinc more strongly than the secondary alkoxide afforded from ring-opening lactide, thereby resulting in a slower polymerization process.

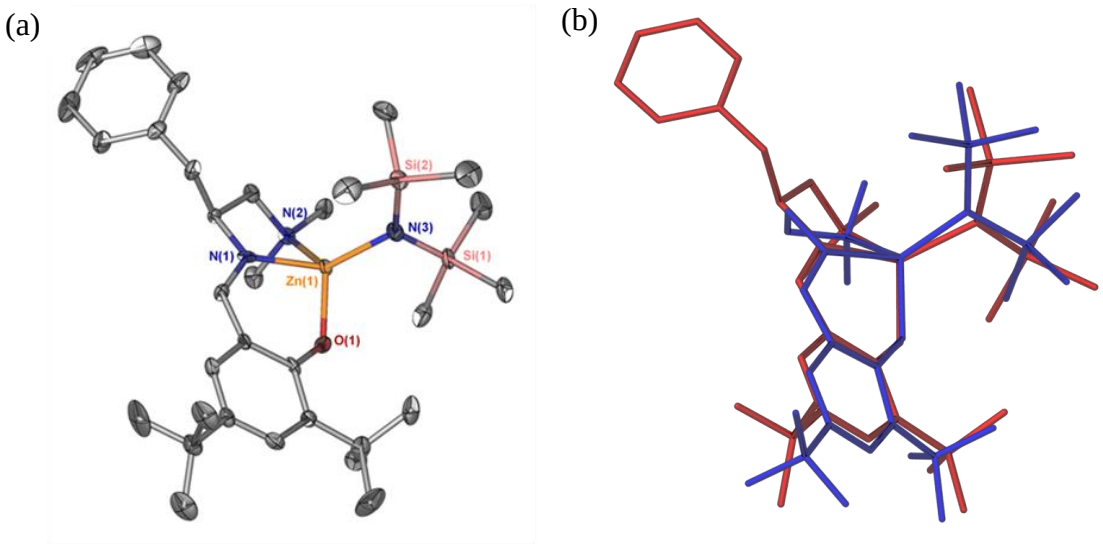

Figure III-2. (a) X-ray crystal structure of complex **III1a**. (b) Stick drawings of complexes **III1a** (red) and **III1b** (blue) obtained for X-ray determined structures.[60]

The preparation of polymer samples of polylactide and polycaprolactone as a function of the monomer-to-initiator ratio was carried out using complex **III1a** as catalyst. The ROP of *rac*-lactide was performed in chloroform at ambient temperature, whereas the ring-opening polymerization of caprolactone was carried out in the melt at 110 °C. The resulting polymers were isolated and purified by precipitation from CH_2Cl_2 with 5% HCl in methanol followed by drying *in vacuo*. Gel permeation chromatography (dual RI and light scattering detectors) using polystyrene as a standard was used to determine the molecular weights and polydispersities of the purified polymers in THF. These experiments revealed that complex **III1a** behaved in a well-controlled manner producing polylactide with narrow PDIs (1.05−1.08) at ambient temperature as shown in Table III-2. Furthermore, the polymerization process displayed a linear correlation between M_n and the monomer/initiator ratio as illustrated in Figure III-3a. A

pseudoliving character for the ROP of ε-caprolactone is seen in the linear relationship between M_n and the monomer/initiator ratio (Table III-3 and Figure III-3b); however, the polydispersity indices are rather broad (1.23−1.56). In addition, the molecular weights of the polycaprolactones were not in agreement with their expected theoretical values. These findings suggest the existence of transesterification occurring during the polymerization process (*vide infra*).

Table III-2. Polylactides Produced from the ROP of *Rac*-Lactide in Chloroform at Ambient Temperature.

			M_n			
entry	M/I	Conversion (%)[a]	Theoretical[b]	GPC	$0.58M_{n,GPC}$[c]	PDI
1	50	97	6 990	8 630	5 000	1.08
2	300	96	41 509	96 191	55 790	1.05
3	700	96	96 855	181 730	105 400	1.08
4	1000	96	138 782	285 108	165 360	1.05
5	2000	96	279 612	530 141	307 480	1.07

[a] Obtained from ^{1}H NMR spectroscopy. For entry 1 the reaction times was 2 hours, all other reactions were carried out for 24 hours. [b] Theoretical M_n = (M/I) x (% conversion) x (mol. wt. of lactide). [c] M_n values corrected by the equation: $M_n = 0.58M_{n,GPC}$.[51]

Copolymerization of L-Lactide and ε-Caprolactone. The random copolymerization of L-lactide and ε-caprolactone was carried out in the melt at 110 °C using complex **III1a** as the catalyst. In order to gain insight into the copolymerization process of these cyclic esters in the presence of this catalytic system, a series of reactions were performed at various molar ratio of L-lactide and ε-caprolactone. These copolymerization were undertaken in sealed ampules stirred at 110 °C for 30 min. The resulting copolymers were purified by precipitation from dichloromethane by the addition of 5% hydrochloric acid in methanol. The copolymers were characterized by ^{1}H and ^{13}C NMR spectroscopy, gel permeation chromatography, and differential scanning

calorimetry. The results of these random copolymerization reactions are summarized in Table III-4.

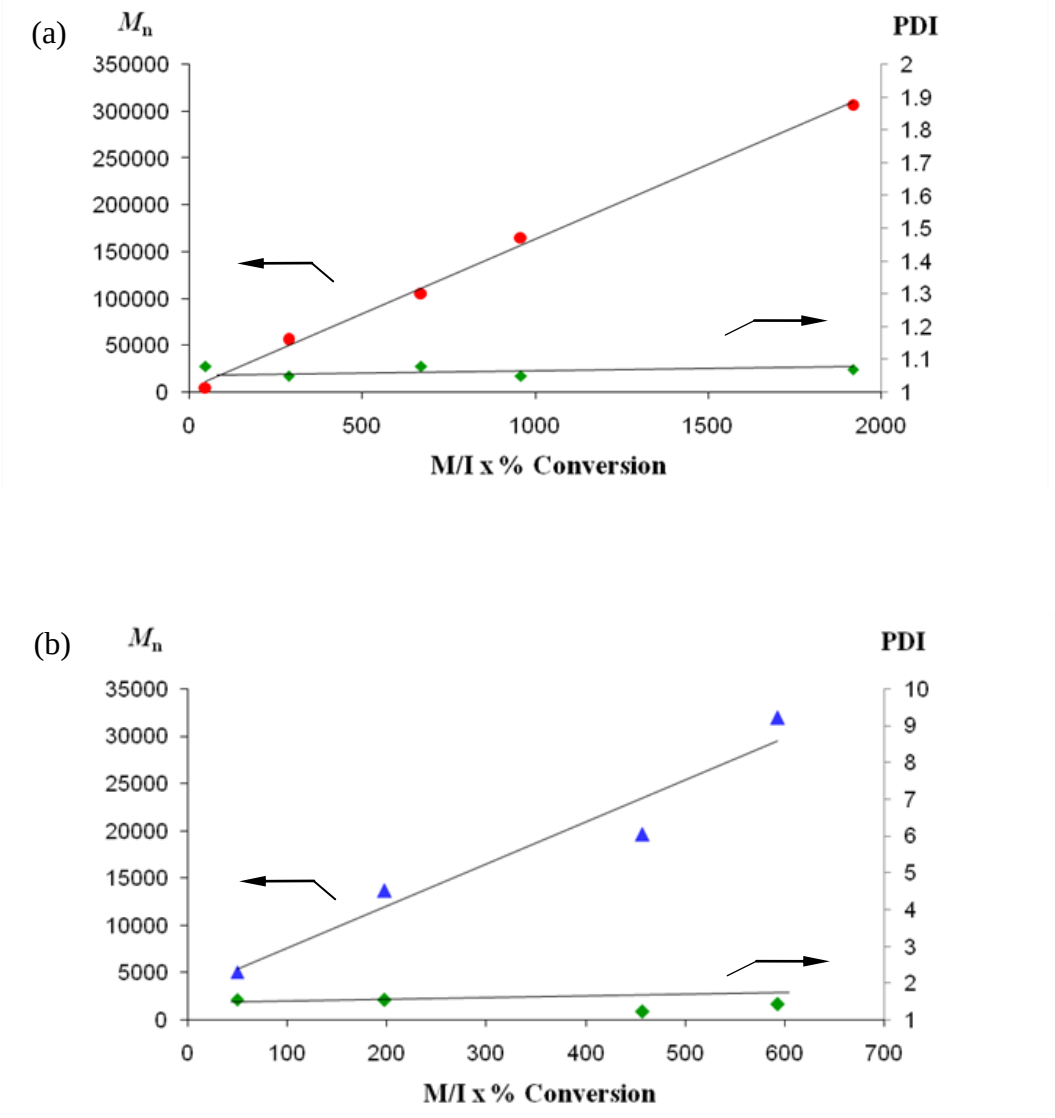

Figure III-3. (a) Linear relationship observed between M_n and monomer/initiator ratio of polylactide from *rac*-lactide catalyzed by complex **III1a** at ambient temperature in $CHCl_3$. (b) Linear relationship observed between M_n and monomer/initiator ratio of polycaprolactone from ε-caprolactone in bulk at 110 ^oC.

Table III-3. Polycaprolactone Produced from the ROP of ε-caprolactone in the melt at 110 ^{o}C.

entry	M/I x monomer conversion	M/I	Conversion (%)[a]	M_n		PDI
				Theoretical[b]	GPC	
1	50	50	100	5 707	5 115	1.56
2	198	200	99	22 828	13 632	1.55
4	460	2000	23	45 656	19 613	1.23
5	595	700	85	67 114	31 887	1.43

[a] Obtained from ^{1}H NMR spectroscopy. The reaction times was 60 mins. [b] Theoretical M_n = (M/I) x (% conversion) x (mol. wt. of ε-caprolactone).

Table III-4. Copolymerization of L-Lactide and ε-Caprolactone with Complex **III1a**.[a]

entry	L-lactide:ε-CL in the feed (mmol); M/I = 200	%conversion		% lactide in the polymer	M_n		PDI
		lactide	CL		Theoritical[b]	GPC	
1	0:100		100	0	22 828	13 632	1.55
2	10:90	98	82	15	19 729	9 253	1.26
3	30:70	98	98	30	24 148	21 341	1.46
4	50:50	99	84	55	23 887	16 330	1.70
5	70:30	98	86	77	26 067	21 062	2.12
6	90:10	99	99	95	28 227	N/A[c]	N/A[c]
7	100:0	99		100	28 828	N/A[c]	N/A[c]

[a] Each reaction was performed in the melt at 110 ^{o}C using complex **III1a** 30 mins: (L-lactide+ε-caprolactone) : complex **III1a** = 200. [b] Theoretical M_n = [(M/I) x (% conversion of L-lactide) x (mol. wt. of L-lactide)] + [(M/I) x (% conversion of ε-caprolactone) x (mol. wt. of ε-caprolactone)]. [c] Molecular weight was not measured because of polymer's insolubility in THF due to its high crystallinity.

The percentage of each monomer incorporated into polymer chains was analyzed by ^{1}H NMR spectroscopy in $CDCl_3$. The methylene signal of polycaprolactone (−COO−CH_2−) is observed around 4.00 ppm, and the methine signal of polylactide (−COO−C*H*CH_3) appears around 5.20 ppm. Experimental observations revealed that the percent of lactide and ε-caprolactone units in the polymer chains corresponded well with the monomer feed ratios. In all the cases, the percent conversion of lactide was 98−99%, while the percent conversion of ε-caprolactone ranged from 82 to 99% (Table III-4). This result correlates with the reactivity of complex **III1a** which displayed a higher

reactivity toward the ROP of L-lactide as discussed earlier. Two additional copolymerization reactions were performed for the 50:50 feed ratio of lactide:CL for shorter reaction times of 8 and 16 min. These runs resulted in 79 and 94% conversions of lactide and 75 and 80% conversions of CL with the percentages of lactide in the copolymers of 51 and 54%, respectively. Hence, these results are not very different from entry 5 which resulted in a copolymer composed of 55% lactide. The dependence of the molecular weights of the copolymers on monomer/initiator ratios was investigated by performing a series of experiments as listed in Table III-5. The experimental results revealed that there is a linear correlation of M_n and monomer/initiator ratio (Figure III-4). All molecular weights of the produced copolymers were lower than their theoretical values, and the polydispersity indices were broad compared to those of their homopolymers.

Table III-5. Molecular Weight of Copolymer Depending on M/I.[a]

entry	M/I (lactide:CL=70:30)	%conversion[b]		% lactide in the polymer[b]	M_n		PDI
		lactide	CL		Theoritical[c]	GPC	
1	100	99	87	73	10 933	8 923	2.50
2	200	98	86	77	22 828	21 062	2.12
3	400	98	54	84	47 754	39 879	2.10
4	800	99	40	90	91 669	N/A[d]	N/A[d]
5	1600	73	20	95	127 191	N/A[d]	N/A[d]

[a] Each reaction was performed in the melt at 110 °C using complex **III1a** for 30 mins. [b] Obtained from ^{1}H NMR spectroscopy. [c] Theoretical M_n = [(M/I0 x (%conversion of L-lactide) x (mol. wt. of L-lactide] + [(M/I) x (% conversion) x (mol. wt. of ε-caprolactone)]. [d] Molecular weight was not measured because of polymer's insolubility in THF due to its high crystallinity.

As illustrated in Table III-4 and Figure III-5, increasing the percentage of L-lactide in the feed from 0 to 100% resulted in the formation of ε-caprolactone and lactide linkages, with the ^{1}H NMR signals for the CL-LA heterodiads resonances increasing.

That is, as seen in Figure III-5a-d, the intensities of the resonances assigned to ε(CL-LA) and α(CL-LA) are increased as the mole ratio of the lactide in the monomer feed increases, indicative of a higher propensity for random copolymerization behavior. In addition, the copolymer's microstructure was assessed by ^{13}C NMR spectroscopy in the carbonyl region of the spectra. Figure III-6 displays the ^{13}C NMR spectrum (a) of a mixture of polylactide and polycaprolactone, with spectra for the random copolymers with increasing lactide compositions in (b) (15%), (c) (30%), and (d) (50%). The ^{13}C NMR carbonyl sequences were assigned according to the reported literature.[62] A ^{13}C NMR resonance at 170.9 ppm corresponds to the carbonyl group of a CapLCap linkage, indicative of transeserification occurring during the copolymerization process.

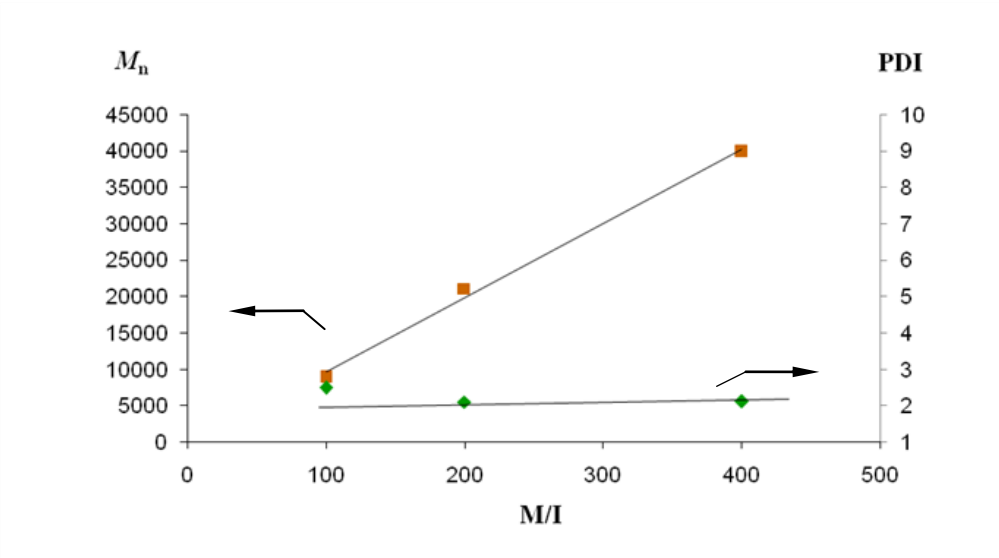

Figure III-4. Linear relationship observed between M_n and monomer/initiator ratio of copolymer from L-lactide and ε-caprolactone catalyzed by complex **III1a** in the melt at 110 ^{o}C.

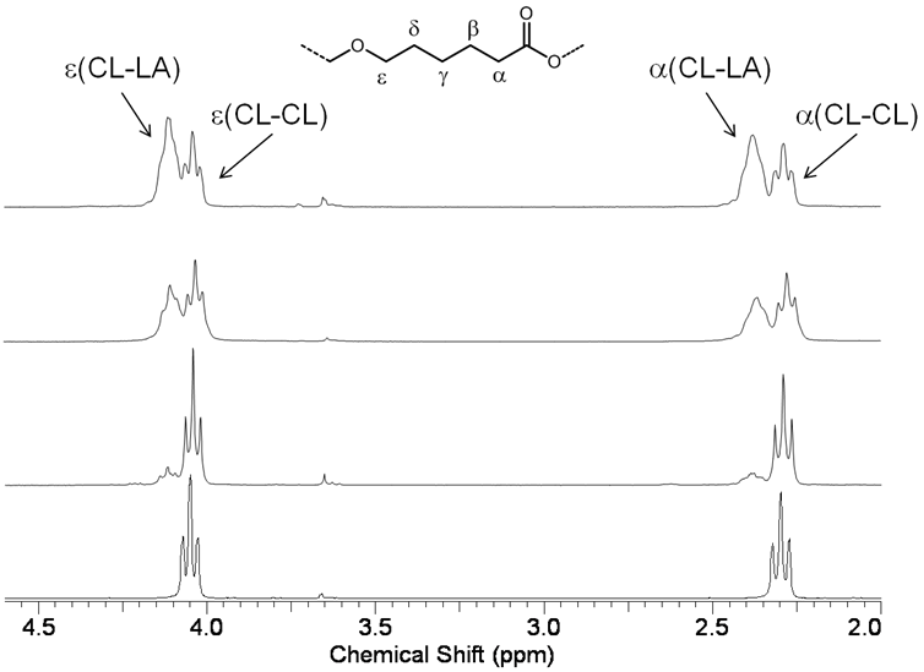

Figure III-5. ^{1}H NMR spectra of the copolymer in $CDCl_3$ at ambient temperature showing the ε- and α-methylene ranges in the copolymers of entry 1 (a), entry 2 (b), entry 3(c), entry 4 (d) from Table III-4.

DSC Studies. The thermal properties of the polymers prepared in this study were measured by differential scanning calorimetry. The thermal parameters are listed in Table III-6 for polylactide, polycaprolactone, and their copolymers. DSC thermograms of the copolymers of varying composition are provided in Figure III-7. As anticipated, the thermal properties for the copolymers are very dependent on the composition of the monomers incorporated in the polymer chains. That is, the T_g of the copolymers increased from −67 °C (pure polycaprolactone) to 60 °C (pure polylactide) as the percent of lactide units in the copolymer increased (Figure III-8). The values calculated from Fox law fit reasonably well with the obtained values listed in Table III-6. The same trend was observed for T_m, as the crystalline units (lactide) increased the T_m increased as noted

in entries 6−10 in Table III-6. By way of contrast, the T_c's of the copolymers decreased with increasing lactide content (entries 7−10).

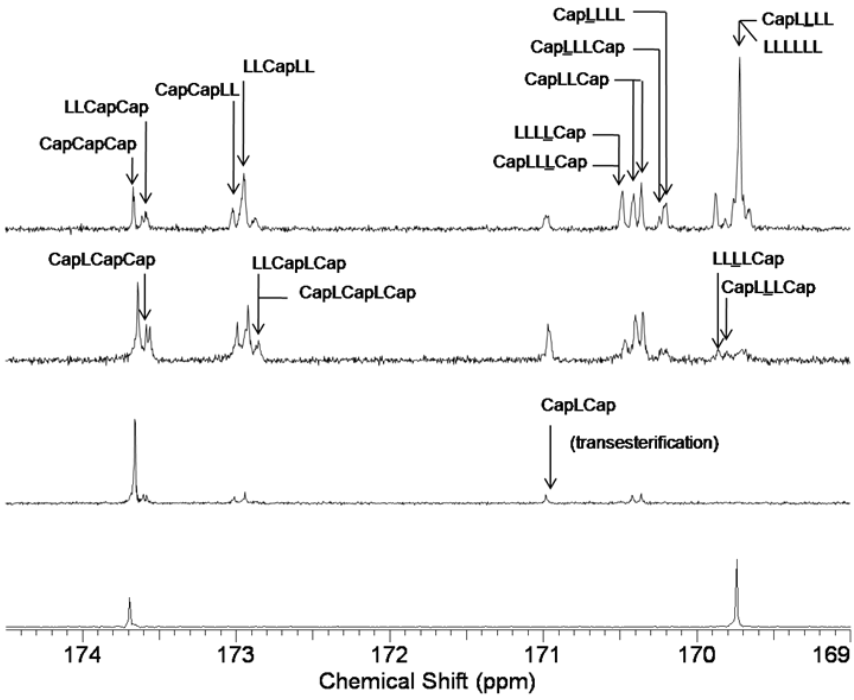

Figure III-6. ^{13}C NMR spectra of the copolymer in $CDCl_3$ at ambient temperature of the mixture of polylactide and polycaprolactone (a), entry 2 (b), entry 3(c), entry 4 (d) from Table III-4.

Table III-6. Thermal Properties of Copolymers of Polylactide and Polycaprolactone.

entry	% lactide in the copolymers[a]	T_g (°C)	T_g[b] (°C)	T_c (°C)	T_m(°C)
1	0	-67	-67	-62	57
2	15	-60	-47	-55	49
3	30	-31	-40	n.d.	49
4	55	9	-24	n.d.	n.d.
5	73	22	12	n.d.	n.d.
6	77	35	19	n.d.	164
7	84	42	30	116	166
8	90	52	41	105	171
9	95	55	50	98	175
10	100	60	60	88	179

[a] Determined by ^1H NMR spectroscopy on purified copolymers. The glass transition temperature (T_g), the crystallization temperature (T_c), and the melting temperature (T_m) of copolymers were determined from the 2nd heating at heating rate of 5 °C/min. [b] Theoretical values calculated by Fox equation according to the literature reported.[58a]

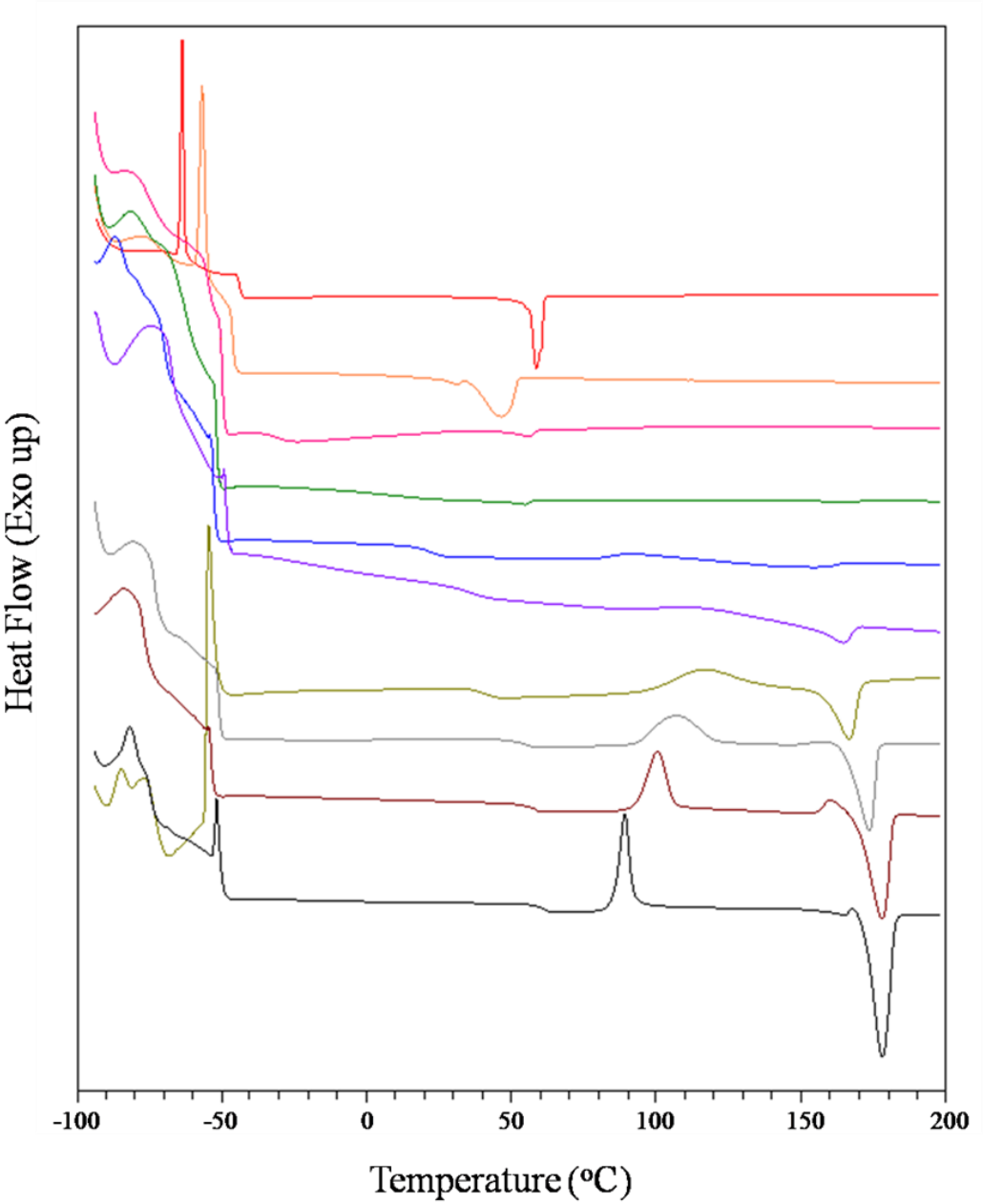

Figure III-7. DSC curves (second heating run) of polymers from table III-5, entries 1-10 from top to bottom.

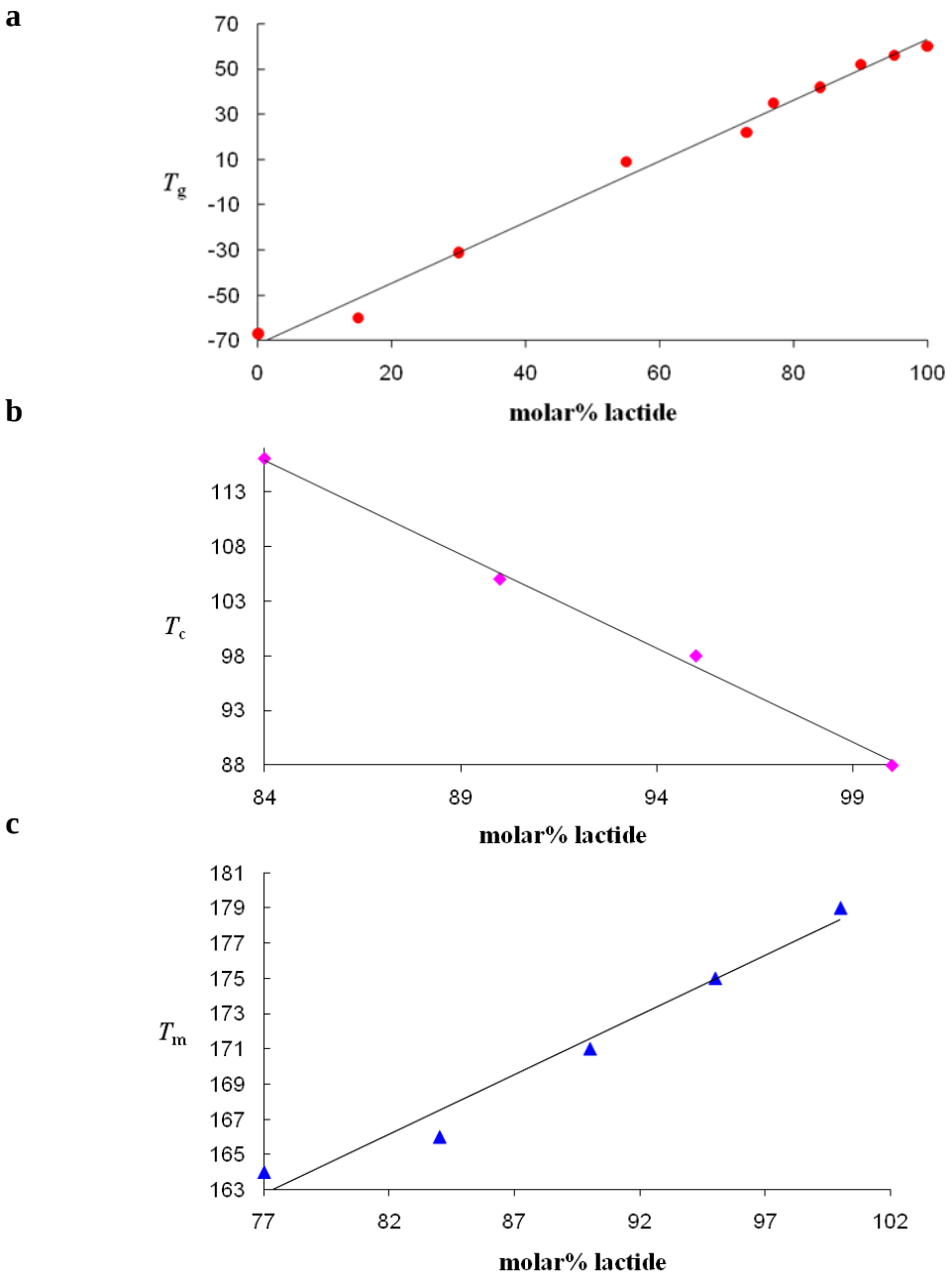

Figure III-8. Plots of the dependence of T_g (**a**), T_c (**b**), and T_m (**c**) of copolymers on the molar % lactide in copolymers.

Summary Remarks

Herein we have reported biocompatible zinc complexes which are effective catalysts for the ring-opening polymerization of L-lactide and ε-caprolactone. The most active catalyst utilized in detailed studies contained a Schiff base ligand derived from the natural amino acid phenylalanine. Although homopolymerization rates in the presence of this initiator of lactide and caprolactone differ significantly in benzene at ambient temperature, the polyester resulting from the copolymerization of equimolar quantity of lactide and caprolactone has a close content of both monomers. That is, copolymerization of L-lactide and caprolactone in the presence of this catalyst in the melt at 110 °C afforded random copolymers of content consistent with the monomer mixture in the feed. This suggests that caprolactone significantly inhibits the reactivity of lactide leading to a matched reactivity of the two monomers during the copolymerization process. Nevertheless, reactions run under these conditions showed evidence of some transesterification occurring during the copolymerization process. Differential scanning calorimetry revealed the thermal properties of the copolymers to be highly dependent upon the monomer compositions. For example, the T_g is adjustable in a linear fashion between −67 and 60 °C by controlling the relative proportions of lactide and caprolactone content. Similar trends were observed in the measured T_c and T_m parameters as a function of monomer ratio in the copolymers.

CHAPTER IV

STEREOSELECTIVE RING-OPENING POLYMERIZATION OF *RAC*-LACTIDES CATALYZED BY CHIRAL AND ACHIRAL ALUMINUM HALF-SALEN COMPLEXES *

Introduction

Polylactides are biodegradable polymers derived from renewable resources such as corn, wheat, and sugar beets.[2a, 20, 38o, 63] These polymeric materials have received much attention over the past decade because of their attractive physical and mechanical properties, which lend them to having numerous applications in medical[6] and microelectronic areas.[64] Of importance, polylactides and various copolymers thereof are readily metabolized in the human body by normal metabolic pathways.[54c] The thermal properties of polylactides are highly dependent on the microstructures of the polylactides. Therefore, researchers have focused their studies on synthesizing stereocomplex polylactides from *rac*-lactide, utilizing catalytic systems which can control the tacticity of the polymers formed. Stereocomplexed polylactides can thereby be produced from a blend of poly-L-lactide and poly-D-lactide which have melting temperatures up to 230 °C.[65]

---

* Reproduced in part with permission from Darensbourg, D. J.; Karroonnirun, O. *Organometallics* **2010**, *29*, 5627-5634.

The use of metal-based catalysts, especially those derived from a biocompatible metal, for the ring-opening polymerization (ROP) of cyclic esters has been the subject of numerous reviews.[6c, 9, 32] Relevant to this topic, in Chapter II, we have reported the ROP of *rac*-lactide using zinc-based half-salen complexes derived from chiral natural amino acids as catalysts.[60] Although these complexes were chiral, our observations revealed these zinc complexes underwent ROP of *rac*-lactide via a chain-end control mechanism to provide heterotactic polylactide.[39t, 66] While chiral ligands bound to active metal centers are typically expected to play a major role in stereoselectivity via an enantiomorphic site control mechanism,[13a, 13b] it is generally not true for the ROP of cyclic esters by zinc-catalyzed systems. Indeed, zinc complexes derived from chiral[38e, 43s, 60, 67] or achiral ligands[21b, 22, 38c, 38l, 43a, 43j, 43l, 43n, 43r, 68] which have been reported in the literature thus far undergo a chain-end control mechanism to produce heterotactic polylactides. On the other hand, chiral[10a, 15, 18, 39b-d, 39o, 65, 69] and achiral[12-13, 17, 39g, 39n, 39r, 39t, 70] complexes of aluminum have shown significant stereocontrol for the ROP of *rac*-lactide to afford polylactides with high degrees of isotactic enrichment. Chisholm and co-workers have shown that, in addition to chiral ligands bound to aluminum, other factors such as the chirality of the alkoxide initiator and solvents can contribute to the stereoselectivity in the ROP of lactides when utilizing aluminum salen catalysts.[18, 39o]

In Chapter IV, we have synthesized and characterized structurally a series of aluminum half-salen complexes containing both chiral and achiral ligands and report some of our preliminary observations on their use as catalysts for the ring-opening polymerization of lactides.

Experimental Section

Methods and Materials. All manipulations were carried out using a double-manifold Schlenk vacuum line under an argon atmosphere or an argon-filled glovebox unless otherwise stated. Toluene was freshly distilled from sodium/benzophenone before use. Methanol and dichloromethane were purified by an MBraun Manual Solvent Purification System packed with Alcoa F200 activated alumina desiccant. Pentane was freshly distilled from CaH_2. Deuterated chloroform and deuterated benzene from Cambridge Isotope Laboratories Inc. were stored in the glovebox and used as received. L- and D-lactide and *rac*-lactide were gifts from PURAC America Inc. These lactides were recrystallized from toluene, dried under vacuum at 40 °C overnight, and stored in the glovebox. 4-Amino-1-butanol and triethylaluminium were purchased from TCI America and Sigma-Aldrich, respectively, and used without further purification. Ethanolamine, 3-amino-1-propanol, 5-amino-1-pentanol, *trans*-2-aminocyclohexanol hydrochloride, 2-hydroxy-3-methoxybenzaldehyde, *rac*-methionine, *rac*-phenylalanine, and *tert*-butyldimethylchlorosilane were purchased from Alfa Aesar and used as received. 3,5-Di-*tert*-butyl-2-hydroxybenzaldehyde and 3-(*tert*-butyldimethylsilyl)-2-hydroxy-5-methylbenzaldehyde were prepared according to the published procedure.[40c, 40d, 48b, 71] All other compounds and reagents were obtained from Sigma-Aldrich and were used without further purification. Analytical elemental analysis was provided by Canadian Microanalytical Services Ltd.

Measurements. ^{1}H NMR spectra were recorded on Unity+ 300 or 500 MHz and VXR 300 or 500 MHz superconducting NMR spectrometers. Molecular weight

determinations were carried out with a Viscotek Modular GPC apparatus equipped with ViscoGEL I-series columns (H + L) and Model 270 dual detector comprised of refractive index and light scattering detectors. DSC measurements were performed with a Polymer DSC instrument by Mettler Toledo. The samples were scanned from −100 to 200 °C under a nitrogen atmosphere. The glass transition temperature (T_g), the crystallization temperature (T_c), and the melting temperature (T_m) of polylatides were determined from the second heating at a heating rate of 5 °C/min. X-ray crystallography was done on a Bruker GADDS X-ray diffractometer under a nitrogen cold stream maintained at 110 K. Crystal data and details of the data collection for complexes **2f** (***cis***) and **2f** (***trans***) are provided in Table on page 93.

General Procedure for Synthesis of Tridentate Schiff Base Ligand IV1a-d. *trans*-2-Aminocyclohexanol hydrochloride (1.1 equiv) and triethylamine (1.09 equiv) were added to the corresponding benzaldehyde (1.0 equiv) in MeOH (30 mL). The solution mixture was heated to reflux overnight, and the solvent was removed under reduced pressure to give a yellow solid. The resulting yellow solid was washed with water (3 × 20 mL) to remove excess *trans*-2-aminocyclohexanol hydrochloride and triethylamine. The organic layer was separated, dried over $NaSO_4$, and concentrated to dryness under reduced pressure to afford the crude products; these were crystallized in pentane to give a yellow powder in 81−95% yield.

(*E*)-2,4-Di-*tert*-butyl-6-(((*trans*-2-hydroxycyclohexyl)imino)methyl)phenol (IV1a; L^1-H). Following the general procedure for synthesis of the tridentate Schiff base ligands **IV1a**−**d**, *trans*-2-aminocyclohexanol (0.711 g, 4.69 mmol, 1.1 equiv) and

triethylamine (0.470 g, 4.65 mmol, 1.09 equiv) were added to 3,5-di-*tert*-butyl-2-hydroxybenzaldehyde (1.00 g, 4.26 mmol, 1.0 equiv) in MeOH (30 mL). The solution mixture was heated to reflux overnight, and the solvent was removed under reduced pressure to give a yellow solid. The resulting yellow solid was washed with water (3 × 20 mL) to remove excess *trans*-2-aminocyclohexanol hydrochloride and triethylamine. The organic layer was separated, dried over $NaSO_4$, and concentrated to dryness under reduced pressure to afford product **IV1a**, which was crystallized in pentane to give a yellow powder in 95% yield. ^{1}H NMR (300 MHz, $CDCl_3$): δ 1.31 (s, 9H, C(C*H*$_3$)$_3$), 1.45 (s, 9H, C(C*H*$_3$)$_3$), 1.35−2.4 (bm, 8H, CH(C*H*$_2$)$_4$CH), 2.99 (m, 1H, NC*H*CH$_2$), 3.69 (m, 1H, OC*H*CH$_2$), 7.12 (d, *J* = 2.38 Hz, 1H, C$_6$*H*$_2$), 7.40 (d, *J* = 2.38 Hz, 1H, C$_6$*H*$_2$), 8.45 (s, 1H, C*H*═N), 13.60 (s, 1H, O*H*). ^{13}C NMR (300 MHz, $CDCl_3$): δ 24.28 (NCHCH$_2$*C*H$_2$CH$_2$), 24.43 (OCHCH$_2$*C*H$_2$CH$_2$), 29.42 (C(^{p}*C*H$_3$)$_3$), 31.47 (C(^{o}*C*H$_3$)$_3$), 32.51 (NCH*C*H$_2$CH$_2$), 32.83 (OCH*C*H$_2$CH$_2$), 34.12 (^{p}*C*CH$_3$), 35.01(^{o}*C*CH$_3$), 73.68 (N*C*HCH$_2$), 75.55 (O*C*HCH$_2$), 117.73, 126.04, 127.06, 136.66, 140.22, 157.97 (Ar), 166.59 (*C*═N). Anal. Calcd for $C_{21}H_{33}NO_2$: C, 76.09; H, 10.03; N, 4.23. Found: C, 75.93; H, 10.13; N, 4.16. HRMS (ESI): *m*/*z* 332.2581 [M + H$^+$], calcd for $C_{21}H_{33}NO_2$ 331.25.

(*E*)-2-(((*trans*-2-Hydroxycyclohexyl)imino)methyl)-6-methoxyphenol (IV1b; L^2-H). Following the general procedure for synthesis of the tridentate Schiff base ligands **IV1a**−**d**, *trans*-2-aminocyclohexanol (1.09 g, 7.22 mmol, 1.1 equiv) and triethylamine (0.724 g, 7.16 mmol, 1.09 equiv) were added to 2-hydroxy-3-methoxybenzaldehyde (1.00 g, 6.57 mmol, 1.0 equiv) in MeOH (30 mL). Compound

IV1b was obtained as a yellow powder in 87% yield. ^{1}H NMR (300 MHz, $CDCl_3$): δ 1.38, 1.62, 1.81, 2.08 (bm, 8H, CH(CH_2)$_4$CH), 3.03 (m, 1H, NCHCH$_2$), 3.66 (m, 1H, OCHCH$_2$), 3.90 (s, 3H, OCH_3) 6.78, 6.81, 6.84, 6.88, 6.91, 6.94 (m, 3H, C$_6H_3$), 8.42 (s, 1H, CH═N), 13.84 (s, 1H, OH). ^{13}C NMR (300 MHz, $CDCl_3$): δ 24.12 (NCHCH$_2$*C*H$_2$CH$_2$), 24.28 (OCHCH$_2$*C*H$_2$CH$_2$), 32.58 (NCH*C*H$_2$CH$_2$), 32.62 (OCH*C*H$_2$CH$_2$), 73.59 (N*C*HCH$_2$), 74.76 (O*C*HCH$_2$), 114.08, 117.97, 118.42, 123.00, 148.50, 151.94 (Ar), 165.41 (*C*═N). Anal. Calcd for $C_{14}H_{19}NO_3$: C, 67.45; H, 7.68; N, 5.62. Found: C, 67.63; H, 7.73; N, 5.60. HRMS (ESI): *m*/*z* 250.1515 [M + H$^+$], calcd for $C_{14}H_{19}NO_3$ 249.14.

(*E*)-2-(((*trans*-2-Hydroxycyclohexyl)imino)methyl)-4-methyl-6(triphenylsilyl) phenol (IV1c; L^3-H). Following the general procedure for the synthesis of tridentate Schiff base ligands **IV1a**−**d**, *trans*-2-aminocyclohexanol (0.338 g, 2.23 mmol, 1.1 equiv) and triethylamine (0.223 g, 2.21 mmol, 1.09 equiv) were added to 2-hydroxy-5-methyl-3-(triphenylsilyl)benzaldehyde[71] (0.800 g, 2.02 mmol, 1.0 equiv) in MeOH (30 mL). Compound **IV1c** was obtained as a yellow powder in 90% yield. ^{1}H NMR (300 MHz, $CDCl_3$): δ 1.31, 1.56, 1.75, 2.03 (bm, 8H, CH(CH_2)$_4$CH), 2.19 (s, 3H, CCH_3), 2.97 (m, 1H, NCHCH$_2$), 3.59 (m, 1H, OCHCH$_2$), 3.90 (s, 3H, OCH_3) 7.07−7.64 (m, 18H, Ar), 8.41 (s, 1H, CH═N), 13.20 (s, 1H, OH). ^{13}C NMR (300 MHz, $CDCl_3$): δ 20.43 (C*C*H$_3$), 24.25 (NCHCH$_2$*C*H$_2$CH$_2$), 24.40 (OCHCH$_2$*C*H$_2$CH$_2$), 32.59 (NCH*C*H$_2$CH$_2$), 32.76 (OCH*C*H$_2$CH$_2$), 73.42 (N*C*HCH$_2$), 75.71 (O*C*HCH$_2$), 117.73, 121.32, 127.40, 127.67, 129.24, 129.76, 134.23, 134.68, 135.16, 135.42, 136.35, 142.04, 163.98 (Ar), 165.54

(*C*═N). Anal. Calcd for $C_{32}H_{33}NO_2Si$: C, 78.17; H, 6.76; N, 2.85. Found: C, 76.99; H, 6.67; N, 2.16. HRMS (ESI): *m*/*z* 492.2625 [M + H^+], calcd for $C_{32}H_{33}NO_2Si$ 491.23.

(*E*)-2-(*tert*-Butyldimethylsilyl)-6-(((*trans*-2-hydroxycyclohexyl)imino) methyl)-4-methylphenol (IV1d; L^4-H). Following the general procedure for synthesis of tridentate Schiff base ligands **IV1a**−**d**, *trans*-2-aminocyclohexanol (0.166 g, 1.09 mmol, 1.1 equiv) and triethylamine (0.110 g, 1.08 mmol, 1.09 equiv) were added to 2-hydroxy-5-methyl-3-(triphenylsilyl)benzaldehyde[71] (0.250 g, 0.99 mmol, 1.0 equiv) in MeOH (30 mL). Compound **IV1d** was obtained as a yellow powder in 81% yield. ^{1}H NMR (300 MHz, $CDCl_3$): δ 0.32 (s, 6H, Si(C*H*$_3$)$_2$), 0.92 (s, 9H, C(C*H*$_3$)$_3$), 1.37, 1.63, 1.80, 2.08 (bm, 8H, CH(C*H*$_2$)$_4$CH), 2.97 (m, 1H, NC*H*CH$_2$), 3.69 (m, 1H, OC*H*CH$_2$), 7.05 (d, *J* = 1.78 Hz, 1H, C$_6$*H*$_2$), 7.20 (d, *J* = 2.09 Hz, 1H, C$_6$*H*$_2$), 8.37 (s, 1H, C*H*═N), 12.98 (s, 1H, O*H*). ^{13}C NMR (300 MHz, $CDCl_3$): δ −4.71 (Si(*C*H$_3$)$_2$), 17.61 (Si*C*(CH$_3$)$_3$), 20.43 (C*C*H$_3$), 24.28 (NCHCH$_2$*C*H$_2$CH$_2$), 24.45 (OCHCH$_2$*C*H$_2$CH$_2$), 27.11 (SiC(*C*H$_3$)$_3$), 32.53 (NCH*C*H$_2$CH$_2$), 32.83 (OCH*C*H$_2$CH$_2$), 73.62 (N*C*HCH$_2$), 75.74 (O*C*HCH$_2$), 117.42, 124.72, 126.81, 133.06, 140.20, 163.73 (Ar), 165.90 (*C*═N). Anal. Calcd for $C_{20}H_{33}NO_2Si$: C, 69.11; H, 9.57; N, 4.03. Found: C, 69.34; H, 9.81; N, 4.01. HRMS (ESI): *m*/*z* 348.2482 [M + H^+], calcd for $C_{20}H_{33}NO_2Si$, 347.23.

General Procedure for Synthesis of Tridentate Schiff Base Ligands IV1e−h. The corresponding benzaldehyde (1.0 equiv) was added to the corresponding amino alcohol (1.0 equiv) in MeOH (30 mL). The solution mixture was heated to reflux overnight and dried over Na_2SO_4 followed by filtration. The volatile component was removed in vacuo to give tridentate Schiff base ligands in quantitative yield.

(*E*)-2,4-Di-*tert*-butyl-6-(((2-hydroxyethyl)imino)methyl)phenol (IV1e; L^5-H). Following the general procedure for synthesis of tridentate Schiff base ligands **IV1e**–**h**, 3,5-di-*tert*-butyl-2-hydroxybenzaldehyde (1.00 g, 4.26 mmol, 1.0 equiv) was added to ethanolamine (0.260 g, 4.26 mmol, 1.0 equiv) in MeOH (30 mL). The solution mixture was heated to reflux overnight and dried over Na_2SO_4, followed by filtration. The volatile component was removed in vacuo to give the tridentate Schiff base ligand **IV1e** in quantitative yield. ^{1}H NMR (300 MHz, $CDCl_3$): δ 1.24 (s, 9H, C(CH_3)$_3$), 1.37 (s, 9H, C(CH_3)$_3$), 3.68 (m, 2H, OCH_2CH$_2$), 3.86 (m, 2H, NCHCH$_2$), 7.03 (d, J = 2.68 Hz, 1H, C$_6H_2$), 7.32 (d, J = 2.68 Hz, 1H, C$_6H_2$), 8.35 (s, 1H, CH═N), 13.49 (s, 1H, OH). ^{13}C NMR (300 MHz, $CDCl_3$): δ 29.40 (C(^{p}CH$_3$)$_3$), 31.48 (C(^{o}CH$_3$)$_3$), 34.35 (^{p}CCH$_3$), 35.01 (^{o}CCH$_3$), 61.82 (OCH_2CH$_2$), 62.33 (NCH_2CH$_2$), 117.73, 126.05, 127.14, 136.71, 140.21, 157.95 (Ar), 168.14 (C═N). Anal. Calcd for $C_{17}H_{27}NO_2$: C, 73.61; H, 9.81; N, 5.05. Found: C, 73.94; H, 10.16; N, 4.70. HRMS (ESI): *m*/*z* 278.2213 [M + H$^+$], calcd for $C_{17}H_{27}NO_2$, 277.20.

(*E*)-2,4-Di-*tert*-butyl-6-(((3-hydroxypropyl)imino)methyl)phenol (IV1f; L^6-H). Following the general procedure for synthesis of tridentate Schiff base ligands **IV1e**–**h**, 3,5-di-*tert*-butyl-2-hydroxybenzaldehyde (0.800 g, 3.41 mmol, 1.0 equiv) was added to 3-amino-1-propanol (0.256 g, 3.41 mmol, 1.0 equiv) in MeOH (30 mL). The solution mixture was heated to reflux overnight and dried over Na_2SO_4, followed by filtration. The volatile component was removed in vacuo to give the tridentate Schiff base ligand **IV1f** in quantitative yield. ^{1}H NMR (300 MHz, $CDCl_3$): δ 1.31 (s, 9H, C(CH_3)$_3$), 1.45 (s, 9H, C(CH_3)$_3$), 1.97 (m, 2H, CH$_2$CH_2CH$_2$), 3.71 (t, J = 6.84 Hz, 2H,

OC*H*$_2$CH$_2$), 3.76 (t, *J* = 6.25 Hz, 2H, NC*H*CH$_2$), 7.09 (d, *J* = 2.38 Hz, 1H, C$_6$*H*$_2$), 7.38 (d, *J* = 2.38 Hz, 1H, C$_6$*H*$_2$), 8.39 (s, 1H, C*H*═N), 13.85 (s, 1H, O*H*). ^{13}C NMR (300 MHz, CDCl$_3$): δ 29.40 (C(^{p}*C*H$_3$)$_3$), 31.48 (C(^{o}*C*H$_3$)$_3$), 33.50 (CH$_2$*C*H$_2$CH$_2$) 34.11 (^{p}*C*CH$_3$), 35.00 (^{o}*C*CH$_3$), 55.84 (OC*H*$_2$CH$_2$), 60.31 (NC*H*$_2$CH$_2$), 117.77, 125.78, 126.83, 136.65, 139.97, 158.08 (Ar), 166.35 (*C*═N). Anal. Calcd for C$_{18}$H$_{29}$NO$_2$: C, 74.18; H, 10.03; N, 4.81. Found: C, 74.05; H, 10.20; N, 4.84. HRMS (ESI): *m*/*z* 292.2394 [M + H$^+$], calcd for C$_{18}$H$_{29}$NO$_2$, 291.22.

(*E*)-2,4-Di-*tert*-butyl-6-(((4-hydroxybutyl)imino)methyl)phenol (IV1g; L^7-H). Following the general procedure for synthesis of tridentate Schiff base ligands **IV1e**−**h**, 3,5-di-*tert*-butyl-2-hydroxybenzaldehyde (1.00 g, 4.26 mmol, 1.0 equiv) was added to 4-amino-1-butanol (0.380 g, 4.26 mmol, 1.0 equiv) in MeOH (30 mL). The solution mixture was heated to reflux overnight and dried over Na$_2$SO$_4$, followed by filtration. The volatile component was removed in vacuo to give the tridentate Schiff base ligand **IV1g** in quantitative yield. ^{1}H NMR (300 MHz, CDCl$_3$): δ 1.31 (s, 9H, C(C*H*$_3$)$_3$), 1.45 (s, 9H, C(C*H*$_3$)$_3$), 1.70 (m, 2H, CH$_2$C*H*$_2$CH$_2$), 1.79 (m, 2H, CH$_2$C*H*$_2$CH$_2$), 3.62 (t, *J* = 6.55 Hz, 2H, OC*H*$_2$CH$_2$), 3.70 (t, *J* = 6.24 Hz, 2H, NC*H*CH$_2$), 7.08 (d, *J* = 2.38 Hz, 1H, C$_6$*H*$_2$), 7.37 (d, *J* = 2.38 Hz, 1H, C$_6$*H*$_2$), 8.36 (s, 1H, C*H*═N), 13.90 (s, 1H, O*H*). ^{13}C NMR (300 MHz, CDCl$_3$): δ 27.19 (CH$_2$*C*H$_2$CH$_2$), 29.39 (C(^{p}*C*H$_3$)$_3$), 30.29 (CH$_2$*C*H$_2$CH$_2$), 31.48 (C(^{o}*C*H$_3$)$_3$), 34.08 (^{p}*C*CH$_3$), 34.98 (^{o}*C*CH$_3$), 59.17 (OC*H*$_2$CH$_2$), 62.56 (NC*H*$_2$CH$_2$), 117.77, 125.70, 126.72, 136.62, 139.88, 158.13 (Ar), 166.83 (*C*═N). Anal. Calcd for C$_{19}$H$_{31}$NO$_2$: C, 74.71; H, 10.23; N, 4.59. Found: C, 74.73; H, 10.32; N, 4.58. HRMS (ESI): *m*/*z* 306.2501 [M + H$^+$], calcd for C$_{19}$H$_{31}$NO$_2$, 305.24.

(*E*)-2,4-Di-*tert*-butyl-6-(((5-hydroxypentyl)imino)methyl)phenol (1h; L^8-H). Following the general procedure for synthesis of tridentate Schiff base ligands **IV1e**−**h**, 3,5-di-*tert*-butyl-2-hydroxybenzaldehyde (1.00 g, 4.26 mmol, 1.0 equiv) was added to 5-amino-1-pentanol (0.440 g, 4.26 mmol, 1.0 equiv) in MeOH (30 mL). The solution mixture was heated to reflux overnight and dried over Na_2SO_4, followed by filtration. The volatile component was removed in vacuo to give the tridentate Schiff base ligand **IV1h** in quantitative yield. ^{1}H NMR (300 MHz, $CDCl_3$): δ 1.31 (s, 9H, C(CH_3)$_3$), 1.45 (s, 9H, C(CH_3)$_3$), 1.48 (m, 2H, $CH_2CH_2CH_2$), 1.63 (m, 2H, $CH_2CH_2CH_2$), 1.74 (m, 2H, $CH_2CH_2CH_2$), 3.59 (t, *J* = 6.84 Hz, 2H, OCH_2CH_2), 3.67 (t, *J* = 6.54 Hz, 2H, NC*H*CH_2), 7.07 (d, *J* = 2.38 Hz, 1H, C_6H_2), 7.37 (d, *J* = 2.38 Hz, 1H, C_6H_2), 8.34 (s, 1H, C*H*═N), 13.95 (s, 1H, O*H*). ^{13}C NMR (300 MHz, $CDCl_3$): δ 23.39 ($CH_2CH_2CH_2$), 29.40 (C($^pCH_3$)$_3$), 30.66 ($CH_2CH_2CH_2$), 31.49 (C($^oCH_3$)$_3$), 33.44 ($CH_2CH_2CH_2$), 34.10 ($^pCCH_3$), 35.00 ($^oCCH_3$), 59.43 (OCH_2CH_2), 62.80 (NCH_2CH_2), 117.80, 125.67, 126.70, 136.63, 139.86, 158.17 (Ar), 158.17 (*C*═N). Anal. Calcd for $C_{20}H_{33}NO_2$: C, 75.19; H, 10.41; N, 4.38. Found: C, 75.10; H, 10.41; N, 4.38. HRMS (ESI): *m*/*z* 320.2708 [M + H^+], calcd for $C_{20}H_{33}NO_2$, 319.25.

General Procedure for Synthesis of Tridentate Schiff Base Ligands 1i,j. The corresponding amino acid (2 equiv) and triethylamine (2 equiv) were added to 3,5-di-*tert*-butyl-2-hydroxybenzaldehyde[40c, 40d, 48b] (1.0 equiv) in MeOH (30 mL). The solution mixture was heated to reflux for overnight, and the solvent was removed under reduced pressure to obtain a yellow solid. The resulting yellow solid was washed with water (3 × 20 mL) to remove excess amino acid and triethylamine. The organic layer was separated,

dried over $NaSO_4$, and concentrated to dryness under reduced pressure to afford the crude products with 0.5 equiv of triethylamine, which were crystallized in pentane to give a yellow powder in 81−85% yield.

(*E*)-2-((3,5-Di-*tert*-butyl-2-hydroxybenzylidene)amino)-4-(methylthio) butanoic acid (IV1i; L^9-H). Following the general procedure for synthesis of tridentate Schiff base ligands **IV1i**,**j**, *rac*-methionine (1.273 g, 8.535 mmol, 2 equiv) and triethylamine (0.863 g, 8.535 mmol, 2 equiv) were added to 3,5-di-*tert*-butyl-2-hydroxybenzaldehyde (1.00 g, 4.26 mmol) in MeOH (30 mL). Compound **IV1i** was obtained as a yellow powder in 81% yield. ^{1}H NMR (300 MHz, $CDCl_3$): δ 1.20 (t, *J* = 7.44 Hz, 4.5H, CH_2CH_3), 1.30 (s, 9H, $C(CH_3)_3$), 1.43 (s, 9H, $C(CH_3)_3$), 2.08 (s, 3H, SCH_3), 2.24 (m, 2H, $CHCH_2CH_2$), 2.52 (m, 2H, CH_2CH_2S), 3.05 (q, *J* = 7.73 Hz, 3H, CH_2CH_3) 4.08 (m, 1H, $NCHCH_2$) 7.10 (d, *J* = 2.67 Hz, 1H, C_6H_2), 7.37 (d, *J* = 2.38 Hz, 1H, C_6H_2), 8.48 (s, 1H, CH═N). ^{13}C NMR (300 MHz, $CDCl_3$): δ 8.41 (CH_2CH_3), 15.19 (SCH_3), 29.25 (CH_2CH_2S), 29.42 ($C(^pCH_3)_3$), 31.30 ($CHCH_2CH_2$), 31.49 ($C(^oCH_3)_3$), 34.10 ($^pCCH_3$), 35.01 ($^oCCH_3$), 44.99 (CH_2CH_3), 71.76 ($NCHCH_2$), 117.90, 126.24, 127.02, 136.52, 139.84, 158.22 (Ar), 167.41 (C═N), 175.78 (C═O). Anal. Calcd for $C_{46}H_{77}N_3O_6S_2$: C, 66.39; H, 9.33; N, 5.05; S, 7.71. Found: C, 66.14; H, 9.28; N, 5.07; S, 8.00. HRMS (ESI): *m*/*z* 366.2241 [M + H^+], calcd for $C_{46}H_{77}N_3O_6S_2$, 365.20.

(*E*)-2-((3,5-Di-*tert*-butyl-2-hydroxybenzylidene)amino)-3-phenylpropanoic acid (IV1j; L^{10}-H). Following the general procedure for synthesis of tridentate Schiff base ligands **IV1i**,**j**, *rac*-phenylalanine (1.409 g, 8.532 mmol, 2 equiv) and triethylamine (0.863 g, 8.532 mmol, 2 equiv) were added to 3,5-di-*tert*-butyl-2-hydroxybenzaldehyde

(1.00 g, 4.26 mmol) in MeOH (30 mL). Compound **IV1j** was obtained as a yellow powder in 85% yield. ^{1}H NMR (300 MHz, $CDCl_3$): δ 1.18 (t, *J* = 7.23 Hz, 4.5H, CH_2CH_3), 1.25 (s, 9H, $C(CH_3)_3$), 1.43 (s, 9H, $C(CH_3)_3$), 3.00 (q, *J* = 7.37 Hz, 3H, CH_2CH_3) 3.14 (m, 1H, $CHCH_2Ph$), 3.37 (m, 1H, $CHCH_2Ph$), 4.10 (m, 1H, $NCHCH_2$), 6.93 (d, *J* = 2.46 Hz, 1H, C_6H_2), 7.10−7.21 (m, 5H, C_6H_5), 7.33 (d, *J* = 2.46 Hz, 1H, C_6H_2), 8.06 (s, 1H, CH═N). ^{13}C NMR (300 MHz, $CDCl_3$): δ 8.37 (CH_2CH_3), 29.42 ($C(^{p}CH_3)_3$), 31.46 ($C(^{o}CH_3)_3$), 34.05 ($^{p}CCH_3$), 35.00 ($^{o}CCH_3$), 40.24 ($CHCH_2Ph$), 45.10 (CH_2CH_3), 74.61 ($NCHCH_2$), 117.87, 126.17, 126.82, 128.23, 129.66, 136.39, 138.33, 139.61, 158.20 (Ar), 166.95 (C═N), 175.23 (C═O). Anal. Calcd for $C_{54}H_{77}N_3O_6$: C, 75.05; H, 8.98; N, 4.68. Found: C, 75.28; H, 9.14; N, 4.90. HRMS (ESI): *m*/*z* 382.2631 [M + H^+], calcd for $C_{54}H_{77}N_3O_6$, 381.23.

Preparation of Aluminum Complexes IV2a−j. A solution of triethylaluminum in toluene (0.10 M, 0.25 mL, 1 equiv) was added to a solution of the corresponding ligands **IV1a−j** in 0.75 mL of toluene in a sealed tube, and the reaction mixture was stirred for 3 h at room temperature.

Polymerization Procedure. In a typical experiment carried out in the argon-filled glovebox, a Teflon-screw-capped heavy-walled pressure vessel containing the corresponding aluminum complex **IV2a−j** and 50 equiv of *rac*-lactide (per aluminum center) in 1.00 mL of toluene was stirred at 70 °C for the designated time period. Upon removal of a small sample of the crude product via syringe, it was analyzed by ^{1}H NMR spectroscopy in $CDCl_3$. The product was isolated and purified by precipitation from

dichloromethane by the addition of 5% hydrochloric acid in methanol. The solid polymer was collected and dried under vacuum to constant weight.

General Procedure for Synthesis of Tridentate Schiff Base Aluminum Complexes (IV2e−g; L^{5-7}AlEthyl). A solution of triethylaluminum (1.0 equiv) in pentane was cannulated to a solution of tridentate Schiff base ligand (1 equiv) in pentane. The reaction mixture was stirred until a yellow precipitate was formed, and this mixture was stirred at room temperature for an additional 3 h. The resulting yellow precipitate was washed with cold pentane (3 × 1 mL). The volatile component was removed under reduced pressure to give light yellow solids of complexes **IV2e**−**g**.

Synthesis of [L^5AlEthyl] (IV2e). A solution of triethylaluminum (0.463 g, 4.06 mmol, 1.0 equiv) in pentane (2 mL) was cannulated to a suspended solution of the tridentate Schiff base ligand **IV1e** (1.12 g, 4.06 mmol, 1 equiv) in pentane (2 mL). Complex **IV2e** was obtained in 62% yield. ^{1}H NMR (300 MHz, $CDCl_3$): δ 0.37 (bm, 2H, C*H*$_2$CH$_3$), 0.79, 0.90 (2 sets of t, 3H, CH$_2$C*H*$_3$), 1.29, 1.31 (2 set of s, 9H, C(C*H*$_3$)$_3$), 1.45, 1.48 (2 set of s, 9H, C(C*H*$_3$)$_3$), 3.52, 3.83 (m, 2H, OC*H*$_2$CH$_2$), 4.10, 4.34 (m, 2H, NC*H*CH$_2$), 7.01, 7.04 (2 set of d, *J* = 2.67 and 2.67 Hz, 1H, C$_6$*H*$_2$), 7.45, 7.48 (d, *J* = 2.67 and 2.38 Hz, 1H, C$_6$*H*$_2$), 8.27, 8.22 (2 set of s, 1H, C*H*═N). ^{13}C NMR (300 MHz, $CDCl_3$): δ 10.10, 14.07, 22.35, 29.25, 31.43, 33.98, 35.39, 55.40, 55.80,59.31, 60.23, 118.66, 119.19, 126.91, 127.07, 129.74, 137.67, 137.93, 139.90, 139.97, 161.66, 161.93, 166.25, 166.55. Anal. Calcd for $C_{19}H_{30}AlNO_2$: C, 68.85; H, 9.12; N, 4.23. Found: C, 68.63; H, 9.40; N, 4.20.

Synthesis of [L^{6}AlEthyl] (IV2f). A solution of triethylaluminum (0.156 g, 1.37 mmol, 1.0 equiv) in pentane (2 mL) was cannulated to a suspended solution of the tridentate Schiff base ligand **IV1f** (0.400 g, 1.37 mmol, 1 equiv) in pentane (2 mL). Complex **IV2f** was obtained in 20% yield. ^{1}H NMR (300 MHz, $CDCl_3$): δ −0.32, −0.14 (2 sets of m, 2H, C*H*$_2$CH$_3$), 0.83, 0.92 (2 set of t, 3H, CH$_2$C*H*$_3$), 1.28, 1.38 (2 set of s, 9H, C(C*H*$_3$)$_3$), 1.31, 1.48 (2 set of s, 9H, C(C*H*$_3$)$_3$), 1.83, 1.93, 2.21, 3.50, 3.86, 4.11, 4.39 (m, 6H, C*H*$_2$C*H*$_2$C*H*$_2$), 6.95, 7.00 (2 set of d, *J* = 2.38 and 2.67 Hz, 1H, C$_6$*H*$_2$), 7.40, 7.47 (d, *J* = 2.68 and 2.68 Hz, 1H, C$_6$*H*$_2$), 8.04, 8.09 (2 set of s, 1H, C*H*═N). ^{13}C NMR (300 MHz, $CDCl_3$): δ 10.22, 10.34, 29.44, 30.36, 31.40, 31.82, 33.89, 35.02, 35.16, 57.45, 60.77, 61.30, 63.52, 118.22, 118.66, 127.37, 127.64, 129.57, 129.69, 137.54, 137.80, 139.24, 139.51, 161.57, 161.68, 167.61, 167.92. Anal. Calcd for $C_{20}H_{32}AlNO_2$: C, 69.54; H, 9.34; N, 4.05. Found: C, 68.81; H, 9.54; N, 4.01.

Synthesis of [L^{7}AlEthyl] (IV2g). A solution of triethylaluminum (0.196 g, 1.71 mmol, 1.0 equiv) in pentane (2 mL) was canulated to a suspended solution of the tridentate Schiff base ligand **IV1g** (0.525 g, 1.71 mmol, 1 equiv) in pentane (2 mL). Complex **IV2g** was obtained in 21% yield. ^{1}H NMR (300 MHz, $CDCl_3$): δ −0.34, −0.15 (m, 2H, C*H*$_2$CH$_3$), 0.82, 0.88 (2 sets of m, 3H, CH$_2$C*H*$_3$), 1.31 (s, 9H, C(C*H*$_3$)$_3$), 1.50 (s, 9H, C(C*H*$_3$)$_3$), 1.72 (m, 2H, CH$_2$C*H*$_2$CH$_2$), 2.17 (m, 2H, CH$_2$C*H*$_2$CH$_2$), 3.44 (m, 2H, OC*H*$_2$CH$_2$), 4.05 (m, 2H, NC*H*CH$_2$), 6.99 (d, *J* = 2.68 Hz, 1H, C$_6$*H*$_2$), 7.45 (d, *J* = 2.68 Hz, 1H, C$_6$*H*$_2$), 8.16 (s, 1H, C*H*═N), 13.90 (s, 1H, O*H*). ^{13}C NMR (300 MHz, $CDCl_3$): δ 10.08, 10.52, 14.07, 22.34, 27.73, 28.68, 29.50, 31.38, 33.85, 33.94, 34.73, 35.44, 58.06,

58.35, 61.56, 62.18. Anal. Calcd for $C_{21}H_{34}AlNO_2$: C, 70.16; H, 9.53; N, 3.90. Found: C, 69.12; H, 9.91; N, 3.57.

Results and Discussion

The ligands used in our studies were derived from either amino alcohols or amino acids by condensation reactions with the corresponding aldehydes to afford compounds **IV1a**–**j**. Reactions of these ligands with triethylaluminum in dry toluene resulted in the formation of complexes **IV2a**–**j**, as depicted in Scheme IV-1. In this manner three series of closely related aluminum half-salen complexes were synthesized whose ligand backbones were easily modified by chiral amino alcohols (**IV2a**–**d**), aliphatic amino alcohols (**IV2e**–**h**), and amino acids (**IV2i**,**j**). The reactivity and selectivity of aluminum complexes **IV2a**–**j** for catalyzing the ROP of *rac*-lactide are provided in Table IV-1.

As noted in Table IV-1, complex **IV2a** did not polymerize *rac*-lactide in $CDCl_3$ after 66 h at 60 °C (entry2); however, in toluene a 57% conversion to polylactide was observed over the same time period at 70 °C (entry4). For complexes in the series **IV2a**–**d** and the substituents (R^2) on the phenoxide of the half-salen ligand increase in size (R^2 = $SiPh_3$) or are more electron donating (R^2 = OMe), the rate of lactide polymerization decreases (entries 6 and 8). Similar observations have been previously reported by Normura and co-workers and Gibson and co-workers.[12, 17] Complex **IV2a** afforded a moderately isotactic polymer with a P_m value of 0.70, while complexes **IV2b**,**c** yielded polylactides with P_m values less than 0.50. The complexes with achiral aliphatic backbone with the exception of **IV2f**, *i.e.*, complexes **IV2e**,**g**,**h**, were found to

catalyze the ROP of *rac*-lactide at rates faster than that of complex **IV2a** to give isotactic polylactides with P_m values of 0.62, 0.76, and 0.73, respectively. Similarly, the complexes derived from *rac*-amino acids, **IV2i**,**j**, were also found to be active for the ring-opening polymerization of *rac*-lactide, providing substantially isotactic polymers with P_m values of 0.74 and 0.72, respectively.

Scheme IV-1

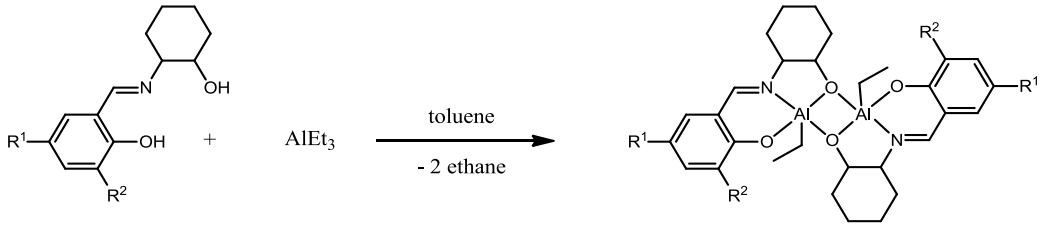

IV1a : R^1 = *t*-Bu, R^2 = *t*-Bu
IV1b : R^1 = H, R^2 = OMe
IV1c : R^1 = Me, R^2 = $SiPh_3$
IV1d : R^1 = Me, R^2 = $SiMe_2{}^tBu$

IV2a : R^1 = *t*-Bu, R^2 = *t*-Bu
IV2b : R^1 = H, R^2 = OMe
IV2c : R^1 = Me, R^2 = $SiPh_3$
IV2d : R^1 = Me, R^2 = $SiMe_2{}^tBu$

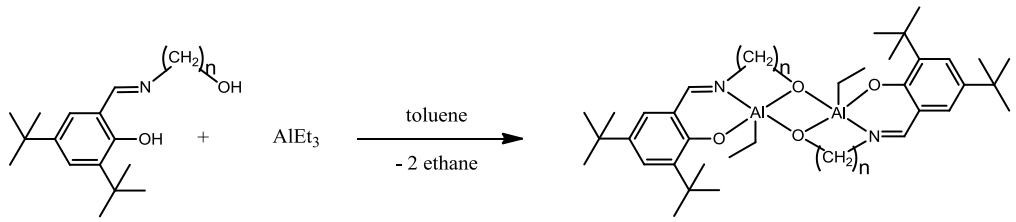

IV1e : n = 2
IV1f : n = 3
IV1g : n = 4
IV1h : n = 5

IV2e : n = 2
IV2f : n = 3
IV2g : n = 4
IV2h : n = 5

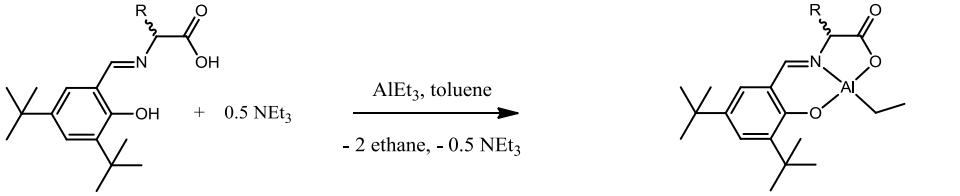

IV1i : R = 2-(methylthio)ethyl
IV1j : R = benzyl

IV2i : R = 2-(methylthio)ethyl
IV2j : R = benzyl

Table IV-1. Reactivity and Selectivity of Aluminum Complexes **IV2a-j** for the ROP of *Rac*-Lactide.[a]

entry	M	time (h)	Conversion (%)[b]	*meso*-[c]	M_n		PDI	P_m[f]
					Theoretical[d]	$0.58M_{n,GPC}$[e]		
1	**IV2a**[g]	20	0	no				
2	**IV2a**[h]	66	0	yes				
3	**IV2a**	15	0	yes				
4	**IV2a**	66	57	yes	4 107	7 938	1.05	70
5	**IV2b**	15	0	yes				
6	**IV2b**	69	43	yes	3 243	3 844	1.08	<50
7	**IV2c**	15	0	yes				
8	**IV2c**	168	45	yes	3 207	4 962	1.09	<50
9	**IV2d**	15	0	yes				
10	**IV2e**	15	64	yes	4 614	6 987	1.04	62
11	**IV2f**	15	0	yes				
12	**IV2g**	15	34	no	2 446	2 456	1.07	76
13	**IV2h**	15	50	no				73
14	**IV2i**	15	36	no	2 594	3 916	1.07	74
15	**IV2j**	15	42	no	3 026	4 043	1.03	72

[a] Unless otherwise specified, the polymerization reactions were performed in sealed reaction tubes with the following conditions: [*rac*-LA]/[Al] = 50, in toluene at 70 °C.[b] Obtained from ^{1}H NMR spectroscopy. [c] *meso*-lactide was obtained from epimerization of L- or D-lactide during the polymerization process. [d] Theoretical M_n = (M/I) x (% conversion) x (mol. wt. of lactide). [e] M_n values were corrected by the equation: $M_n = 0.58\ M_{n,\ GPC}$.[51] [f] P_m values were calculated from the ratio of the (area of iii)/(total area in methine proton region). [g] $CDCl_3$ was used as the solvent at ambient temperature. [h] $CDCl_3$ was used as the solvent at 60 °C.

A noteworthy point of importance is that for several of these aluminum-catalyzed systems, namely **IV2a**–**f**, a ^{1}H NMR signal at 1.70 ppm appears during the polymerization process, while polymerization reactions catalyzed by complexes **IV2g**–**j** did not exhibit such a ^{1}H NMR signal (see resonance labeled **a** in Figure IV-1). This ^{1}H NMR peak is assigned to intermediate formation of *meso*-lactide from epimerization of L- and D-lactide during the ROP process. In order to further confirm this occurrence, select aluminum complexes **IV2e**–**g**,**i**,**j** were used to catalyze the ROP of L-lactide. In these instances, if there is no epimerization occurring during the polymerization process, only isotactic polylactide will be formed. As anticipated, complexes **IV2e**,**f** polymerized L-lactide to afford atactic polylactide with P_m values of 0.52 and <0.50, respectively,

while complexes **IV2g**,**i**,**j** provided isotactic polylactide with a P_m value of 1, indicative of an absence of epimerization in these instances (Table IV-2).

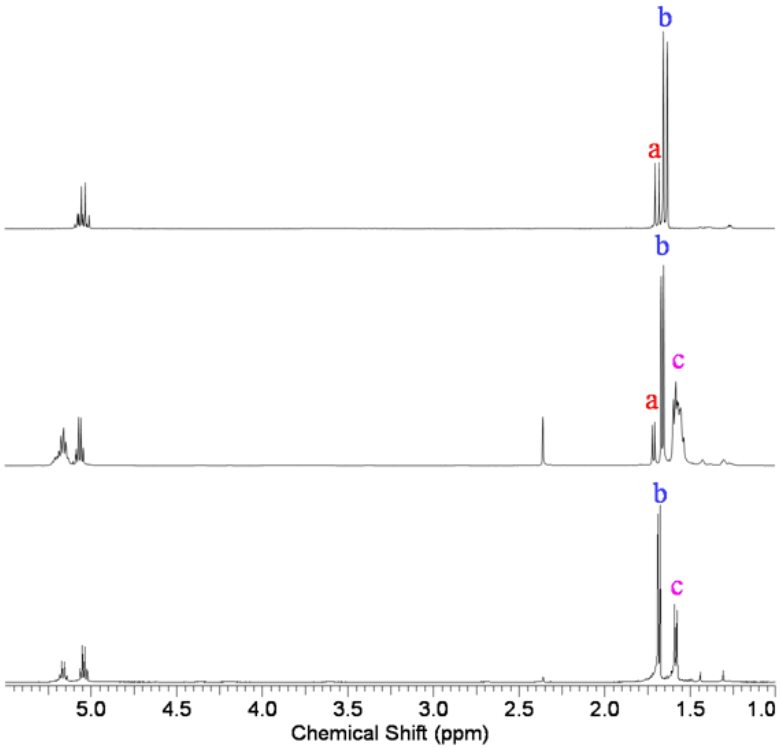

Figure IV-1. ^{1}H NMR spectrum ($CDCl_3$, rt) of the reaction mixtures during the ROP of L-lactide in the presence of complex **IV2a** (A), **IV2e** (B), **IV2g** (C) (entries 3, 10, 12; Table IV-1, respectively). The polymerization reactions were performed in toluene at 70 ^{o}C for 15 h. Methyl proton of *meso*-lactide, L-lactide, and polylactide were observed at 1.70 (a), 1.66 (b), and 1.57 (c) respectively.

The observed molecular weights of all the polymer produced via catalysis with the aluminum complexes employed in this study, *i.e.*, complexes **IV2a**−**j**, were found to closely parallel the theoretical values. In addition, the polymers thus afforded had polydispersity indices ranging from 1.03 to 1.08. The ring-opening polymerization was shown to be first order in [monomer] and [catalyst]. Hence, these catalytic systems have

the characteristic of well-controlled polymerization processes. The thermal properties of a purified polylactide sample produced from the ROP of *rac*-lactide by complex **IV2i** (P_m = 74%) were determined by differential scanning calorimetry (DSC). The T_m and T_g values of the polymer were found to be 158 and 52 °C, respectively (Figure IV-2). The observed T_m value is consistent with a moderately isotactic polylactide.

Table IV-2. The ROP of *rac*- and L-Lactide Using Aluminum Complexes **2IVe-g**, **2IVi-j**.[a]

entry	M	lactide	conversion (%)[b]	*meso*[c]	M_n		PDI	P_m[f]
					theoretical[d]	$0.58M_{n,GPC}$[e]		
1	**IV2e**	*rac*	64	yes	4 614	6 987	1.04	62
2	**IV2e**	L	77	yes	4 107	7 938	1.05	52
3	**IV2f**	*rac*	0	yes				
4	**IV2f**[g]	L	36	yes	2 600	3 726	1.07	<50
5	**IV2g**	*rac*	34	no	2 446	2 456	1.07	76
6	**IV2g**	L	44	no	3 164	N/A[h]	N/A[h]	100
7	**IV2i**	*rac*	34	no	2 594	3 916	1.07	74
8	**IV2i**	L	54	no	3 891	N/A[h]	N/A[h]	100
9	**IV2j**	*rac*	42	no	3 026	4 043	1.03	72
10	**IV2j**	L	45	no	3 243	N/A[h]	N/A[h]	100

[a] Unless otherwise specified, the polymerization reactions were performed in sealed reaction tubes under the following conditions: [LA]/[Al] = 50, in toluene at 70 °C for 15 h.[b] Obtained from ^{1}H NMR spectroscopy. [c] *meso*-lactide was obtained from epimerization of L- or D-lactide during the polymerization process. [d] Theoretical M_n = (M/I) x (% conversion) x (mol. wt. of lactide). [e] M_n values were corrected by the equation: $M_n = 0.58\ M_{n,\ GPC}$.[51] [f] P_m values were calculated from the ratio of the (area of iii)/(total area in methine proton region). [g] The reaction time was 76 h. [h] Molecular weight was not measure because of polymer's insolubility in THF due to its high crystallinity.

In an effort to understand the catalytic differences noted for the ROP of lactides by the closely related aluminum complexes **IV2e**−**h**, we report here the structural characterization of one of these derivatives. Specifically, complex **IV2f** was synthesized and isolated according to Scheme IV-1, except pentane was used as solvent, which

allowed the complex to precipitate out of solution during its preparation. Single crystals suitable for X-ray structural analysis were obtained upon recrystallization from dichloromethane at −10 °C. In this manner both platelike crystals and blocklike crystals were obtained. X-ray crystallography revealed the blocklike crystals to be dimeric, with bridging oxygen atoms. The two five-coordinate aluminum centers possess a distorted-bipyramidal geometry with the ethyl group of each metal *cis* to one another, as shown in Figure IV-3a. Similarly, the solid-state structure of the platelike crystals was shown to be dimeric, except that the ethyl groups on the aluminum centers were *trans* to one another (Figure IV-3b).

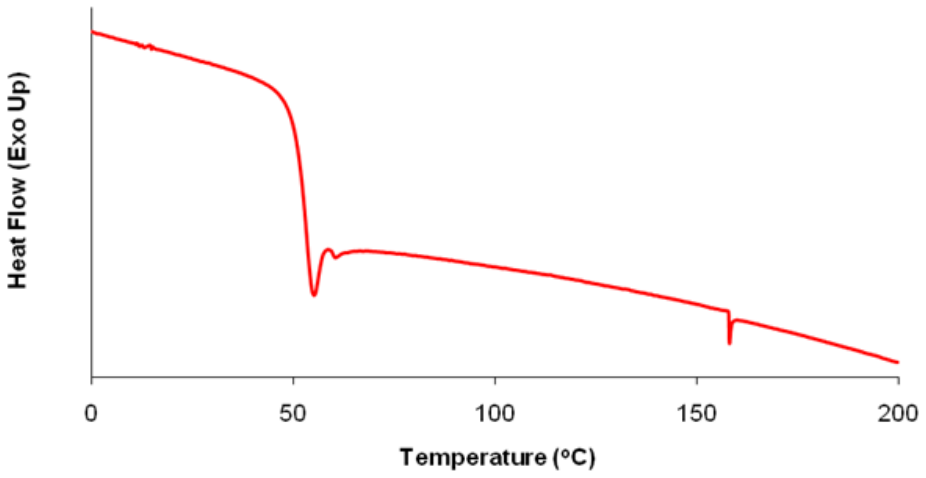

Figure IV-2. DSC curves (second heating run) of polylactide from *rac*-lactide catalyzed by complex **IV2i.**

a)

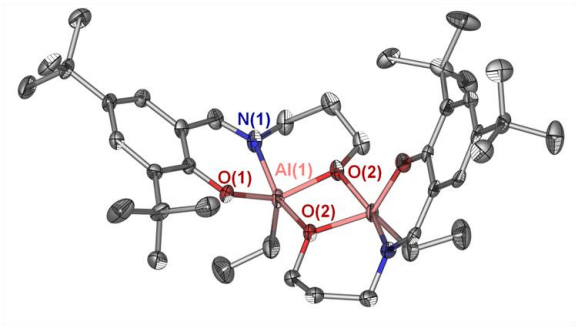

b)

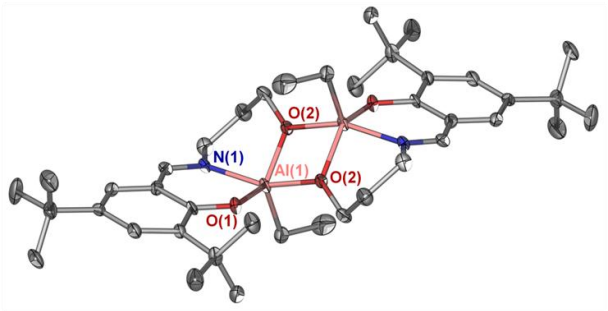

Figure IV-3. X-ray crystal structures of (a) **IV2f** (*cis*-), (b) **IV2f** (*trans*-). Thermal ellipsoids represent the 50% probability surfaces. Hydrogen atoms are omitted for the sake of clarity.

Since this difference in dimeric aluminum structures may be related to the disparity in catalytic reactivity for the ROP of lactides noted above, and the ROP processes are carried out in solution at 70 °C, it is important to examine the structures of these aluminum complexes in solution. We therefore performed variable-temperature ^{1}H NMR spectroscopic studies of complex **IV2f** in deuterated toluene. As observed in Figure IV-4, the ^{1}H NMR spectrum of complex **IV2f** at ambient temperature reveals two sets of methyl group protons from the *tert*-butyl substituents of the phenoxide ligands (resonances **a** and **a′** and **b** and **b′**). As the temperature was increased, the intensity of

the proton signals **a′** and **b′** increased with a concomitant decrease in the ^{1}H NMR signals at **a** and **b**. Both set of resonances were noted at 100 °C, with those of **a′** and **b′** being more intense. Once the distribution of the isomeric complex mixture was reached at 100 °C, this complex mixture remained the same after the solution stood at ambient temperature for 2 days (spectrum **E** in Figure IV-4). As indicated in Figure IV-4, we

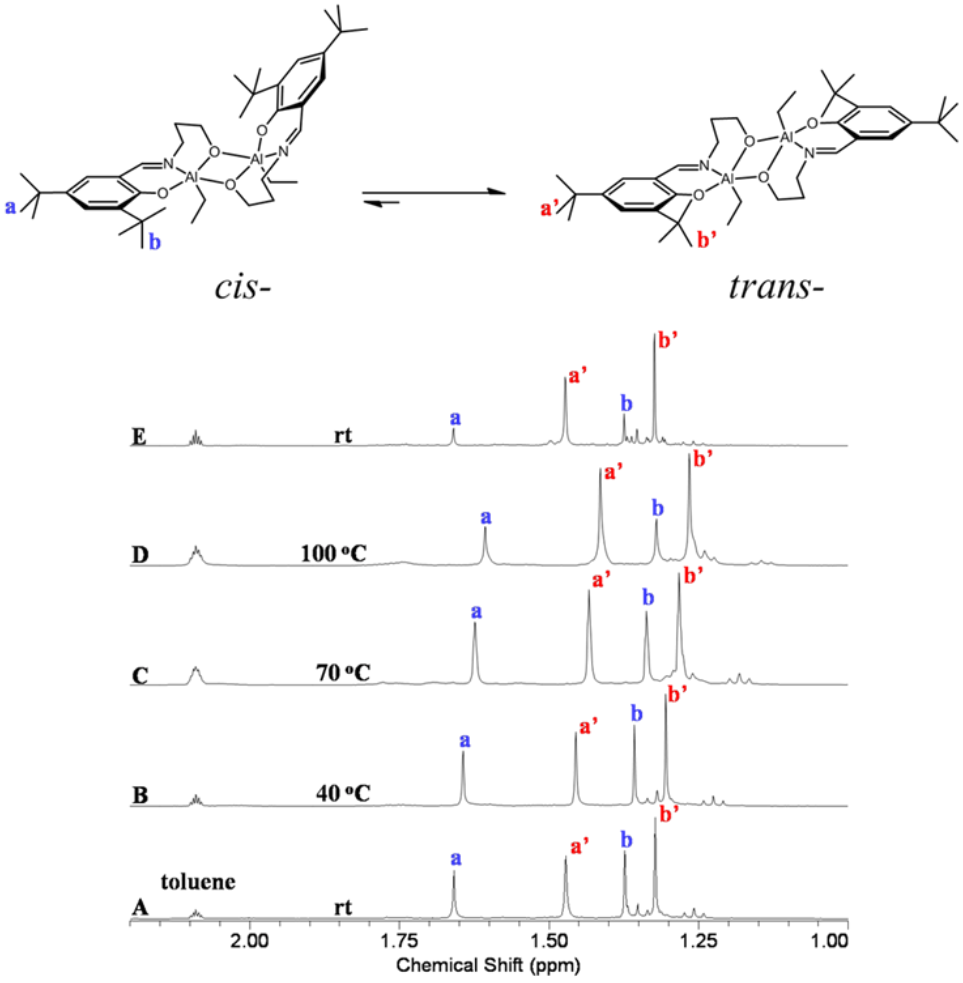

Figure IV-4. Variable-temperature ^{1}H NMR spectrum (500 MHz) of complex **IV2f** in deuterated toluene taken sequentially at different temperatures. (**A**) room temperature, (**B**) 40 ^{o}C, (**C**) 70 ^{o}C, (**D**) 100 ^{o}C, (**E**) sample cooled down from 100 ^{o}C to room temperature, spectrum taken two days later.

propose the isomeric mixture of aluminum complexes favors the *trans* arrangement of ethyl groups. That is, due to the decrease in steric repulsion of the bulky phenyl ring, the *trans* isomer is thermodynamically more stable.

As indicated by the variable-temperature ^{1}H NMR study, complex **IV2f** exists as both the *cis* and *trans* isomers in toluene solution at the ROP temperature of 70 °C. We propose that one of these isomeric forms of the aluminum complex **IV2f** is responsible for *meso*-lactide formation: *i.e.*, the *cis* form (*vide infra*). In much the same way, the ^{1}H NMR spectrum of complex **IV2e** exhibited two sets of *tert*-butyl group methyl protons at ambient temperature. However, in this case, upon increasing the temperature to 100 °C with periodic monitoring of the spectra, no spectral changes were observed. This result strongly suggests that the structural rearrangements seen in these aluminum dimers are related to the length of the carbon chain backbone in the amino−alkoxide bridging ligand, with the five-membered ring (**IV2e**) being, as expected, more stable than the six-membered ring (**IV2f**). In support of this contention, upon examination of the variable-temperature ^{1}H NMR spectra of complex **IV2g**, which contains a longer four-carbon-chain backbone leading to a seven-membered amino−alkoxide bridging ligand, a facile isomeric exchange reaction was observed (Figure IV-5). That is, at ambient temperature the ^{1}H NMR spectrum revealed the presence of both isomers in solution, with the *cis* isomer in larger quantity. As the temperature was increased, the distribution of isomers converted to all *trans* by 70 °C, with no further change occurring with either an increase in temperature to 100 °C or a decrease down to ambient temperature.[72] As evident from Table IV-1, when complexes **IV2g**,**h** (four- or five-membered carbon chain backbone)

were employed as catalysts for the ROP of *rac*-lactide, no *meso*-lactide formation was observed. These observations confirm our suggestion that the *cis* isomer is responsible for the epimerization of lactide prior to the ring-opening polymerization process. Crystal data and details of the data collection for complexes **IV2f** (*cis*-) and **IV2f** (*trans*-) are provided in Table IV-3.

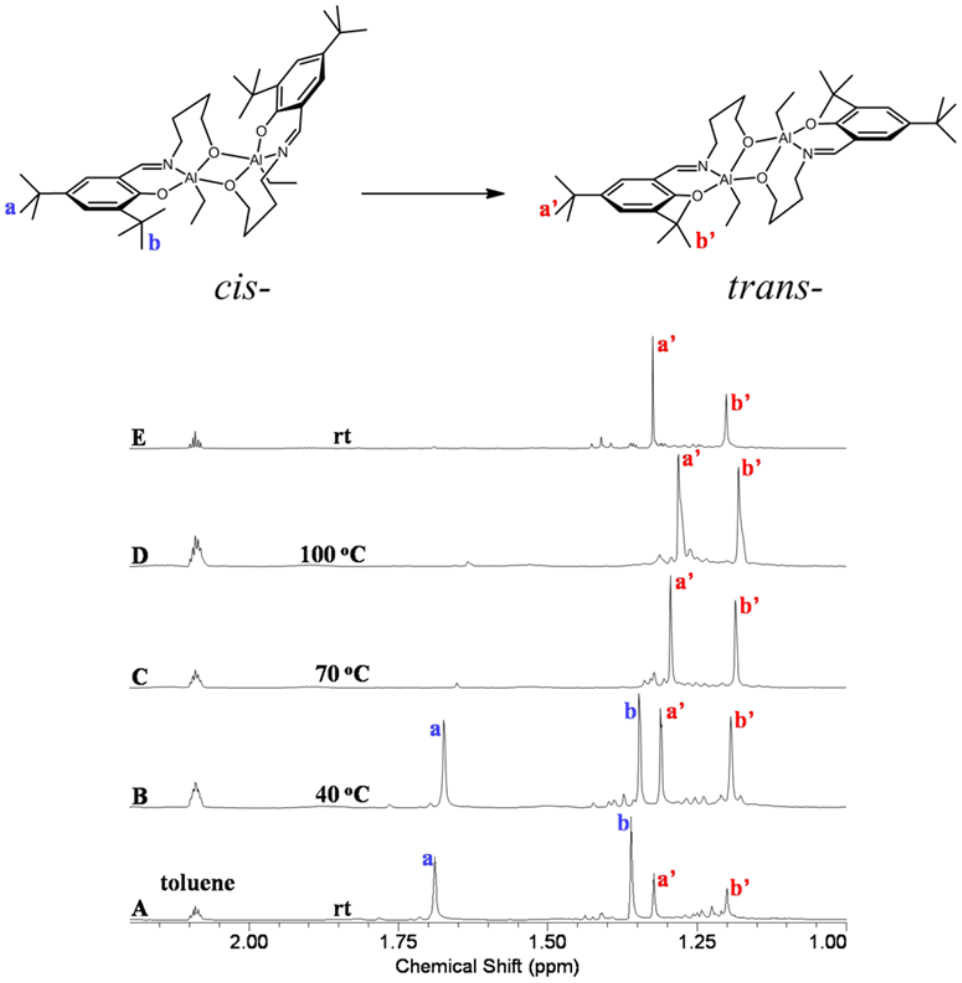

Figure IV-5. Variable-temperature ^{1}H NMR spectrum (500 MHz) of complex **IV2g** in deuterated toluene taken sequentially at different temperatures. (**A**) room temperature, (**B**) 40 ^{o}C, (**C**) 70 ^{o}C, (**D**) 100 ^{o}C, (**E**) sample cooled down from 100 ^{o}C to room temperature, spectrum taken two days later.

Table IV-3. Crystallographic Data for Complexes **IV2f** (*cis*-) and **IV2f** (*trans*-).

	IV2f (*cis*-)	**IV2f** (*trans*-)
empirical formula	$C_{40}\ H_{64}\ Al_2\ N_2\ O_4$	$C_{40}\ H_{64}\ Al_2\ N_2\ O_4$
fw	690.89	690.89
temperature (K)	110(2) K	110(2) K
crystal system	orthorhombic	monoclinic
space group	Pbcn	P21/C
a(Å)	32.810(7)	14.234(4)
b(Å)	20.945(5)	8.985(3)
c(Å)	17.910(4)	18.655(5)
α(deg)	90	90
β(deg)	90	123.063(16)
γ(deg)	90	90
V(Å)	12308(5)	1999.5(10)
D_c(Mg/m^3)	1.119	1.148
Z	12	2
abs coeff(mm^{-1})	0.940	0.964
reflections collected	71247	12357
independent reflections	9145 [*R*(int) = 0.0715]	2689 [*R*(int) = 0.1829]
data/restrains/parameters	9145 / 34 / 696	2689 / 0 / 225
GOF on F^2	1.066	1.019
final *R* indices	R_1 = 0.0873	R_1 = 0.0945
[$I > 2\sigma(I)$]	R_w = 0.2201	R_w = 0.2215
final *R* indices	R_1 = 0.1077	R_1 = 0.1233
final *R* indices (all data)	R_w = 0.2348	R_w = 0.2334

Summary Remarks

Herein we have reported the synthesis of a series of tridentate NOO Schiff base ligands along with their aluminum complexes. These metal complexes were dimeric and exhibited two isomeric structures, one with the initiators on the two aluminum centers *cis* to one another and the other with the *trans* arrangement. The latter form was shown to be thermodynamically more stable by variable-temperature ^{1}H NMR studies. All complexes were shown to polymerize *rac*-lactide in toluene at 70 °C. The molecular weights of the afforded polylactides correlated well with monomer/initiator and conversion level and displayed narrow distributions with PDI values ranging from 1.03 to 1.08. It was established that complexes which existed in both *cis* and *trans* forms under the conditions of the ring-opening polymerization reaction led to partial

epimerization of D- and L-lactide to *meso*-lactide prior to polymerization. On the other hand, complexes which exist in the *trans* isomeric form led to polymerization of *rac*-lactide with no epimerization and concomitantly a polylactide with a high degree of isotacticity (P_m = 76%). More detailed studies of the mechanistic aspects of the ROP of lactides, employing a complete series of structurally well-characterized aluminum dimeric complexes will be presented in Chapter V.

CHAPTER V

RING-OPENING POLYMERIZATION OF CYCLIC ESTERS AND TRIMETHYLENE CARBONATE CATALYZED BY ALUMINUM HALF-SALEN COMPLEXES

Introduction

Much research is currently focused on the development of polymers with sophisticated macromolecular structures derived from renewable resources.[73] Among the most well-studied of these non-petrochemical based polymeric materials are those synthesized from lactides. Polylactides (PLA) which originate from replenishable resources such as corn, wheat, and sugar beets are biodegradable polymers widely used not only in commodity plastics, *i.e.*, the textile industry,[74] but also in medical applications such as drug delivery[64a, 75] and tissue engineering.[6a, 6b] On the other hand, polyhydroxybutyrate (PHB) is an aliphatic polyester produced by a variety of microorganisms and bacteria.[76] Hence, PHB can be degraded by microorganisms and used as a source of internal energy and carbon reserve. Importantly, over 300 bacterial species are known to synthesize polyhydroxyalkonoates (PHAs).[77] The mechanical properties of PHB are similar to those of petrochemical-based polymers, allowing PHB to be a potential replacement polymer for the packaging and agricultural industries.[77-78] It is also worthy to note that both PLA and PHA exhibit very good green design assessments as well as moderate life cycle assessments.[79]

Poly-ε-caprolactone (PCL) and poly-δ-valerolactone (PVL) are other examples of biobased aliphatic polyesters that have emerged as important materials in industrial processes that require biodegradable high performance plastics. In addition, PCL, because of various valuable properties of the polymer, finds uses in the construction industry.[80] Polytrimethylene carbonate (PTMC) is a biodegradable polymer which degrades without forming acidic compounds. This property of PTMC makes it ideal for applications involving protein delivery, since low pH conditions tend to lead to protein denaturation.[81] Although these biobased polymers can be employed in numerous applications, a common use of these biodegradable polymers is in drug delivery, for they are readily removed from the human body *via* normal metabolic pathways.[54c]

We have recently demonstrated in Chapter IV that aluminum half-salen complexes are effective catalysts for the ring-opening polymerization (ROP) of *rac*-lactide.[60] Herein, we wish to report extensive studies of these catalysts for the ring-opening polymerization of cyclic monomers, *rac*-lactide, trimethylene carbonate (TMC), *rac*-β-butyrolactone (*rac*-β-BL), δ-valerolactone (δ-VL), and ε-caprolactone (ε-CL). Included in these investigations are X-ray structural analysis of the aluminum complexes, kinetic studies for the ROP of various cyclic monomers, as well as kinetic studies of copolymerization reactions of *rac*-lactide and δ-VL.

Experimental Section

Methods and Materials. All manipulations were carried out using a double manifold Schlenk vacuum line under an argon atmosphere or an argon filled glove box unless otherwise stated. Toluene was freshly distilled from sodium/benzophenone before

use. Methanol and dichloromethane were purified by an MBraun Manual Solvent Purification System packed with Alcoa F200 activated alumina desiccant. Pentane was freshly distilled from CaH_2. Deuterated chloroform, deuterated benzene and deuterated toluene from Cambridge Isotope Laboratories Inc. were stored in the glove box and used as received. L-, D-lactide and *rac*-lactide were gifts from PURAC America Inc. These lactides were recrystallized from toluene, dried under vacuum at 40 ^{o}C overnight, and stored in the glove box. β-butyrolactone, γ-butyrolactone, δ-valerolactone and ε-caprolactone were distilled under vacuum from CaH_2 and storred in the glove box. Trimethylene carbonate (Boehringer Ingelheim) was recrystallized from tetrahydrofuran and diethyl ether, dried under vacuo and stored in the glove box. 4-amino-1-butanol and triethylaluminium were purchased from TCI America and Sigma-Aldrich respectively and used without further purification. Ethanolamine, 3-amino-1-propanol, 5-amino-1-pentanol, *trans*-2-aminocyclohexanol hydrochloride, 2-hydroxy-3-methoxybenzaldehyde, *rac*-methionine, *rac*-phenylalanine, and *tert*-butyldimethylchlorosilane were purchased from Alfa Aesar and used as received. 3,5-di-*tert*-butyl-2-hydroxybenzaldehyde, 3-(*tert*-butyldimethylsilyl)-2-hydroxy-5-methylbenzaldehyde, and 2-hydroxy-5-methyl-3-(triphenylsilyl)benzaldehyde were prepared according to published procedure.[40c, 40d, 48b, 71] All other compounds and reagents were obtained from Sigma-Aldrich and were used without further purification. The preparation and spectral characterization of all ligands and their aluminum complexes have previously been reported in detail in an earlier publication.[60] Analytical elemental analysis was provided by Canadian Microanalytical Services Ltd.

Measurements. ^{1}H NMR spectra were recorded on Unity+ 300 or 500 MHz and VXR 300 or 500 MHz superconducting NMR spectrometers. Molecular weight determinations were carried out with Viscotek Modular GPC apparatus equipped with ViscoGEL^{TM} I-series columns (H + L) and Model 270 dual detector comprised of refractive index and light scattering detectors. DSC measurements were performed with a Polymer DSC by Mettler Toledo. The samples were scanned from -100 ^{o}C to 200 ^{o}C under nitrogen atmosphere. The glass transition temperature (T_g), was determined from the 2nd heating at heating rate of 5 ^{o}C/min. X-ray crystallography was done on a Bruker GADDS X-ray diffractometer in a nitrogen cold stream maintained at 110K. Crystal data and details of the data collection for complexes **V2a, V3b, V2d, V2f** (***cis***), **V2f** (***trans***), **V3e**, **V4e** are provided in Tables on pages 127-128.

Lactide Polymerization Procedure. In a typical experiment carried out in the argon filled glovebox a Teflon-screw-capped heavy walled pressure vessel containing the corresponding aluminum complex (**V2a-k**) and 50 equivalents of *rac*-lactide (per aluminum center) in 1.00 mL of toluene was stirred at 70 ^{o}C for the designated time period. Upon removal of a small sample of the crude product *via* syringe, it was analyze by ^{1}H NMR spectroscopy in $CDCl_3$. The product was isolated and purified by precipitation from dichloromethane by the addition of 5% hydrochloric acid in methanol. The solid polymer was collected and dried under vacuum to constant weight.

Kinetic Studies for Homopolymers. In a typical experiment carried out in the argon filled glovebox (Table on page 111, entry 3), a J. Young NMR tube containing 0.41 mmol of an appropriate monomer (*rac*-lactide, trimethylene carbonate (TMC), *β*-

butyrolactone, γ-butyrolactone, δ-valorolactone, or ε-caprolactone) was added 0.1 ml of complex **V2g** in deuterated toluene from a 8.94 mM stock solution. Next, 0.5 ml of deuterated toluene was added to adjust the total volume to 0.6 ml. The NMR tube was then placed to the preheated NMR spectrometer at corresponding temperature (70-105 ^{o}C, typically 90 ^{o}C), and the % conversion was investigated from the integration of polymer and monomer signals. The characteristic chemical shift for each monomer in deuterated toluene is 4.12 (q, -C*H*-; lactide), 3.62(m, -CH_2-; TMC), 3.93 (m, -C*H*-; β-butyrolactone), 3.63 (t, -CH_2-; δ-valerolactone), and 3.63 (m, -CH_2-; ε-caprolactone). The characteristic chemical shif for each polymer in deuterated toluene is 5.12 (q, -C*H*-; polylactide), 4.06(t, -CH_2-; TMC), 5.31 (m, -C*H*-; poly-β-butyrolactone), 3.95 (t, -CH_2-; poly-δ-valerolactone), and 4.00 (t, -CH_2-; poly-ε-caprolactone).

Kinetic Studies for Copolymers. In a typical experiment carried out in the argon filled glovebox (Table on page 110, entry 3), a J. Young NMR tube containing 0.41 mmol of *rac*-lactide and 0.41 mmol of δ-VL was added 0.1 ml of complex **V2g** in deuterated toluene from a 8.94 mM stock solution. Next, 0.5 ml of deuterated toluene was added to adjust the total volume to 0.6 ml. The NMR tube was then placed to the preheated NMR spectrometer at corresponding temperature (70-105 ^{o}C, typically 90 ^{o}C), and the % conversion was investigated from the integration of polymer and monomer signals.

Results and Discussions

Synthesis and X-ray Structural Characterization of Aluminum Complexes. As described in our earlier report the aluminum complexes were prepared by treatment

of the appropriate Schiff base ligand with a stoichiometric quantity of $AlEt_3$ in dry toluene.[60] Scheme V-1 illustrates the synthesis of these dimeric aluminum complexes, along with their designated numeric label, derived from the reaction of triethylaluminum and chiral amino alcohols (**V2a-d**), aliphatic amino alcohols (**V2e-i**), and amino acids (**V2j**,**k**). Suitable single crystals of the chiral amino alcohol complexes **V2a** and **V2d** were obtained upon recrystallization from dichloromethane at -10 ^{o}C. On the other hand, the other two derivatives, **V2b** and **V2c**, failed to provide single crystals under similar conditions. Instead the addition of one equivalent of benzyl alcohol to a crystal tube containing complex **V2b** afforded crystals of complex **V3b**, where the ethyl group was replaced by the benzyloxide group as evidenced by X-ray crystallography (Scheme V-2).

Scheme V-1

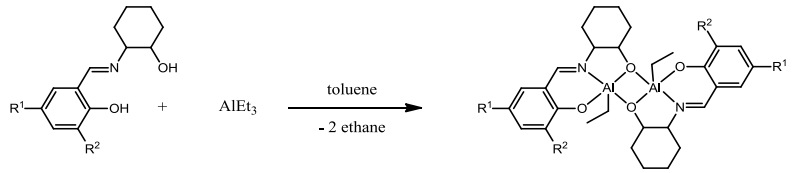

V1a : R^1 = *t*-Bu, R^2 = *t*-Bu
V1b : R^1 = H, R^2 = OMe
V1c : R^1 = Me, R^2 = $SiPh_3$
V1d : R^1 = Me, R^2 = $SiMe_2{}^tBu$

V2a : R^1 = *t*-Bu, R^2 = *t*-Bu
V2b : R^1 = H, R^2 = OMe
V2c : R^1 = Me, R^2 = $SiPh_3$
V2d : R^1 = Me, R^2 = $SiMe_2{}^tBu$

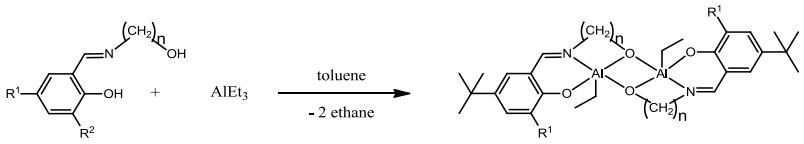

V1e : n = 2, R^1 = *t*-Bu, R^2 = *t*-Bu
V1f : n = 3, R^1 = *t*-Bu, R^2 = *t*-Bu
V1g : n = 4, R^1 = *t*-Bu, R^2 = *t*-Bu
V1h : n = 5, R^1 = *t*-Bu, R^2 = *t*-Bu
V1i : n = 4, R^1 = Me, R^2 = $SiMe_2{}^tBu$

V2e : n = 2, R^1 = *t*-Bu, R^2 = *t*-Bu
V2f : n = 3, R^1 = *t*-Bu, R^2 = *t*-Bu
V2g : n = 4, R^1 = *t*-Bu, R^2 = *t*-Bu
V2h : n = 5, R^1 = *t*-Bu, R^2 = *t*-Bu
V2i : n = 4, R^1 = Me, R^2 = $SiMe_2{}^tBu$

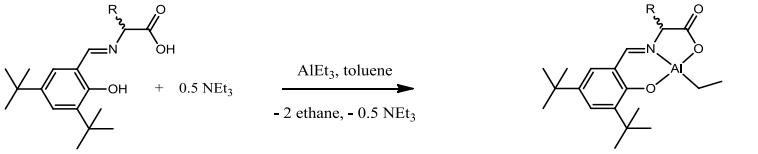

V1j : R = 2-(methylthio)ethyl
V1k : R = benzyl

V2j : R = 2-(methylthio)ethyl
V2k : R = benzyl

Scheme V-2

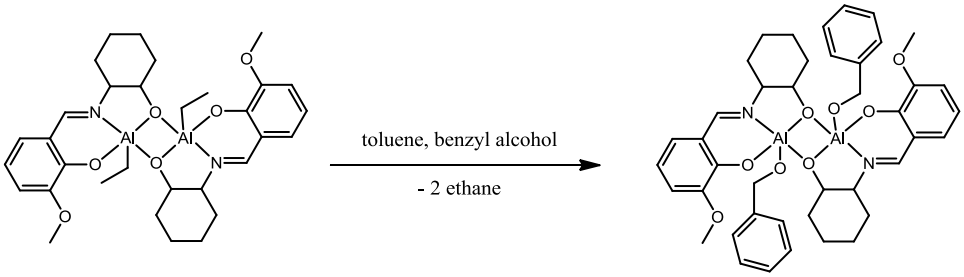

V2b **V3b**

The X-ray structures of the closely related aluminum complexes **V2a**, **V2d**, and **V3b** derived from chiral amino alcohols are illustrated in Figure V-1, where all

complexes are shown to be dimeric. The aluminum centers coordinated to these Schiff base ligands are held together by bridging oxygen atoms with each metal adopting a distorted-bipyramidal geometry with an ethyl group (**V2a** and **V2d**) or a benzyloxide (**V3b**) on the metal centers arranged *cis* to one another. Selected bond distances and bond angles for these derivatives are provided in Table V-1. All bond lengths within the three complexes are quite similar with the exception of the Al(1)–O(1) distance which is slightly shorter in complex **V3b** as a result of the electron donating methoxy substituent on the phenoxide ring. The bond angles in complex **V3b** were also found to be slightly different from those in complexes **V2a** and **V2d** due to less steric hindrance of OMe as compared to the bulky ^{t}Bu and SiMe$_2$^{t}Bu substituents on the phenoxide ring.

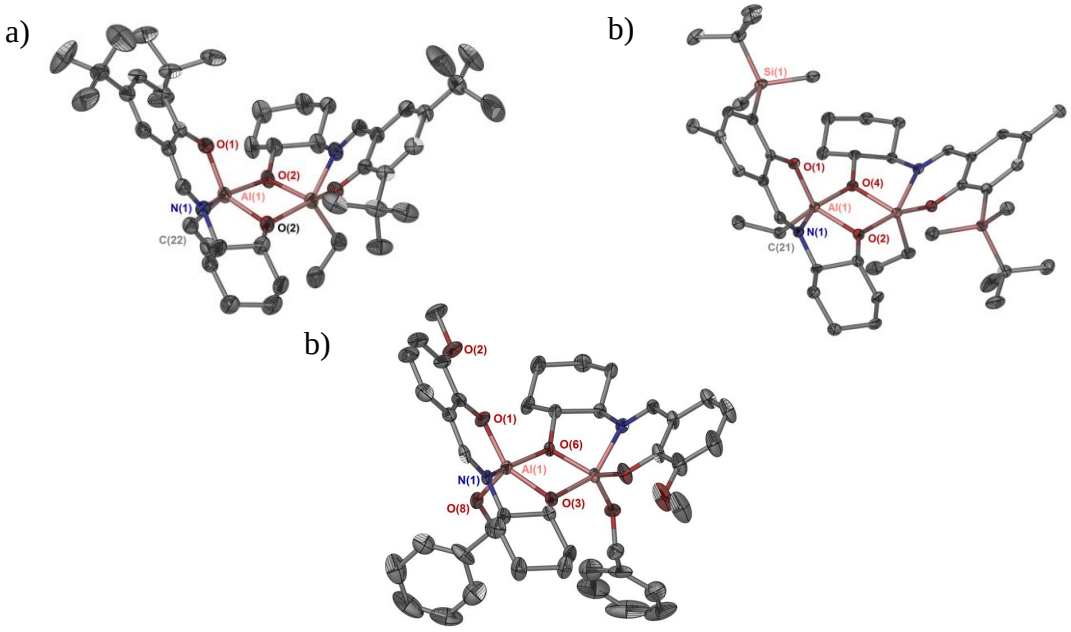

Figure V-1. X-ray crystal structures of (a) complex **V2a**, (b) complex **V2d**, and (c) complex **V3b**. Thermal ellipsoids represent the 50% probability levels with hydrogen atoms omitted for the sake of clarity.

Table V-1. Selected Bond Lengths (Å) and Angles (deg) for Al Complexes **V2a**, **V2b**, **V2d**, **V2f** (*cis*-), **V2f** (*trans*-), and **V2g** (*trans*-).

	V2a	**V2b**	**V2d**	**V2f** (*cis*-)	**V2f** (*trans*-)	**V2g**
			Bond lengths			
Al1-O1	1.811 (2)	1.778 (3)	1.8142 (15)	1.796 (3)	1.797 (4)	1.792 (4)
Al1-N1	2.011 (3)	1.978 (4)	2.2041 (18)	2.030 (4)	2.034 (4)	2.047 (5)
Al1-X[a]	1.873 (2)	1.850 (3)	1.8716 (15)	1.846 (3)	1.851 (3)	1.831 (5)
Al1-Y[b]	1.899 (2)	1.899 (3)	1.8959 (15)	1.915 (3)	1.905 (3)	1.935 (5)
Al1-Z[c]	1.963 (3)	1.733 (3)	1.977 (2)	1.992 (5)	1.993 (5)	2.002 (7)
			Bond angles			
O1-Al1-N1	88.31 (10)	90.26 (16)	88.93 (7)	88.75 (14)	89.83 (16)	90.3 (2)
O1-Al1-X[a]	94.78 (10)	92.39 (15)	97.19 (7)	89.61 (13)	92.14 (16)	91.3 (2)
[a]X-Al1-Y[b]	75.30 (10)	76.66 (14)	74.61(6)	75.94 (14)	74.91 (17)	77.2 (2)
[b]Y-Al1-N1	79.52 (10)	82.12 (15)	79.36 (7)	88.58 (14)	87.52 (16)	90.6 (2)
O1-Al1-Z[c]	111.65 (13)	108.04 (18)	110.56 (8)	113.62 (17)	113.4 (2)	116.2 (3)
N1-Al1-X[a]	147.29 (11)	145.38 (16)	149.03 (7)	157.52 (15)	158.63 (17)	167.1(2)

[a]X = O2 (red), O6, O2, O2 (red), O2 (red), O2 (red) in **V2a**, **V2b**, **V2d**, **V2f** (*cis*-), **V2f** (*trans*-), **V2g** respectively. [b]Y = O2 (black), O3, O4, O2 (black), O2 (black), O2 (black) in **V2a**, **V2b**, **V2d**, **V2f** (*cis*-) respectively. [c]Z = C22, O8, C21, C19, in **V2a**, **V2b**, **V2d**, **V2f** (*cis*-) respectively.

The solid state structures of the aliphatic amino alcohol derivatives of aluminum were also obtained in this study. As we previously noted based on variable-temperature ^{1}H NMR studies, in these instances the isomer isolated, *i.e.*, *cis* or *trans* arrangement of apical ligands, depends on temperature.[60] For example, complex **V2g** was recrystallized following heating of the complex at 50 ^{o}C in methylene chloride in a sealed tube until complete dissolution. Upon cooling the solution and maintaining it at -10 ^{o}C, the *trans*

isomer was exclusively afforded (Figure V-2a). On the other hand, complex **V2f** was dissolved in methylene chloride at ambient temperature and kept at -10 ^{o}C resulting in formation of crystals of both *cis* and *trans* isomers. The two five-coordinate aluminum centers in this series of aluminum complex possess distorted-bipyramidal geometries with the ethyl groups on each metal center *cis* to one another in complex **V2f** (*cis*) and *trans* to each other in complex **V2f** (*trans*) and **V2g**. Thermal ellipsoid representations of these structures are shown in Figure V-2, with selected bond distances and bond angles listed in Table V-1. Although we have thusfar not been successful in obtaining crystals of complexes **V2j** and **V2k**, these are most likely similarly dimeric in structure.

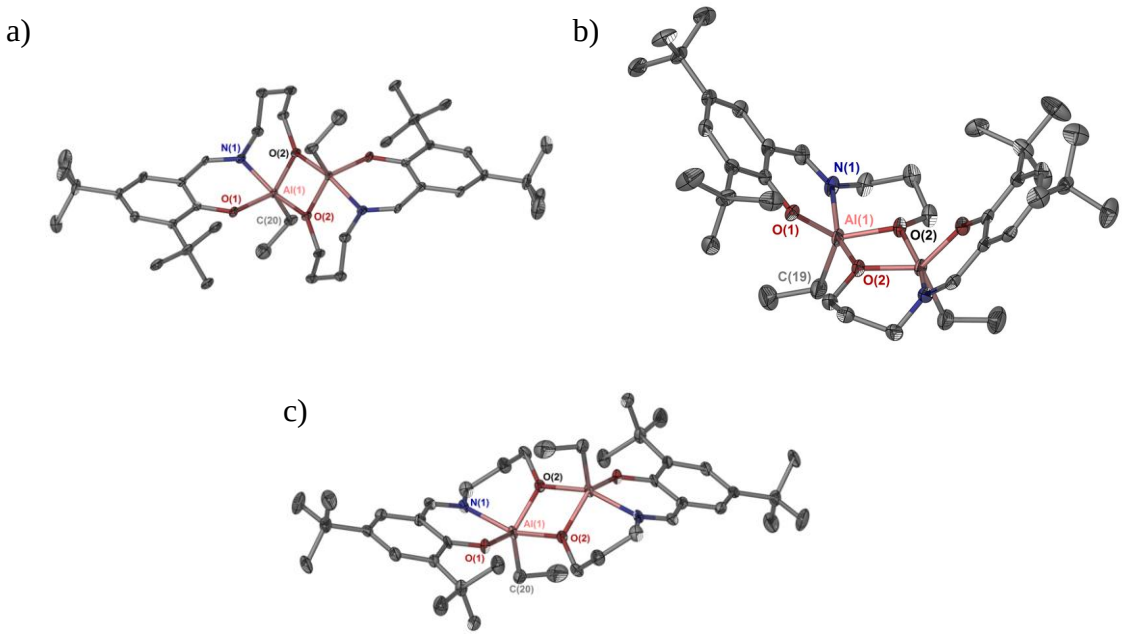

Figure V-2. X-ray crystal structures of (a) **V2g** (*trans*-), (b) **V2f** (*cis*), and (c) **V2f** (*trans*-). Thermal ellipsoids represent the 50% probability surfaces. Hydrogen atoms are omitted for the sake of clarity.

Polymerization Studies: **Ring-Opening Polymerization of Lactides**. The aluminum complexes shown in Scheme V-1 were examined as catalysts for the ROP of *rac*-lactide in solution, where Table V-2 summarizes the relative reactivity and selectivity observed for this polymerization process under similar reaction conditions. Although complex **V2a** was not efficient at catalyzing *rac*-lactide in $CDCl_3$ after an extended period of time at 60 ^oC

Table V-2. Reactivity and Selectivity of Aluminum Complexes **V2a-k** for the ROP of *Rac*-Lactide.[a]

entry	M	time (h)	conversion (%)[b]	*meso*-[c]	M_n		PDI	P_m[f]
					Theoretical[d]	$0.58M_{n,GPC}$[e]		
1	**V2a**[g]	20	0	no				
2	**V2a**[h]	66	0	yes				
3	**V2a**	15	0	yes				
4	**V2a**	66	57	yes	4 107	7 938	1.05	70
5	**V2b**	15	0	yes				
6	**V2b**	69	43	yes	3 243	3 844	1.08	<50
7	**V2c**	15	0	yes				
8	**V2c**	168	45	yes	3 207	4 962	1.09	<50
9	**V2d**	15	0	yes				
10	**V2e**	15	64	yes	4 614	6 987	1.04	62
11	**V2f**	15	0	yes				
12	**V2g**	15	34	no	2 446	2 456	1.07	76
13	**V2h**	15	50	no				73
14	**V2i**	15	21	no				82
15	**V2j**	15	36	no	2 594	3 916	1.07	74
16	**V2k**	15	42	no	3 026	4 043	1.03	72

[a] Unless otherwise specified, the polymerization reactions were performed in sealed reaction tubes with the following conditions: [*rac*-LA]/[Al] = 50, in toluene at 70 ^oC.[b] Obtained from ^1H NMR spectroscopy. [c] *meso*-lactide was obtained from epimerization of L- or D-lactide during the polymerization process. [d] Theoretical M_n = (M/I) x (% conversion) x (mol. wt. of lactide). [e] M_n values were corrected by the equation: $M_n = 0.58\ M_{n,\ GPC}$.[51] [f] P_m values were calculated from the ratio of the (area of iii)/(total area in methine proton region). [g]$CDCl_3$ was used as the solvent at ambient temperature. [h] $CDCl_3$ was used as the solvent at 60 ^oC.

(*entry 2*); over the same time period a 57% conversion to polylactide was noted in toluene at 70 ^{o}C (*entry 4*). In the series of aluminum complexes **V2a-d** when the substituents (R^2) on the phenoxide portion of the Schiff base ligand increased in size (R^2 = $SiPh_3$) or is more electron donating (R^2 = OMe), the rate of polymerization decreased (*entries 6 and 8*). Similar results have been reported previously in related systems by Gibson and coworkers, as well as by Nomura and coworkers.[12, 17] Complex **V2a** afforded a moderately isotactic polylactide with a P_m value of 0.70, whereas, complexes **V2b**, **c** produced atactic polylactide with P_m values less than 0.50. The aluminum complexes with achiral aliphatic backbones with the exception of **V2f**, *i.e.*, complexes **V2e**, **g**, **h**, **I** were observed to polymerize *rac*-lactide at faster rates than complex **V2a** to provide isotactic polymers with P_m values of 0.62, 0.76, 0.73, and 0.82, respectively. It should also be noted here that when the substituents on the phenoxide (R^2) of the half-salen ligand in the series of complexes **V2e-i** increased in size from ^{t}Bu to $SiMe_2{}^{t}$Bu, the percent of isotacticity of the polymer increased from 0.76 to 0.82.

The complexes derived from *rac*-amino acids, **V2j** and **V2k**, were also active for catalyzing the ROP of *rac*-lactide, providing isotactic polylactide with P_m values of 0.74 and 0.72 as shown in Table V-2. Previously we established that aluminum complexes which existed in both *cis* and *trans* forms, e.g., **V2e** and **V2f**, under conditions of the ring-opening polymerization reaction led to partial epimerization of D- and L-lactide to *meso*-lactide prior to polymerization.[60] Similarly, upon utilizing complexes **V2a-d** as catalysts for the ROP of *rac*-lactide, *meso*-lactide was observed to be produced during the polymerization process. Presumably, the *cis* isomeric form of the series of complexes

V2a-d is responsible for the formation of *meso*-lactide. As evident from X-ray crystallography only the *cis* isomeric form of complexes **V2a**, **V3b**, and **V2d** was obtained in the solid state. On the contrary, when complexes which exist in the *trans* isomeric form are used to catalyze the ROP of *rac*-lactide in toluene at 70 ^{o}C, no epimerization was observed and concomitantly a polylactide was produced with a high degree of isotacticity (P_m = 82%).

There are two proposed mechanisms for the stereoselective ROP of *rac*-lactide,[13c] that is, an enantiomorphic site-control,[13a, 13b] and a chain-end control mechanism.[12] Chisholm and coworkers have shown in addition to chiral ligands bound to aluminum centers, other factors can also contribute to the stereoselectivity in the ROP of lactides when utilizing aluminum salen complexes as catalysts.[18, 39o] These include considerations of the chirality of the initiator as well as the solvent. In order to better understand the origin of the stereoselectivity of *rac*-lactide during the polymerization process in our catalytic system, we attempted to obtain crystal structures of lactide binding to the aluminum centers in our complexes. The ethyl group on the aluminum center can be removed upon reaction with $[H(OEt_2)_2]^+[B(C_6H_3(CF_3)_2)_4]^-$ as illustrated in equation 1 in Scheme V-3. Zwitterion formation and aryl transfer to aluminum can be avoided when using the non-nucleophilic $[B(C_6H_3(CF_3)_2)_4]^-$ as counter anion.[82] X-ray quality crystals obtained from a $CHCl_3$ solution of complex **V2e** in the presence of $[H(OEt_2)_2]^+[B(C_6H_3(CF_3)_2)_4]^-$ and one equivalent of *rac*-lactide were found to consist of two morphological forms, *i.e.*, plate-like and block-like crystals. The plate-like crystals were shown to be a tetrameric aluminum complex with two $[B(C_6H_3(CF_3)_2)_4]^-$ counter

Scheme V-3

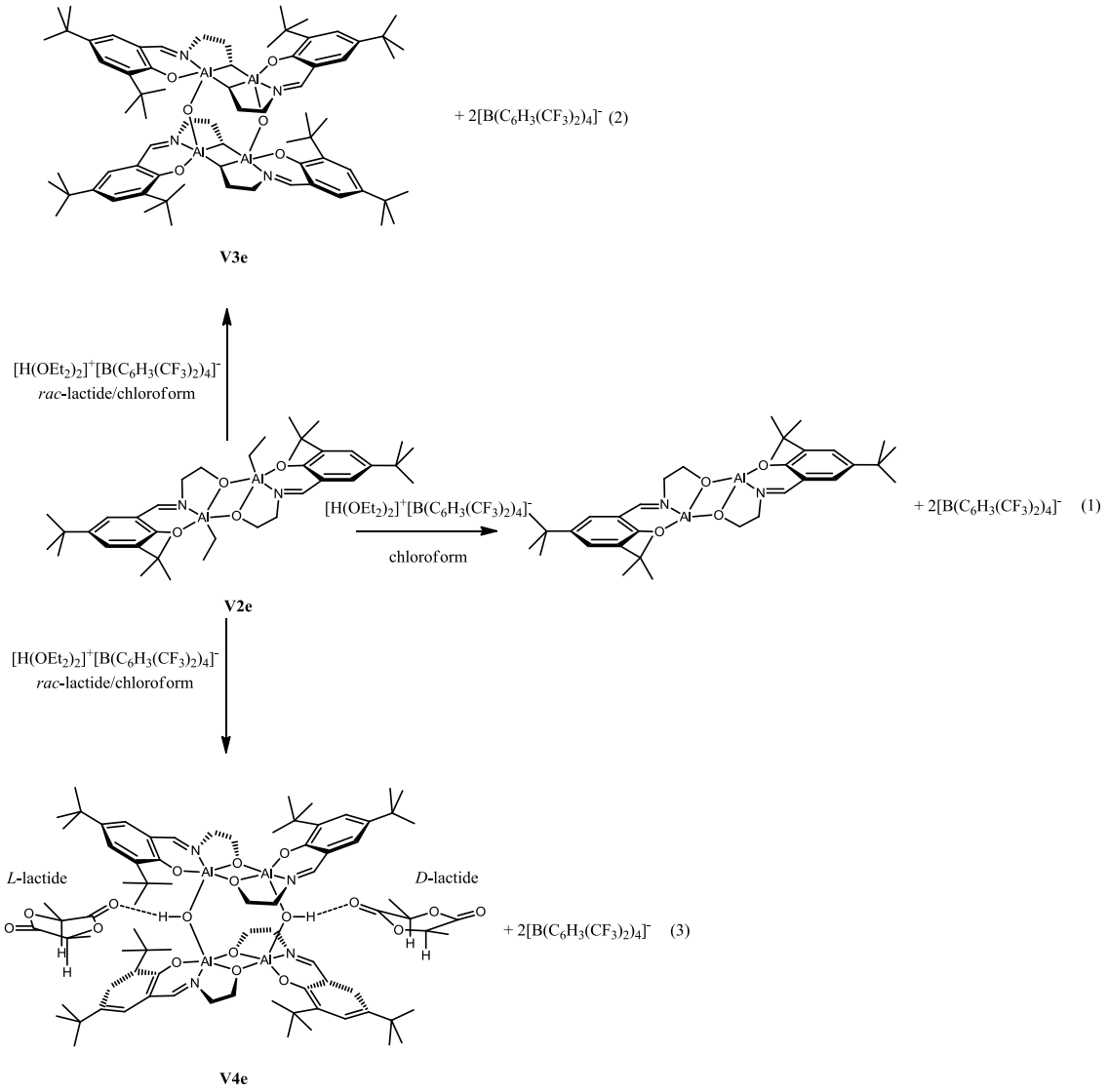

ions. All four aluminum centers are five-coordinate with bridging oxygen atoms from the Schiff base ligands and hydroxyl groups as illustrated in Figure V-3 and Scheme V-3, equation 2. The molecular structure of the block-like crystals are also tetrameric and similar to that observed in **V3e**, except the ^{t}Bu substituents were found in this derivative, complex **V4e**, on opposite sides as seen in Figure V-4 and Scheme V-3, equation 3. In

addition, complex **V4e** contains two lactide molecules located between the phenoxides of the half-salen ligands with hydrogen bonds from the carbonyl oxygen of the lactide to the bridging hydroxyl ligands (1.876 Å). Both L-lactide (left) and D-lactide (right) were found in the solid state structure as shown in Figure V-4 and Scheme V-3, equation 3. This observation suggests that the stereoselectivity noted for the ROP of *rac*-lactide in the presence of the aluminum complexes **V2e-i** results from an enantiomorphic site control mechanism dictated by the bulky ^{t}Bu substituents in the R^1 position. The bond distance of Al1–O9 of 1.805 Å lies within the range of those reported in the literature.[83] We assume the hydroxyl bridging ligands result from adventitious water being present during the crystal growth process.

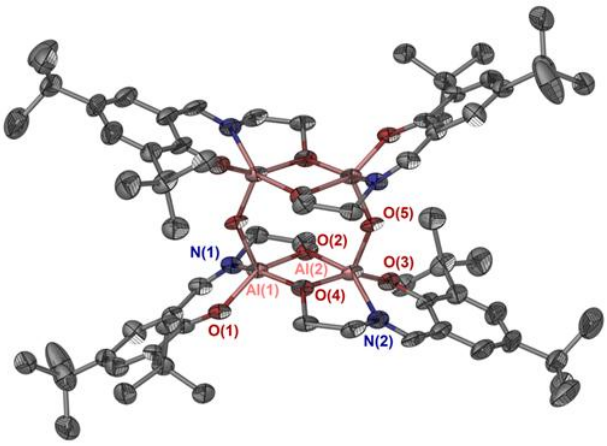

Figure V-3. X-ray crystal structure of complex **V3e**. Thermal ellipsoids represent the 50% probability surfaces. Hydrogen atoms and $2[B(C_6H_3(CF_3)_2)_4]^-$ are omitted for the sake of clarity. Selected bond lengths (Å) and angles (deg): Al1-N1: 1.944 (4), Al1-O1: 1.779 (4), Al1-O2: 1.873 (4), Al1-O4: 1.862 (3), Al2-N2: 1.959 (4), Al2-O3: 1.765 (4), Al2-O4: 1.876 (4), Al2-O5: 1.817 (4), N1-Al1-O1: 92.06 (18), N1-Al1-O2: 82.50 (17), O1-Al1-O4: 96.97 (16), O2-Al1-O4: 76.15 (15), N1-Al1-O4: 150.00 (19), O1-Al1-O2: 152.03 (17), N2-Al2-O3: 91.67 (19), N2-Al2-O4: 81.80 (17), O2-Al2-O4: 76.79 (15), O2-Al2-O3: 97. 18 (17), N2-Al2-O2: 150.29 (19), O3-Al2-O4: 151.12 (18), O3-Al2-O5: 105.53 (18).

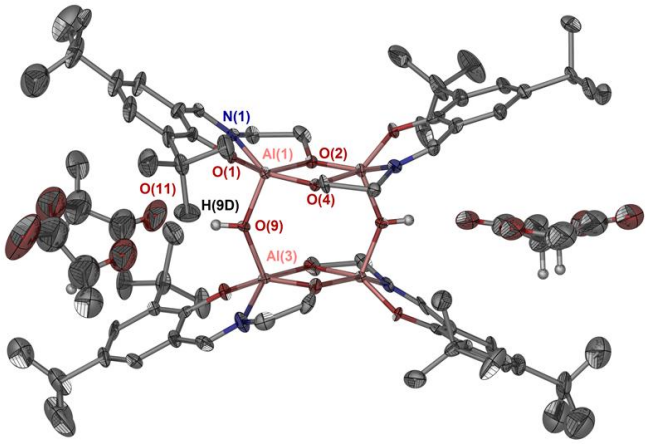

Figure V-4. X-ray crystal structure of complex **V4e**. Thermal ellipsoids represent the 50% probability surfaces. Hydrogen atoms and $2[B(C_6F_5)_4]^-$ are omitted for the sake of clarity. Selected bond lengths (Å) and angles (deg): Al1-N1: 1.948 (8), Al1-O1: 1.756 (7), Al1-O2: 1.886 (6), Al1-O4: 1.839 (6), Al1-O9: 1.805 (6), O11-H9D: 1.876 (8), N1-Al1-O1: 92.4 (3), N1-Al1-O2: 81.7 (3), O2-Al1-O4: 76.5 (3), O1-Al1-O4: 96.7 (3), N1-Al1-O4: 149.7 (3), O1-Al1-O2: 151.4 (3), O1-Al1-O9: 104.6 (3), Al1-O9-Al3: 139.2 (3).

Ring-Opening of Other Cyclic Monomers. Complex **V2g** was selected to investigate the ring-opening polymerization for other cyclic monomers (Chart V-1) because of its greater reactivity and selectivity compared to the other aluminum complexes for the ROP of lactides. Table V-3 summarizes the reactivity of complex **V2g** for the various cyclic monomers in toluene at 70 ^oC with a monomer:initiator of 50:1. The percent conversion of each monomer to polymer was monitored by ^1H NMR after 15 h of reaction, with the resulting polymers isolated and purified by precipitation from CH_2Cl_2 with 5% HCl in methanol followed by drying in vacuo.

Chart V-1

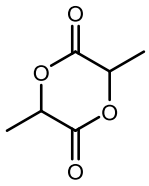

lactide

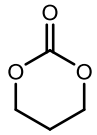

TMC

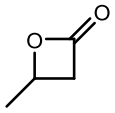

β-butyrolactone

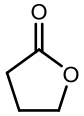

γ-butyrolactone

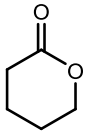

δ-valerolactone

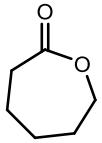

ε-caprolactone

Table V-3. Reactivity of Aluminum Complex **V2g** for the ROP of Cyclic Monomers.[a]

entry	Monomer	conversion (%)[b]	M_n		PDI
			Theoretical[c]	$M_{n,GPC}$	
1	*rac*-lactide	34	2 446	2 456[d]	1.07
2	TMC	99	5 050	2 567	1.66
3	*rac*-β-butyrolactone	26	1 118	1 450	1.23
4	γ-butyrolactone[e]	0	N/A	N/A	N/A
5	δ-valerolactone	30	1 501	1 819	1.89
6	ε-caprolactone	99	5 649	2 356	1.75

[a] Unless otherwise specified, the polymerization reactions were performed in sealed reaction tubes with the following conditions: monomer/[Al] = 50, in toluene at 70 ^{o}C.[b] Obtained from ^{1}H NMR spectroscopy. [c] Theoretical M_n = (M/I) x (% conversion) x (mol. wt. of lactide). [d] M_n values were corrected by the equation: $M_n = 0.58\ M_{n,\ GPC}$.[51] [e]The reaction was both performed in toluene at 70 and 105 ^{o}C.

As indicated in Table V-3, complex **V2g** was found to catalyze all of the cyclic monomers examined except for the five-membered cyclic lactone (γ-butyrolactone), even at 105 ^{o}C in toluene. This is explained based on the fact that the geometric

distortion in the ester group in γ-butyrolactone is much less than that in δ-valerolactone resulting in lower ring strain.[84] Complex **V2g** was more effective at catalyzing the ROP of trimethylene carbonate and ε-caprolactone than the other cyclic monomer, with 99% conversion being observed in 15 h. Although complex **V2g** catalyzed the ROP of *rac*-lactide to isotactic polylactide with a P_m value of 0.76, β-butyrolactone similarly underwent ROP to afford an atactic polymer as evidenced by ^{13}C NMR spectroscopy.[85]

Table V-4. Polylactide Produced from the ROP of *Rac*-Lactide in Toluene at 70 ^{o}C.

entry	M/I	conversion (%)[a]	M_n			PDI
			Theoretical[b]	GPC	$0.58M_{n,GPC}$[c]	
1	115	96	15 913	28 024	16 254	1.12
2	155	96	21 448	40 598	23 457	1.09
3	230	96	31 826	59 694	34 632	1.18
4	460	96	63 552	109 513	63 518	1.10

[a] Obtained from ^{1}H NMR spectroscopy. [b] Theoretical M_n = (M/I) x (% conversion) x (mol. wt. of lactide). [c] M_n values were corrected by the equation: $M_n = 0.58\ M_{n,\ GPC}$.[51]

Table V-5. Poly-β-Butyrolactone Produced from the ROP of *Rac*-Lactide in Toluene at 70 ^{o}C.

entry	M/I x monmer conversion	M/I	conversion (%)[a]	M_n		PDI
				Theoretical[b]	GPC	
1	142	160	89	12 347	12 753	1.12
2	177	217	82	15 235	15 601	1.22
3	202	317	64	17 552	18 248	1.28

[a] Obtained from ^{1}H NMR spectroscopy. [b] Theoretical M_n = (M/I) x (% conversion) x (mol. wt. of β-butyrolactone).

The dependence of the molecular weights of polylactide and poly-*β*-butyrolactone produced on the monomer/initiator ratios was investigated and the results are provided in Tables V-4 and V-5, respectively. As illustrated in Figure V-5 there is a linear

a)

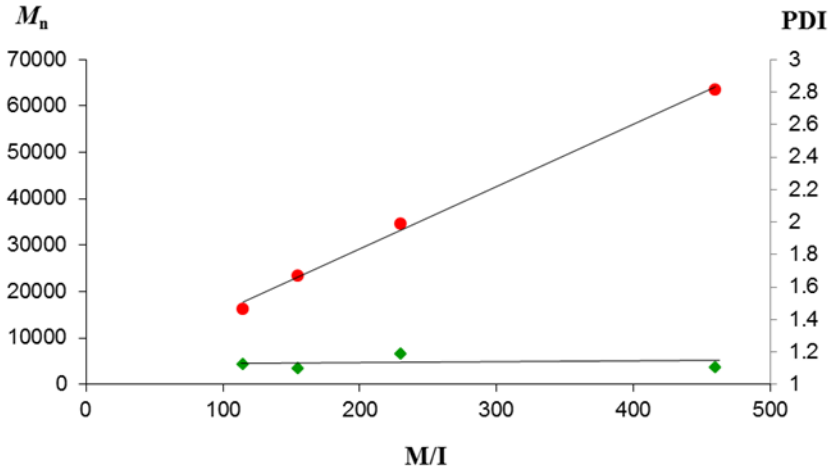

b)

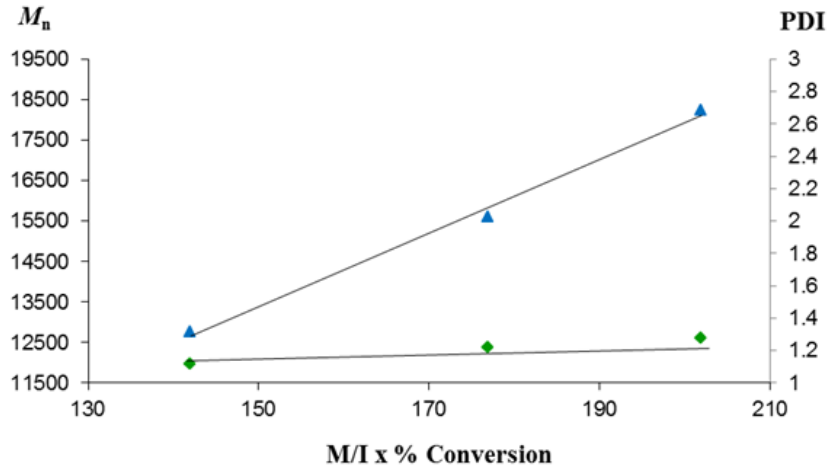

Figure V-5. (a) Linear relationship observed between M_n and monomer/initiator ratio of polylactide from *rac*-lactide catalyzed by complex **V2g** at 70 ^{o}C in toluene. (b) Linear relationship observed between M_n and monomer/initiator ratio of poly-*β*-butyrolactone from *rac*-*β*-butyrolactone catalyzed by complex **V2g** at 70 ^{o}C in toluene.

correlation of M_n and the monomer/initiator ratio, indicative of a well-controlled polymerization process. The living character of these polymerization processes is further noted in the low polydispersities observed, where the PDIs for polylactide and poly-β-butyrolactone span the range of 1.09 – 1.18 and 1.12 – 1.18, respectively. However, the molecular weights of poly(TMC), poly-δ-valerolactone, and poly-ε-caprolactone observed for the polymers produced by the ROP of the corresponding monomers catalyzed by complex **V2g** did not agree with the expected values. Furthermore, the PDIs of these polymers were found to be rather broad, see Table V-3. These results are suggestive of transesterification occurring during the polymerization process possibly resulting from less steric hindrance of the alkoxide formed at the metal center from the ring-opening of these cyclic monomers.

Kinetic Studies of the Ring-Opening Polymerization of *rac*-lactide. Kinetic measurements of the ring-opening polymerization of *rac*-lactide were carried out in modest pressure NMR tubes employing complex **V2g** as catalyst in toluene solution. *It should be noted here that rac-lactide is not very soluble in deuterated toluene at ambient temperature, therefore, all reactions were preheated at 90 ^{o}C prior to be placed in the preheated NMR spectrometer.* The observed rate constants (k_{obsd}) were extracted from a plot of ln(*rac*-LA]$_0$/[*rac*-LA]$_t$) *vs* time (Figure V-6). The reaction order in catalyst concentration was determined from a plot of k_{obsd} *vs* [Al] and the ln[k_{obsd}] *vs* ln[Al] as shown in Figure V-7. As seen from the linearity of the plot of k_{obsd} *vs* [catalyst]

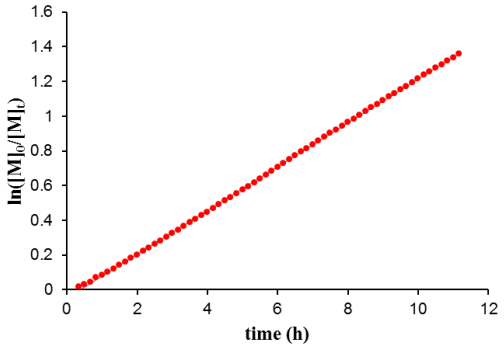

Figure V-6. ln([*rac*-LA]$_0$/[*rac*-LA]$_t$) *vs* time plot depicting a reaction order of unity with respect to monomer concentration (R^2 = 0.999).

as well as the near unity of the slope of the ln[k_{obsd}] *vs* ln[catalyst] plot, the ROP of *rac*-lactide in the presence of complex **V2g** is first order in catalyst concentration. This kinetic data is listed in Table V-6, along with analogous temperature dependent data. The activation parameters for the ROP of *rac*-lactide catalyzed by complex **V2g** in deuterated toluene were determined from the data in Table V-6 to be $\Delta H^{\neq}$ = 59.7 ± 2.8 kJ/mol and $\Delta S^{\neq}$ = -129.1 ± 7.7 J/mol-k (see Eyring plot in Figure V-8). The corresponding free energy of activation for this polymerization process was calculated to be 106.6 kJ/mol at 90 ^{o}C.

a)

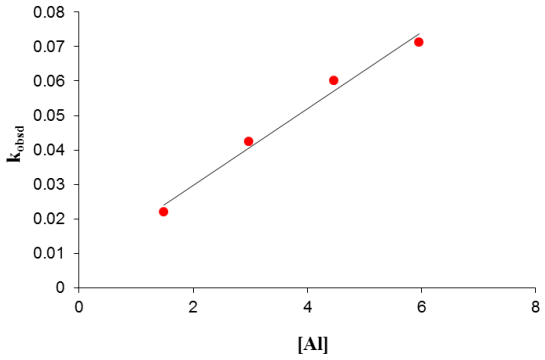

b)

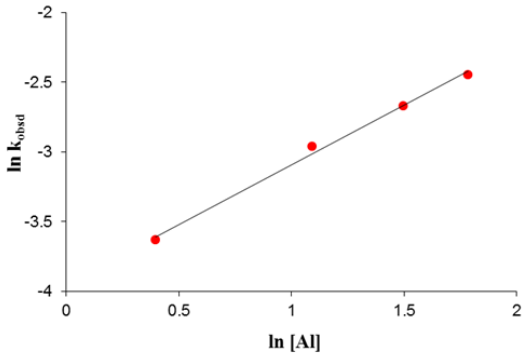

Figure V-7. (a) Plot of k_{obsd} *vs* [Al] with slope = 0.011 and R^2 = 0.984. (b) Plot of ln k_{obsd} *vs* ln[Al] with slope = 0.86 and R^2 = 0.984.

Table V-6. Rate Constants Dependence on the Concentration of the Catalyst (**V2g)** and Temperature for the Ring-Opening Polymerization of *Rac*-Lactide.[a]

entry	[Al] (mM)	temp (^{o}C)	k_{obsd} (h^{-1})	K_p (m^{-1}-sec^{-1})
1	1.49	90	0.0219	
2	2.98	90	0.0424	average value
3	4.47	90	0.0600	3.77×10^{-3}
4	5.96	90	0.0713	
5	4.47	80	0.0304	1.89×10^{-3}
6	4.47	100	0.0985	6.12×10^{-3}
7	4.47	105	0.1263	7.85×10^{-3}

[a] Monomer concentration was held constant at 0.69 M and reactions carried out in toluene-d_8.

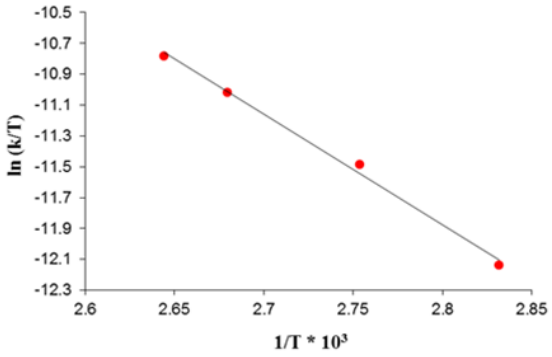

Figure V-8. Eyring plot of ROP of *rac*-lactide in the presence of catalyst **V2g** in toluene-d_8. Slope = -7.180 with R^2 = 0.995.

Kinetic measurements of the ring-opening polymerization of the other cyclic monomers examined in this report were conducted in the same manner as those for *rac*-lactide. The polymerization processes were shown to be first-order in monomer concentration for all monomers investigated as evidenced by the plot of $\ln([M]_0/[M]_t)$ *vs* time as depicted in Figure V-9. Table V-7 listed the k_{obsd} values for each monomer as a function of both catalyst concentration and temperature. It is noteworthy that in each case there is a brief initiation period involved. Furthermore, plots of $\ln[k_{obsd}]$ *vs* ln[Al] as shown in Figure V-10 reveal the order of the reaction with respect to catalyst (**V2g**) concentration to be 0.73, 0.85, 0.48, and 0.55 for the ROP of TMC, *rac*-β-BL, δ-VL, and ε-CL, respectively. Fractional dependencies on [catalyst] have previously been reported for the ROP of lactones with other aluminum complexes.[86] A fractional order on [catalyst] can be explained by an aggregation of the active species during the

polymerization process. Hence, a determination of the propagation rate constant (k_p) in the polymerization process is complicated.[55c] The fractional order will be equal to the reciprocal of the degree of aggregation when the majority of the active species is aggregated and only a small fraction is unaggregated.[87]

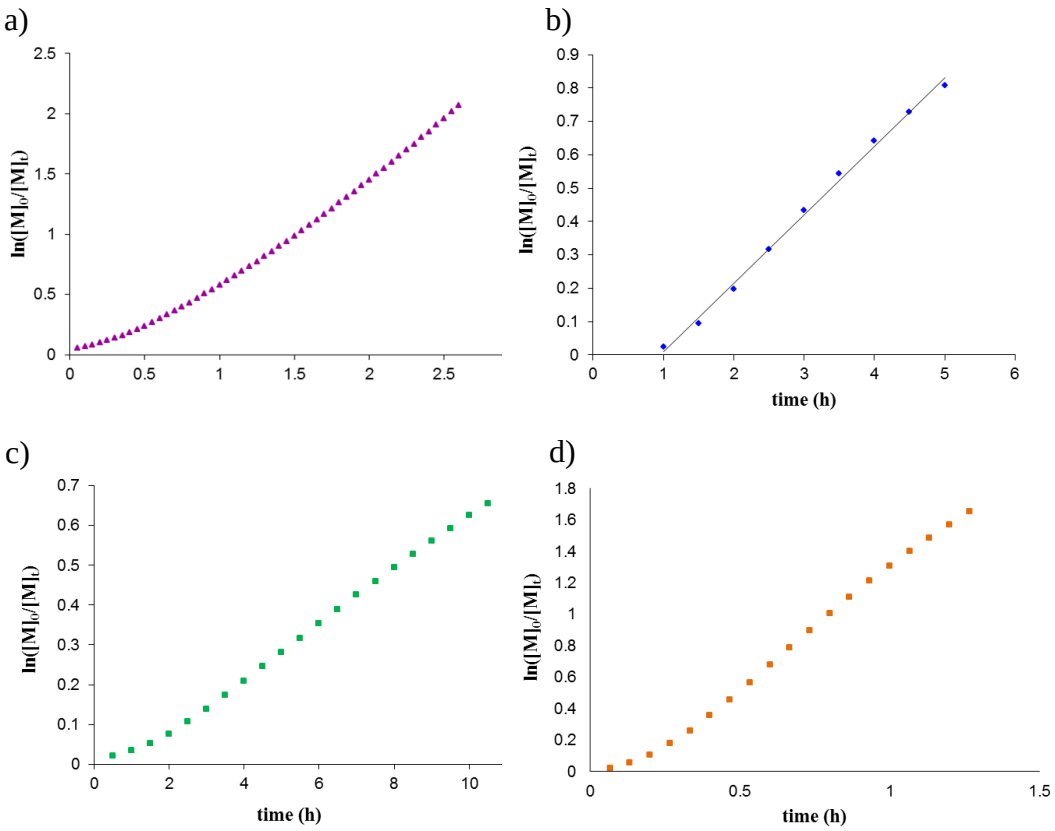

Figure V-9. $\ln([M]_0/[M]_t)$ *vs* time plot depicting a reaction order of unity with respect to a) [TMC] (R^2 = 0.987), b) [*rac*-*β*-BL] (R^2 = 0.996), c) [*δ*-VL] (R^2 = 0.997), and d) [*ε*-CL] (R^2 = 0.995).

Table V-7. Rate Constants Dependence on the Concentration of the Catalyst (**V2g)** and Temperature in the ROP of Cyclic Monomers.[a]

entry	[Al] (mM)	temp (^{o}C)	*rac*-lactide k_{obsd} (h^{-1})	TMC k_{obsd} (h^{-1})	*rac*-β-BL k_{obsd} (h^{-1})	δ-VL k_{obsd} (h^{-1})	ε-CL k_{obsd} (h^{-1})
1	0.74	90	-	-	-	0.047	-
2	1.49	90	0.0219	1.0015	0.0264	-	1.2779
3	2.98	90	0.0424	1.6584	0.0519	0.0777	1.8167
4	4.47	90	0.0600	2.1617	0.0692	0.1187	2.2469
5	5.96	90	0.0713	2.7963	0.0868	0.1279	2.7790
6	4.47	70	-	0.8863	-	0.0355	-
7	4.47	80	0.0304	1.5420	0.0230	0.0617	1.4593
8	4.47	100	0.0985	-	0.1481	0.1743	4.0329
9	4.47	105	0.1263	4.0881	0.2051	-	5.3720

[a] Monomer concentration was held constant at 0.69 M and reactions carried out in toluene-d_8.

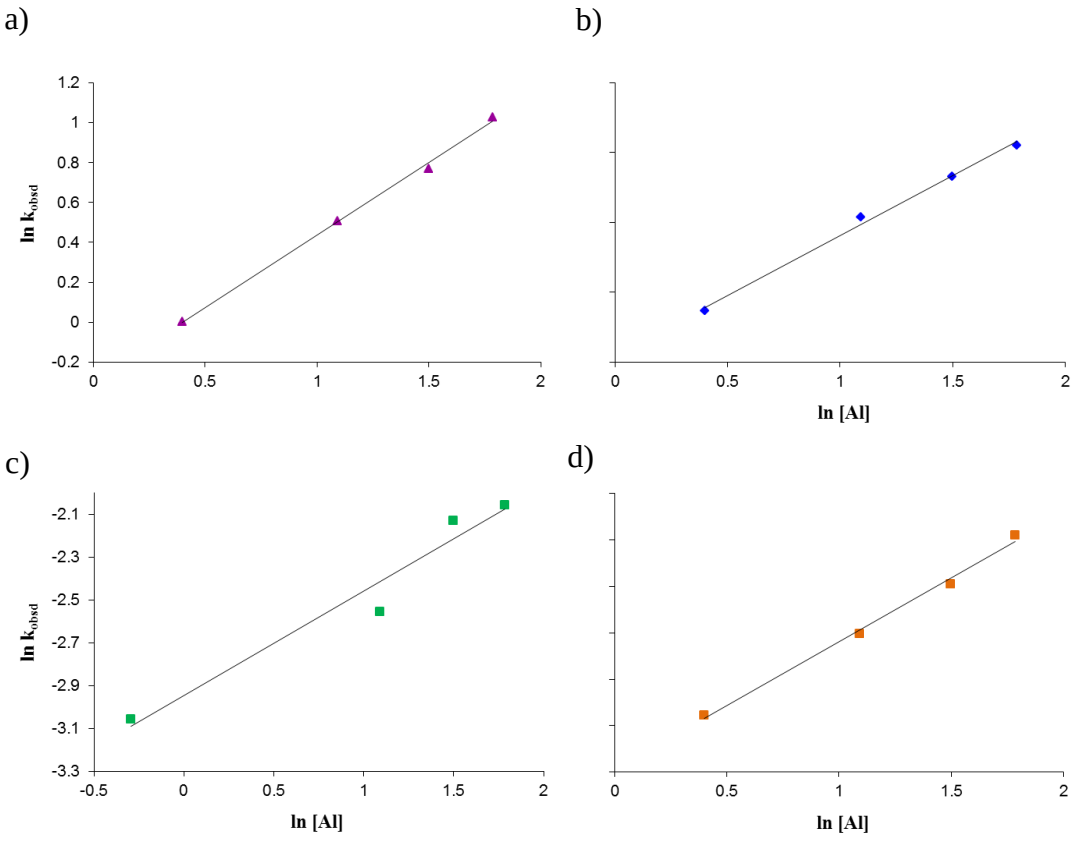

Figure V-10. Plot of ln k_{obsd} *vs* ln[Al] from the ROP of a) TMC (slope = 0.73, R^2 = 0.997), b) *rac*-β-BL (slope = 0.85, R^2 = 0.994), c) δ-VL (slope = 0.48, R^2 = 0.954), and d) ε-CL (slope = 0.54, R^2 = 0.994).

It is apparent that the steric of methyl group on polylactide and poly-β-BL affects the degree of aggregation during the polymerization process. The more steric alkoxide resulting from the ROP of a *rac*-lactide and *rac*-β-BL monomer is a secondary alkoxide. The more steric hindrance of this methyl group should decrease the degree of aggregation during the polymerization process when compared to the primary alkoxide derived from the ROP of TMC, δ-VL and ε-CL. The rates for the ROP of each cyclic monomer under the same condition were compared (entry 4, Table V-7). The experimental results indicated that complex **V2g** catalyzed ε-CL and TMC at similar rates with k_{obsd} values of 2.2469 h^{-1} and 2.1617 h^{-1} respectively. The k_{obsd} value for the ROP of δ-VL (0.1187 h^{-1}) catalyzed by complex **V2g** is slightly higher than that of the polymerization reactions of *rac*-β-BL (0.0692 h^{-1}) and *rac*-lactide (0.0600 h^{-1}).

The ring-opening polymerizations of *rac*-β-bL, TMC, δ-VL and ε-CL were carried out over the temperature range 70-105 ^{o}C in order to obtain the activation parameters for these processes. The activation parameters $\Delta H^{\neq}$ and $\Delta S^{\neq}$ calculated from the Eyring plot shown in Figure V-11 were determined and are listed in Table V-8. The $\Delta G^{\neq}$ values for the ROP of these cyclic monomers at 90 ^{o}C were also calculated and listed in Table V-8. The $\Delta G^{\neq}$ values at 90 ^{o}C of 95.4 kJ/mol and 95.2 kJ/mol for the ROP of TMC and ε-CL are similar. This results demonstrates that the two processes are energetically the same. Likewise, the $\Delta G^{\neq}$ values at 90 ^{o}C for the ROP of *rac*-lactide (106.6 kJ/mol) and *rac*-β-BL (106.3 kJ/mol) were similar and are slightly higher than the $\Delta G^{\neq}$ value for the ROP of δ-VL (104.5 kJ/mol) at 90 ^{o}C.

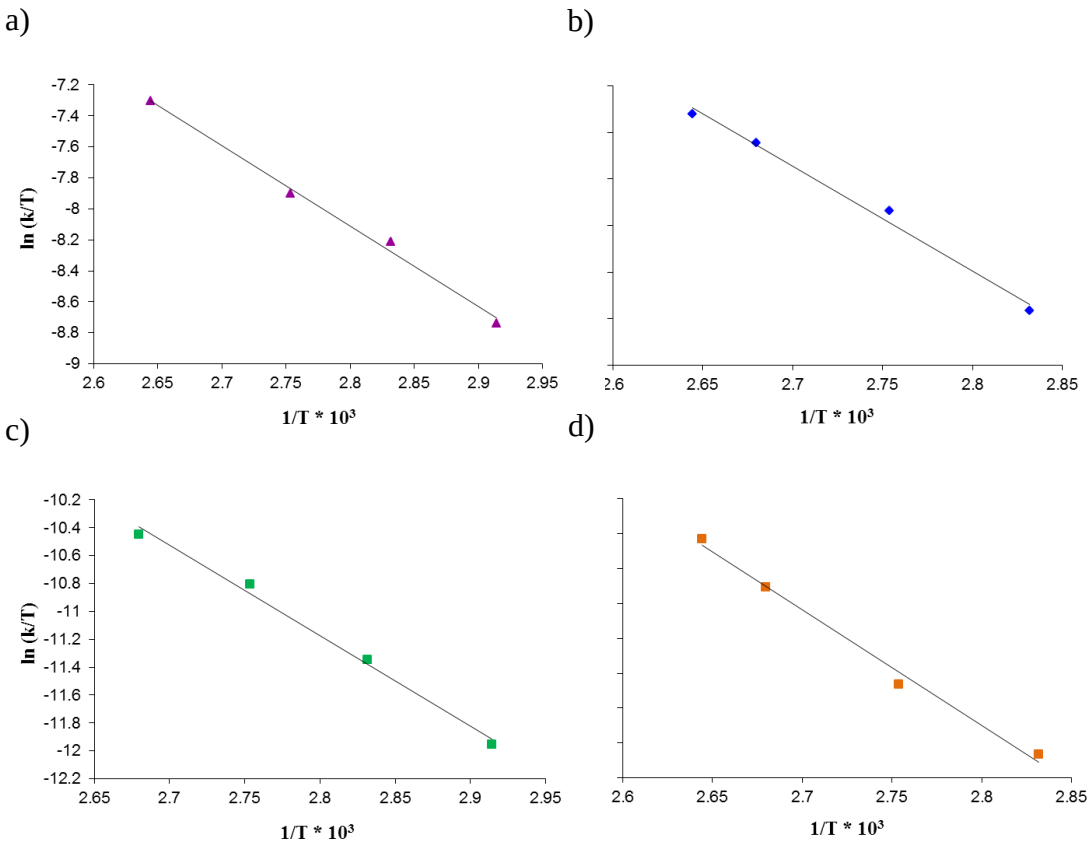

Figure V-11. Eyring plot of ROP of a) TMC (Slope = -5.193 with R^2 = 0.994), b) *rac*-β-BL (Slope = -11.285 with R^2 = 0.990), c) δ-VL (Slope = -6500 with R^2 = 0.992), and d) ε-CL (Slope = -6.645 with R^2 = 0.991) in the presence of catalyst **V2g** in toluene-d_8.

Table V-8. Activation Parameter in Homopolymerization.

entry	monomer	k ($M^{-1}h^{-1}$)	$\Delta H^{\neq}$ (kJ/mol)	$\Delta S^{\neq}$ (J/mol.K)	$\Delta G^{\neq}$ (kJ/mol)
1	*rac*-lactide	0.0111	59.7 ± 2.8	-129.1 ± 7.7	106.6
2	TMC	0.3951	43.1 ± 2.2	-144.1 ± 6.3	95.4
3	*rac*-β-BL	0.0133	93.8 ± 6.3	-34.5 ± 17.1	106.3
4	δ-VL	0.0165	54.0 ± 3.3	-139.1 ± 9.3	104.5
5	ε-CL	0.3311	55.2 ± 3.6	-110.2 ± 9.8	95.2

Copolymerization of Cyclic Monomers. Although complex **V2g** was shown to effectively catalyze the ROP of *rac*-lactide and *rac*-β-BL in toluene at 90 ^{o}C with similar k_{obsd} values (0.060 h^{-1} *vs* 0.069 h^{-1}, see Table V-7), in a copolymerization reaction (50:50 monomer feed) only *rac*-lactide was polymerized after an extended time period with no evidence of polybutyrolactone being formed. A similar copolymerization reaction was carried out involving *rac*-lactide and δ-VL. In this instance a tapered polylactide-polyvalerolactone copolymer, where the lactide monomer conversion was initially high, was obtained as evidenced by ^{1}H NMR spectroscopy. A series of experiments were performed as indicated in Table V-9 in order to determine the monomer reactivity ratios as defined by the Fineman-Ross equations 4 and 5.[88] From the mole fraction of δ-VL in the monomer feed (F) and in the copolymer (f) as determined by ^{1}H NMR spectroscopy of the purified copolymer, a Fineman-Ross plot was created as indicated in Figure V-12.

$$\frac{(f-1)}{F} = -r_{lactide}\frac{f}{F^2} + r_{valero} \qquad (4)$$

$$r_{lactide} = \frac{k_{LL}}{k_{LV}} \quad \text{and} \quad r_{valero} = \frac{k_{VV}}{k_{VL}} \qquad (5)$$

The reactivity ratios determined from the slope ($r_{lactide}$) and the intercept (r_{valero}) of the Fineman-Ross plot were found to be 2.78 and 0.140, respectively. The value of

$r_{lactide}$ indicates that the polymer's lactide unit prefers to ring open *rac*-lactide over δ-VL, and the r_{valero} designates that upon insertion of δ-VL in the polymer chain, it also prefers to ring open a *rac*-lactide monomer as opposed to a δ-VL monomer. This result clearly demonstrates that a tapered polylactide-polyvalerolactone copolymer with high lactide composition should be observed early on in the copolymerization process. A purified copolymer, which was precipitated from 5% HCl in methanol followed by drying, with a composition of *rac*-lactide to δ-valerolactone of 6.50:1.74 (entry 3 in Table V-9) displayed a M_n value of 9600 (PDI = 1.69) which is in good agreement with the theoretical molecular weight of 11,000. The T_g of this copolymer was determined to be 7.69 ^oC which lies between the T_g of pure polylactide (55 ^oC) and poly-δ-VL (-63 ^oC).[27]

Table V-9. The Data Set of Mole Fraction of the Fineman-Ross Plot.[a]

entry	*rac*-lactide : δ-valerolactone in the feed	F [b]	*rac*-lactide : δ-valerolactone in the copolymer[c]	f [d]
1	29:71	2.44	7.96:2.34	0.305
2	34:66	1.94	6.81:1.86	0.273
3	44:56	1.27	6.50:1.74	0.268
4	49:51	1.04	6.69:1.56	0.233
7	53:47	0.88	8.11:1.66	0.204

[a] Polymerization conditions: *rac*-lactide + δ-VL (818 μmol), ([*rac*-lactide]/[δ-VL])/[Al] = 100, in toluene-d_8 at 90 ^oC. [b] Mole fraction of δ-VL in the feed ($F = X_{VL,\ monomer}/X_{LA,\ monomer}$). [c] Determined by ^1H NMR. [d] Mole fraction of δ-VL in the polymer ($f = X_{VL,\ polymer}/X_{LA,\ polymer}$).

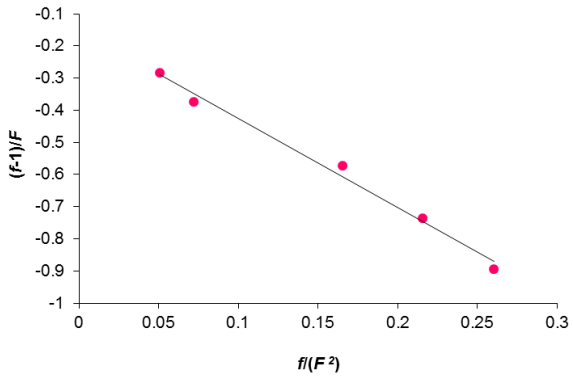

Figure V-12. Plot of (f-1)/F *vs* f/F^2 with slope = 2.78 and R^2 = 0.98, the interception = 0.14.

Kinetic measurements of the copolymerization of *rac*-lactide and δ-VL catalyzed by complex **V2g** in deuterated toluene were carried out at 90 ^{o}C and monitored by ^{1}H NMR spectroscopy. As expected based on the Fineman-Ross analysis above the rate of enchainment of *rac*-lactide was observed to be faster than that of δ-VL. The copolymerization process was found to be first order in both *rac*-lactide and δ-VL concentrations as illustrated from the plots of $\ln([M]_0/[M]_t)$ *vs* time in Figure V-13. As previously noted in the homopolymerization processes there is a brief initiation period seen in the copolymerization process. From the plots of k_{obsd} *vs* [catalyst] or ln k_{obsd} *vs* ln[catalyst], the reaction order in complex **V2g** concentration was also found to be unity (Figure V-14). Table V-10 lists the rate constants (k_{obsd}) for the copolymerization of *rac*-lactide and δ-VL as a function of both catalyst concentration and temperature. Hence, the rate law for the copolymerization process can be expressed as shown in equation 6.

$$\text{rate} = [\text{Al}](k_{\text{LA}}[\textit{rac}\text{-lactide}]+k_{\delta\text{-VL}}[\delta\text{-VL}]) \quad (6)$$

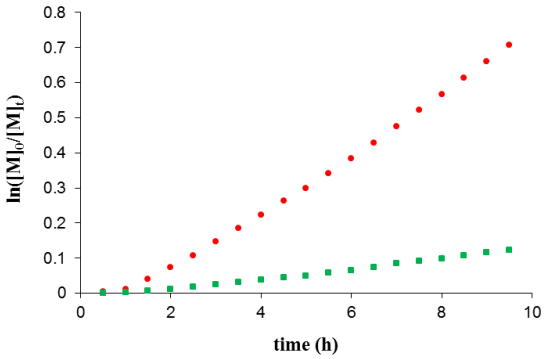

Figure V-13. $\ln([M]_0/[M]_t)$ *vs* time plot depicting a reaction order of unity with respect to *rac*-lactide (red solid circles) and ε-VL (green solid squares) concentration (R^2 = 0.993 for polylactide and R^2 = 0.991 for poly-δ-VL).

The activation parameters for the enchainment of *rac*-lactide and δ-VL in the copolymerization reaction were calculated from the temperature dependent data in Table V-10. In both instances the $\Delta H^{\neq}$ values for the copolymerization processes were larger and the $\Delta S^{\neq}$ values less negative than for the corresponding homopolymerization processes. Table V-11 compiles the Eyring derived activation parameter for the two ROP processes, which illustrates the observation that the $\Delta G^{\neq}$ at 90 ^{o}C for the copolymerization and homopolymerization processes to be quite similar. Nevertheless, the $\Delta G^{\neq}$ for the ROP of δ-VL in the copolymerization has increased somewhat as anticipated from the Fineman-Ross analysis. Crystal data and details of the data collection for complexes **V2a, V3b, V2d, V2f** (***cis***), **V2f** (***trans***), **V3e**, **V4e** are provided in Table V-12-V14.

a)

b)

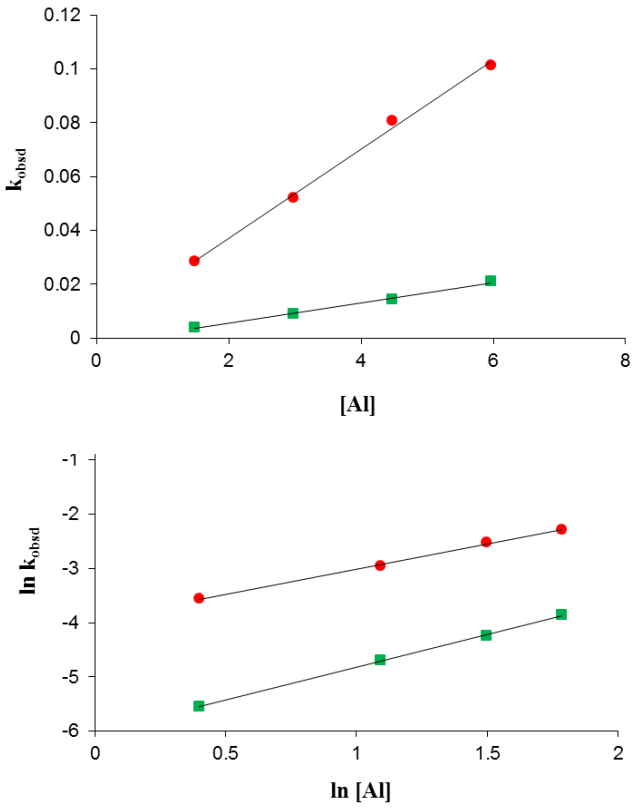

Figure V-14. (a) Plot of k_{obsd} *vs* [Al] with slope = 0.016 for *rac*-lactide (red solid circles ,R^2 = 0.996) and slope = 0.038 for δ-VL(green solid squares, R^2 = 0.995). (b) Plot of ln k_{obsd} *vs* ln[Al] with slope = 0.92 for *rac*-lactide (red solid circles ,R^2 = 0.997) and slope = 1.20 for δ-VL(green solid squares, R^2 = 0.999).

Table V-10. Rate Constants Dependence on the Concentration of the Catalyst (**V2g)** and Temperature in Copolymerization of *Rac*-Lactide and δ-Velerolactone.[a]

entry	[Al] (mM)	temp (^{o}C)	k_{obsd} (h^{-1})	k_{obsd}(h^{-1})
1	1.49	90	0.0285	0.0039
2	2.98	90	0.0520	0.0091
3	4.47	90	0.0808	0.0143
4	5.96	90	0.1014	0.0211
5	4.47	80	0.0379	0.0061
6	4.47	100	0.1472	0.0345
7	4.47	105	0.1938	0.0425

[a] Monomer concentration was held constant at 0.69 M and reactions carried out in toluene-d_8.

Table V-11. Comparison of Rates and Activation Parameters in Homopolymerization and Copolymerization of *Rac*-Lactide and δ-VL Catalyzed by Complex **V2g**.

	homopolymerizatoin		copolymerization	
	rac-lactide	δ-VL	*rac*-lactide	δ-VL
$\Delta H^{\neq}$ (kJ/mol)	59.7 ± 2.8	54.0 ± 3.3	69.7 ± 2.5	85.7 ± 4.9
$\Delta S^{\neq}$ (J/mol.K)	-129.1 ± 7.7	-139.1 ± 9.3	-100.2 ± 6.9	-68.8 ± 13.3
$\Delta G^{\neq}$ (kJ/mol)	106.6	104.5	106.1	110.7

[a] Free energy of activated calculated at 90 °C.

Table **V-12**. Crystallographic Data for Complexes **V2a,** V**3b,** and V**2d**.

	V2a	**V3b**	**V2d**
empirical formula	$C_{46}H_{72}Al_2N_2O_4$	$C_{42}H_{48}Al_2N_2O_8$	$C_{44}H_{72}Al_2N_2O_4Si_2$
fw	771.02	762.78	803.18
temperature (K)	110(2) K	110(2) K	110(2) K
crystal system	orthorhombic	monoclinic	triclinic
space group	P4/ncc	P21/c	P -1
a(Å)	23.795(3)	20.036(2)	9.5815(12)
b(Å)	23.795(3)	13.6282(14)	13.506(2)
c(Å)	18.707(3)	17.6152(19)	18.158(3)
α(deg)	90	90	89.262(9)
β(deg)	90	96.586(6)	86.668(9)
γ(deg)	90	90	75.039(9)
V(Å)	10592(2)	4778.2(9)	2266.4(6)
D_c(Mg/m^3)	0.967	1.060	1.177
Z	8	4	2
abs coeff(mm^{-1})	0.769	0.923	1.407
reflections collected	79230	37179	15570
independent reflections	3958 [*R*(int) = 0.1174]	7055 [*R*(int) = 0.0390]	6277 [*R*(int) = 0.0274]
data/restrains/parameters	3958 / 0 / 257	7055 / 6 / 501	6277 / 0 / 513
GOF on F^2	1.104	1.128	1.045
final *R* indices	R_1 = 0.0633	R_1 = 0.0964	R_1 = 0.0369
[$I > 2\sigma(I)$]	R_w = 0.1578	R_w = 0.2061	R_w = 0.0962
final *R* indices	R_1 = 0.0927	R_1 = 0.1061	R_1 = 0.0435
final *R* indices (all data)	R_w = 0.1712	R_w = 0.2099	R_w = 0.1052

Table V-13. Crystallographic Data for Complexes **V2f** (cis-), **V2f** (*trans*-), and **V2g** (*trans*-).

	V2f (*cis*-)	**V2f** (*trans*-)	**V2g** (*trans*-)
empirical formula	C_{40} H_{64} Al_2 N_2 O_4	C_{40} H_{64} Al_2 N_2 O_4	C_{44} H_{72} Al_2 Cl_4 N_2 O_4
fw	690.89	690.89	888.80
temperature (K)	110(2) K	110(2) K	110(2)K
crystal system	orthorhombic	monoclinic	triclinic
space group	Pbcn	P21/C	P -1
a(Å)	32.810(7)	14.234(4)	10.847(4)
b(Å)	20.945(5)	8.985(3)	12.387(5)
c(Å)	17.910(4)	18.655(5)	18.808(7)
α(deg)	90	90	106.82(2)
β(deg)	90	123.063(16)	91.91(2)
γ(deg)	90	90	90.50(2)
V(Å)	12308(5)	1999.5(10)	2417.1(16)
D_c(Mg/m^3)	1.119	1.148	1.221
Z	12	2	2
abs coeff(mm^{-1})	0.940	0.964	2.893
reflections collected	71247	12357	16050
independent reflections	9145 [R(int) = 0.0715]	2689 [*R*(int) = 0.1829]	6270 [*R*(int) = 0.0880]
data/restrains/parameters	9145 / 34 / 696	2689 / 0 / 225	6270 / 114 / 519
GOF on F^2	1.066	1.019	1.235
final *R* indices	R1 = 0.0873	R_1 = 0.0945	R_1 = 0.1225
[$I > 2\sigma(I)$]	Rw = 0.2201	R_w = 0.2215	R_w = 0.3020
final *R* indices	R1 = 0.1077	R_1 = 0.1233	R_1 = 0.1508
final *R* indices (all data)	Rw = 0.2348	R_w = 0.2334	R_w = 0.3281

Table V-14. Crystallographic Data for Complexes **V3e**, and **V4e**.

	V3e	**V4e**
empirical formula	C_{132} H_{124} Al_4 B_2 F_{48} N_4 O_{10}	C_{150} H_{145} Al_4 B_2 Cl_{18} F_{48} N_4 O_{18}
fw	2967.89	3971.34
temperature (K)	110(2)K	110(2)K
crystal system	triclinic	monoclinic
space group	P -1	P21/c
a(Å)	16.202(6)	29.458(2)
b(Å)	17.644(7)	20.3463(15)
c(Å)	18.126(6)	30.256(2)
α(deg)	74.59(2)	90
β(deg)	66.12(2)	102.383
γ(deg)	75.58(2)	90
V(Å)	4509(3)	17712(2)
D_c(Mg/m^3)	1.093	1.489
Z	1	4
abs coeff(mm^{-1})	1.077	3.725
reflections collected	34543	129138
independent reflections	12628 [*R*(int) = 0.1016]	26167 [*R*(int) = 0.0959]
data/restrains/parameters	12628 / 42 / 913	26167 / 1005 / 2194
GOF on F^2	0.916	3.754
final *R* indices	R_1 = 0.1010	R_1 = 0.1655
[$I > 2\sigma(I)$]	R_w = 0.2435	R_W = 0.3270
final *R* indices	R_1 = 0.1486	R_1 = 0.2258
final *R* indices (all data)	R_w = 0.2762	R_1 = 0.3404

Summary Remarks

In summary, we have reported the synthesis of a series of aluminum half-salen complexes derived from tridentate Schiff base ligands synthesized from either the chiral amino alcohols, achiral amino alcohols, or amino acids. X-ray crystallographic analysis of a closely related complexes **V2a**, **V3b**, and **V2d** reveal that the solid state structures are dimeric with two five-coordinate aluminum centers with bridging oxygen atoms. The ethyl (**V2a**, **V2d**) or benzyl alkoxide (**V3b**) groups located on each aluminum enter are positioned *cis* to one another across the molecule. However, the greater flexibility of the backbones derived from aliphatic amino alcohols allow *trans* conformation to occur as observed for complexes **V2f** and **V2g**. Each of the aluminum complexes **V2a-k** polymerized *rac*-lactide in toluene at 70 ^{o}C. Among these aluminum complexes, complex **V2i** was found to give isotactic polylactide with P_m of up to 0.82. In addition, complex **V2g** has shown reactivity toward the ring-opening polymerization of TMC, *rac*-β-butyrolactone, δ-valerolactone, ε-caprolactone in toluene at 70 ^{o}C. However, only the polymerization processes of *rac*-lactide and *rac*-β-butyrolactone appear to be living system as illustrated by a linear relationship between M_n and % conversion, as well as a low dispersity indices. The solution kinetic studies using complex **V2g** for the ROP of the cyclic monomer were determined to be first order in monomer concentration. And, the fractional orders in catalyst concentration, *i.e.* 0.86, 0.73, 0.85, 0.48 and 0.55 for *rac*-lactide, TMC, *rac*-β-butyrolactone, δ-valerolactone, and ε-caprolactone, respectively, were observed. This is due to the differences in bulk surrounding the alkoxide, resulting in different degree of aggregation of active species during the processes. The activation

parameters for all cyclic monomers were determined, and the $\Delta G^{\neq}$ values are as follows $\Delta G^{\neq}_{LA}$ (106.6 kJ/mol) $\cong$ $\Delta G^{\neq}_{BL}$ (106.3 kJ/mol) $>$ $\Delta G^{\neq}_{VL}$ (104.5 kJ/mol) $>$ $\Delta G^{\neq}_{TMC}$ (95.4 kJ/mol) $\cong$ $\Delta G^{\neq}_{CL}$ (95.2 kJ/mol). The activation parameters for copolymerization of *rac*-lactide and δ-VL have also been determined from an Eyring plot and compared with those of their homopolymerizations. In addition, the monomer reactivity ratios were determined from a Fineman-Ross plot, the results revealed that polymer lactide unit favors to ring-open *rac*-lactide more than ring open δ-VL molecule resulting in a tapered polylactide/polyvalerolactone copolymer.

CHAPTER VI

SUMMARY AND CONCLUSIONS

For decades, petroleum-based plastics have been increasing used across the globe. However, the accumulations of the waste from these non-biodegradable plastics as well as the concerns of limitation of petroleum feedstock have pushed scientific community to find alternative bio-based polymers. Among these polymeric materials, polylactide is a promising candidate as a replacement for petrochemical thermoplastics in several applications due to its outstanding physical and mechanical properties. These properties rely strongly upon the microstructures of the polymer which can be affected directly by the catalysts employed during the lactide polymerization process. This dissertation has focused on newly designed catalytic systems based on zinc and aluminum for the stereoselective ring-opening polymerization of *rac*-lactide as well as copolymerization of lactide with other cyclic monomers. Efforts have been made to understand stereoselectivity and kinetic aspects of these new catalysts for the ring-opening polymerization of these cyclic monomers.

As discussed in Chapter II, a series of chiral NNO-tridentate Schiff base ligands derived from natural amino acids along with their corresponding zinc complexes have been designed and synthesized. X-ray crystallographic analysis revealed that the solid state structures of zinc complexes **II6a-e** are similar to each other. They have all shown to have a distorted tetrahedron geometry with zinc at the center as shown in Figure II-1.

Polymerization studies of these newly designed zinc complexes **II6a-e** were found to be reactive for the ring-opening polymerization of both D- and L-lactide in C_6D_6 at ambient temperature, and the resulting polymers were obtained with the expected molecular weights and narrow polydispersity indices. Kinetic studies of the ring-opening polymerization of D- and L-lactide revealed to be first order in monomer concentration. The rates of the reaction for the ROP of D- and L-lactide were compared for each catalyst, and the experimental results indicate that enantiomerically pure complexes did not favorably catalyze one enantiomer over the other as evidenced from the ratio of $k_{D(obsd)}/k_{L(obsd)}$ being close to unity for all catalysts employed. Since the chiral center in complexes **II6a-c** did not affect the selectivity in the ring-opening polymerization of D- or L-lactide, we suggest that stereoselectivity in the polymerization of *rac*-lactide occurs via a chain-end control mechanism rather than enantiomorphic site control mechanism. In addition, the rates of the polymerization were found to be independent of the coordinating solvent, e.g. THF. Although the chiral center on tridentate Schiff base ligands did not play a role in stereregularity for these zinc complexes, the subsituent of the chiral tridentate Schiff base ligands did however play a significant role in producing heterotactic polylactide from *rac*-lactide. It was shown that complex **II6c** yielded the highest degree of heterotactic polylactide with P_r values of 0.84 and 0.89 at ambient temperature and -30 ^oC, respectively. Furthermore, the sterically bulky substituent of the tridentate Schiff base ligands can prevent the formation of *meso*-lactide during the polymerization process. That is, when complex **II6d** was employed, a methine proton resonance at 4.15 ppm is observed which corresponds to a *meso*-lactide, demonstrating

that epimerization of the lactide monomer occurs during the polymerization process. Conversely, when complexes **II6a-c** containing more steric bulk were used for the ring-opening polymerization of *rac*-lactide, there is no evidence of *meso*-lacitde formation, as observed from ^{1}H NMR.

In Chapter III, it is of interest to explore the reactivity of the zinc complexes from Chapter II for the ring-opening polymerization of ε-caprolactone, since lactides and lactones undergo similar ring-opening polymerization processes as lactides via a coordination-insertion mechanism. The results revealed that complexes **III1a** and **III1b** were both reactive for the ring-opening polymerization of ε-caprolactone in C_6D_6 at ambient temperature. And, these polymerization processes appear to be living systems affording polymers with the expected molecular weights and low polydispersity indices. It was also shown that complex **III1a** polymerizes L-lactide significantly faster than ε-caprolactone, with k_{obsd} value determinded to be 12.4 at room temperature. This may be explained by the difference in Lewis basicity of lactides and ε-carprolactone. In addition, the fact that latides contain two carbonyl groups increases the probability of coordination of the lactide monomer to the metal center, facilitating the rate of the polymerization. Another explanation is that the less sterically encumbering primary alkoxide generated from the ROP of an ε-caprolactone unit should bind more strongly to the zinc center as opposed to the secondary alkoxide from a lactide monomer unit. This stronger binding should slow down the polymerization process. The copolymerization of lactide and ε-caprolactone in melt at 110 ^{o}C by complex **III1a** revealed that the polyester afforded by this catalyst was a random copolymer evidenced by ^{1}H NMR and ^{13}C NMR spectra.

Additionally, the resulting copolymers have the composition of lactide and ε-caprolactone consistent with monomer mixture in the feed. The random copolymers produced from this catalyst system suggest that ε-caprolactone dramatically hinders the reactivity of lactide leading to a matched reactivity of the two monomers during the polymerization process, even though the polymerization rates for the ring-opening homopolymerizations of lactide and ε-caprolactone are different in benzene solution. Differential scanning calorimetry showed that the thermal properties of copolymers are strongly dependent upon the monomer compositions. That is, the T_g of the resulting copolymers increased from -67 ^oC (pure polycaprolactone) to 60 ^oC (pure polylactide) as the molar ratio of lactide units in the copolymer increased, and the calculated T_g correspond well with the values obtained from Fox equation. Similar trends were observed for both T_m and T_c of the copolymers as evidenced from the plot of T_m or T_c versus monomer ratio in the copolymers.

Based on the results obtained in Chapter II, the chiral zinc complexes **II2a-c** are reactive for the ring-opening polymerization of lactide, however, the complexes did not show stereoselectivity toward either L- or D-lactide. Although chiral complexes are anticipated to control the selectivity via an enantiomorphic site control mechanism, it has not been always true for zinc-catalyzed systems. In fact, both chiral and achiral zinc complexes reported in the literature thus far catalyze *rac*-lactide to heterotactic polylactide by a chain-end control mechanism. Our newly designed zinc complexes from Chapter II are some of the few examples of chiral zinc complexes for the ring-opening

polymerization of lactide, and they yet polymerize *rac*-lactide to heterotactic polylactide via a chain-end control mechanism rather than by an enantiomorphic site control.

On the other hand, chiral and achiral aluminum complexes have shown excellent stereocontrol toward the ring-opening polymerization of *rac*-lactide via an enantiomorphic site control mechanism as reported in the literature. We thus wanted to compare the roles of zinc and aluminum with regards to the stereocontrol in the ring-opening polymerization of *rac*-lactide. In Chapter IV, aluminum half-salen complexes closely related to our zinc complexes have been synthesized from both chiral and achiral ligands. The results revealed that both chiral and achiral aluminum complexes **IV2a**, **IV2e**, and **IV2g-j** in fact are reactive for the ring-opening polymerization of *rac*-lactide in toluene at 70 ^{o}C, affording isotactic polylactide with a P_m value of up to 0.76. The findings indicated that metal center has a great impact on the mechanism involved in polymerization process. The molecular weights of the resulting polymers correspond well with the theoretical values and the polydispersity indexes range from 1.03-1.08. From the variable-temperature ^{1}H NMR studies, complexes which existed in both *cis* and *trans* forms under the reaction condition, *i.e.* in toluene at 70 ^{o}C, epimerize *rac*-lactide to *meso*-lactide during the polymerization process. Complexes existing in only *trans* form did not show existence of *meso*-lactide during the ring-opening polymerization of *rac*-lactide. As a result, the produced polylactide was found to have a high degree of isotacticity (P_m = 76%).

Some of the aluminum complexes from Chapter IV were characterized by X-ray crystallography and presented here in Chapter V. Additionally, the exploration of the

ring-opening polymerization of cyclic monomers, *i.e. rac*-lactide, trimethylene carbonate, β-butyrolactone, δ-valerolactone, and ε-caprolactone, were examined by using an aluminum complex **V2g**. The solid state structures of closely related aluminum complexes **V2a**, **V3b**, **V2d**, and **V2f** showed to be dimeric with bridging of oxygen atoms from the ligands, and the aluminum center adopts a distorted-bipyramidal geometry with the ligands positioned *cis* to one another. However, with the more flexible back bone found in aluminum complexe **V2g**, the solid state structures display both *cis* and trans isomer. In addition, aluminum complex **V2g** was found to catalyze all of the cyclic monomers mentioned above. Polylactide obtained by this catalytic system was found to have a high degree of isotacticity, but the produced polybutyrolactone was found to be a completely atactic polymer. The ring-opening polymerizations of both *rac*-lactide and β-butyrolactone were found to be living processes as evidenced by the linear relationship between molecular weights and monomer/initiator ratios. The molecular weights of the resulting polymers were in good agreement with the theoretical values. Narrow polydispersity indexes were also observed from the resulting polymers. Kinetic studies of these cyclic monomers utilizing complex **V2g** revealed to be first order with respect to monomer concentration and to be fractional order in catalyst concentration, that is 0.86, 0.73, 0.85, 0.48 and 0.55 for *rac*-lactide, TMC, *rac*-β-butyrolactone, δ-valerolactone, and ε-caprolactone, respectively. The fractional order can be explained by some aggregation of the active species during the polymerization process as explained in detail in Chapter V. Activation parameters for all homopolymerization have been determined from Eyring plots and it was determined that the ring-opening

polymerization of *rac*-lactide and *rac*-β-butyrolactone are more energetically similar than that of TMC. It was also found that the ring-opening polymerization of δ-valerolactone and ε-caprolactone are also similar but less energetically favorable than that of TMC. In addition, copolymerization of *rac*-lactide and δ-valerolactone were studies and the activation parameters for such process were determined and compared with those in homopolymerization. A Fineman-Ross relationship was plotted, and the experimental results revealed that chain-end lactide units prefer to ring-open *rac*-lactide as opposed to δ-valerolactone monomer, resulting in a tapered polylactide/ polyvalerolactone copolymer.

In summary, I hope that the work presented in this dissertation has contributed to the understanding of the stereoselective ring-opening polymerization of lactide as well as the ring-opening polymerization of other cyclic monomers, and that the discoveries in this dissertation will allow for new development in catalysts for the better production of polylactide and its copolymers.

REFERENCES

(1) Madhavan Nampoothiri, K.; Nair, N. R.; John, R. P. *Bioresour. Technol.* **2010,** *101*, 8493-8501.

(2) (a) Drumright, R. E.; Gruber, P. R.; Henton, D. E. *Adv. Mater.* **2000,** *12*, 1841-1846; (b) Gross, R. A.; Kalra, B. *Science* **2002,** *297*, 803-807.

(3) Bourbigot, S.; Fontaine, G. *Polym. Chem.* **2010,** *1*, 1413-1422.

(4) Sawyer, D. J. *Macromol. Symp.* **2003,** *201*, 271-282.

(5) Albertsson, A.-C.; Varma, I. K. *Biomacromolecules* **2003,** *4*, 1466-1486.

(6) (a) Penco, M.; Donetti, R.; Mendichi, R.; Ferruti, P. *Macromol. Chem. Phys.* **1998,** *199*, 1737-1745; (b) Ikada, Y.; Tsuji, H. *Macromol. Rapid Commun.* **2000,** *21*, 117-132; (c) Platel, R. H.; Hodgson, L. M.; Williams, C. K. *Polym. Rev.* **2008,** *48*, 11-63.

(7) Becker, J. M.; Pounder, R. J.; Dove, A. P. *Macromol. Rapid Commun.* **2010,** *31*, 1923-1937.

(8) Avinc, O.; Khoddami, A. *Fibre Chem.* **2010,** *42*, 68-78.

(9) Thomas, C. M. *Chem. Soc. Rev.* **2010,** *39*, 165-173.

(10) (a) Ovitt, T. M.; Coates, G. W. *J. Am. Chem. Soc.* **1999,** *121*, 4072-4073; (b) Chisholm, M. H.; Eilerts, N. W.; Huffman, J. C.; Iyer, S. S.; Pacold, M.; Phomphrai, K. *J. Am. Chem. Soc.* **2000,** *122*, 11845-11854.

(11) Zell, M. T.; Padden, B. E.; Paterick, A. J.; Thakur, K. A. M.; Kean, R. T.; Hillmyer, M. A.; Munson, E. J. *Macromolecules* **2002,** *35*, 7700-7707.

(12) Nomura, N.; Ishii, R.; Yamamoto, Y.; Kondo, T. *Chem.-Eur. J.* **2007,** *13*, 4433-4451.

(13) (a) Nomura, N.; Ishii, R.; Akakura, M.; Aoi, K. *J. Am. Chem. Soc.* **2002,** *124*, 5938-5939; (b) Ovitt, T. M.; Coates, G. W. *J. Am. Chem. Soc.* **2002,** *124*, 1316-1326; (c) Zhang, L.; Nederberg, F.; Messman, J. M.; Pratt, R. C.; Hedrick, J. L.; Wade, C. G. *J. Am. Chem. Soc.* **2007,** *129*, 12610-12611.

(14) Schwach, G.; Coudane, J.; Engel, R.; Vert, M. *Polym. Bull.* **1996,** *37*, 771-776.

(15) Spassky, N.; Wisniewski, M.; Pluta, C.; Borgne, A. L. *Macromol. Chem. Phys.* **1996,** *197*, 2627-2637.

(16) Zhong, Z; Dijkstra, P. J.; Feijen, J. *Angew. Chem., Int. Ed.* **2002,** *41*, 4510-4513.

(17) Hormnirun, P.; Marshall, E. L.; Gibson, V. C.; White, A. J. P.; Williams, D. J. *J. Am. Chem. Soc.* **2004,** *126*, 2688-2689.

(18) Chisholm, M. H.; Patmore, N. J.; Zhou, Z. *Chem. Commun.* **2005**, 127 - 129.

(19) International Zinc Association. *http://www.zinc.org/zinc_health.html*.

(20) Stanford, M. J.; Dove, A. P. *Chem. Soc. Rev.* **2010,** *39*, 486-494.

(21) (a) Allen, S. D.; Moore, D. R.; Lobkovsky, E. B.; Coates, G. W. *J. Organomet. Chem.* **2003,** *683*, 137-148; (b) Cheng, M.; Attygalle, A. B.; Lobkovsky, E. B.; Coates, G. W. *J. Am. Chem. Soc.* **1999,** *121*, 11583-11584.

(22) (a) Chisholm, M. H.; Huffman, J. C.; Phomphrai, K. *J. Chem. Soc., Dalton Trans.* **2001**, 222-224; (b) Chisholm, M. H.; Gallucci, J.; Phomphrai, K. *Inorg. Chem.* **2002,** *41*, 2785-2794.

(23) (a) Chisholm, M. H.; Gallucci, J.; Phomphrai, K. *Chem. Commun.* **2003**, 48-49; (b) Chisholm, M. H.; Gallucci, J. C.; Phomphrai, K. *Inorg. Chem.* **2004,** *43*, 6717-6725.

(24) Middleton, J. C.; Tipton, A. J. *Biomaterials* **2000,** *21*, 2335-2346.

(25) Pêgo, A. P.; Van Luyn, M. J. A.; Brouwer, L. A.; van Wachem, P. B.; Poot, A. A.; Grijpma, D. W.; Feijen, J. *J. Biomed. Mater. Res. Part A* **2003,** *67A*, 1044-1054.

(26) Albertsson, A.-C.; Eklund, M. *J. Appl. Polym. Sci.* **1995,** *57*, 87-103.

(27) Coulembier, O.; Degée, P.; Hedrick, J. L.; Dubois, P. *Prog. Polym. Sci.* **2006,** *31*, 723-747.

(28) Schindler, A.; Jeffcoat, R.; Kimmel, G. L.; Pitt, C. G.; Wall, M. E.; Zweidinger, R.; Pearce, E. M.; Schaefgen, J. R., *Contemporary Topics in Polymer Science*; Plenum: New York, 1977; Vol. 2, p 251.

(29) (a) Gandini, A. *Macromolecules* **2008,** *41*, 9491-9504; (b) Platel, R. H.; Hodgson, L. M.; Williams, C. K. *Polymer. Rev.* **2008,** *48*, 11-63; (c) Coates, G. W.; Hillmyer, M. A. *Macromolecules* **2009,** *42*, 7987-7989.

(30) Morschbacker, A. *Polym. Rev.* **2009,** *49*, 79-84.

(31) (a) *Sci. News. Phys. Chem.* **2008**, September 23; (b) *C&E News* **2009,** *87*, No. 21, 29.

(32) (a) O'Keefe, B. J.; Hillmyer, M. A.; Tolman, W. B. *J. Chem. Soc., Dalton Trans.* **2001**, 2215-2224; (b) Dechy-Cabaret, O.; Martin-Vaca, B.; Bourissou, D. *Chem. Rev.* **2004,** *104*, 6147-6176; (c) Kamber, N. E.; Jeong, W.; Waymouth, R. M.; Pratt, R. C.; Lohmeijer, B. G. G.; Hedrick, J. L. *Chem. Rev.* **2007,** *107*, 5813-5840.

(33) (a) Ruckenstein, E.; Yuan, Y. *J. Appl. Polym. Sci.* **1998,** *69*, 1429-1434; (b) Kricheldorf, H. R.; Stricker, A. *Macromol. Chem. Phys.* **1999,** *200*, 1726-1733; (c) Pospiech, D.; Komber, H.; Jehnichen, D.; Haussler, L.; Eckstein, K.; Scheibner, H.; Janke, A.; Kricheldorf, H. R.; Petermann, O. *Biomacromolecules* **2005,** *6*, 439-446; (d) Chisholm, M. H.; Gallucci, J. C.; Krempner, C. *Polyhedron* **2007,** *26*, 4436-4444; (e) Grafov, A.; Vuorinen, S.; Repo, T.; Kemell, M.; Nieger, M.; Leskelä, M. *Eur. Polym. J.* **2008,** *44*, 3797-3805.

(34) Chmura, A. J.; Chuck, C. J.; Davidson, M. G.; Jones, M. D.; Lunn, M. D.; Bull, S. D.; Mahon, M. F. *Angew. Chem., Int. Ed.* **2007,** *46*, 2280-2283.

(35) Simic, V.; Pensec, S.; Spassky, N. *Macromol. Symp.* **2000,** *153*, 109-121.

(36) (a) Stolt, M.; Sodergard, A. *Macromolecules* **1999,** *32*, 6412-6417; (b) O'Keefe, B. J.; Monnier, S. M.; Hillmyer, M. A.; Tolman, W. B. *J. Am. Chem. Soc.* **2001,** *123*, 339-340; (c) Gibson, V. C.; Marshall, E. L.; Navarro-Llobet, D.; White, A. J. P.; Williams, D. J. *J. Chem. Soc., Dalton Trans.* **2002**, 4321 - 4322; (d) O'Keefe, B. J.; Breyfogle, L. E.; Hillmyer, M. A.; Tolman, W. B. *J. Am. Chem. Soc.* **2002,** *124*, 4384-4393; (e) McGuinness, D. S.; Marshall, E. L.; Gibson, V. C.; Steed, J. W. *J. Polym. Sci., Part A: Polym. Chem.* **2003,** *41*, 3798-3803; (f) Stolt, M.; Krasowska, K.; Rutkowska, M.; Janik, H.; Rosling, A.; Södergård, A. *Polym. Int.* **2005,** *54*, 362-368; (g) Wang, X.; Liao, K.; Quan, D.; Wu, Q. *Macromolecules* **2005,** *38*, 4611-4617.

(37) (a) Kim, Y.; Verkade, J. G. *Organometallics* **2002,** *21*, 2395-2399; (b) Kim, Y.; Jnaneshwara, G. K.; Verkade, J. G. *Inorg. Chem.* **2003,** *42*, 1437-1447; (c) Russell, S. K.; Gamble, C. L.; Gibbins, K. J.; Juhl, K. C. S.; Mitchell, W. S.; Tumas, A. J.; Hofmeister, G. E. *Macromolecules* **2005,** *38*, 10336-10340; (d) Chmura, A. J.; Davidson, M. G.; Jones, M. D.; Lunn, M. D.; Mahon, M. F.; Johnson, A. F.; Khunkamchoo, P.; Roberts, S. L.; Wong, S. S. F. *Macromolecules* **2006,** *39*, 7250-7257; (e) Gregson, C. K. A.; Gibson, V. C.; Long, N. J.; Marshall, E. L.; Oxford, P. J.; White, A. J. P. *J. Am. Chem. Soc.* **2006,** *128*, 7410-7411; (f) Gendler, S.; Segal, S.; Goldberg, I.; Goldschmidt, Z.;

Kol, M. *Inorg. Chem.* **2006,** *45*, 4783-4790; (g) Chmura, Amanda J.; Davidson, M. G.; Jones, M. D.; Lunn, M. D.; Mahon, M. F. *Dalton Trans.* **2006**, 887 - 889; (h) Atkinson, R. C. J.; Gerry, K.; Gibson, V. C.; Long, N. J.; Marshall, E. L.; West, L. J. *Organometallics* **2006,** *26*, 316-320; (i) Lee, J.; Kim, Y.; Do, Y. *Inorg. Chem.* **2007,** *46*, 7701-7703; (j) Chmura, A. J.; Cousins, D. M.; Davidson, M. G.; Jones, M. D.; Lunn, M. D.; Mahon, M. F. *Dalton Trans.* **2008**, 1437 - 1443.

(38) (a) Chisholm, M. H.; Phomphrai, K. *Inorg. Chim. Acta* **2003,** *350*, 121-125; (b) Dove, A. P.; Gibson, V. C.; Marshall, E. L.; White, A. J. P.; Williams, D. J. *Dalton Trans.* **2004**, 570 - 578; (c) Chisholm, M. H.; Gallucci, J. C.; Phomphrai, K. *Inorg. Chem.* **2005,** *44*, 8004-8010; (d) Ejfler, J.; Micha, K.; Jerzykiewicz, L. B.; Sobota, P. *Dalton Trans.* **2005**, 2047 - 2050; (e) Wu, J.-C.; Huang, B.-H.; Hsueh, M.-L.; Lai, S.-L.; Lin, C.-C. *Polymer* **2005,** *46*, 9784-9792; (f) Yu, T.-L.; Wu, C.-C.; Chen, C.-C.; Huang, B.-H.; Wu, J.; Lin, C.-C. *Polymer* **2005,** *46*, 5909-5917; (g) Sanchez-Barba, L. F.; Hughes, D. L.; Humphrey, S. M.; Bochmann, M. *Organometallics* **2006,** *25*, 1012-1020; (h) Lian, B.; Thomas, C. M.; Casagrande Jr, O. L.; Roisnel, T.; Carpentier, J.-F. *Polyhedron* **2007,** *26*, 3817-3824; (i) Sanchez-Barba, L. F.; Garces, A.; Fajardo, M.; Alonso-Moreno, C.; Fernandez-Baeza, J.; Otero, A.; Antinolo, A.; Tejeda, J.; Lara-Sanchez, A.; Lopez-Solera, M. I. *Organometallics* **2007,** *26*, 6403-6411; (j) Tang, H.-Y.; Chen, H.-Y.; Huang, J.-H.; Lin, C.-C. *Macromolecules* **2007,** *40*, 8855-8860; (k) Wu, J.; Chen, Y.-Z.; Hung, W.-C.; Lin, C.-C. *Organometallics* **2008,** *27*, 4970-4978; (l) Huang, Y.; Hung, W.-C.; Liao, M.-Y.; Tsai, T.-E.; Peng, Y.-L.; Lin, C.-C. *J. Polym. Sci., Part A: Polym. Chem.* **2009,** *47*, 2318-2329; (m) Hung, W.-C.; Lin, C.-C. *Inorg. Chem.* **2009,** *48*, 728-734; (n) Tsai, Y.-H.; Lin, C.-H.; Lin, C.-C.; Ko, B.-T. *J. Polym. Sci., Part A: Polym. Chem.* **2009,** *47*, 4927-4936; (o) Wheaton, C. A.; Hayes, P. G.; Ireland, B. J. *Dalton Trans.* **2009**, 4832 - 4846.

(39) (a) Cameron, P. A.; Jhurry, D.; Gibson, V. C.; White, A. J. P.; Williams, D. J.; Williams, S. *Macromol. Rapid Commun.* **1999,** *20*, 616-618; (b) Radano, C. P.; Baker, G. L.; Smith, M. R. *J. Am. Chem. Soc.* **2000,** *122*, 1552-1553; (c) Zhong, Z.; Dijkstra, P. J.; Feijen, J. *Angew. Chem., Int. Ed.* **2002,** *41*, 4510-4513; (d) Zhong, Z.; Dijkstra, P. J.; Feijen, J. *J. Am. Chem. Soc.* **2003,** *125*, 11291-11298; (e) Doherty, S.; Errington, R. J.; Housley, N.; Clegg, W. *Organometallics* **2004,** *23*, 2382-2388; (f) Li, H.; Wang, C.; Bai, F.; Yue, J.; Woo, H.-G. *Organometallics* **2004,** *23*, 1411-1415; (g) Tang, Z.; Chen, X.; Pang, X.; Yang, Y.; Zhang, X.; Jing, X. *Biomacromolecules* **2004,** *5*, 965-970; (h) Ma, H.; Melillo, G.; Oliva, L.; Spaniol, T. P.; Englert, U.; Okuda, J. *Dalton Trans.* **2005**, 721 - 727; (i) Tang, Z.; Yang, Y.; Pang, X.; Hu, J.; Chen, X.; Hu, N.; Jing, X. *J. Appl. Polym. Sci.* **2005,** *98*, 102-108; (j) Tang, Z.; Pang, X.; Sun, J.; Du, H.; Chen, X.; Wang, X.; Jing, X. *J. Polym. Sci., Part A: Polym. Chem.* **2006,** *44*, 4932-4938; (k) Du, H.; Pang, X.; Yu, H.; Zhuang, X.; Chen, X.; Cui, D.; Wang, X.; Jing, X. *Macromolecules* **2007,** *40*, 1904-1913; (l) Tang, Z.; Gibson, V. C.

Eur. Polym. J. **2007,** *43*, 150-155; (m) Wu, J.; Pan, X.; Tang, N.; Lin, C.-C. *Eur. Polym. J.* **2007,** *43*, 5040-5046; (n) Bouyahyi, M.; Grunova, E.; Marquet, N.; Kirillov, E.; Thomas, C. M.; Roisnel, T.; Carpentier, J.-F. o. *Organometallics* **2008,** *27*, 5815-5825; (o) Chisholm, M. H.; Gallucci, J. C.; Quisenberry, K. T.; Zhou, Z. *Inorg. Chem.* **2008,** *47*, 2613-2624; (p) Iwasa, N.; Fujiki, M.; Nomura, K. *J. Mol. Catal. A: Chem.* **2008,** *292*, 67-75; (q) Zhang, C.; Wang, Z.-X. *J. Organomet. Chem.* **2008,** *693*, 3151-3158; (r) Alaaeddine, A.; Thomas, C. M.; Roisnel, T.; Carpentier, J.-F. o. *Organometallics* **2009,** *28*, 1469-1475; (s) Du, H.; Velders, Aldrik H.; Dijkstra, Pieter J.; Sun, J.; Zhong, Z.; Chen, X.; Feijen, J. *Chem.-Eur. J.* **2009,** *15*, 9836-9845; (t) Du, H.; Velders, A. H.; Dijkstra, P. J.; Zhong, Z.; Chen, X.; Feijen, J. *Macromolecules* **2009,** *42*, 1058-1066; (u) Pappalardo, D.; Annunziata, L.; Pellecchia, C. *Macromolecules* **2009,** *42*, 6056-6062.

(40) (a) Zhong, Z.; Schneiderbauer, S.; Dijkstra, P. J.; Westerhausen, M.; Feijen, J. *Polym. Bull.* **2003,** *51*, 175-182; (b) Chen, H.-Y.; Tang, H.-Y.; Lin, C.-C. *Polymer* **2007,** *48*, 2257-2262; (c) Darensbourg, D. J.; Choi, W.; Richers, C. P. *Macromolecules* **2007,** *40*, 3521-3523; (d) Darensbourg, D. J.; Choi, W.; Karroonnirun, O.; Bhuvanesh, N. *Macromolecules* **2008,** *41*, 3493-3502.

(41) Chen, H.-Y.; Zhang, C.; Lin, C.-C.; Reibenspies, J. H.; Miller, S. A. *Green Chem.* **2007,** *9*, 1038 - 1040.

(42) Hsueh, M.-L.; Huang, B.-H.; Wu, J.; Lin, C.-C. *Macromolecules* **2005,** *38*, 9482-9487.

(43) (a) Chamberlain, B. M.; Cheng, M.; Moore, D. R.; Ovitt, T. M.; Lobkovsky, E. B.; Coates, G. W. *J. Am. Chem. Soc.* **2001,** *123*, 3229-3238; (b) Chisholm, M. H.; Gallucci, J. C.; Zhen, H.; Huffman, J. C. *Inorg. Chem.* **2001,** *40*, 5051-5054; (c) Chisholm, M. H.; Huffman, J. C.; Phomphrai, K. *J. Chem. Soc., Dalton Trans.* **2001**, 222 - 224; (d) Hill, M. S.; Hitchcock, P. B. *J. Chem. Soc., Dalton Trans.* **2002**, 4694 - 4702; (e) Williams, C. K.; Brooks, N. R.; Hillmyer, M. A.; Tolman, W. B. *Chem. Commun.* **2002**, 2132 - 2133; (f) Che, C.-M.; Huang, J.-S. *Coord. Chem. Rev.* **2003,** *242*, 97-113; (g) Williams, C. K.; Breyfogle, L. E.; Choi, S. K.; Nam, W.; Young, V. G.; Hillmyer, M. A.; Tolman, W. B. *J. Am. Chem. Soc.* **2003,** *125*, 11350-11359; (h) Jensen, T. R.; Breyfogle, L. E.; Hillmyer, M. A.; Tolman, W. B. *Chem. Commun.* **2004**, 2504 - 2505; (i) Bukhaltsev, E.; Frish, L.; Cohen, Y.; Vigalok, A. *Org. Lett.* **2005,** *7*, 5123-5126; (j) Chen, H.-Y.; Huang, B.-H.; Lin, C.-C. *Macromolecules* **2005,** *38*, 5400-5405; (k) Jensen, T. R.; Schaller, C. P.; Hillmyer, M. A.; Tolman, W. B. *J. Organomet. Chem.* **2005,** *690*, 5881-5891; (l) Chen, H.-Y.; Tang, H.-Y.; Lin, C.-C. *Macromolecules* **2006,** *39*, 3745-3752; (m) Börner, J.; Herres-Pawlis, S.; Flörke, U.; Huber, K. *Eur. J. Inorg. Chem.* **2007,** *2007*, 5645-5651; (n) Bunge, S. D.; Lance, J. M.; Bertke, J. A. *Organometallics* **2007,** *26*, 6320-6328; (o) Chen, C.-C.; Chen, C.-Y.; Huang,

C.-A.; Chen, M.-T.; Peng, K.-F. *Dalton Trans.* **2007**, 4073 - 4078; (p) Hung, W.-C.; Huang, Y.; Lin, C.-C. *J. Polym. Sci., Part A: Polym. Chem.* **2008,** *46*, 6466-6476; (q) Börner, J.; Flörke, U.; Huber, K.; Döring, A.; Kuckling, D.; Herres-Pawlis, S. *Chem.-Eur. J.* **2009,** *15*, 2362-2376; (r) Jones, M. D.; Davidson, M. G.; Keir, C. G.; Hughes, L. M.; Mahon, M. F.; Apperley, D. C. *Eur. J. Inorg. Chem.* **2009,** *2009*, 635-642; (s) Labourdette, G.; Lee, D. J.; Patrick, B. O.; Ezhova, M. B.; Mehrkhodavandi, P. *Organometallics* **2009,** *28*, 1309-1319.

(44) (a) Douglas, A. F.; Patrick, B. O.; Mehrkhodavandi, P. *Angew. Chem., Int. Ed.* **2008,** *47*, 2290-2293; (b) Peckermann, I.; Kapelski, A.; Spaniol, T. P.; Okuda, J. *Inorg. Chem.* **2009,** *48*, 5526-5534; (c) Pietrangelo, A.; Hillmyer, M. A.; Tolman, W. B. *Chem. Commun.* **2009**, 2736-2737.

(45) (a) Sarasua, J.-R.; Prud'homme, R. E.; Wisniewski, M.; Le Borgne, A.; Spassky, N. *Macromolecules* **1998,** *31*, 3895-3905; (b) Tsuji, H.; Ikada, Y. *Polymer* **1999,** *40*, 6699-6708.

(46) Spinu, M.; Jackson, C.; Keating, M. Y. *J. Macromol. Sci., Pure, Appl. Chem.* **1996,** *A33*, 1497-1530.

(47) (a) Chisholm, M. H.; Zhou, Z. *J. Mater. Chem.* **2004,** *14*, 3081-3092; (b) Wu, J.; Yu, T.-L.; Chen, C.-T.; Lin, C.-C. *Coord. Chem. Rev.* **2006,** *250*, 602-626.

(48) (a) Darensbourg, D. J.; Holtcamp, M. W.; Struck, G. E.; Zimmer, M. S.; Niezgoda, S. A.; Rainey, P.; Robertson, J. B.; Draper, J. D.; Reibenspies, J. H. *J. Am. Chem. Soc.* **1999,** *121*, 107-116; (b) Hansen, T. V.; Skattebøl, L. *Tetrahedron Lett.* **2005,** *46*, 3829-3830.

(49) Coldham, I.; O'Brien, P.; Patel, J. J.; Raimbault, S.; Sanderson, A. J.; Stead, D.; Whittaker, D. T. E. *Tetrahedron: Asym.* **2007,** *18*, 2113-2119.

(50) Cameron, P. A.; Gibson, V. C.; Redshaw, C.; Segal, J. A.; Bruce, M. D.; White, A. J. P.; Williams, D. J. *Chem. Commun.* **1999**, 1883-1884.

(51) Baran, J.; Duda, A.; Kowalski, A.; Szymanski, R.; Penczek, S. *Macromol. Rapid Commun.* **1997,** *18*, 325-333.

(52) (a) MacDonald, R. T.; McCarthy, S. P.; Gross, R. A. *Macromolecules* **1996,** *29*, 7356-7361; (b) Stevels, W. M.; Ankone, M. J. K.; Dijkstra, P. J.; Feijen, J. *Macromolecules* **1996,** *29*, 6132-6138.

(53) From expanded version of the ^{1}H NMR spectra illustrated in Figure II-9, and assuming the sis and isi peaks are symmetrical, the areas of these peaks *vs* that of the total methine proton region were measured using a planimeter. This

mechanical integrating instrument used to measure the area under a curve by moving a point attached to an arm of the device around the perimeter of the defined curve can be easily demonstrated to accurately assess areas as indicated by concomitant area measurements of known dimensions.

(54) (a) Chiellini, E.; Solaro, R. *Adv. Mater.* **1996,** *8*, 305-313; (b) Qian, H.; Bei, J.; Wang, S. *Polym. Degrad. Stab.* **2000,** *68*, 423-429; (c) Ghosh, S. *J. Chem. Res.* **2004,** *2004*, 241-246.

(55) (a) Gref, R.; Minamitake, Y.; Peracchia, M. T.; Trubetskov, V.; Torchilin, V.; Langer, R. *Science* **1994,** *263*, 1600-1603; (b) Bhardwaj, R.; Blanchard, J. *Int. J. Pharm.* **1998,** *170*, 109-117; (c) Chamberlain, B. M.; Jazdzewski, B. A.; Pink, M.; Hillmyer, M. A.; Tolman, W. B. *Macromolecules* **2000,** *33*, 3970-3977.

(56) (a) Van Butsele, K.; Jérôme, R.; Jérôme, C. *Polymer* **2007,** *48*, 7431-7443; (b) Shen, Y.; Zhu, K. J.; Shen, Z.; Yao, K.-M. *J. Polym. Sci., Part A: Polym. Chem.* **1996,** *34*, 1799-1805.

(57) Okada, M. *Prog. Polym. Sci.* **2001,** *27*, 87-133.

(58) (a) Vanhoorne, P.; Dubois, P.; Jerome, R.; Teyssie, P. *Macromolecules* **1992,** *25*, 37-44; (b) Bero, M.; Kasperczyk, J. *Macromol. Chem. Phys.* **1996,** *197*, 3251-3258; (c) Kister, G.; Cassanas, G.; Bergounhon, M.; Hoarau, D.; Vert, M. *Polymer* **2000,** *41*, 925-932; (d) Faÿ, F.; Renard, E.; Langlois, V.; Linossier, I.; Vallée-Rehel, K. *Eur. Polym. J.* **2007,** *43*, 4800-4813; (e) Calandrelli, L.; Calarco, A.; Laurienzo, P.; Malinconico, M.; Petillo, O.; Peluso, G. *Biomacromolecules* **2008,** *9*, 1527-1534; (f) Nomura, N.; Akita, A.; Ishii, R.; Mizuno, M. *J. Am. Chem. Soc.* **2010,** *132*, 1750-1751.

(59) (a) Song, C. X.; Feng, X. D. *Macromolecules* **1984,** *17*, 2764-2767; (b) Huang, M.-H.; Li, S.; Coudane, J.; Vert, M. *Macromol. Chem. Phys.* **2003,** *204*, 1994-2001; (c) Jeon, O.; Lee, S.-H.; Kim, S. H.; Lee, Y. M.; Kim, Y. H. *Macromolecules* **2003,** *36*, 5585-5592; (d) Lahcini, M.; Castro, P. M.; Kalmi, M.; Leskela, M.; Repo, T. *Organometallics* **2004,** *23*, 4547-4549; (e) Wang, J.-L.; Dong, C.-M. *Macromol. Chem. Phys.* **2006,** *207*, 554-562; (f) Zhao, Z.; Yang, L.; Hu, Y.; He, Y.; Wei, J.; Li, S. *Polym. Degrad. Stab.* **2007,** *92*, 1769-1777; (g) Wei, Z.; Liu, L.; Yu, F.; Wang, P.; Qu, C.; Qi, M. *Polym. Bull.* **2008,** *61*, 407-413.

(60) Darensbourg, D. J.; Karroonnirun, O. *Inorg. Chem.* **2010,** *49*, 2360-2371.

(61) (a) Kricheldorf, H. R.; Berl, M.; Scharnagl, N. *Macromolecules* **1988,** *21*, 286-293; (b) Dubois, P.; Jacobs, C.; Jérôme, R.; Teyssié, P. *Macromolecules* **1991,** *24*, 2266-2270; (c) Kricheldorf, H. R.; Sumbél, M. V.; Kreiser-Saunders, I.

Macromolecules **1991,** *24*, 1944-1949; (d) Nijenhuis, A. J.; Grijpma, D. W.; Pennings, A. J. *Macromolecules* **1992,** *25*, 6419-6424; (e) Nishiura, M.; Hou, Z.; Koizumi, T.-A.; Imamoto, T.; Wakatsuki, Y. *Macromolecules* **1999,** *32*, 8245-8251; (f) Kricheldorf, H. R.; Kreiser-Saunders, I. *Polymer* **2000,** *41*, 3957-3963; (g) Lewinski, J.; Horeglad, P.; Wojcik, K.; Justyniak, I. *Organometallics* **2005,** *24*, 4588-4593.

(62) (a) Kasperczyk, J.; Bero, M. *Makromol. Chem.* **1991,** *192*, 1777-1787; (b) Kasperczyk, J.; Bero, M. *Makromol. Chem.* **1993,** *194*, 913-925.

(63) Dove, A. P. *Chem. Commun.* **2008**, 6446 - 6470.

(64) (a) Uhrich, K. E.; Cannizzaro, S. M.; Langer, R. S.; Shakesheff, K. M. *Chem. Rev.* **1999,** *99*, 3181-3198; (b) Auras, R.; Harte, B.; Selke, S. *Macromol. Biosci.* **2004,** *4*, 835-864.

(65) Ovitt, T. M.; Coates, G. W. *J. Polym. Sci., Part A: Polym. Chem.* **2000,** *38*, 4686-4692.

(66) Zhang, Z.; Xu, X.; Sun, S.; Yao, Y.; Zhang, Y.; Shen, Q. *Chem. Commun.* **2009**, 7414-7416.

(67) Drouin, F. d. r.; Oguadinma, P. O.; Whitehorne, T. J. J.; Prud'homme, R. E.; Schaper, F. *Organometallics* **2010,** *29*, 2139-2147.

(68) Xu, X.; Chen, Y.; Zou, G.; Ma, Z.; Li, G. *J. Organomet. Chem.* **2010,** *695*, 1155-1162.

(69) (a) Wisniewski, M.; Borgne, A. L.; Spassky, N. *Macromol. Chem. Phys.* **1997,** *198*, 1227-1238; (b) Majerska, K.; Duda, A. *J. Am. Chem. Soc.* **2004,** *126*, 1026-1027; (c) Lian, B.; Ma, H.; Spaniol, T. P.; Okuda, J. *Dalton Trans.* **2009**, 9033-9042.

(70) (a) Pang, X.; Chen, X.; Du, H.; Wang, X.; Jing, X. *J. Organomet. Chem.* **2007,** *692*, 5605-5613; (b) Phomphrai, K.; Chumsaeng, P.; Sangtrirutnugul, P.; Kongsaeree, P.; Pohmakotr, M. *Dalton Trans.* **2010,** *39*, 1865-1871.

(71) Thadani, A. N.; Huang, Y.; Rawal, V. H. *Org. Lett.* **2007,** *9*, 3873-3876.

(72) Complex **2g** was recrystallized by heating the complex in a sealed test tube at 50 ^{o}C in dichloromethane until all of the complex was dissolved. The crystal tube was kept at -10 ^{o}C and provided crystals of the *trans* form exclusively, as evidenced by X-ray crystallographic studies.

(73) Williams, C. K.; Hillmyer, M. A. *Polym. Rev.* **2008,** *48*, 1-10.

(74) (a) Schmack, G.; Tändler, B.; Vogel, R.; Beyreuther, R.; Jacobsen, S.; Fritz, H. G. *J. Appl. Polym. Sci.* **1999,** *73*, 2785-2797; (b) Perepelkin, K. E. *Fibre Chem.* **2002,** *34*, 85-100; (c) Avinc, O.; Khoddami, A. *Fibre Chem.* **2009,** *41*, 391-401.

(75) Paulsson, M.; Singh, S. K. *J. Pharm. Sci.* **1999,** *88*, 406-411.

(76) Reichardt, R.; Vagin, S.; Reithmeier, R.; Ott, A. K.; Rieger, B. *Macromolecules* **2010,** *43*, 9311-9317.

(77) Dobroth, Z. T.; Hu, S.; Coats, E. R.; McDonald, A. G. *Bioresour. Technol.* **2011,** *102*, 3352-3359.

(78) van der Walle, G.; de Koning, G.; Weusthuis, R.; Eggink, G., Properties, Modifications and Applications of Biopolyesters. In *Biopolyesters*, Babel, W.; Steinbüchel, A., Eds. Springer Berlin / Heidelberg: 2001; Vol. 71, pp 263-291.

(79) Tabone, M. D.; Cregg, J. J.; Beckman, E. J.; Landis, A. E. *Environ. Sci. Technol.* **2010,** *44*, 8264-8269.

(80) Toncheva, N.; Jerome, R.; Mateva, R. *Eur. Polym. J.* **2011,** *47*, 238-247.

(81) Jansen, J.; Bosman, M. B.; Boerakker, M. J.; Feijen, J.; Grijpma, D. W. *J. Controlled Release* **2010,** *148*, e79-e80.

(82) Brookhart, M.; Grant, B.; Volpe, A. F. *Organometallics* **1992,** *11*, 3920-3922.

(83) (a) Adams, J. *Acta Crystallogr., Sect. B* **1979,** *35*, 1084-1088; (b) Valle, G. C.; Bombi, G. G.; Corain, B.; Favarato, M.; Zatta, P. *J. Chem. Soc., Dalton Trans.* **1989**, 1513-1517; (c) Mason, M. R.; Smith, J. M.; Bott, S. G.; Barron, A. R. *J. Am. Chem. Soc.* **1993,** *115*, 4971-4984; (d) Schnitter, C.; Roesky, H. W.; Albers, T.; Schmidt, H.-G.; Röpken, C.; Parisini, E.; Sheldrick, G. M. *Chem.-Eur. J.* **1997,** *3*, 1783-1792; (e) Veith, M.; Jarczyk, M.; Huch, V. *Angew. Chem., Int. Ed.* **1998,** *37*, 105-108; (f) Chen, H.-L.; Ko, B.-T.; Huang, B.-H.; Lin, C.-C. *Organometallics* **2001,** *20*, 5076-5083; (g) Zhu, H.; Chai, J.; He, C.; Bai, G.; Roesky, H. W.; Jancik, V.; Schmidt, H.-G.; Noltemeyer, M. *Organometallics* **2004,** *24*, 380-384; (h) Joszai, R.; Kerekes, I.; Satoshi, I.; Sawada, K.; Zekany, L.; Toth, I. *Dalton Trans.* **2006**, 3221-3227; (i) Li, X.; Song, H.; Duan, L.; Cui, C.; Roesky, H. W. *Inorg. Chem.* **2006,** *45*, 1912-1914; (j) Cametti, M.; Dalla Cort, A.; Colapietro, M.; Portalone, G.; Russo, L.; Rissanen, K. *Inorg. Chem.* **2007,** *46*, 9057-9059.

(84) Alemán, C.; Betran, O.; Casanovas, J.; Houk, K. N.; Hall, H. K. *J. Org. Chem.* **2009,** *74*, 6237-6244.

(85) Rieth, L. R.; Moore, D. R.; Lobkovsky, E. B.; Coates, G. W. *J. Am. Chem. Soc.* **2002,** *124*, 15239-15248.

(86) (a) Ouhadi, T.; Hamitou, A.; Jerome, R.; Teyssie, P. *Macromolecules* **1976,** *9*, 927-931; (b) Dubois, P.; Jacobs, C.; Jerome, R.; Teyssie, P. *Macromolecules* **1991,** *24*, 2266-2270; (c) Beila, T.; Duda, A.; Penczek, S. *Polym. Prepr., Am. Chem. Soc., Div. Polym. Chem.* **1994,** *35*, 508-508.

(87) Duda, A.; Penczek, S. *Macromol. Rapid Commun.* **1994,** *15*, 559-566.

(88) Fineman, M.; Ross, S. D. *J. Polym. Sci.* **1950,** *5*, 259-262.

APPENDIX A

COPYRIGHT INFORMATION

American Chemical Society's Policy on Theses and Dissertations

If your university requires a signed copy of this letter see contact information below.

Thank you for your request for permission to include **your** paper(s) or portions of text from **your** paper(s) in your thesis. Permission is now automatically granted; please pay special attention to the implications paragraph below. The Copyright Subcommittee of the Joint Board/Council Committees on Publications approved the following:

Copyright permission for published and submitted material from theses and dissertations
ACS extends blanket permission to students to include in their theses and dissertations their own articles, or portions thereof, that have been published in ACS journals or submitted to ACS journals for publication, provided that the ACS copyright credit line is noted on the appropriate page(s).

Publishing implications of electronic publication of theses and dissertation material
Students and their mentors should be aware that posting of theses and dissertation material on the Web prior to submission of material from that thesis or dissertation to an ACS journal may affect publication in that journal. Whether Web posting is considered prior publication may be evaluated on a case-by-case basis by the journal's editor. If an ACS journal editor considers Web posting to be "prior publication", the paper will not be accepted for publication in that journal. If you intend to submit your unpublished paper to ACS for publication, check with the appropriate editor prior to posting your manuscript electronically.

If your paper has **not** yet been published by ACS, we have no objection to your including the text or portions of the text in your thesis/dissertation in **print and microfilm formats**; please note, however, that electronic distribution or Web posting of the unpublished paper as part of your thesis in electronic formats might jeopardize publication of your paper by ACS. Please print the following credit line on the first page of your article: "Reproduced (or 'Reproduced in part') with permission from [JOURNAL NAME], in press (or 'submitted for publication'). Unpublished work copyright [CURRENT YEAR] American Chemical Society." Include appropriate information.

If your paper has already been published by ACS and you want to include the text or portions of the text in your thesis/dissertation in **print or microfilm formats**, please print the ACS copyright credit line on the first page of your article: "Reproduced (or 'Reproduced in part') with permission from [FULL REFERENCE CITATION.] Copyright [YEAR] American Chemical Society." Include appropriate information.

Submission to a Dissertation Distributor: If you plan to submit your thesis to UMI or to another dissertation distributor, you should not include the unpublished ACS paper in your thesis if the thesis will be disseminated electronically, until ACS has published your paper. After publication of the paper by ACS, you may release the entire thesis (**not the individual ACS article by itself**) for electronic dissemination through the distributor; ACS's copyright credit line should be printed on the first page of the ACS paper.

Use on an Intranet: The inclusion of your ACS unpublished or published manuscript is permitted in your thesis in print and microfilm formats. If ACS has published your paper you may include the manuscript in your thesis on an intranet that is not publicly available. Your ACS article cannot be posted electronically on a publicly available medium (i.e. one that is not password protected), such as but not limited to, electronic archives, Internet, library server, etc. The only material from your paper that can be posted on a public electronic medium is the article abstract, figures, and tables, and you may link to the article's DOI or post the article's author-directed URL link provided by ACS. This paragraph does not pertain to the dissertation distributor paragraph above.

Questions? Call +1 202/872-4368/4367. Send e-mail to copyright@acs.org or fax to +1 202-776-8112. 10/10/03, 01/15/04, 06/07/06

APPENDIX B

TABLES OF CRYSTALLOGRAPHIC DATA

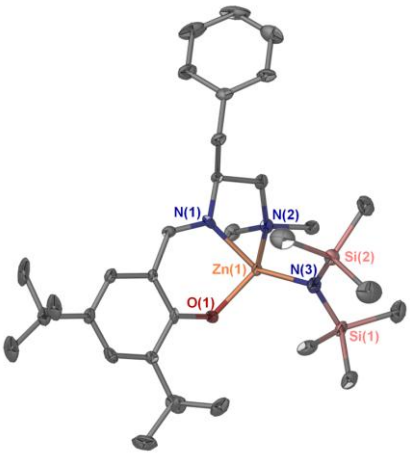

Complex II6a

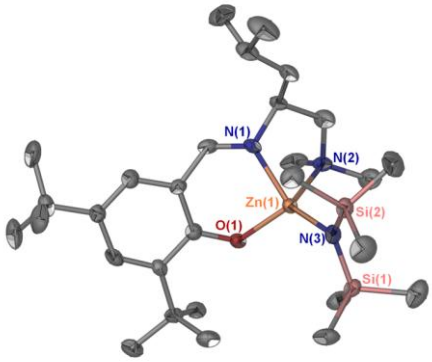

Complex II6b

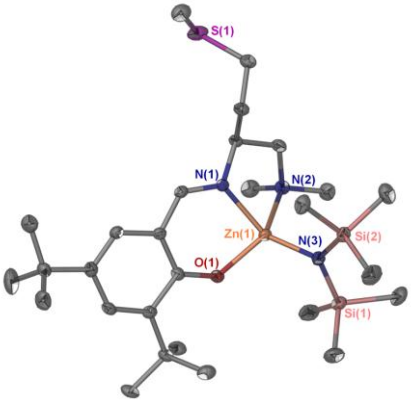

Complex II6c

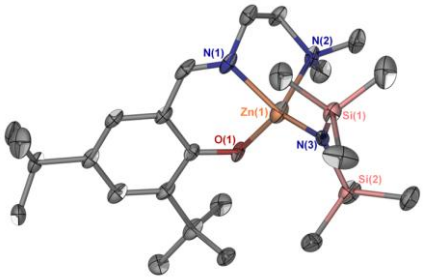

Complex II6d

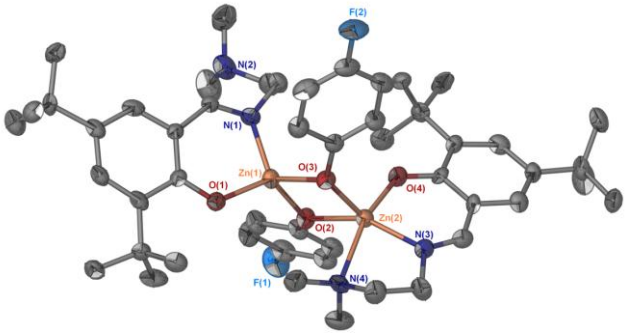

Complex II6e

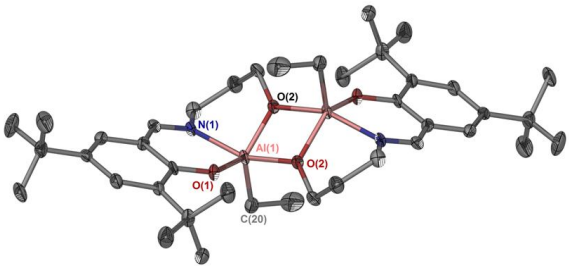

Complex IV2f (*trans*-)
Complex V2f (*trans*-)

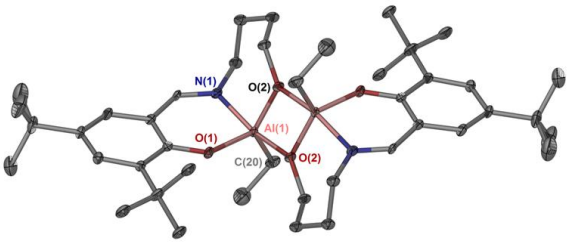

Complex IV2g
Complex V2g

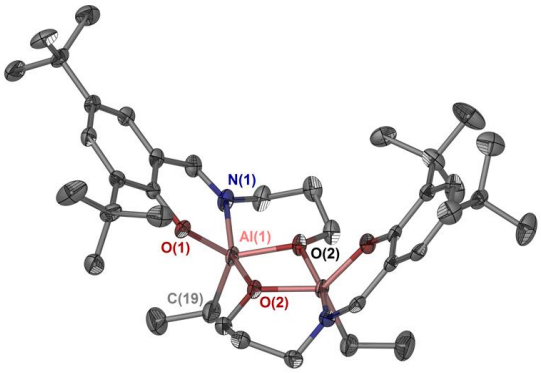

Complex V2f (*cis*-)

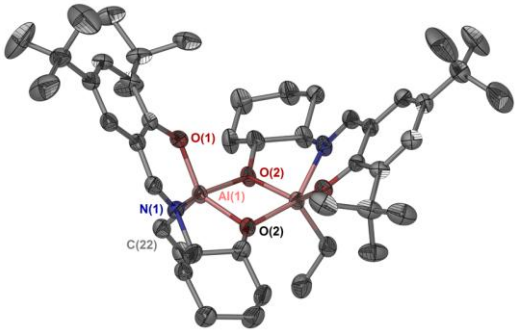

Complex V2a

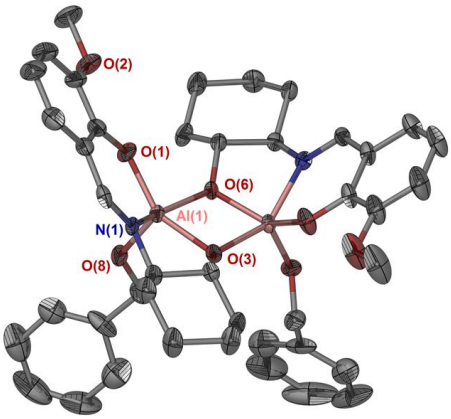

Complex V3b

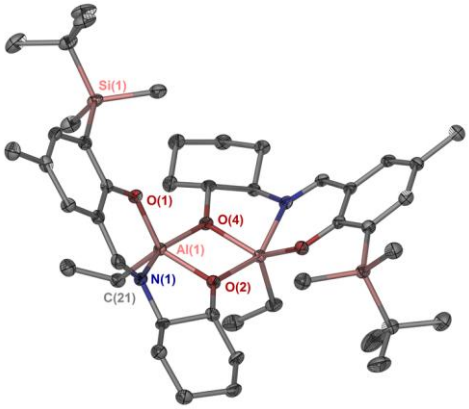

Complex V2d

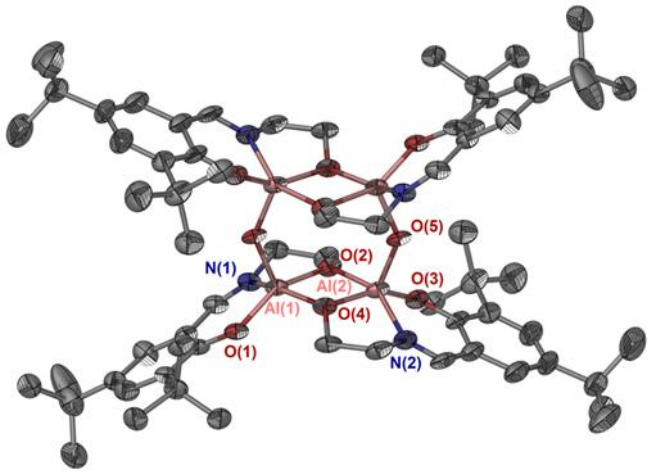

Complex V3e

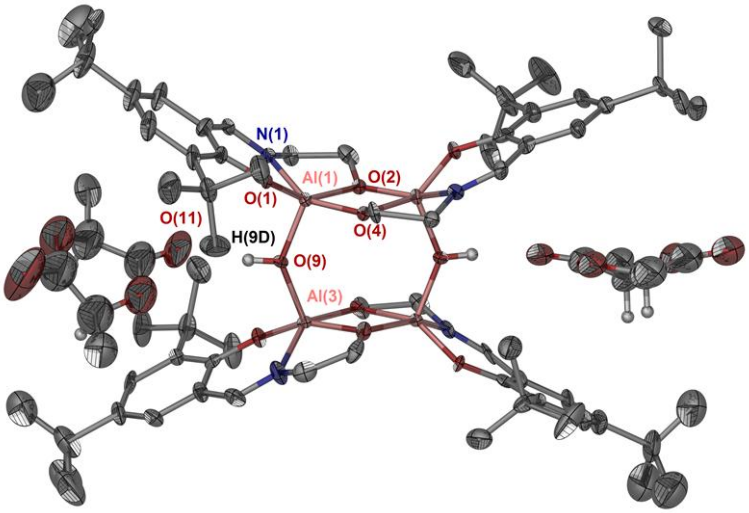

Complex V4e

Table B-1. Crystal Data and Structure Refinement for Complex **II6a**.

Identification code	Complex **II6a**	
Empirical formula	C32 H55 N3 O Si2 Zn	
Formula weight	619.34	
Temperature	150(2) K	
Wavelength	0.71073 Å	
Crystal system	Orthorhombic	
Space group	P(2)1(2)1(2)1	
Unit cell dimensions	a = 8.719(4) Å	α= 90°.
	b = 16.535(8) Å	β= 90°.
	c = 24.901(12) Å	γ = 90°.
Volume	3590(3) $Å^3$	
Z	4	
Density (calculated)	1.146 Mg/m^3	
Absorption coefficient	0.777 mm^{-1}	
F(000)	1336	
Crystal size	0.20 x 0.20 x 0.18 mm^3	
Theta range for data collection	2.05 to 25.99°.	
Index ranges	-10<=h<=10, -20<=k<=20, -30<=l<=30	
Reflections collected	32055	
Independent reflections	7063 [R(int) = 0.1231]	
Completeness to theta = 25.99°	99.9 %	
Absorption correction	Semi-empirical from equivalents	
Max. and min. transmission	0.8728 and 0.8601	
Refinement method	Full-matrix least-squares on F^2	
Data / restraints / parameters	7063 / 4 / 373	
Goodness-of-fit on F^2	1.014	
Final R indices [I>2sigma(I)]	R1 = 0.0539, wR2 = 0.1190	
R indices (all data)	R1 = 0.0779, wR2 = 0.1299	
Absolute structure parameter	0.012(15)	
Largest diff. peak and hole	0.620 and -0.538 $e.Å^{-3}$	

Table B-2. Bond Lengths [Å] and Angles [°] for Complex **II6a**.

C(1)-O(1)	1.293(5)	C(1)-C(2)	1.419(6)
C(1)-C(6)	1.444(6)	C(2)-C(3)	1.408(6)
C(2)-C(15)	1.444(6)	C(3)-C(4)	1.376(6)
C(4)-C(5)	1.386(6)	C(4)-C(11)	1.524(6)
C(5)-C(6)	1.386(6)	C(6)-C(7)	1.533(7)
C(7)-C(8)	1.525(7)	C(7)-C(10)	1.530(7)
C(7)-C(9)	1.541(7)	C(11)-C(14A)	1.46(11)
C(11)-C(12B)	1.527(3)	C(11)-C(13B)	1.527(3)
C(11)-C(13A)	1.529(3)	C(11)-C(12A)	1.531(3)
C(11)-C(14B)	1.55(5)	C(15)-N(1)	1.280(5)
C(16)-N(1)	1.480(5)	C(16)-C(26)	1.515(6)
C(16)-C(17)	1.522(6)	C(17)-N(2)	1.472(6)
C(18)-N(2)	1.466(6)	C(19)-N(2)	1.470(6)
C(20)-Si(2)	1.878(6)	C(21)-Si(2)	1.872(6)
C(22)-Si(2)	1.868(6)	C(23)-Si(1)	1.859(5)
C(24)-Si(1)	1.866(5)	C(25)-Si(1)	1.879(5)
C(26)-C(27)	1.517(6)	C(27)-C(28)	1.374(7)
C(27)-C(32)	1.379(7)	C(28)-C(29)	1.397(7)
C(29)-C(30)	1.357(9)	C(30)-C(31)	1.376(9)
C(31)-C(32)	1.401(8)	N(1)-Zn(1)	2.017(4)
N(2)-Zn(1)	2.198(3)	N(3)-Si(2)	1.697(4)
N(3)-Si(1)	1.703(4)	N(3)-Zn(1)	1.920(4)
O(1)-Zn(1)	1.933(3)		
O(1)-C(1)-C(2)	123.5(4)	O(1)-C(1)-C(6)	119.8(4)
C(2)-C(1)-C(6)	116.6(4)	C(3)-C(2)-C(1)	121.9(4)
C(3)-C(2)-C(15)	115.8(4)	C(1)-C(2)-C(15)	121.8(4)
C(4)-C(3)-C(2)	121.4(4)	C(3)-C(4)-C(5)	116.5(4)
C(3)-C(4)-C(11)	121.5(4)	C(5)-C(4)-C(11)	122.0(4)
C(4)-C(5)-C(6)	125.7(4)	C(5)-C(6)-C(1)	117.9(4)
C(5)-C(6)-C(7)	122.8(4)	C(1)-C(6)-C(7)	119.3(4)
C(8)-C(7)-C(10)	107.5(5)	C(8)-C(7)-C(6)	111.4(4)
C(10)-C(7)-C(6)	110.5(4)	C(8)-C(7)-C(9)	108.0(4)

C(10)-C(7)-C(9)	110.2(4)	C(6)-C(7)-C(9)	109.1(4)
C(14A)-C(11)-C(4)	113(4)	C(14A)-C(11)-C(12B)	108(3)
C(4)-C(11)-C(12B)	108.9(5)	C(14A)-C(11)-C(13B)	129(3)
C(4)-C(11)-C(13B)	113.5(7)	C(12B)-C(11)-C(13B)	77.0(8)
C(14A)-C(11)-C(13A)	110(3)	C(4)-C(11)-C(13A)	110.8(5)
C(12B)-C(11)-C(13A)	106.9(6)	C(13B)-C(11)-C(13A)	31.3(6)
C(14A)-C(11)-C(12A)	82(3)	C(4)-C(11)-C(12A)	107.3(7)
C(12B)-C(11)-C(12A)	29.9(7)	C(13B)-C(11)-C(12A)	104.6(9)
C(13A)-C(11)-C(12A)	131.1(8)	C(14A)-C(11)-C(14B)	14(4)
C(4)-C(11)-C(14B)	113.0(18)	C(12B)-C(11)-C(14B)	119.4(17)
C(13B)-C(11)-C(14B)	120.3(19)	C(13A)-C(11)-C(14B)	97.0(18)
C(12A)-C(11)-C(14B)	95.3(18)	N(1)-C(15)-C(2)	126.7(4)
N(1)-C(16)-C(26)	112.5(4)	N(1)-C(16)-C(17)	106.6(3)
C(26)-C(16)-C(17)	111.7(4)	N(2)-C(17)-C(16)	112.9(4)
C(16)-C(26)-C(27)	111.4(4)	C(28)-C(27)-C(32)	119.0(5)
C(28)-C(27)-C(26)	121.1(4)	C(32)-C(27)-C(26)	119.9(4)
C(27)-C(28)-C(29)	120.8(5)	C(30)-C(29)-C(28)	119.6(6)
C(29)-C(30)-C(31)	120.9(5)	C(30)-C(31)-C(32)	119.2(6)
C(27)-C(32)-C(31)	120.4(5)	C(15)-N(1)-C(16)	118.2(4)
C(15)-N(1)-Zn(1)	122.6(3)	C(16)-N(1)-Zn(1)	116.3(3)
C(18)-N(2)-C(19)	110.0(4)	C(18)-N(2)-C(17)	107.9(3)
C(19)-N(2)-C(17)	110.5(3)	C(18)-N(2)-Zn(1)	115.5(3)
C(19)-N(2)-Zn(1)	113.2(3)	C(17)-N(2)-Zn(1)	99.0(2)
Si(2)-N(3)-Si(1)	126.6(2)	Si(2)-N(3)-Zn(1)	118.6(2)
Si(1)-N(3)-Zn(1)	114.7(2)	C(1)-O(1)-Zn(1)	125.7(3)
N(3)-Si(1)-C(23)	109.7(2)	N(3)-Si(1)-C(24)	111.8(2)
C(23)-Si(1)-C(24)	108.0(3)	N(3)-Si(1)-C(25)	114.5(2)
C(23)-Si(1)-C(25)	105.8(2)	C(24)-Si(1)-C(25)	106.7(3)
N(3)-Si(2)-C(22)	112.4(2)	N(3)-Si(2)-C(21)	110.7(2)
C(22)-Si(2)-C(21)	107.6(3)	N(3)-Si(2)-C(20)	113.4(2)
C(22)-Si(2)-C(20)	105.6(3)	C(21)-Si(2)-C(20)	106.9(3)
N(3)-Zn(1)-O(1)	115.60(14)	N(3)-Zn(1)-N(1)	136.85(16)
O(1)-Zn(1)-N(1)	91.24(13)	N(3)-Zn(1)-N(2)	110.14(14)
O(1)-Zn(1)-N(2)	121.26(14)	N(1)-Zn(1)-N(2)	78.64(14)

Table B-3. Crystal Data and Structure Refinement for Complex **II6b**

Identification code	Complex **II6b**	
Empirical formula	C58 H114 N6 O2 Si4 Zn2	
Formula weight	1170.65	
Temperature	110(2) K	
Wavelength	1.54178 Å	
Crystal system	Monoclinic	
Space group	P2(1)	
Unit cell dimensions	a = 10.616(3) Å	α= 90°.
	b = 18.225(4) Å	β= 91.995(13)°.
	c = 17.992(4) Å	γ = 90°.
Volume	3478.7(14) $Å^3$	
Z	2	
Density (calculated)	1.118 Mg/m^3	
Absorption coefficient	1.805 mm^{-1}	
F(000)	1272	
Crystal size	0.18 x 0.17 x 0.15 mm^3	
Theta range for data collection	2.46 to 60.51°.	
Index ranges	-11<=h<=11, -19<=k<=20, -20<=l<=19	
Reflections collected	27837	
Independent reflections	9520 [R(int) = 0.0627]	
Completeness to theta = 60.51°	97.0 %	
Absorption correction	Semi-empirical from equivalents	
Max. and min. transmission	0.7735 and 0.7371	
Refinement method	Full-matrix least-squares on F^2	
Data / restraints / parameters	9520 / 4 / 694	
Goodness-of-fit on F^2	1.077	
Final R indices [I>2sigma(I)]	R1 = 0.0402, wR2 = 0.0963	
R indices (all data)	R1 = 0.0515, wR2 = 0.1030	
Absolute structure parameter	-0.01(2)	
Largest diff. peak and hole	0.418 and -0.541 $e.Å^{-3}$	

Table B-4. Bond Lengths [Å] and Angles [°] for Complex **II6b**.

C(1)-O(1)	1.324(6)	C(1)-C(2)	1.420(6)
C(1)-C(6)	1.441(7)	C(2)-C(3)	1.415(6)
C(2)-C(15)	1.445(6)	C(3)-C(4)	1.377(7)
C(3)-H(3)	0.9500	C(4)-C(5)	1.403(7)
C(4)-C(11)	1.538(7)	C(5)-C(6)	1.378(7)
C(5)-H(5)	0.9500	C(6)-C(7)	1.530(6)
C(7)-C(9)	1.530(7)	C(7)-C(8)	1.540(7)
C(7)-C(10)	1.541(7)	C(8)-H(8A)	0.9800
C(8)-H(8B)	0.9800	C(8)-H(8C)	0.9800
C(9)-H(9A)	0.9800	C(9)-H(9B)	0.9800
C(9)-H(9C)	0.9800	C(10)-H(10A)	0.9800
C(10)-H(10B)	0.9800	C(10)-H(10C)	0.9800
C(11)-C(13)	1.518(8)	C(11)-C(14)	1.525(7)
C(11)-C(12)	1.541(7)	C(12)-H(12A)	0.9800
C(12)-H(12B)	0.9800	C(12)-H(12C)	0.9800
C(13)-H(13A)	0.9800	C(13)-H(13B)	0.9800
C(13)-H(13C)	0.9800	C(14)-H(14A)	0.9800
C(14)-H(14B)	0.9800	C(14)-H(14C)	0.9800
C(15)-N(1)	1.294(6)	C(15)-H(15)	0.9500
C(16)-N(1)	1.485(6)	C(16)-C(26)	1.516(6)
C(16)-C(17)	1.542(6)	C(16)-H(16)	1.0000
C(17)-N(2)	1.453(6)	C(17)-H(17A)	0.9900
C(17)-H(17B)	0.9900	C(18)-N(2)	1.480(6)
C(18)-H(18A)	0.9800	C(18)-H(18B)	0.9800
C(18)-H(18C)	0.9800	C(19)-N(2)	1.498(6)
C(19)-H(19A)	0.9800	C(19)-H(19B)	0.9800
C(19)-H(19C)	0.9800	C(20)-Si(1)	1.886(5)
C(20)-H(20A)	0.9800	C(20)-H(20B)	0.9800
C(20)-H(20C)	0.9800	C(21)-Si(1)	1.867(5)
C(21)-H(21A)	0.9800	C(21)-H(21B)	0.9800
C(21)-H(21C)	0.9800	C(22)-Si(1)	1.878(6)
C(22)-H(22A)	0.9800	C(22)-H(22B)	0.9800
C(22)-H(22C)	0.9800	C(23)-Si(2)	1.876(5)

C(23)-H(23A)	0.9800	C(23)-H(23B)	0.9800
C(23)-H(23C)	0.9800	C(24)-Si(2)	1.888(6)
C(24)-H(24A)	0.9800	C(24)-H(24B)	0.9800
C(24)-H(24C)	0.9800	C(25)-Si(2)	1.882(6)
C(25)-H(25A)	0.9800	C(25)-H(25B)	0.9800
C(25)-H(25C)	0.9800	C(26)-C(27)	1.534(7)
C(26)-H(26A)	0.9900	C(26)-H(26B)	0.9900
C(27)-C(28)	1.531(7)	C(27)-C(29)	1.532(8)
C(27)-H(27)	1.0000	C(28)-H(28A)	0.9800
C(28)-H(28B)	0.9800	C(28)-H(28C)	0.9800
C(29)-H(29A)	0.9800	C(29)-H(29B)	0.9800
C(29)-H(29C)	0.9800	C(30)-O(2)	1.315(5)
C(30)-C(31)	1.430(6)	C(30)-C(35)	1.447(7)
C(31)-C(32)	1.398(6)	C(31)-C(44)	1.447(6)
C(32)-C(33)	1.377(7)	C(32)-H(32)	0.9500
C(33)-C(34)	1.409(6)	C(33)-C(40)	1.528(6)
C(34)-C(35)	1.385(7)	C(34)-H(34)	0.9500
C(35)-C(36)	1.536(6)	C(36)-C(37)	1.530(7)
C(36)-C(38)	1.537(6)	C(36)-C(39)	1.542(6)
C(37)-H(37A)	0.9800	C(37)-H(37B)	0.9800
C(37)-H(37C)	0.9800	C(38)-H(38A)	0.9800
C(38)-H(38B)	0.9800	C(38)-H(38C)	0.9800
C(39)-H(39A)	0.9800	C(39)-H(39B)	0.9800
C(39)-H(39C)	0.9800	C(40)-C(43A)	1.472(17)
C(40)-C(41)	1.493(8)	C(40)-C(41A)	1.498(17)
C(40)-C(43)	1.521(8)	C(40)-C(42)	1.598(8)
C(40)-C(42A)	1.648(16)	C(41)-H(41A)	0.9800
C(41)-H(41B)	0.9800	C(41)-H(41C)	0.9800
C(42)-H(42A)	0.9800	C(42)-H(42B)	0.9800
C(42)-H(42C)	0.9800	C(43)-H(43A)	0.9800
C(43)-H(43B)	0.9800	C(43)-H(43C)	0.9800
C(44)-N(4)	1.279(6)	C(44)-H(44)	0.9500
C(45)-N(4)	1.475(5)	C(45)-C(55)	1.519(6)
C(45)-C(46)	1.527(6)	C(45)-H(45)	1.0000

C(46)-N(5)	1.483(5)	C(46)-H(46A)	0.9900
C(46)-H(46B)	0.9900	C(47)-N(5)	1.459(6)
C(47)-H(47A)	0.9800	C(47)-H(47B)	0.9800
C(47)-H(47C)	0.9800	C(48)-N(5)	1.482(6)
C(48)-H(48A)	0.9800	C(48)-H(48B)	0.9800
C(48)-H(48C)	0.9800	C(49)-Si(3)	1.886(5)
C(49)-H(49A)	0.9800	C(49)-H(49B)	0.9800
C(49)-H(49C)	0.9800	C(50)-Si(3)	1.881(5)
C(50)-H(50A)	0.9800	C(50)-H(50B)	0.9800
C(50)-H(50C)	0.9800	C(51)-Si(3)	1.875(6)
C(51)-H(51A)	0.9800	C(51)-H(51B)	0.9800
C(51)-H(51C)	0.9800	C(52)-Si(4)	1.865(5)
C(52)-H(52A)	0.9800	C(52)-H(52B)	0.9800
C(52)-H(52C)	0.9800	C(53)-Si(4)	1.877(5)
C(53)-H(53A)	0.9800	C(53)-H(53B)	0.9800
C(53)-H(53C)	0.9800	C(54)-Si(4)	1.882(5)
C(54)-H(54A)	0.9800	C(54)-H(54B)	0.9800
C(54)-H(54C)	0.9800	C(55)-C(56)	1.523(7)
C(55)-H(55A)	0.9900	C(55)-H(55B)	0.9900
C(56)-C(57)	1.508(7)	C(56)-C(58)	1.534(7)
C(56)-H(56)	1.0000	C(57)-H(57A)	0.9800
C(57)-H(57B)	0.9800	C(57)-H(57C)	0.9800
C(58)-H(58A)	0.9800	C(58)-H(58B)	0.9800
C(58)-H(58C)	0.9800	C(41A)-H(41D)	0.9800
C(41A)-H(41E)	0.9800	C(41A)-H(41F)	0.9800
C(42A)-H(42D)	0.9800	C(42A)-H(42E)	0.9800
C(42A)-H(42F)	0.9800	C(43A)-H(43D)	0.9800
C(43A)-H(43E)	0.9800	C(43A)-H(43F)	0.9800
N(1)-Zn(1)	2.030(4)	N(2)-Zn(1)	2.193(4)
N(3)-Si(2)	1.706(4)	N(3)-Si(1)	1.711(4)
N(3)-Zn(1)	1.921(4)	N(4)-Zn(2)	2.007(4)
N(5)-Zn(2)	2.232(4)	N(6)-Si(3)	1.697(4)
N(6)-Si(4)	1.707(4)	N(6)-Zn(2)	1.927(4)
O(1)-Zn(1)	1.930(3)	O(2)-Zn(2)	1.922(3)

		O(1)-C(1)-C(2)	122.2(4)
O(1)-C(1)-C(6)	119.6(4)	C(2)-C(1)-C(6)	118.1(4)
C(3)-C(2)-C(1)	119.8(4)	C(3)-C(2)-C(15)	116.9(4)
C(1)-C(2)-C(15)	122.9(4)	C(4)-C(3)-C(2)	123.1(4)
C(4)-C(3)-H(3)	118.5	C(2)-C(3)-H(3)	118.5
C(3)-C(4)-C(5)	115.2(4)	C(3)-C(4)-C(11)	122.7(4)
C(5)-C(4)-C(11)	122.1(5)	C(6)-C(5)-C(4)	126.0(5)
C(6)-C(5)-H(5)	117.0	C(4)-C(5)-H(5)	117.0
C(5)-C(6)-C(1)	117.5(4)	C(5)-C(6)-C(7)	122.3(4)
C(1)-C(6)-C(7)	120.2(4)	C(9)-C(7)-C(6)	110.2(4)
C(9)-C(7)-C(8)	107.5(4)	C(6)-C(7)-C(8)	112.0(4)
C(9)-C(7)-C(10)	109.6(4)	C(6)-C(7)-C(10)	110.5(4)
C(8)-C(7)-C(10)	106.9(4)	C(7)-C(8)-H(8A)	109.5
C(7)-C(8)-H(8B)	109.5	H(8A)-C(8)-H(8B)	109.5
C(7)-C(8)-H(8C)	109.5	H(8A)-C(8)-H(8C)	109.5
H(8B)-C(8)-H(8C)	109.5	C(7)-C(9)-H(9A)	109.5
C(7)-C(9)-H(9B)	109.5	H(9A)-C(9)-H(9B)	109.5
C(7)-C(9)-H(9C)	109.5	H(9A)-C(9)-H(9C)	109.5
H(9B)-C(9)-H(9C)	109.5	C(7)-C(10)-H(10A)	109.5
C(7)-C(10)-H(10B)	109.5	H(10A)-C(10)-H(10B)	109.5
C(7)-C(10)-H(10C)	109.5	H(10A)-C(10)-H(10C)	109.5
H(10B)-C(10)-H(10C)	109.5	C(13)-C(11)-C(14)	109.7(5)
C(13)-C(11)-C(4)	112.0(4)	C(14)-C(11)-C(4)	107.6(4)
C(13)-C(11)-C(12)	107.6(5)	C(14)-C(11)-C(12)	108.3(5)
C(4)-C(11)-C(12)	111.6(4)	C(11)-C(12)-H(12A)	109.5
C(11)-C(12)-H(12B)	109.5	H(12A)-C(12)-H(12B)	109.5
C(11)-C(12)-H(12C)	109.5	H(12A)-C(12)-H(12C)	109.5
H(12B)-C(12)-H(12C)	109.5	C(11)-C(13)-H(13A)	109.5
C(11)-C(13)-H(13B)	109.5	H(13A)-C(13)-H(13B)	109.5
C(11)-C(13)-H(13C)	109.5	H(13A)-C(13)-H(13C)	109.5
H(13B)-C(13)-H(13C)	109.5	C(11)-C(14)-H(14A)	109.5
C(11)-C(14)-H(14B)	109.5	H(14A)-C(14)-H(14B)	109.5
C(11)-C(14)-H(14C)	109.5	H(14A)-C(14)-H(14C)	109.5
H(14B)-C(14)-H(14C)	109.5	N(1)-C(15)-C(2)	126.9(4)

N(1)-C(15)-H(15)	116.6	C(2)-C(15)-H(15)	116.6
N(1)-C(16)-C(26)	113.3(4)	N(1)-C(16)-C(17)	106.1(4)
C(26)-C(16)-C(17)	109.0(4)	N(1)-C(16)-H(16)	109.4
C(26)-C(16)-H(16)	109.4	C(17)-C(16)-H(16)	109.4
N(2)-C(17)-C(16)	114.8(4)	N(2)-C(17)-H(17A)	108.6
C(16)-C(17)-H(17A)	108.6	N(2)-C(17)-H(17B)	108.6
C(16)-C(17)-H(17B)	108.6	H(17A)-C(17)-H(17B)	107.6
N(2)-C(18)-H(18A)	109.5	N(2)-C(18)-H(18B)	109.5
H(18A)-C(18)-H(18B)	109.5	N(2)-C(18)-H(18C)	109.5
H(18A)-C(18)-H(18C)	109.5	H(18B)-C(18)-H(18C)	109.5
N(2)-C(19)-H(19A)	109.5	N(2)-C(19)-H(19B)	109.5
H(19A)-C(19)-H(19B)	109.5	N(2)-C(19)-H(19C)	109.5
H(19A)-C(19)-H(19C)	109.5	H(19B)-C(19)-H(19C)	109.5
Si(1)-C(20)-H(20A)	109.5	Si(1)-C(20)-H(20B)	109.5
H(20A)-C(20)-H(20B)	109.5	Si(1)-C(20)-H(20C)	109.5
H(20A)-C(20)-H(20C)	109.5	H(20B)-C(20)-H(20C)	109.5
Si(1)-C(21)-H(21A)	109.5	Si(1)-C(21)-H(21B)	109.5
H(21A)-C(21)-H(21B)	109.5	Si(1)-C(21)-H(21C)	109.5
H(21A)-C(21)-H(21C)	109.5	H(21B)-C(21)-H(21C)	109.5
Si(1)-C(22)-H(22A)	109.5	Si(1)-C(22)-H(22B)	109.5
H(22A)-C(22)-H(22B)	109.5	Si(1)-C(22)-H(22C)	109.5
H(22A)-C(22)-H(22C)	109.5	H(22B)-C(22)-H(22C)	109.5
Si(2)-C(23)-H(23A)	109.5	Si(2)-C(23)-H(23B)	109.5
H(23A)-C(23)-H(23B)	109.5	Si(2)-C(23)-H(23C)	109.5
H(23A)-C(23)-H(23C)	109.5	H(23B)-C(23)-H(23C)	109.5
Si(2)-C(24)-H(24A)	109.5	Si(2)-C(24)-H(24B)	109.5
H(24A)-C(24)-H(24B)	109.5	Si(2)-C(24)-H(24C)	109.5
H(24A)-C(24)-H(24C)	109.5	H(24B)-C(24)-H(24C)	109.5
Si(2)-C(25)-H(25A)	109.5	Si(2)-C(25)-H(25B)	109.5
H(25A)-C(25)-H(25B)	109.5	Si(2)-C(25)-H(25C)	109.5
H(25A)-C(25)-H(25C)	109.5	H(25B)-C(25)-H(25C)	109.5
C(16)-C(26)-C(27)	116.9(4)	C(16)-C(26)-H(26A)	108.1
C(27)-C(26)-H(26A)	108.1	C(16)-C(26)-H(26B)	108.1
C(27)-C(26)-H(26B)	108.1	H(26A)-C(26)-H(26B)	107.3

C(28)-C(27)-C(29)	109.8(5)	C(28)-C(27)-C(26)	109.8(5)
C(29)-C(27)-C(26)	112.9(4)	C(28)-C(27)-H(27)	108.1
C(29)-C(27)-H(27)	108.1	C(26)-C(27)-H(27)	108.1
C(27)-C(28)-H(28A)	109.5	C(27)-C(28)-H(28B)	109.5
H(28A)-C(28)-H(28B)	109.5	C(27)-C(28)-H(28C)	109.5
H(28A)-C(28)-H(28C)	109.5	H(28B)-C(28)-H(28C)	109.5
C(27)-C(29)-H(29A)	109.5	C(27)-C(29)-H(29B)	109.5
H(29A)-C(29)-H(29B)	109.5	C(27)-C(29)-H(29C)	109.5
H(29A)-C(29)-H(29C)	109.5	H(29B)-C(29)-H(29C)	109.5
O(2)-C(30)-C(31)	123.4(4)	O(2)-C(30)-C(35)	119.3(4)
C(31)-C(30)-C(35)	117.3(4)	C(32)-C(31)-C(30)	120.6(4)
C(32)-C(31)-C(44)	116.8(4)	C(30)-C(31)-C(44)	122.3(4)
C(33)-C(32)-C(31)	123.0(4)	C(33)-C(32)-H(32)	118.5
C(31)-C(32)-H(32)	118.5	C(32)-C(33)-C(34)	115.8(4)
C(32)-C(33)-C(40)	122.3(4)	C(34)-C(33)-C(40)	121.8(4)
C(35)-C(34)-C(33)	125.0(4)	C(35)-C(34)-H(34)	117.5
C(33)-C(34)-H(34)	117.5	C(34)-C(35)-C(30)	118.1(4)
C(34)-C(35)-C(36)	121.7(4)	C(30)-C(35)-C(36)	120.2(4)
C(37)-C(36)-C(35)	112.4(4)	C(37)-C(36)-C(38)	107.7(4)
C(35)-C(36)-C(38)	110.2(4)	C(37)-C(36)-C(39)	107.1(4)
C(35)-C(36)-C(39)	110.2(4)	C(38)-C(36)-C(39)	109.2(4)
C(36)-C(37)-H(37A)	109.5	C(36)-C(37)-H(37B)	109.5
H(37A)-C(37)-H(37B)	109.5	C(36)-C(37)-H(37C)	109.5
H(37A)-C(37)-H(37C)	109.5	H(37B)-C(37)-H(37C)	109.5
C(36)-C(38)-H(38A)	109.5	C(36)-C(38)-H(38B)	109.5
H(38A)-C(38)-H(38B)	109.5	C(36)-C(38)-H(38C)	109.5
H(38A)-C(38)-H(38C)	109.5	H(38B)-C(38)-H(38C)	109.5
C(36)-C(39)-H(39A)	109.5	C(36)-C(39)-H(39B)	109.5
H(39A)-C(39)-H(39B)	109.5	C(36)-C(39)-H(39C)	109.5
H(39A)-C(39)-H(39C)	109.5	H(39B)-C(39)-H(39C)	109.5
C(43A)-C(40)-C(41)	130.5(10)	C(43A)-C(40)-C(41A)	109.6(15)
C(41)-C(40)-C(41A)	46.6(11)	C(43A)-C(40)-C(43)	46.6(10)
C(41)-C(40)-C(43)	111.1(5)	C(41A)-C(40)-C(43)	132.3(10)
C(43A)-C(40)-C(33)	116.6(10)	C(41)-C(40)-C(33)	112.9(5)

C(41A)-C(40)-C(33)	115.3(10)	C(43)-C(40)-C(33)	112.4(4)
C(43A)-C(40)-C(42)	59.7(11)	C(41)-C(40)-C(42)	107.6(6)
C(41A)-C(40)-C(42)	62.3(12)	C(43)-C(40)-C(42)	105.6(5)
C(33)-C(40)-C(42)	106.7(4)	C(43A)-C(40)-C(42A)	107.3(14)
C(41)-C(40)-C(42A)	55.3(10)	C(41A)-C(40)-C(42A)	100.3(14)
C(43)-C(40)-C(42A)	64.0(10)	C(33)-C(40)-C(42A)	106.1(9)
C(42)-C(40)-C(42A)	147.0(9)	C(40)-C(41)-H(41A)	109.5
C(40)-C(41)-H(41B)	109.5	C(40)-C(41)-H(41C)	109.5
C(40)-C(42)-H(42A)	109.5	C(40)-C(42)-H(42B)	109.5
C(40)-C(42)-H(42C)	109.5	C(40)-C(43)-H(43A)	109.5
C(40)-C(43)-H(43B)	109.5	C(40)-C(43)-H(43C)	109.5
N(4)-C(44)-C(31)	126.0(4)	N(4)-C(44)-H(44)	117.0
C(31)-C(44)-H(44)	117.0	N(4)-C(45)-C(55)	118.0(4)
N(4)-C(45)-C(46)	103.6(3)	C(55)-C(45)-C(46)	112.5(4)
N(4)-C(45)-H(45)	107.4	C(55)-C(45)-H(45)	107.4
C(46)-C(45)-H(45)	107.4	N(5)-C(46)-C(45)	112.1(4)
N(5)-C(46)-H(46A)	109.2	C(45)-C(46)-H(46A)	109.2
N(5)-C(46)-H(46B)	109.2	C(45)-C(46)-H(46B)	109.2
H(46A)-C(46)-H(46B)	107.9	N(5)-C(47)-H(47A)	109.5
N(5)-C(47)-H(47B)	109.5	H(47A)-C(47)-H(47B)	109.5
N(5)-C(47)-H(47C)	109.5	H(47A)-C(47)-H(47C)	109.5
H(47B)-C(47)-H(47C)	109.5	N(5)-C(48)-H(48A)	109.5
N(5)-C(48)-H(48B)	109.5	H(48A)-C(48)-H(48B)	109.5
N(5)-C(48)-H(48C)	109.5	H(48A)-C(48)-H(48C)	109.5
H(48B)-C(48)-H(48C)	109.5	Si(3)-C(49)-H(49A)	109.5
Si(3)-C(49)-H(49B)	109.5	H(49A)-C(49)-H(49B)	109.5
Si(3)-C(49)-H(49C)	109.5	H(49A)-C(49)-H(49C)	109.5
H(49B)-C(49)-H(49C)	109.5	Si(3)-C(50)-H(50A)	109.5
Si(3)-C(50)-H(50B)	109.5	H(50A)-C(50)-H(50B)	109.5
Si(3)-C(50)-H(50C)	109.5	H(50A)-C(50)-H(50C)	109.5
H(50B)-C(50)-H(50C)	109.5	Si(3)-C(51)-H(51A)	109.5
Si(3)-C(51)-H(51B)	109.5	H(51A)-C(51)-H(51B)	109.5
Si(3)-C(51)-H(51C)	109.5	H(51A)-C(51)-H(51C)	109.5
H(51B)-C(51)-H(51C)	109.5	Si(4)-C(52)-H(52A)	109.5

Si(4)-C(52)-H(52B)	109.5	H(52A)-C(52)-H(52B)	109.5
Si(4)-C(52)-H(52C)	109.5	H(52A)-C(52)-H(52C)	109.5
H(52B)-C(52)-H(52C)	109.5	Si(4)-C(53)-H(53A)	109.5
Si(4)-C(53)-H(53B)	109.5	H(53A)-C(53)-H(53B)	109.5
Si(4)-C(53)-H(53C)	109.5	H(53A)-C(53)-H(53C)	109.5
H(53B)-C(53)-H(53C)	109.5	Si(4)-C(54)-H(54A)	109.5
Si(4)-C(54)-H(54B)	109.5	H(54A)-C(54)-H(54B)	109.5
Si(4)-C(54)-H(54C)	109.5	H(54A)-C(54)-H(54C)	109.5
H(54B)-C(54)-H(54C)	109.5	C(45)-C(55)-C(56)	116.2(4)
C(45)-C(55)-H(55A)	108.2	C(56)-C(55)-H(55A)	108.2
C(45)-C(55)-H(55B)	108.2	C(56)-C(55)-H(55B)	108.2
H(55A)-C(55)-H(55B)	107.4	C(57)-C(56)-C(55)	111.0(4)
C(57)-C(56)-C(58)	109.6(4)	C(55)-C(56)-C(58)	111.7(4)
C(57)-C(56)-H(56)	108.2	C(55)-C(56)-H(56)	108.2
C(58)-C(56)-H(56)	108.2	C(56)-C(57)-H(57A)	109.5
C(56)-C(57)-H(57B)	109.5	H(57A)-C(57)-H(57B)	109.5
C(56)-C(57)-H(57C)	109.5	H(57A)-C(57)-H(57C)	109.5
H(57B)-C(57)-H(57C)	109.5	C(56)-C(58)-H(58A)	109.5
C(56)-C(58)-H(58B)	109.5	H(58A)-C(58)-H(58B)	109.5
C(56)-C(58)-H(58C)	109.5	H(58A)-C(58)-H(58C)	109.5
H(58B)-C(58)-H(58C)	109.5	C(40)-C(41A)-H(41D)	109.5
C(40)-C(41A)-H(41E)	109.5	H(41D)-C(41A)-H(41E)	109.5
C(40)-C(41A)-H(41F)	109.5	H(41D)-C(41A)-H(41F)	109.5
H(41E)-C(41A)-H(41F)	109.5	C(40)-C(42A)-H(42D)	109.5
C(40)-C(42A)-H(42E)	109.5	H(42D)-C(42A)-H(42E)	109.5
C(40)-C(42A)-H(42F)	109.5	H(42D)-C(42A)-H(42F)	109.5
H(42E)-C(42A)-H(42F)	109.5	C(40)-C(43A)-H(43D)	109.5
C(40)-C(43A)-H(43E)	109.5	H(43D)-C(43A)-H(43E)	109.5
C(40)-C(43A)-H(43F)	109.5	H(43D)-C(43A)-H(43F)	109.5
H(43E)-C(43A)-H(43F)	109.5	C(15)-N(1)-C(16)	119.4(4)
C(15)-N(1)-Zn(1)	121.3(3)	C(16)-N(1)-Zn(1)	115.6(3)
C(17)-N(2)-C(18)	109.7(4)	C(17)-N(2)-C(19)	111.1(4)
C(18)-N(2)-C(19)	109.0(4)	C(17)-N(2)-Zn(1)	100.5(3)
C(18)-N(2)-Zn(1)	114.1(3)	C(19)-N(2)-Zn(1)	112.4(3)

Si(2)-N(3)-Si(1)	124.9(2)	Si(2)-N(3)-Zn(1)	119.0(2)
Si(1)-N(3)-Zn(1)	115.9(2)	C(44)-N(4)-C(45)	124.0(4)
C(44)-N(4)-Zn(2)	122.7(3)	C(45)-N(4)-Zn(2)	109.2(3)
C(47)-N(5)-C(48)	109.8(4)	C(47)-N(5)-C(46)	110.5(4)
C(48)-N(5)-C(46)	110.4(4)	C(47)-N(5)-Zn(2)	111.0(3)
C(48)-N(5)-Zn(2)	109.8(3)	C(46)-N(5)-Zn(2)	105.4(3)
Si(3)-N(6)-Si(4)	127.2(2)	Si(3)-N(6)-Zn(2)	116.1(2)
Si(4)-N(6)-Zn(2)	116.5(2)	C(1)-O(1)-Zn(1)	125.6(3)
C(30)-O(2)-Zn(2)	124.2(3)	N(3)-Si(1)-C(21)	110.9(2)
N(3)-Si(1)-C(22)	112.4(2)	C(21)-Si(1)-C(22)	106.1(3)
N(3)-Si(1)-C(20)	113.5(2)	C(21)-Si(1)-C(20)	106.8(2)
C(22)-Si(1)-C(20)	106.7(3)	N(3)-Si(2)-C(23)	111.1(2)
N(3)-Si(2)-C(25)	112.2(2)	C(23)-Si(2)-C(25)	108.2(3)
N(3)-Si(2)-C(24)	113.8(2)	C(23)-Si(2)-C(24)	105.2(3)
C(25)-Si(2)-C(24)	105.9(3)	N(6)-Si(3)-C(51)	112.5(3)
N(6)-Si(3)-C(50)	113.2(2)	C(51)-Si(3)-C(50)	106.9(3)
N(6)-Si(3)-C(49)	110.6(2)	C(51)-Si(3)-C(49)	106.7(3)
C(50)-Si(3)-C(49)	106.6(3)	N(6)-Si(4)-C(52)	112.0(2)
N(6)-Si(4)-C(53)	112.3(2)	C(52)-Si(4)-C(53)	107.6(2)
N(6)-Si(4)-C(54)	113.4(2)	C(52)-Si(4)-C(54)	105.6(3)
C(53)-Si(4)-C(54)	105.4(3)	N(3)-Zn(1)-O(1)	119.64(15)
N(3)-Zn(1)-N(1)	133.83(15)	O(1)-Zn(1)-N(1)	92.20(13)
N(3)-Zn(1)-N(2)	114.20(16)	O(1)-Zn(1)-N(2)	112.07(14)
N(1)-Zn(1)-N(2)	77.40(14)	O(2)-Zn(2)-N(6)	122.97(15)
O(2)-Zn(2)-N(4)	92.78(13)	N(6)-Zn(2)-N(4)	126.87(15)
O(2)-Zn(2)-N(5)	111.59(14)	N(6)-Zn(2)-N(5)	113.90(16)
N(4)-Zn(2)-N(5)	80.37(14)		

Table B-5. Crystal Data and Structure Refinement for Complex **II6c**.

Identification code	Complex **II6c**	
Empirical formula	C33 H67 N3 O S Si2 Zn	
Formula weight	675.51	
Temperature	110(2) K	
Wavelength	0.71073 Å	
Crystal system	Monoclinic	
Space group	P2(1)	
Unit cell dimensions	a = 15.315(7) Å	α= 90°.
	b = 10.089(5) Å	β= 104.946(6)°.
	c = 26.190(13) Å	γ = 90°.
Volume	3910(3) $Å^3$	
Z	4	
Density (calculated)	1.148 Mg/m^3	
Absorption coefficient	0.770 mm^{-1}	
F(000)	1472	
Crystal size	0.15 x 0.14 x 0.12 mm^3	
Theta range for data collection	1.38 to 27.50°.	
Index ranges	-19<=h<=19, -13<=k<=13, -34<=l<=33	
Reflections collected	44430	
Independent reflections	17705 [R(int) = 0.0242]	
Completeness to theta = 27.50°	99.6 %	
Absorption correction	Semi-empirical from equivalents	
Max. and min. transmission	0.9133 and 0.8933	
Refinement method	Full-matrix least-squares on F^2	
Data / restraints / parameters	17705 / 44 / 818	
Goodness-of-fit on F^2	1.032	
Final R indices [I>2sigma(I)]	R1 = 0.0347, wR2 = 0.0899	
R indices (all data)	R1 = 0.0408, wR2 = 0.0927	
Absolute structure parameter	0.004(6)	
Largest diff. peak and hole	0.827 and -0.583 $e.Å^{-3}$	

Table B-6. Bond Lengths [Å] and Angles [°] for Complex **II6c**.

C(1)-O(1)	1.299(3)	C(1)-C(6)	1.430(3)
C(1)-C(2)	1.442(3)	C(2)-C(3)	1.364(4)
C(2)-C(7)	1.540(3)	C(3)-C(4)	1.410(3)
C(3)-H(3)	0.9500	C(4)-C(5)	1.364(3)
C(4)-C(11)	1.532(4)	C(5)-C(6)	1.415(3)
C(5)-H(5)	0.9500	C(6)-C(15)	1.435(3)
C(7)-C(8)	1.532(4)	C(7)-C(9)	1.537(4)
C(7)-C(10)	1.544(3)	C(8)-H(8A)	0.9800
C(8)-H(8B)	0.9800	C(8)-H(8C)	0.9800
C(9)-H(9A)	0.9800	C(9)-H(9B)	0.9800
C(9)-H(9C)	0.9800	C(10)-H(10A)	0.9800
C(10)-H(10B)	0.9800	C(10)-H(10C)	0.9800
C(11)-C(14)	1.522(8)	C(11)-C(13A)	1.527(13)
C(11)-C(14A)	1.528(13)	C(11)-C(12)	1.533(4)
C(11)-C(13)	1.535(9)	C(12)-H(12A)	0.9800
C(12)-H(12B)	0.9800	C(12)-H(12C)	0.9800
C(13)-H(13A)	0.9800	C(13)-H(13B)	0.9800
C(13)-H(13C)	0.9800	C(14)-H(14A)	0.9800
C(14)-H(14B)	0.9800	C(14)-H(14C)	0.9800
C(13A)-H(13D)	0.9800	C(13A)-H(13E)	0.9800
C(13A)-H(13F)	0.9800	C(14A)-H(14D)	0.9800
C(14A)-H(14E)	0.9800	C(14A)-H(14F)	0.9800
C(15)-N(1)	1.290(3)	C(15)-H(15)	0.9500
C(16)-N(1)	1.471(3)	C(16)-C(17)	1.529(3)
C(16)-C(26)	1.533(3)	C(16)-H(16)	1.0000
C(17)-N(2)	1.478(3)	C(17)-H(17A)	0.9900
C(17)-H(17B)	0.9900	C(18)-N(2)	1.469(3)
C(18)-H(18A)	0.9800	C(18)-H(18B)	0.9800
C(18)-H(18C)	0.9800	C(19)-N(2)	1.472(3)
C(19)-H(19A)	0.9800	C(19)-H(19B)	0.9800
C(19)-H(19C)	0.9800	C(20)-Si(1)	1.861(3)
C(20)-H(20A)	0.9800	C(20)-H(20B)	0.9800

C(20)-H(20C)	0.9800	C(21)-Si(1)	1.877(3)
C(21)-H(21A)	0.9800	C(21)-H(21B)	0.9800
C(21)-H(21C)	0.9800	C(22)-Si(1)	1.881(3)
C(22)-H(22A)	0.9800	C(22)-H(22B)	0.9800
C(22)-H(22C)	0.9800	C(23)-Si(2)	1.869(3)
C(23)-H(23A)	0.9800	C(23)-H(23B)	0.9800
C(23)-H(23C)	0.9800	C(24)-Si(2)	1.878(3)
C(24)-H(24A)	0.9800	C(24)-H(24B)	0.9800
C(24)-H(24C)	0.9800	C(25)-Si(2)	1.871(3)
C(25)-H(25A)	0.9800	C(25)-H(25B)	0.9800
C(25)-H(25C)	0.9800	C(26)-C(27)	1.521(3)
C(26)-H(26A)	0.9900	C(26)-H(26B)	0.9900
C(27)-S(1)	1.810(3)	C(27)-H(27A)	0.9900
C(27)-H(27B)	0.9900	C(28)-S(1)	1.800(3)
C(28)-H(28A)	0.9800	C(28)-H(28B)	0.9800
C(28)-H(28C)	0.9800	C(29)-O(2)	1.309(3)
C(29)-C(34)	1.424(3)	C(29)-C(30)	1.427(3)
C(30)-C(31)	1.386(3)	C(30)-C(35)	1.539(3)
C(31)-C(32)	1.417(3)	C(31)-H(31)	0.9500
C(32)-C(33)	1.365(3)	C(32)-C(39)	1.535(3)
C(33)-C(34)	1.417(3)	C(33)-H(33)	0.9500
C(34)-C(43)	1.434(3)	C(35)-C(38)	1.530(3)
C(35)-C(36)	1.528(4)	C(35)-C(37)	1.530(3)
C(36)-H(36A)	0.9800	C(36)-H(36B)	0.9800
C(36)-H(36C)	0.9800	C(37)-H(37A)	0.9800
C(37)-H(37B)	0.9800	C(37)-H(37C)	0.9800
C(38)-H(38A)	0.9800	C(38)-H(38B)	0.9800
C(38)-H(38C)	0.9800	C(39)-C(40)	1.523(4)
C(39)-C(42)	1.525(4)	C(39)-C(41)	1.535(4)
C(40)-H(40A)	0.9800	C(40)-H(40B)	0.9800
C(40)-H(40C)	0.9800	C(41)-H(41A)	0.9800
C(41)-H(41B)	0.9800	C(41)-H(41C)	0.9800
C(42)-H(42A)	0.9800	C(42)-H(42B)	0.9800
C(42)-H(42C)	0.9800	C(43)-N(4)	1.288(3)

C(43)-H(43)	0.9500	C(44)-N(4)	1.477(3)
C(44)-C(54)	1.515(3)	C(44)-C(45)	1.535(3)
C(44)-H(44)	1.0000	C(45)-N(5)	1.481(3)
C(45)-H(45A)	0.9900	C(45)-H(45B)	0.9900
C(46)-N(5)	1.474(3)	C(46)-H(46A)	0.9800
C(46)-H(46B)	0.9800	C(46)-H(46C)	0.9800
C(47)-N(5)	1.477(3)	C(47)-H(47A)	0.9800
C(47)-H(47B)	0.9800	C(47)-H(47C)	0.9800
C(48)-Si(3)	1.867(3)	C(48)-H(48A)	0.9800
C(48)-H(48B)	0.9800	C(48)-H(48C)	0.9800
C(49)-Si(3)	1.870(3)	C(49)-H(49A)	0.9800
C(49)-H(49B)	0.9800	C(49)-H(49C)	0.9800
C(50)-Si(3)	1.875(3)	C(50)-H(50A)	0.9800
C(50)-H(50B)	0.9800	C(50)-H(50C)	0.9800
C(51)-Si(4)	1.862(3)	C(51)-H(51A)	0.9800
C(51)-H(51B)	0.9800	C(51)-H(51C)	0.9800
C(52)-Si(4)	1.874(3)	C(52)-H(52A)	0.9800
C(52)-H(52B)	0.9800	C(52)-H(52C)	0.9800
C(53)-Si(4)	1.880(3)	C(53)-H(53A)	0.9800
C(53)-H(53B)	0.9800	C(53)-H(53C)	0.9800
C(54)-C(55)	1.520(3)	C(54)-H(54A)	0.9900
C(54)-H(54B)	0.9900	C(55)-S(2)	1.802(3)
C(55)-H(55A)	0.9900	C(55)-H(55B)	0.9900
C(56)-S(2)	1.797(3)	C(56)-H(56A)	0.9800
C(56)-H(56B)	0.9800	C(56)-H(56C)	0.9800
C(80)-C(81)	1.5400(11)	C(80)-H(80A)	0.9800
C(80)-H(80B)	0.9800	C(80)-H(80C)	0.9800
C(81)-C(82)	1.5393(12)	C(81)-H(81A)	0.9900
C(81)-H(81B)	0.9900	C(82)-C(83)	1.5378(11)
C(82)-H(82A)	0.9900	C(82)-H(82B)	0.9900
C(83)-C(84)	1.5420(12)	C(83)-H(83A)	0.9900
C(83)-H(83B)	0.9900	C(84)-H(84A)	0.9800
C(84)-H(84B)	0.9800	C(84)-H(84C)	0.9800
C(90)-C(91)	1.5376(12)	C(90)-H(90A)	0.9800

C(90)-H(90B)	0.9800	C(90)-H(90C)	0.9800
C(91)-C(92)	1.5404(12)	C(91)-H(91A)	0.9900
C(91)-H(91B)	0.9900	C(92)-C(93)	1.5394(12)
C(92)-H(92A)	0.9900	C(92)-H(92B)	0.9900
C(93)-C(94)	1.5393(12)	C(93)-H(93A)	0.9900
C(93)-H(93B)	0.9900	C(94)-H(94A)	0.9800
C(94)-H(94B)	0.9800	C(94)-H(94C)	0.9800
C(80A)-C(81A)	1.5394(12)	C(80A)-H(80D)	0.9800
C(80A)-H(80E)	0.9800	C(80A)-H(80F)	0.9800
C(81A)-C(82A)	1.5393(12)	C(81A)-H(81C)	0.9900
C(81A)-H(81D)	0.9900	C(82A)-C(83A)	1.5404(12)
C(82A)-H(82C)	0.9900	C(82A)-H(82D)	0.9900
C(83A)-C(84A)	1.470(12)	C(83A)-H(83C)	0.9900
C(83A)-H(83D)	0.9900	C(84A)-H(84D)	0.9800
C(84A)-H(84E)	0.9800	C(84A)-H(84F)	0.9800
C(90A)-C(91A)	1.598(11)	C(90A)-H(90D)	0.9800
C(90A)-H(90E)	0.9800	C(90A)-H(90F)	0.9800
C(91A)-C(92A)	1.5380(11)	C(91A)-H(91C)	0.9900
C(91A)-H(91D)	0.9900	C(92A)-C(93A)	1.5385(12)
C(92A)-H(92C)	0.9900	C(92A)-H(92D)	0.9900
C(93A)-C(94A)	1.5406(11)	C(93A)-H(93C)	0.9900
C(93A)-H(93D)	0.9900	C(94A)-H(94D)	0.9800
C(94A)-H(94E)	0.9800	C(94A)-H(94F)	0.9800
N(1)-Zn(1)	2.022(2)	N(2)-Zn(1)	2.211(2)
N(3)-Si(2)	1.702(2)	N(3)-Si(1)	1.714(2)
N(3)-Zn(1)	1.913(2)	N(4)-Zn(2)	1.999(2)
N(5)-Zn(2)	2.226(2)	N(6)-Si(3)	1.707(2)
N(6)-Si(4)	1.711(2)	N(6)-Zn(2)	1.911(2)
O(1)-Zn(1)	1.9406(18)	O(2)-Zn(2)	1.9351(17)
		O(1)-C(1)-C(6)	122.7(2)
O(1)-C(1)-C(2)	120.4(2)	C(6)-C(1)-C(2)	116.8(2)
C(3)-C(2)-C(1)	118.7(2)	C(3)-C(2)-C(7)	122.0(2)
C(1)-C(2)-C(7)	119.3(2)	C(2)-C(3)-C(4)	125.3(2)
C(2)-C(3)-H(3)	117.4	C(4)-C(3)-H(3)	117.4

C(5)-C(4)-C(3)	116.1(2)	C(5)-C(4)-C(11)	124.0(2)
C(3)-C(4)-C(11)	119.8(2)	C(4)-C(5)-C(6)	122.3(2)
C(4)-C(5)-H(5)	118.8	C(6)-C(5)-H(5)	118.8
C(5)-C(6)-C(1)	120.6(2)	C(5)-C(6)-C(15)	116.4(2)
C(1)-C(6)-C(15)	122.5(2)	C(8)-C(7)-C(9)	110.4(2)
C(8)-C(7)-C(2)	110.4(2)	C(9)-C(7)-C(2)	109.7(2)
C(8)-C(7)-C(10)	108.1(2)	C(9)-C(7)-C(10)	106.9(2)
C(2)-C(7)-C(10)	111.3(2)	C(7)-C(8)-H(8A)	109.5
C(7)-C(8)-H(8B)	109.5	H(8A)-C(8)-H(8B)	109.5
C(7)-C(8)-H(8C)	109.5	H(8A)-C(8)-H(8C)	109.5
H(8B)-C(8)-H(8C)	109.5	C(7)-C(9)-H(9A)	109.5
C(7)-C(9)-H(9B)	109.5	H(9A)-C(9)-H(9B)	109.5
C(7)-C(9)-H(9C)	109.5	H(9A)-C(9)-H(9C)	109.5
H(9B)-C(9)-H(9C)	109.5	C(7)-C(10)-H(10A)	109.5
C(7)-C(10)-H(10B)	109.5	H(10A)-C(10)-H(10B)	109.5
C(7)-C(10)-H(10C)	109.5	H(10A)-C(10)-H(10C)	109.5
H(10B)-C(10)-H(10C)	109.5	C(14)-C(11)-C(13A)	97.3(16)
C(14)-C(11)-C(14A)	14.6(11)	C(13A)-C(11)-C(14A)	108(2)
C(14)-C(11)-C(4)	108.7(9)	C(13A)-C(11)-C(4)	110(2)
C(14A)-C(11)-C(4)	113.2(15)	C(14)-C(11)-C(12)	114.7(9)
C(13A)-C(11)-C(12)	116.0(16)	C(14A)-C(11)-C(12)	100.4(11)
C(4)-C(11)-C(12)	109.4(2)	C(14)-C(11)-C(13)	107.8(11)
C(13A)-C(11)-C(13)	12.9(19)	C(14A)-C(11)-C(13)	116.2(17)
C(4)-C(11)-C(13)	112.2(12)	C(12)-C(11)-C(13)	104.1(11)
C(11)-C(12)-H(12A)	109.5	C(11)-C(12)-H(12B)	109.5
H(12A)-C(12)-H(12B)	109.5	C(11)-C(12)-H(12C)	109.5
H(12A)-C(12)-H(12C)	109.5	H(12B)-C(12)-H(12C)	109.5
C(11)-C(13)-H(13A)	109.5	C(11)-C(13)-H(13B)	109.5
C(11)-C(13)-H(13C)	109.5	C(11)-C(14)-H(14A)	109.5
C(11)-C(14)-H(14B)	109.5	C(11)-C(14)-H(14C)	109.5
C(11)-C(13A)-H(13D)	109.5	C(11)-C(13A)-H(13E)	109.5
H(13D)-C(13A)-H(13E)	109.5	C(11)-C(13A)-H(13F)	109.5
H(13D)-C(13A)-H(13F)	109.5	H(13E)-C(13A)-H(13F)	109.5
C(11)-C(14A)-H(14D)	109.5	C(11)-C(14A)-H(14E)	109.5

H(14D)-C(14A)-H(14E)	109.5	C(11)-C(14A)-H(14F)	109.5
H(14D)-C(14A)-H(14F)	109.5	H(14E)-C(14A)-H(14F)	109.5
N(1)-C(15)-C(6)	127.0(2)	N(1)-C(15)-H(15)	116.5
C(6)-C(15)-H(15)	116.5	N(1)-C(16)-C(17)	107.37(19)
N(1)-C(16)-C(26)	112.1(2)	C(17)-C(16)-C(26)	110.55(19)
N(1)-C(16)-H(16)	108.9	C(17)-C(16)-H(16)	108.9
C(26)-C(16)-H(16)	108.9	N(2)-C(17)-C(16)	113.21(19)
N(2)-C(17)-H(17A)	108.9	C(16)-C(17)-H(17A)	108.9
N(2)-C(17)-H(17B)	108.9	C(16)-C(17)-H(17B)	108.9
H(17A)-C(17)-H(17B)	107.7	N(2)-C(18)-H(18A)	109.5
N(2)-C(18)-H(18B)	109.5	H(18A)-C(18)-H(18B)	109.5
N(2)-C(18)-H(18C)	109.5	H(18A)-C(18)-H(18C)	109.5
H(18B)-C(18)-H(18C)	109.5	N(2)-C(19)-H(19A)	109.5
N(2)-C(19)-H(19B)	109.5	H(19A)-C(19)-H(19B)	109.5
N(2)-C(19)-H(19C)	109.5	H(19A)-C(19)-H(19C)	109.5
H(19B)-C(19)-H(19C)	109.5	Si(1)-C(20)-H(20A)	109.5
Si(1)-C(20)-H(20B)	109.5	H(20A)-C(20)-H(20B)	109.5
Si(1)-C(20)-H(20C)	109.5	H(20A)-C(20)-H(20C)	109.5
H(20B)-C(20)-H(20C)	109.5	Si(1)-C(21)-H(21A)	109.5
Si(1)-C(21)-H(21B)	109.5	H(21A)-C(21)-H(21B)	109.5
Si(1)-C(21)-H(21C)	109.5	H(21A)-C(21)-H(21C)	109.5
H(21B)-C(21)-H(21C)	109.5	Si(1)-C(22)-H(22A)	109.5
Si(1)-C(22)-H(22B)	109.5	H(22A)-C(22)-H(22B)	109.5
Si(1)-C(22)-H(22C)	109.5	H(22A)-C(22)-H(22C)	109.5
H(22B)-C(22)-H(22C)	109.5	Si(2)-C(23)-H(23A)	109.5
Si(2)-C(23)-H(23B)	109.5	H(23A)-C(23)-H(23B)	109.5
Si(2)-C(23)-H(23C)	109.5	H(23A)-C(23)-H(23C)	109.5
H(23B)-C(23)-H(23C)	109.5	Si(2)-C(24)-H(24A)	109.5
Si(2)-C(24)-H(24B)	109.5	H(24A)-C(24)-H(24B)	109.5
Si(2)-C(24)-H(24C)	109.5	H(24A)-C(24)-H(24C)	109.5
H(24B)-C(24)-H(24C)	109.5	Si(2)-C(25)-H(25A)	109.5
Si(2)-C(25)-H(25B)	109.5	H(25A)-C(25)-H(25B)	109.5
Si(2)-C(25)-H(25C)	109.5	H(25A)-C(25)-H(25C)	109.5
H(25B)-C(25)-H(25C)	109.5	C(27)-C(26)-C(16)	113.7(2)

C(27)-C(26)-H(26A)	108.8	C(16)-C(26)-H(26A)	108.8
C(27)-C(26)-H(26B)	108.8	C(16)-C(26)-H(26B)	108.8
H(26A)-C(26)-H(26B)	107.7	C(26)-C(27)-S(1)	114.23(18)
C(26)-C(27)-H(27A)	108.7	S(1)-C(27)-H(27A)	108.7
C(26)-C(27)-H(27B)	108.7	S(1)-C(27)-H(27B)	108.7
H(27A)-C(27)-H(27B)	107.6	S(1)-C(28)-H(28A)	109.5
S(1)-C(28)-H(28B)	109.5	H(28A)-C(28)-H(28B)	109.5
S(1)-C(28)-H(28C)	109.5	H(28A)-C(28)-H(28C)	109.5
H(28B)-C(28)-H(28C)	109.5	O(2)-C(29)-C(34)	122.3(2)
O(2)-C(29)-C(30)	119.9(2)	C(34)-C(29)-C(30)	117.8(2)
C(31)-C(30)-C(29)	118.8(2)	C(31)-C(30)-C(35)	120.7(2)
C(29)-C(30)-C(35)	120.4(2)	C(30)-C(31)-C(32)	124.1(2)
C(30)-C(31)-H(31)	118.0	C(32)-C(31)-H(31)	118.0
C(33)-C(32)-C(31)	116.3(2)	C(33)-C(32)-C(39)	123.9(2)
C(31)-C(32)-C(39)	119.7(2)	C(32)-C(33)-C(34)	122.7(2)
C(32)-C(33)-H(33)	118.7	C(34)-C(33)-H(33)	118.7
C(33)-C(34)-C(29)	120.1(2)	C(33)-C(34)-C(43)	115.6(2)
C(29)-C(34)-C(43)	123.8(2)	C(38)-C(35)-C(36)	106.88(19)
C(38)-C(35)-C(37)	107.5(2)	C(36)-C(35)-C(37)	110.4(2)
C(38)-C(35)-C(30)	112.5(2)	C(36)-C(35)-C(30)	109.1(2)
C(37)-C(35)-C(30)	110.42(19)	C(35)-C(36)-H(36A)	109.5
C(35)-C(36)-H(36B)	109.5	H(36A)-C(36)-H(36B)	109.5
C(35)-C(36)-H(36C)	109.5	H(36A)-C(36)-H(36C)	109.5
H(36B)-C(36)-H(36C)	109.5	C(35)-C(37)-H(37A)	109.5
C(35)-C(37)-H(37B)	109.5	H(37A)-C(37)-H(37B)	109.5
C(35)-C(37)-H(37C)	109.5	H(37A)-C(37)-H(37C)	109.5
H(37B)-C(37)-H(37C)	109.5	C(35)-C(38)-H(38A)	109.5
C(35)-C(38)-H(38B)	109.5	H(38A)-C(38)-H(38B)	109.5
C(35)-C(38)-H(38C)	109.5	H(38A)-C(38)-H(38C)	109.5
H(38B)-C(38)-H(38C)	109.5	C(40)-C(39)-C(42)	109.7(2)
C(40)-C(39)-C(41)	108.2(2)	C(42)-C(39)-C(41)	108.2(2)
C(40)-C(39)-C(32)	110.5(2)	C(42)-C(39)-C(32)	108.8(2)
C(41)-C(39)-C(32)	111.4(2)	C(39)-C(40)-H(40A)	109.5
C(39)-C(40)-H(40B)	109.5	H(40A)-C(40)-H(40B)	109.5

C(39)-C(40)-H(40C)	109.5	H(40A)-C(40)-H(40C)	109.5
H(40B)-C(40)-H(40C)	109.5	C(39)-C(41)-H(41A)	109.5
C(39)-C(41)-H(41B)	109.5	H(41A)-C(41)-H(41B)	109.5
C(39)-C(41)-H(41C)	109.5	H(41A)-C(41)-H(41C)	109.5
H(41B)-C(41)-H(41C)	109.5	C(39)-C(42)-H(42A)	109.5
C(39)-C(42)-H(42B)	109.5	H(42A)-C(42)-H(42B)	109.5
C(39)-C(42)-H(42C)	109.5	H(42A)-C(42)-H(42C)	109.5
H(42B)-C(42)-H(42C)	109.5	N(4)-C(43)-C(34)	126.0(2)
N(4)-C(43)-H(43)	117.0	C(34)-C(43)-H(43)	117.0
N(4)-C(44)-C(54)	116.2(2)	N(4)-C(44)-C(45)	103.08(19)
C(54)-C(44)-C(45)	112.9(2)	N(4)-C(44)-H(44)	108.1
C(54)-C(44)-H(44)	108.1	C(45)-C(44)-H(44)	108.1
N(5)-C(45)-C(44)	111.9(2)	N(5)-C(45)-H(45A)	109.2
C(44)-C(45)-H(45A)	109.2	N(5)-C(45)-H(45B)	109.2
C(44)-C(45)-H(45B)	109.2	H(45A)-C(45)-H(45B)	107.9
N(5)-C(46)-H(46A)	109.5	N(5)-C(46)-H(46B)	109.5
H(46A)-C(46)-H(46B)	109.5	N(5)-C(46)-H(46C)	109.5
H(46A)-C(46)-H(46C)	109.5	H(46B)-C(46)-H(46C)	109.5
N(5)-C(47)-H(47A)	109.5	N(5)-C(47)-H(47B)	109.5
H(47A)-C(47)-H(47B)	109.5	N(5)-C(47)-H(47C)	109.5
H(47A)-C(47)-H(47C)	109.5	H(47B)-C(47)-H(47C)	109.5
Si(3)-C(48)-H(48A)	109.5	Si(3)-C(48)-H(48B)	109.5
H(48A)-C(48)-H(48B)	109.5	Si(3)-C(48)-H(48C)	109.5
H(48A)-C(48)-H(48C)	109.5	H(48B)-C(48)-H(48C)	109.5
Si(3)-C(49)-H(49A)	109.5	Si(3)-C(49)-H(49B)	109.5
H(49A)-C(49)-H(49B)	109.5	Si(3)-C(49)-H(49C)	109.5
H(49A)-C(49)-H(49C)	109.5	H(49B)-C(49)-H(49C)	109.5
Si(3)-C(50)-H(50A)	109.5	Si(3)-C(50)-H(50B)	109.5
H(50A)-C(50)-H(50B)	109.5	Si(3)-C(50)-H(50C)	109.5
H(50A)-C(50)-H(50C)	109.5	H(50B)-C(50)-H(50C)	109.5
Si(4)-C(51)-H(51A)	109.5	Si(4)-C(51)-H(51B)	109.5
H(51A)-C(51)-H(51B)	109.5	Si(4)-C(51)-H(51C)	109.5
H(51A)-C(51)-H(51C)	109.5	H(51B)-C(51)-H(51C)	109.5
Si(4)-C(52)-H(52A)	109.5	Si(4)-C(52)-H(52B)	109.5

H(52A)-C(52)-H(52B)	109.5	Si(4)-C(52)-H(52C)	109.5
H(52A)-C(52)-H(52C)	109.5	H(52B)-C(52)-H(52C)	109.5
Si(4)-C(53)-H(53A)	109.5	Si(4)-C(53)-H(53B)	109.5
H(53A)-C(53)-H(53B)	109.5	Si(4)-C(53)-H(53C)	109.5
H(53A)-C(53)-H(53C)	109.5	H(53B)-C(53)-H(53C)	109.5
C(44)-C(54)-C(55)	113.5(2)	C(44)-C(54)-H(54A)	108.9
C(55)-C(54)-H(54A)	108.9	C(44)-C(54)-H(54B)	108.9
C(55)-C(54)-H(54B)	108.9	H(54A)-C(54)-H(54B)	107.7
C(54)-C(55)-S(2)	113.11(18)	C(54)-C(55)-H(55A)	109.0
S(2)-C(55)-H(55A)	109.0	C(54)-C(55)-H(55B)	109.0
S(2)-C(55)-H(55B)	109.0	H(55A)-C(55)-H(55B)	107.8
S(2)-C(56)-H(56A)	109.5	S(2)-C(56)-H(56B)	109.5
H(56A)-C(56)-H(56B)	109.5	S(2)-C(56)-H(56C)	109.5
H(56A)-C(56)-H(56C)	109.5	H(56B)-C(56)-H(56C)	109.5
C(82)-C(81)-C(80)	108.55(10)	C(82)-C(81)-H(81A)	110.0
C(80)-C(81)-H(81A)	110.0	C(82)-C(81)-H(81B)	110.0
C(80)-C(81)-H(81B)	110.0	H(81A)-C(81)-H(81B)	108.4
C(83)-C(82)-C(81)	108.71(10)	C(83)-C(82)-H(82A)	109.9
C(81)-C(82)-H(82A)	109.9	C(83)-C(82)-H(82B)	109.9
C(81)-C(82)-H(82B)	109.9	H(82A)-C(82)-H(82B)	108.3
C(82)-C(83)-C(84)	108.76(10)	C(82)-C(83)-H(83A)	109.9
C(84)-C(83)-H(83A)	109.9	C(82)-C(83)-H(83B)	109.9
C(84)-C(83)-H(83B)	109.9	H(83A)-C(83)-H(83B)	108.3
C(90)-C(91)-C(92)	108.37(10)	C(90)-C(91)-H(91A)	110.0
C(92)-C(91)-H(91A)	110.0	C(90)-C(91)-H(91B)	110.0
C(92)-C(91)-H(91B)	110.0	H(91A)-C(91)-H(91B)	108.4
C(93)-C(92)-C(91)	108.53(10)	C(93)-C(92)-H(92A)	110.0
C(91)-C(92)-H(92A)	110.0	C(93)-C(92)-H(92B)	110.0
C(91)-C(92)-H(92B)	110.0	H(92A)-C(92)-H(92B)	108.4
C(94)-C(93)-C(92)	108.59(10)	C(94)-C(93)-H(93A)	110.0
C(92)-C(93)-H(93A)	110.0	C(94)-C(93)-H(93B)	110.0
C(92)-C(93)-H(93B)	110.0	H(93A)-C(93)-H(93B)	108.4
C(81A)-C(80A)-H(80D)	109.5	C(81A)-C(80A)-H(80E)	109.5
H(80D)-C(80A)-H(80E)	109.5	C(81A)-C(80A)-H(80F)	109.5

H(80D)-C(80A)-H(80F)	109.5	H(80E)-C(80A)-H(80F)	109.5
C(80A)-C(81A)-C(82A)	108.58(10)	C(80A)-C(81A)-H(81C)	110.0
C(82A)-C(81A)-H(81C)	110.0	C(80A)-C(81A)-H(81D)	110.0
C(82A)-C(81A)-H(81D)	110.0	H(81C)-C(81A)-H(81D)	108.4
C(81A)-C(82A)-C(83A)	108.55(11)	C(81A)-C(82A)-H(82C)	110.0
C(83A)-C(82A)-H(82C)	110.0	C(81A)-C(82A)-H(82D)	110.0
C(83A)-C(82A)-H(82D)	110.0	H(82C)-C(82A)-H(82D)	108.4
C(84A)-C(83A)-C(82A)	116.2(9)	C(84A)-C(83A)-H(83C)	108.2
C(82A)-C(83A)-H(83C)	108.2	C(84A)-C(83A)-H(83D)	108.2
C(82A)-C(83A)-H(83D)	108.2	H(83C)-C(83A)-H(83D)	107.4
C(83A)-C(84A)-H(84D)	109.5	C(83A)-C(84A)-H(84E)	109.5
H(84D)-C(84A)-H(84E)	109.5	C(83A)-C(84A)-H(84F)	109.5
H(84D)-C(84A)-H(84F)	109.5	H(84E)-C(84A)-H(84F)	109.5
C(92A)-C(91A)-C(90A)	111.7(6)	C(92A)-C(91A)-H(91C)	109.3
C(90A)-C(91A)-H(91C)	109.3	C(92A)-C(91A)-H(91D)	109.3
C(90A)-C(91A)-H(91D)	109.3	H(91C)-C(91A)-H(91D)	107.9
C(91A)-C(92A)-C(93A)	108.80(10)	C(91A)-C(92A)-H(92C)	109.9
C(93A)-C(92A)-H(92C)	109.9	C(91A)-C(92A)-H(92D)	109.9
C(93A)-C(92A)-H(92D)	109.9	H(92C)-C(92A)-H(92D)	108.3
C(92A)-C(93A)-C(94A)	108.59(10)	C(92A)-C(93A)-H(93C)	110.0
C(94A)-C(93A)-H(93C)	110.0	C(92A)-C(93A)-H(93D)	110.0
C(94A)-C(93A)-H(93D)	110.0	H(93C)-C(93A)-H(93D)	108.4
C(15)-N(1)-C(16)	117.8(2)	C(15)-N(1)-Zn(1)	122.36(16)
C(16)-N(1)-Zn(1)	116.82(16)	C(18)-N(2)-C(19)	110.1(2)
C(18)-N(2)-C(17)	108.48(19)	C(19)-N(2)-C(17)	111.5(2)
C(18)-N(2)-Zn(1)	114.65(17)	C(19)-N(2)-Zn(1)	111.78(16)
C(17)-N(2)-Zn(1)	99.96(14)	Si(2)-N(3)-Si(1)	123.91(13)
Si(2)-N(3)-Zn(1)	121.22(12)	Si(1)-N(3)-Zn(1)	114.83(11)
C(43)-N(4)-C(44)	120.9(2)	C(43)-N(4)-Zn(2)	123.54(16)
C(44)-N(4)-Zn(2)	111.61(16)	C(46)-N(5)-C(47)	108.8(2)
C(46)-N(5)-C(45)	109.29(19)	C(47)-N(5)-C(45)	110.32(19)
C(46)-N(5)-Zn(2)	113.60(15)	C(47)-N(5)-Zn(2)	108.56(16)
C(45)-N(5)-Zn(2)	106.21(14)	Si(3)-N(6)-Si(4)	122.66(12)
Si(3)-N(6)-Zn(2)	115.44(10)	Si(4)-N(6)-Zn(2)	121.80(11)

C(1)-O(1)-Zn(1)	127.00(15)	C(29)-O(2)-Zn(2)	127.26(14)
C(28)-S(1)-C(27)	99.97(14)	C(56)-S(2)-C(55)	100.80(14)
N(3)-Si(1)-C(20)	113.16(14)	N(3)-Si(1)-C(21)	111.49(12)
C(20)-Si(1)-C(21)	106.73(15)	N(3)-Si(1)-C(22)	111.49(12)
C(20)-Si(1)-C(22)	106.46(15)	C(21)-Si(1)-C(22)	107.13(15)
N(3)-Si(2)-C(23)	110.60(12)	N(3)-Si(2)-C(25)	113.01(13)
C(23)-Si(2)-C(25)	107.01(14)	N(3)-Si(2)-C(24)	113.63(13)
C(23)-Si(2)-C(24)	106.15(15)	C(25)-Si(2)-C(24)	105.96(16)
N(6)-Si(3)-C(48)	111.03(12)	N(6)-Si(3)-C(49)	113.32(13)
C(48)-Si(3)-C(49)	106.98(13)	N(6)-Si(3)-C(50)	112.74(12)
C(48)-Si(3)-C(50)	106.15(14)	C(49)-Si(3)-C(50)	106.14(15)
N(6)-Si(4)-C(51)	111.72(12)	N(6)-Si(4)-C(52)	113.50(12)
C(51)-Si(4)-C(52)	106.28(13)	N(6)-Si(4)-C(53)	113.39(12)
C(51)-Si(4)-C(53)	105.48(14)	C(52)-Si(4)-C(53)	105.83(15)
N(3)-Zn(1)-O(1)	116.01(9)	N(3)-Zn(1)-N(1)	138.63(9)
O(1)-Zn(1)-N(1)	91.58(8)	N(3)-Zn(1)-N(2)	108.68(9)
O(1)-Zn(1)-N(2)	120.65(8)	N(1)-Zn(1)-N(2)	78.21(8)
N(6)-Zn(2)-O(2)	118.54(8)	N(6)-Zn(2)-N(4)	134.15(8)
O(2)-Zn(2)-N(4)	92.19(8)	N(6)-Zn(2)-N(5)	111.19(9)
O(2)-Zn(2)-N(5)	115.33(7)	N(4)-Zn(2)-N(5)	80.05(8)

Table B-7. Crystal Data and Structure Refinement for Complex **II6d**.

Identification code	Complex **II6d**	
Empirical formula	C55 H108 N6 O2 Si4 Zn2	
Formula weight	1128.57	
Temperature	110(2) K	
Wavelength	0.71073 Å	
Crystal system	Monoclinic	
Space group	P2(1)/c	
Unit cell dimensions	a = 13.530(5) Å	α= 90.000(5)°.
	b = 23.298(5) Å	β= 99.190(5)°.
	c = 10.488(5) Å	γ = 90.000(5)°.
Volume	3264(2) $Å^3$	
Z	2	
Density (calculated)	1.148 Mg/m^3	
Absorption coefficient	0.848 mm^{-1}	
F(000)	1224	
Crystal size	0.22 x 0.20 x 0.18 mm^3	
Theta range for data collection	1.52 to 23.47°.	
Index ranges	-15<=h<=15, -26<=k<=25, -11<=l<=11	
Reflections collected	22528	
Independent reflections	4681 [R(int) = 0.1202]	
Completeness to theta = 23.47°	97.4 %	
Absorption correction	None	
Max. and min. transmission	0.8623 and 0.8353	
Refinement method	Full-matrix least-squares on F^2	
Data / restraints / parameters	4681 / 2 / 337	
Goodness-of-fit on F^2	0.965	
Final R indices [I>2sigma(I)]	R1 = 0.0756, wR2 = 0.1935	
R indices (all data)	R1 = 0.1165, wR2 = 0.2405	
Extinction coefficient	0.040(3)	
Largest diff. peak and hole	0.784 and -1.130 $e.Å^{-3}$	

Table B-8. Bond Lengths [Å] and Angles [°] for Complex **II6d**.

C(1)-O(1)	1.318(7)	C(1)-C(6)	1.437(8)
C(1)-C(2)	1.446(9)	C(2)-C(3)	1.386(9)
C(2)-C(7)	1.558(8)	C(3)-C(4)	1.415(9)
C(4)-C(5)	1.372(9)	C(4)-C(11)	1.559(9)
C(5)-C(6)	1.411(9)	C(6)-C(15)	1.473(10)
C(7)-C(8)	1.527(10)	C(7)-C(9)	1.537(10)
C(7)-C(10)	1.546(10)	C(11)-C(13)	1.531(10)
C(11)-C(14)	1.541(10)	C(11)-C(12)	1.557(10)
C(15)-N(1)	1.276(9)	C(16)-N(1)	1.466(9)
C(16)-C(17)	1.534(9)	C(17)-N(2)	1.501(8)
C(18)-N(2)	1.472(9)	C(19)-N(2)	1.476(8)
C(20)-Si(1)	1.864(8)	C(21)-Si(1)	1.857(9)
C(22)-Si(1)	1.882(10)	C(23)-Si(2)	1.881(7)
C(24)-Si(2)	1.880(7)	C(25)-Si(2)	1.871(8)
C(30)-C(31)#1	1.322(18)	C(30)-C(31)	1.322(18)
C(30)-C(31A)#1	1.397(19)	C(30)-C(31A)	1.397(19)
C(31)-C(32)	1.55(2)	C(31A)-C(32A)	1.55(2)
N(1)-Zn(1)	2.010(5)	N(2)-Zn(1)	2.211(6)
N(3)-Si(2)	1.713(5)	N(3)-Si(1)	1.725(5)
N(3)-Zn(1)	1.917(5)	O(1)-Zn(1)	1.930(4)
		O(1)-C(1)-C(6)	123.2(6)
O(1)-C(1)-C(2)	121.6(5)	C(6)-C(1)-C(2)	115.2(5)
C(3)-C(2)-C(1)	120.0(6)	C(3)-C(2)-C(7)	120.9(6)
C(1)-C(2)-C(7)	119.1(6)	C(2)-C(3)-C(4)	123.6(7)
C(5)-C(4)-C(3)	116.7(6)	C(5)-C(4)-C(11)	121.8(6)
C(3)-C(4)-C(11)	121.3(6)	C(4)-C(5)-C(6)	122.0(6)
C(5)-C(6)-C(1)	121.8(6)	C(5)-C(6)-C(15)	117.5(6)
C(1)-C(6)-C(15)	120.4(6)	C(8)-C(7)-C(9)	109.8(6)
C(8)-C(7)-C(10)	108.3(6)	C(9)-C(7)-C(10)	108.0(6)
C(8)-C(7)-C(2)	110.7(5)	C(9)-C(7)-C(2)	108.5(6)
C(10)-C(7)-C(2)	111.4(5)	C(13)-C(11)-C(14)	109.8(6)
C(13)-C(11)-C(12)	108.7(6)	C(14)-C(11)-C(12)	108.5(6)

C(13)-C(11)-C(4)	108.3(6)	C(14)-C(11)-C(4)	109.0(6)
C(12)-C(11)-C(4)	112.6(5)	N(1)-C(15)-C(6)	125.3(6)
N(1)-C(16)-C(17)	105.0(5)	N(2)-C(17)-C(16)	111.0(5)
C(31)#1-C(30)-C(31)	179.999(10)	C(31)#1-C(30)-C(31A)#1	48.7(11)
C(31)-C(30)-C(31A)#1	131.3(11)	C(31)#1-C(30)-C(31A)	131.3(11)
C(31)-C(30)-C(31A)	48.7(11)	C(31A)#1-C(30)-C(31A)	180.0(10)
C(30)-C(31)-C(32)	119.0(18)	C(30)-C(31A)-C(32A)	128(2)
C(15)-N(1)-C(16)	119.0(6)	C(15)-N(1)-Zn(1)	125.1(5)
C(16)-N(1)-Zn(1)	110.5(4)	C(18)-N(2)-C(19)	109.1(5)
C(18)-N(2)-C(17)	109.5(6)	C(19)-N(2)-C(17)	108.9(5)
C(18)-N(2)-Zn(1)	110.3(4)	C(19)-N(2)-Zn(1)	113.2(4)
C(17)-N(2)-Zn(1)	105.7(4)	Si(2)-N(3)-Si(1)	123.3(3)
Si(2)-N(3)-Zn(1)	113.9(3)	Si(1)-N(3)-Zn(1)	122.7(3)
C(1)-O(1)-Zn(1)	127.5(4)	N(3)-Si(1)-C(21)	112.7(3)
N(3)-Si(1)-C(20)	111.9(3)	C(21)-Si(1)-C(20)	104.5(5)
N(3)-Si(1)-C(22)	114.8(3)	C(21)-Si(1)-C(22)	106.0(5)
C(20)-Si(1)-C(22)	106.2(4)	N(3)-Si(2)-C(25)	113.5(3)
N(3)-Si(2)-C(24)	110.0(3)	C(25)-Si(2)-C(24)	105.1(4)
N(3)-Si(2)-C(23)	110.9(3)	C(25)-Si(2)-C(23)	108.3(4)
C(24)-Si(2)-C(23)	108.8(3)	N(3)-Zn(1)-O(1)	122.2(2)
N(3)-Zn(1)-N(1)	132.3(2)	O(1)-Zn(1)-N(1)	90.6(2)
N(3)-Zn(1)-N(2)	112.0(2)	O(1)-Zn(1)-N(2)	110.9(2)
N(1)-Zn(1)-N(2)	81.4(2)		

Table B-9. Crystal Data and Structure Refinement for Complex **II6e**.

Identification code	Complex **II6e**	
Empirical formula	C50 H70 F2 N4 O4 Zn2	
Formula weight	959.84	
Temperature	110(2) K	
Wavelength	0.71073 Å	
Crystal system	Monoclinic	
Space group	P2(1)/n	
Unit cell dimensions	a = 12.128(12) Å	α= 90°.
	b = 21.45(2) Å	β= 105.529(12)°.
	c = 20.25(2) Å	γ = 90°.
Volume	5074(9) $Å^3$	
Z	4	
Density (calculated)	1.257 Mg/m^3	
Absorption coefficient	0.997 mm^{-1}	
F(000)	2032	
Crystal size	0.19 x 0.18 x 0.16 mm^3	
Theta range for data collection	1.78 to 27.50°.	
Index ranges	-15<=h<=15, -27<=k<=27, -26<=l<=26	
Reflections collected	48125	
Independent reflections	11309 [R(int) = 0.1135]	
Completeness to theta = 27.50°	97.1 %	
Absorption correction	Semi-empirical from equivalents	
Max. and min. transmission	0.8567 and 0.8331	
Refinement method	Full-matrix least-squares on F^2	
Data / restraints / parameters	11309 / 0 / 575	
Goodness-of-fit on F^2	1.036	
Final R indices [I>2sigma(I)]	R1 = 0.0932, wR2 = 0.2505	
R indices (all data)	R1 = 0.1435, wR2 = 0.3180	
Largest diff. peak and hole	1.794 and -2.246 $e.Å^{-3}$	

Table B-10. Bond Lengths [Å] and Angles [°] for Complex **II6e**.

C(1)-O(1)	1.315(7)	C(1)-C(6)	1.420(8)
C(1)-C(2)	1.463(8)	C(2)-C(3)	1.393(9)
C(2)-C(7)	1.535(8)	C(3)-C(4)	1.421(8)
C(4)-C(5)	1.388(8)	C(4)-C(11)	1.536(8)
C(5)-C(6)	1.418(8)	C(6)-C(15)	1.454(8)
C(7)-C(9)	1.529(9)	C(7)-C(8)	1.542(8)
C(7)-C(10)	1.559(9)	C(11)-C(13)	1.539(9)
C(11)-C(14)	1.547(9)	C(11)-C(12)	1.562(9)
C(15)-N(1)	1.276(8)	C(16)-N(1)	1.484(8)
C(16)-C(17)	1.500(9)	C(17)-N(3)	1.492(8)
C(18)-N(3)	1.489(8)	C(19)-N(3)	1.479(9)
C(20)-O(2)	1.330(7)	C(20)-C(25)	1.424(8)
C(20)-C(21)	1.440(8)	C(21)-C(22)	1.393(9)
C(21)-C(26)	1.541(8)	C(22)-C(23)	1.425(8)
C(23)-C(24)	1.378(8)	C(23)-C(30)	1.554(9)
C(24)-C(25)	1.443(9)	C(25)-C(34)	1.440(8)
C(26)-C(27)	1.555(9)	C(26)-C(29)	1.557(8)
C(26)-C(28)	1.557(8)	C(30)-C(33)	1.535(8)
C(30)-C(31)	1.545(8)	C(30)-C(32)	1.546(9)
C(34)-N(2)	1.311(8)	C(35)-N(2)	1.470(8)
C(35)-C(36)	1.532(9)	C(36)-N(4)	1.470(10)
C(37)-N(4)	1.467(8)	C(38)-N(4)	1.470(10)
C(39)-O(3)	1.362(6)	C(39)-C(44)	1.385(9)
C(39)-C(40)	1.389(9)	C(40)-C(41)	1.410(8)
C(41)-C(42)	1.369(10)	C(42)-C(43)	1.357(10)
C(42)-F(1)	1.394(7)	C(43)-C(44)	1.413(8)
C(45)-O(4)	1.367(6)	C(45)-C(46)	1.392(8)
C(45)-C(50)	1.442(9)	C(46)-C(47)	1.389(8)
C(47)-C(48)	1.389(11)	C(48)-F(2)	1.372(7)
C(48)-C(49)	1.380(10)	C(49)-C(50)	1.383(8)
N(1)-Zn(1)	2.050(6)	N(2)-Zn(2)	1.980(5)
N(3)-Zn(1)	2.301(5)	O(1)-Zn(1)	1.977(4)

O(2)-Zn(2)	1.907(4)	O(3)-Zn(2)	1.965(5)
O(3)-Zn(1)	2.080(4)	O(4)-Zn(2)	2.001(4)
O(4)-Zn(1)	2.016(5)		
O(1)-C(1)-C(6)	123.0(5)	O(1)-C(1)-C(2)	119.1(5)
C(6)-C(1)-C(2)	118.0(5)	C(3)-C(2)-C(1)	117.2(5)
C(3)-C(2)-C(7)	121.9(5)	C(1)-C(2)-C(7)	120.9(5)
C(2)-C(3)-C(4)	125.5(5)	C(5)-C(4)-C(3)	116.1(5)
C(5)-C(4)-C(11)	124.8(5)	C(3)-C(4)-C(11)	119.0(5)
C(4)-C(5)-C(6)	121.9(6)	C(5)-C(6)-C(1)	121.3(5)
C(5)-C(6)-C(15)	116.0(5)	C(1)-C(6)-C(15)	122.6(5)
C(9)-C(7)-C(2)	108.9(5)	C(9)-C(7)-C(8)	107.7(5)
C(2)-C(7)-C(8)	111.8(5)	C(9)-C(7)-C(10)	110.4(6)
C(2)-C(7)-C(10)	110.7(5)	C(8)-C(7)-C(10)	107.3(5)
C(4)-C(11)-C(13)	112.2(5)	C(4)-C(11)-C(14)	109.9(6)
C(13)-C(11)-C(14)	107.4(5)	C(4)-C(11)-C(12)	109.9(5)
C(13)-C(11)-C(12)	108.5(6)	C(14)-C(11)-C(12)	108.7(6)
N(1)-C(15)-C(6)	128.5(6)	N(1)-C(16)-C(17)	110.1(6)
N(3)-C(17)-C(16)	111.4(5)	O(2)-C(20)-C(25)	122.5(5)
O(2)-C(20)-C(21)	118.7(5)	C(25)-C(20)-C(21)	118.8(5)
C(22)-C(21)-C(20)	118.3(5)	C(22)-C(21)-C(26)	122.1(5)
C(20)-C(21)-C(26)	119.5(5)	C(21)-C(22)-C(23)	124.7(6)
C(24)-C(23)-C(22)	116.0(6)	C(24)-C(23)-C(30)	123.5(6)
C(22)-C(23)-C(30)	120.5(5)	C(23)-C(24)-C(25)	122.8(6)
C(20)-C(25)-C(34)	126.4(5)	C(20)-C(25)-C(24)	119.3(5)
C(34)-C(25)-C(24)	114.3(5)	C(21)-C(26)-C(27)	111.3(5)
C(21)-C(26)-C(29)	110.3(5)	C(27)-C(26)-C(29)	106.8(5)
C(21)-C(26)-C(28)	111.1(4)	C(27)-C(26)-C(28)	107.3(5)
C(29)-C(26)-C(28)	109.8(5)	C(33)-C(30)-C(31)	110.0(5)
C(33)-C(30)-C(32)	109.3(5)	C(31)-C(30)-C(32)	108.3(5)
C(33)-C(30)-C(23)	109.7(5)	C(31)-C(30)-C(23)	109.3(5)
C(32)-C(30)-C(23)	110.2(5)	N(2)-C(34)-C(25)	127.9(5)
N(2)-C(35)-C(36)	109.9(5)	N(4)-C(36)-C(35)	110.6(6)
O(3)-C(39)-C(44)	120.9(6)	O(3)-C(39)-C(40)	120.1(5)
C(44)-C(39)-C(40)	119.0(5)	C(39)-C(40)-C(41)	121.2(6)

C(42)-C(41)-C(40)	117.9(7)	C(43)-C(42)-C(41)	122.7(6)
C(43)-C(42)-F(1)	118.5(6)	C(41)-C(42)-F(1)	118.7(7)
C(42)-C(43)-C(44)	119.3(6)	C(39)-C(44)-C(43)	120.0(7)
O(4)-C(45)-C(46)	122.6(6)	O(4)-C(45)-C(50)	118.4(5)
C(46)-C(45)-C(50)	119.0(5)	C(47)-C(46)-C(45)	120.8(6)
C(46)-C(47)-C(48)	119.3(6)	F(2)-C(48)-C(49)	119.4(7)
F(2)-C(48)-C(47)	119.0(6)	C(49)-C(48)-C(47)	121.6(6)
C(48)-C(49)-C(50)	120.1(6)	C(49)-C(50)-C(45)	119.2(6)
C(15)-N(1)-C(16)	118.0(5)	C(15)-N(1)-Zn(1)	125.0(4)
C(16)-N(1)-Zn(1)	116.6(4)	C(34)-N(2)-C(35)	116.5(5)
C(34)-N(2)-Zn(2)	119.1(4)	C(35)-N(2)-Zn(2)	124.4(4)
C(19)-N(3)-C(18)	111.3(6)	C(19)-N(3)-C(17)	108.9(5)
C(18)-N(3)-C(17)	110.7(6)	C(19)-N(3)-Zn(1)	115.7(4)
C(18)-N(3)-Zn(1)	108.8(4)	C(17)-N(3)-Zn(1)	101.1(4)
C(37)-N(4)-C(38)	110.1(6)	C(37)-N(4)-C(36)	110.6(6)
C(38)-N(4)-C(36)	111.3(5)	C(1)-O(1)-Zn(1)	130.9(4)
C(20)-O(2)-Zn(2)	125.3(4)	C(39)-O(3)-Zn(2)	128.5(4)
C(39)-O(3)-Zn(1)	131.3(4)	Zn(2)-O(3)-Zn(1)	97.04(16)
C(45)-O(4)-Zn(2)	117.8(4)	C(45)-O(4)-Zn(1)	133.6(4)
Zn(2)-O(4)-Zn(1)	98.01(16)	O(1)-Zn(1)-O(4)	106.69(17)
O(1)-Zn(1)-N(1)	89.61(18)	O(4)-Zn(1)-N(1)	126.78(19)
O(1)-Zn(1)-O(3)	95.69(16)	O(4)-Zn(1)-O(3)	80.79(16)
N(1)-Zn(1)-O(3)	148.99(18)	O(1)-Zn(1)-N(3)	161.08(19)
O(4)-Zn(1)-N(3)	92.24(18)	N(1)-Zn(1)-N(3)	78.79(19)
O(3)-Zn(1)-N(3)	87.10(17)	O(2)-Zn(2)-O(3)	117.98(18)
O(2)-Zn(2)-N(2)	98.5(2)	O(3)-Zn(2)-N(2)	127.02(19)
O(2)-Zn(2)-O(4)	118.13(17)	O(3)-Zn(2)-O(4)	84.05(17)
N(2)-Zn(2)-O(4)	112.40(18)		

Table B-11. Crystal Data and Structure Refinement for Complex **IV2f**, **V2f** (*trans*-).

Identification code	Complex **IV2f**, **V2f** (*trans*-)	
Empirical formula	C40 H64 Al2 N2 O4	
Formula weight	690.89	
Temperature	110(2) K	
Wavelength	1.54178 Å	
Crystal system	Monoclinic	
Space group	P21/C	
Unit cell dimensions	a = 14.234(4) Å	α= 90°.
	b = 8.985(3) Å	β= 123.063(16)°.
	c = 18.655(5) Å	γ = 90°.
Volume	1999.5(10) $Å^3$	
Z	2	
Density (calculated)	1.148 Mg/m^3	
Absorption coefficient	0.964 mm^{-1}	
F(000)	752	
Crystal size	0.15 x 0.12 x 0.05 mm^3	
Theta range for data collection	3.71 to 58.83°.	
Index ranges	-15<=h<=15, -9<=k<=9, -20<=l<=20	
Reflections collected	12357	
Independent reflections	2689 [R(int) = 0.1829]	
Completeness to theta = 58.83°	94.1 %	
Absorption correction	Semi-empirical from equivalents	
Max. and min. transmission	0.9534 and 0.8689	
Refinement method	Full-matrix least-squares on F^2	
Data / restraints / parameters	2689 / 0 / 225	
Goodness-of-fit on F^2	1.019	
Final R indices [I>2sigma(I)]	R1 = 0.0945, wR2 = 0.2215	
R indices (all data)	R1 = 0.1233, wR2 = 0.2334	
Extinction coefficient	0.0038(9)	
Largest diff. peak and hole	1.250 and -0.360 e.$Å^{-3}$	

Table B-12. Bond Lengths [Å] and Angles [°] for Complex **IV2f**, **V2f** (*trans*-).

Al(1)-O(1)	1.797(4)	Al(1)-O(2)	1.851(3)
Al(1)-O(2)#1	1.905(3)	Al(1)-C(20)	1.993(5)
Al(1)-N(1)	2.034(4)	Al(1)-Al(1)#1	2.982(3)
O(1)-C(2)	1.325(6)	O(2)-C(19)	1.422(6)
O(2)-Al(1)#1	1.905(3)	N(1)-C(16)	1.299(6)
N(1)-C(17)	1.455(6)	C(2)-C(3)	1.415(7)
C(2)-C(7)	1.442(7)	C(3)-C(4)	1.395(7)
C(3)-C(16)	1.441(7)	C(4)-C(5)	1.390(7)
C(4)-H(4)	0.9500	C(5)-C(6)	1.405(7)
C(5)-C(12)	1.528(7)	C(6)-C(7)	1.378(7)
C(6)-H(6)	0.9500	C(7)-C(8)	1.529(7)
C(8)-C(9)	1.527(7)	C(8)-C(10)	1.535(7)
C(8)-C(11)	1.538(8)	C(9)-H(9A)	0.9800
C(9)-H(9B)	0.9800	C(9)-H(9C)	0.9800
C(10)-H(10A)	0.9800	C(10)-H(10B)	0.9800
C(10)-H(10C)	0.9800	C(11)-H(11A)	0.9800
C(11)-H(11B)	0.9800	C(11)-H(11C)	0.9800
C(12)-C(13)	1.526(8)	C(12)-C(15)	1.531(7)
C(12)-C(14)	1.547(8)	C(13)-H(13A)	0.9800
C(13)-H(13B)	0.9800	C(13)-H(13C)	0.9800
C(14)-H(14A)	0.9800	C(14)-H(14B)	0.9800
C(14)-H(14C)	0.9800	C(15)-H(15A)	0.9800
C(15)-H(15B)	0.9800	C(15)-H(15C)	0.9800
C(16)-H(16)	0.9500	C(17)-C(18)	1.542(7)
C(17)-H(17A)	0.9900	C(17)-H(17B)	0.9900
C(18)-C(19)	1.510(7)	C(18)-H(18A)	0.9900
C(18)-H(18B)	0.9900	C(19)-H(19A)	0.9900
C(19)-H(19B)	0.9900	C(20)-C(21)	1.541(8)
C(20)-H(20A)	0.9900	C(20)-H(20B)	0.9900
C(21)-H(21A)	0.9800	C(21)-H(21B)	0.9800
C(21)-H(21C)	0.9800		
O(1)-Al(1)-O(2)	129.73(17)	O(1)-Al(1)-O(2)#1	92.14(16)

O(2)-Al(1)-O(2)#1	74.91(17)	O(1)-Al(1)-C(20)	113.4(2)
O(2)-Al(1)-C(20)	116.57(19)	O(2)#1-Al(1)-C(20)	99.24(19)
O(1)-Al(1)-N(1)	89.83(16)	O(2)-Al(1)-N(1)	87.52(16)
O(2)#1-Al(1)-N(1)	158.63(17)	C(20)-Al(1)-N(1)	99.48(19)
O(1)-Al(1)-Al(1)#1	114.88(13)	O(2)-Al(1)-Al(1)#1	38.09(10)
O(2)#1-Al(1)-Al(1)#1	36.83(10)	C(20)-Al(1)-Al(1)#1	112.34(16)
N(1)-Al(1)-Al(1)#1	124.62(14)	C(2)-O(1)-Al(1)	135.9(3)
C(19)-O(2)-Al(1)	126.7(3)	C(19)-O(2)-Al(1)#1	127.9(3)
Al(1)-O(2)-Al(1)#1	105.09(17)	C(16)-N(1)-C(17)	117.0(4)
C(16)-N(1)-Al(1)	124.4(3)	C(17)-N(1)-Al(1)	118.6(3)
O(1)-C(2)-C(3)	121.3(4)	O(1)-C(2)-C(7)	121.0(4)
C(3)-C(2)-C(7)	117.7(4)	C(4)-C(3)-C(2)	121.2(5)
C(4)-C(3)-C(16)	117.3(5)	C(2)-C(3)-C(16)	121.3(5)
C(5)-C(4)-C(3)	122.1(5)	C(5)-C(4)-H(4)	118.9
C(3)-C(4)-H(4)	118.9	C(4)-C(5)-C(6)	115.7(5)
C(4)-C(5)-C(12)	124.6(5)	C(6)-C(5)-C(12)	119.8(5)
C(7)-C(6)-C(5)	125.4(5)	C(7)-C(6)-H(6)	117.3
C(5)-C(6)-H(6)	117.3	C(6)-C(7)-C(2)	117.8(5)
C(6)-C(7)-C(8)	121.2(5)	C(2)-C(7)-C(8)	121.0(4)
C(9)-C(8)-C(7)	112.8(4)	C(9)-C(8)-C(10)	107.7(5)
C(7)-C(8)-C(10)	110.2(4)	C(9)-C(8)-C(11)	106.9(5)
C(7)-C(8)-C(11)	108.7(4)	C(10)-C(8)-C(11)	110.5(4)
C(8)-C(9)-H(9A)	109.5	C(8)-C(9)-H(9B)	109.5
H(9A)-C(9)-H(9B)	109.5	C(8)-C(9)-H(9C)	109.5
H(9A)-C(9)-H(9C)	109.5	H(9B)-C(9)-H(9C)	109.5
C(8)-C(10)-H(10A)	109.5	C(8)-C(10)-H(10B)	109.5
H(10A)-C(10)-H(10B)	109.5	C(8)-C(10)-H(10C)	109.5
H(10A)-C(10)-H(10C)	109.5	H(10B)-C(10)-H(10C)	109.5
C(8)-C(11)-H(11A)	109.5	C(8)-C(11)-H(11B)	109.5
H(11A)-C(11)-H(11B)	109.5	C(8)-C(11)-H(11C)	109.5
H(11A)-C(11)-H(11C)	109.5	H(11B)-C(11)-H(11C)	109.5
C(13)-C(12)-C(5)	111.9(5)	C(13)-C(12)-C(15)	108.5(5)
C(5)-C(12)-C(15)	111.0(4)	C(13)-C(12)-C(14)	109.4(5)
C(5)-C(12)-C(14)	108.4(4)	C(15)-C(12)-C(14)	107.5(5)

C(12)-C(13)-H(13A)	109.5	C(12)-C(13)-H(13B)	109.5
H(13A)-C(13)-H(13B)	109.5	C(12)-C(13)-H(13C)	109.5
H(13A)-C(13)-H(13C)	109.5	H(13B)-C(13)-H(13C)	109.5
C(12)-C(14)-H(14A)	109.5	C(12)-C(14)-H(14B)	109.5
H(14A)-C(14)-H(14B)	109.5	C(12)-C(14)-H(14C)	109.5
H(14A)-C(14)-H(14C)	109.5	H(14B)-C(14)-H(14C)	109.5
C(12)-C(15)-H(15A)	109.5	C(12)-C(15)-H(15B)	109.5
H(15A)-C(15)-H(15B)	109.5	C(12)-C(15)-H(15C)	109.5
H(15A)-C(15)-H(15C)	109.5	H(15B)-C(15)-H(15C)	109.5
N(1)-C(16)-C(3)	126.9(5)	N(1)-C(16)-H(16)	116.6
C(3)-C(16)-H(16)	116.6	N(1)-C(17)-C(18)	113.1(4)
N(1)-C(17)-H(17A)	109.0	C(18)-C(17)-H(17A)	109.0
N(1)-C(17)-H(17B)	109.0	C(18)-C(17)-H(17B)	109.0
H(17A)-C(17)-H(17B)	107.8	C(19)-C(18)-C(17)	114.2(4)
C(19)-C(18)-H(18A)	108.7	C(17)-C(18)-H(18A)	108.7
C(19)-C(18)-H(18B)	108.7	C(17)-C(18)-H(18B)	108.7
H(18A)-C(18)-H(18B)	107.6	O(2)-C(19)-C(18)	111.4(4)
O(2)-C(19)-H(19A)	109.3	C(18)-C(19)-H(19A)	109.3
O(2)-C(19)-H(19B)	109.3	C(18)-C(19)-H(19B)	109.3
H(19A)-C(19)-H(19B)	108.0	C(21)-C(20)-Al(1)	114.2(4)
C(21)-C(20)-H(20A)	108.7	Al(1)-C(20)-H(20A)	108.7
C(21)-C(20)-H(20B)	108.7	Al(1)-C(20)-H(20B)	108.7
H(20A)-C(20)-H(20B)	107.6	C(20)-C(21)-H(21A)	109.5
C(20)-C(21)-H(21B)	109.5	H(21A)-C(21)-H(21B)	109.5
C(20)-C(21)-H(21C)	109.5	H(21A)-C(21)-H(21C)	109.5
H(21B)-C(21)-H(21C)	109.5		

Table B-13. Crystal Data and Structure Refinement for Complex **IV2g**, **V2g**.

Identification code	Complex **IV2g, V2g**	
Empirical formula	C44 H72 Al2 Cl4 N2 O4	
Formula weight	888.80	
Temperature	110(2) K	
Wavelength	1.54178 Å	
Crystal system	Triclinic	
Space group	P_-1	
Unit cell dimensions	a = 10.847(4) Å	α= 106.82(2)°.
	b = 12.387(5) Å	β= 91.91(2)°.
	c = 18.808(7) Å	γ = 90.50(2)°.
Volume	2417.1(16) $Å^3$	
Z	2	
Density (calculated)	1.221 Mg/m^3	
Absorption coefficient	2.893 mm^{-1}	
F(000)	952	
Crystal size	0.20 x 0.20 x 0.15 mm^3	
Theta range for data collection	2.46 to 59.90°.	
Index ranges	-12<=h<=11, -13<=k<=13, -21<=l<=20	
Reflections collected	16050	
Independent reflections	6270 [R(int) = 0.0880]	
Completeness to theta = ACTA 50°	ACTA 50 %	
Absorption correction	Semi-empirical from equivalents	
Max. and min. transmission	0.6708 and 0.5954	
Refinement method	Full-matrix least-squares on F^2	
Data / restraints / parameters	6270 / 114 / 519	
Goodness-of-fit on F^2	1.235	
Final R indices [I>2sigma(I)]	R1 = 0.1225, wR2 = 0.3020	
R indices (all data)	R1 = 0.1508, wR2 = 0.3281	
Largest diff. peak and hole	1.569 and -0.825 e.$Å^{-3}$	

Table B-14. Bond Lengths [Å] and Angles [°] for Complex **IV2g**, **V2g**.

Al(1)-O(1)	1.792(4)	Al(1)-O(2)	1.831(5)
Al(1)-O(2)#1	1.935(5)	Al(1)-C(20)	2.002(7)
Al(1)-N(1)	2.047(5)	Al(1)-Al(1)#1	2.943(4)
Al(2)-O(3)	1.791(4)	Al(2)-O(4)	1.820(5)
Al(2)-O(4)#2	1.941(5)	Al(2)-C(41)	1.991(7)
Al(2)-N(2)	2.070(6)	Al(2)-Al(2)#2	2.949(4)
C(1)-O(1)	1.334(8)	C(1)-C(6)	1.409(9)
C(1)-C(2)	1.430(9)	C(2)-C(3)	1.402(9)
C(2)-C(15)	1.439(9)	C(3)-C(4)	1.367(10)
C(4)-C(5)	1.414(10)	C(4)-C(11)	1.549(10)
C(5)-C(6)	1.385(9)	C(6)-C(7)	1.547(9)
C(7)-C(8)	1.521(10)	C(7)-C(9)	1.538(10)
C(7)-C(10)	1.551(10)	C(11)-C(14)	1.503(12)
C(11)-C(13)	1.508(11)	C(11)-C(12)	1.542(11)
C(15)-N(1)	1.281(8)	C(16)-N(1)	1.477(8)
C(16)-C(17)	1.529(10)	C(17)-C(18)	1.502(10)
C(18)-C(19)	1.555(9)	C(19)-O(2)	1.417(8)
C(20)-C(21)	1.534(10)	C(22)-O(3)	1.336(7)
C(22)-C(27)	1.405(9)	C(22)-C(23)	1.428(9)
C(23)-C(24)	1.399(9)	C(23)-C(36)	1.439(9)
C(24)-C(25)	1.378(9)	C(25)-C(26)	1.411(9)
C(25)-C(32)	1.536(10)	C(26)-C(27)	1.403(9)
C(27)-C(28)	1.539(9)	C(28)-C(31)	1.520(10)
C(28)-C(29)	1.534(10)	C(28)-C(30)	1.540(9)
C(32)-C(35)	1.498(14)	C(32)-C(33)	1.521(14)
C(32)-C(34)	1.530(12)	C(36)-N(2)	1.262(8)
C(37)-N(2)	1.466(8)	C(37)-C(38)	1.547(10)
C(38)-C(39)	1.512(10)	C(39)-C(40)	1.512(10)
C(40)-O(4)	1.441(8)	C(41)-C(42)	1.503(11)
C(43)-Cl(2)	1.751(9)	C(43)-Cl(1)	1.752(9)
C(44)-Cl(3)	1.754(9)	C(44)-Cl(4)	1.767(8)
O(2)-Al(1)#1	1.935(5)	O(4)-Al(2)#2	1.941(5)

		O(1)-Al(1)-O(2)	116.4(2)
O(1)-Al(1)-O(2)#1	91.3(2)	O(2)-Al(1)-O(2)#1	77.2(2)
O(1)-Al(1)-C(20)	116.2(3)	O(2)-Al(1)-C(20)	127.4(3)
O(2)#1-Al(1)-C(20)	99.2(2)	O(1)-Al(1)-N(1)	90.3(2)
O(2)-Al(1)-N(1)	90.6(2)	O(2)#1-Al(1)-N(1)	167.1(2)
C(20)-Al(1)-N(1)	91.5(3)	O(1)-Al(1)-Al(1)#1	106.97(17)
O(2)-Al(1)-Al(1)#1	39.87(14)	O(2)#1-Al(1)-Al(1)#1	37.35(13)
C(20)-Al(1)-Al(1)#1	118.8(2)	N(1)-Al(1)-Al(1)#1	130.38(18)
O(3)-Al(2)-O(4)	117.7(2)	O(3)-Al(2)-O(4)#2	91.3(2)
O(4)-Al(2)-O(4)#2	76.8(2)	O(3)-Al(2)-C(41)	119.4(3)
O(4)-Al(2)-C(41)	122.8(3)	O(4)#2-Al(2)-C(41)	98.4(3)
O(3)-Al(2)-N(2)	89.1(2)	O(4)-Al(2)-N(2)	91.2(2)
O(4)#2-Al(2)-N(2)	166.6(2)	C(41)-Al(2)-N(2)	93.0(3)
O(3)-Al(2)-Al(2)#2	107.55(17)	O(4)-Al(2)-Al(2)#2	39.85(14)
O(4)#2-Al(2)-Al(2)#2	36.92(13)	C(41)-Al(2)-Al(2)#2	115.5(2)
N(2)-Al(2)-Al(2)#2	130.79(18)	O(1)-C(1)-C(6)	120.7(6)
O(1)-C(1)-C(2)	120.4(6)	C(6)-C(1)-C(2)	119.0(6)
C(3)-C(2)-C(1)	119.6(6)	C(3)-C(2)-C(15)	118.5(6)
C(1)-C(2)-C(15)	121.8(6)	C(4)-C(3)-C(2)	122.6(6)
C(3)-C(4)-C(5)	116.3(6)	C(3)-C(4)-C(11)	123.9(6)
C(5)-C(4)-C(11)	119.7(6)	C(6)-C(5)-C(4)	124.5(6)
C(5)-C(6)-C(1)	118.0(6)	C(5)-C(6)-C(7)	120.9(6)
C(1)-C(6)-C(7)	121.2(6)	C(8)-C(7)-C(9)	107.7(6)
C(8)-C(7)-C(6)	112.9(6)	C(9)-C(7)-C(6)	109.2(6)
C(8)-C(7)-C(10)	107.9(6)	C(9)-C(7)-C(10)	109.9(6)
C(6)-C(7)-C(10)	109.2(5)	C(14)-C(11)-C(13)	109.1(8)
C(14)-C(11)-C(12)	108.8(7)	C(13)-C(11)-C(12)	109.3(7)
C(14)-C(11)-C(4)	109.5(6)	C(13)-C(11)-C(4)	109.5(6)
C(12)-C(11)-C(4)	110.6(6)	N(1)-C(15)-C(2)	127.3(6)
N(1)-C(16)-C(17)	111.8(5)	C(18)-C(17)-C(16)	115.4(6)
C(17)-C(18)-C(19)	116.2(5)	O(2)-C(19)-C(18)	113.9(5)
C(21)-C(20)-Al(1)	110.9(5)	O(3)-C(22)-C(27)	120.9(5)
O(3)-C(22)-C(23)	120.2(5)	C(27)-C(22)-C(23)	118.8(6)
C(24)-C(23)-C(22)	120.2(6)	C(24)-C(23)-C(36)	117.8(6)

C(22)-C(23)-C(36)	121.9(6)	C(25)-C(24)-C(23)	122.5(6)
C(24)-C(25)-C(26)	116.2(6)	C(24)-C(25)-C(32)	121.5(6)
C(26)-C(25)-C(32)	122.3(6)	C(27)-C(26)-C(25)	124.3(6)
C(26)-C(27)-C(22)	118.0(6)	C(26)-C(27)-C(28)	121.6(6)
C(22)-C(27)-C(28)	120.4(6)	C(31)-C(28)-C(29)	108.1(6)
C(31)-C(28)-C(27)	109.4(5)	C(29)-C(28)-C(27)	111.7(6)
C(31)-C(28)-C(30)	110.4(6)	C(29)-C(28)-C(30)	106.9(6)
C(27)-C(28)-C(30)	110.3(5)	C(35)-C(32)-C(33)	108.6(8)
C(35)-C(32)-C(34)	111.4(8)	C(33)-C(32)-C(34)	105.7(7)
C(35)-C(32)-C(25)	109.0(7)	C(33)-C(32)-C(25)	111.1(7)
C(34)-C(32)-C(25)	111.1(7)	N(2)-C(36)-C(23)	127.0(6)
N(2)-C(37)-C(38)	111.1(6)	C(39)-C(38)-C(37)	114.2(6)
C(38)-C(39)-C(40)	118.2(6)	O(4)-C(40)-C(39)	114.4(6)
C(42)-C(41)-Al(2)	116.5(5)	Cl(2)-C(43)-Cl(1)	113.0(5)
Cl(3)-C(44)-Cl(4)	112.3(5)	C(15)-N(1)-C(16)	116.5(5)
C(15)-N(1)-Al(1)	123.6(4)	C(16)-N(1)-Al(1)	119.8(4)
C(36)-N(2)-C(37)	116.4(5)	C(36)-N(2)-Al(2)	124.7(4)
C(37)-N(2)-Al(2)	118.8(4)	C(1)-O(1)-Al(1)	135.8(4)
C(19)-O(2)-Al(1)	130.6(4)	C(19)-O(2)-Al(1)#1	121.6(4)
Al(1)-O(2)-Al(1)#1	102.8(2)	C(22)-O(3)-Al(2)	136.3(4)
C(40)-O(4)-Al(2)	132.2(4)	C(40)-O(4)-Al(2)#2	121.3(4)
Al(2)-O(4)-Al(2)#2	103.2(2)		

Table B-15. Crystal Data and Structure Refinement for Complex **Vf** (*cis*-).

Identification code	Complex **Vf** (*cis*-)	
Empirical formula	C40 H64 Al2 N2 O4	
Formula weight	690.89	
Temperature	110(2) K	
Wavelength	1.54178 Å	
Crystal system	Orthorhombic	
Space group	Pbcn	
Unit cell dimensions	a = 32.810(7) Å	α= 90°.
	b = 20.945(5) Å	β= 90°.
	c = 17.910(4) Å	γ = 90°.
Volume	12308(5) $Å^3$	
Z	12	
Density (calculated)	1.119 Mg/m^3	
Absorption coefficient	0.940 mm^{-1}	
F(000)	4512	
Crystal size	0.20 x 0.16 x 0.15 mm^3	
Theta range for data collection	2.50 to 60.54°.	
Index ranges	-36<=h<=36, -23<=k<=23, -19<=l<=20	
Reflections collected	71247	
Independent reflections	9145 [R(int) = 0.0715]	
Completeness to theta = 60.54°	98.4 %	
Absorption correction	Semi-empirical from equivalents	
Max. and min. transmission	0.8719 and 0.8343	
Refinement method	Full-matrix least-squares on F^2	
Data / restraints / parameters	9145 / 34 / 696	
Goodness-of-fit on F^2	1.066	
Final R indices [I>2sigma(I)]	R1 = 0.0873, wR2 = 0.2201	
R indices (all data)	R1 = 0.1077, wR2 = 0.2348	
Largest diff. peak and hole	0.734 and -0.755 $e.Å^{-3}$	

Table B-16. Bond Lengths [Å] and Angles [°] for Complex **Vf** (*cis*-).

Al(1)-O(1)	1.796(3)	Al(1)-O(2)	1.846(3)
Al(1)-O(2)#1	1.915(3)	Al(1)-C(19)	1.992(5)
Al(1)-N(1)	2.030(4)	Al(1)-Al(1)#1	2.944(2)
Al(2)-O(3)	1.793(3)	Al(2)-O(4)	1.846(3)
Al(2)-O(6)	1.923(4)	Al(2)-C(39)	2.000(5)
Al(2)-N(2)	2.028(4)	Al(2)-Al(3)	2.951(2)
Al(3)-O(5)	1.797(3)	Al(3)-O(6)	1.843(3)
Al(3)-O(4)	1.907(3)	Al(3)-C(59)	1.988(5)
Al(3)-N(3)	2.022(4)	O(1)-C(1)	1.325(5)
O(2)-C(18)	1.433(5)	O(2)-Al(1)#1	1.915(3)
O(3)-C(21)	1.324(5)	O(4)-C(38)	1.436(5)
O(5)-C(41)	1.325(6)	O(6)-C(58)	1.435(5)
N(1)-C(15)	1.282(5)	N(1)-C(16)	1.472(5)
N(2)-C(35)	1.278(6)	N(2)-C(36)	1.472(6)
N(3)-C(55)	1.285(6)	N(3)-C(56)	1.466(6)
C(1)-C(2)	1.419(6)	C(1)-C(6)	1.424(6)
C(2)-C(3)	1.409(6)	C(2)-C(15)	1.438(6)
C(3)-C(4)	1.373(6)	C(3)-H(3)	0.9500
C(4)-C(5)	1.409(6)	C(4)-C(11)	1.539(6)
C(5)-C(6)	1.396(6)	C(5)-H(5)	0.9500
C(6)-C(7)	1.530(6)	C(7)-C(8)	1.536(6)
C(7)-C(9)	1.536(7)	C(7)-C(10)	1.551(7)
C(8)-H(8A)	0.9800	C(8)-H(8B)	0.9800
C(8)-H(8C)	0.9800	C(9)-H(9A)	0.9800
C(9)-H(9B)	0.9800	C(9)-H(9C)	0.9800
C(10)-H(10A)	0.9800	C(10)-H(10B)	0.9800
C(10)-H(10C)	0.9800	C(11)-C(12)	1.517(6)
C(11)-C(13)	1.522(6)	C(11)-C(14)	1.536(7)
C(12)-H(12A)	0.9800	C(12)-H(12B)	0.9800
C(12)-H(12C)	0.9800	C(13)-H(13A)	0.9800
C(13)-H(13B)	0.9800	C(13)-H(13C)	0.9800
C(14)-H(14A)	0.9800	C(14)-H(14B)	0.9800

C(14)-H(14C)	0.9800	C(15)-H(15)	0.9500
C(16)-C(17)	1.520(6)	C(16)-H(16A)	0.9900
C(16)-H(16B)	0.9900	C(17)-C(18)	1.517(6)
C(17)-H(17A)	0.9900	C(17)-H(17B)	0.9900
C(18)-H(18A)	0.9900	C(18)-H(18B)	0.9900
C(19)-C(20)	1.509(7)	C(19)-H(19A)	0.9900
C(19)-H(19B)	0.9900	C(20)-H(20A)	0.9800
C(20)-H(20B)	0.9800	C(20)-H(20C)	0.9800
C(21)-C(26)	1.416(6)	C(21)-C(22)	1.421(6)
C(22)-C(23)	1.405(7)	C(22)-C(35)	1.439(7)
C(23)-C(24)	1.373(7)	C(23)-H(23)	0.9500
C(24)-C(25)	1.398(7)	C(24)-C(31)	1.535(7)
C(25)-C(26)	1.384(7)	C(25)-H(25)	0.9500
C(26)-C(27)	1.535(7)	C(27)-C(28)	1.536(7)
C(27)-C(29)	1.538(7)	C(27)-C(30)	1.550(7)
C(28)-H(28A)	0.9800	C(28)-H(28B)	0.9800
C(28)-H(28C)	0.9800	C(29)-H(29A)	0.9800
C(29)-H(29B)	0.9800	C(29)-H(29C)	0.9800
C(30)-H(30A)	0.9800	C(30)-H(30B)	0.9800
C(30)-H(30C)	0.9800	C(31)-C(32)	1.494(11)
C(31)-C(33)	1.513(15)	C(31)-C(33A)	1.514(15)
C(31)-C(34A)	1.514(13)	C(31)-C(34)	1.602(13)
C(31)-C(32A)	1.612(13)	C(32)-H(32A)	0.9800
C(32)-H(32B)	0.9800	C(32)-H(32C)	0.9800
C(33)-H(33A)	0.9800	C(33)-H(33B)	0.9800
C(33)-H(33C)	0.9800	C(34)-H(34A)	0.9800
C(34)-H(34B)	0.9800	C(34)-H(34C)	0.9800
C(35)-H(35)	0.9500	C(36)-C(37)	1.520(7)
C(36)-H(36A)	0.9900	C(36)-H(36B)	0.9900
C(37)-C(38)	1.515(7)	C(37)-H(37A)	0.9900
C(37)-H(37B)	0.9900	C(38)-H(38A)	0.9900
C(38)-H(38B)	0.9900	C(39)-C(40)	1.509(8)
C(39)-H(39A)	0.9900	C(39)-H(39B)	0.9900
C(40)-H(40A)	0.9800	C(40)-H(40B)	0.9800

C(40)-H(40C)	0.9800	C(41)-C(42)	1.409(6)
C(41)-C(46)	1.413(6)	C(42)-C(43)	1.411(7)
C(42)-C(55)	1.442(6)	C(43)-C(44)	1.374(7)
C(43)-H(43)	0.9500	C(44)-C(45)	1.407(7)
C(44)-C(51)	1.533(7)	C(45)-C(46)	1.387(7)
C(45)-H(45)	0.9500	C(46)-C(47)	1.543(7)
C(47)-C(50)	1.535(8)	C(47)-C(49)	1.535(7)
C(47)-C(48)	1.537(7)	C(48)-H(48A)	0.9800
C(48)-H(48B)	0.9800	C(48)-H(48C)	0.9800
C(49)-H(49A)	0.9800	C(49)-H(49B)	0.9800
C(49)-H(49C)	0.9800	C(50)-H(50A)	0.9800
C(50)-H(50B)	0.9800	C(50)-H(50C)	0.9800
C(51)-C(53A)	1.447(16)	C(51)-C(52)	1.488(9)
C(51)-C(53)	1.522(8)	C(51)-C(54A)	1.535(16)
C(51)-C(54)	1.581(8)	C(51)-C(52A)	1.585(18)
C(52)-H(52A)	0.9800	C(52)-H(52B)	0.9800
C(52)-H(52C)	0.9800	C(53)-H(53A)	0.9800
C(53)-H(53B)	0.9800	C(53)-H(53C)	0.9800
C(54)-H(54A)	0.9800	C(54)-H(54B)	0.9800
C(54)-H(54C)	0.9800	C(55)-H(55)	0.9500
C(56)-C(57)	1.524(8)	C(56)-H(56A)	0.9900
C(56)-H(56B)	0.9900	C(57)-C(58)	1.506(7)
C(57)-H(57A)	0.9900	C(57)-H(57B)	0.9900
C(58)-H(58A)	0.9900	C(58)-H(58B)	0.9900
C(59)-C(60)	1.471(8)	C(59)-H(59A)	0.9900
C(59)-H(59B)	0.9900	C(60)-H(60A)	0.9800
C(60)-H(60B)	0.9800	C(60)-H(60C)	0.9800
C(32A)-H(32D)	0.9800	C(32A)-H(32E)	0.9800
C(32A)-H(32F)	0.9800	C(33A)-H(33D)	0.9800
C(33A)-H(33E)	0.9800	C(33A)-H(33F)	0.9800
C(34A)-H(34D)	0.9800	C(34A)-H(34E)	0.9800
C(34A)-H(34F)	0.9800	C(52A)-H(52D)	0.9800
C(52A)-H(52E)	0.9800	C(52A)-H(52F)	0.9800
C(53A)-H(53D)	0.9800	C(53A)-H(53E)	0.9800

C(53A)-H(53F)	0.9800	C(54A)-H(54D)	0.9800
C(54A)-H(54E)	0.9800	C(54A)-H(54F)	0.9800
		O(1)-Al(1)-O(2)	131.81(14)
O(1)-Al(1)-O(2)#1	89.61(13)	O(2)-Al(1)-O(2)#1	75.94(14)
O(1)-Al(1)-C(19)	113.62(17)	O(2)-Al(1)-C(19)	114.37(17)
O(2)#1-Al(1)-C(19)	102.88(18)	O(1)-Al(1)-N(1)	88.75(14)
O(2)-Al(1)-N(1)	88.58(14)	O(2)#1-Al(1)-N(1)	157.52(15)
C(19)-Al(1)-N(1)	98.31(19)	O(1)-Al(1)-Al(1)#1	119.55(10)
O(2)-Al(1)-Al(1)#1	39.32(9)	O(2)#1-Al(1)-Al(1)#1	37.64(9)
C(19)-Al(1)-Al(1)#1	106.92(14)	N(1)-Al(1)-Al(1)#1	127.67(12)
O(3)-Al(2)-O(4)	129.01(15)	O(3)-Al(2)-O(6)	89.84(15)
O(4)-Al(2)-O(6)	75.72(15)	O(3)-Al(2)-C(39)	113.4(2)
O(4)-Al(2)-C(39)	117.2(2)	O(6)-Al(2)-C(39)	100.1(2)
O(3)-Al(2)-N(2)	88.98(16)	O(4)-Al(2)-N(2)	88.54(16)
O(6)-Al(2)-N(2)	158.62(16)	C(39)-Al(2)-N(2)	100.0(2)
O(3)-Al(2)-Al(3)	117.44(12)	O(4)-Al(2)-Al(3)	38.92(10)
O(6)-Al(2)-Al(3)	37.47(10)	C(39)-Al(2)-Al(3)	108.11(19)
N(2)-Al(2)-Al(3)	127.23(13)	O(5)-Al(3)-O(6)	130.12(15)
O(5)-Al(3)-O(4)	89.40(15)	O(6)-Al(3)-O(4)	76.16(15)
O(5)-Al(3)-C(59)	114.8(2)	O(6)-Al(3)-C(59)	114.9(2)
O(4)-Al(3)-C(59)	102.1(2)	O(5)-Al(3)-N(3)	88.79(16)
O(6)-Al(3)-N(3)	88.79(16)	O(4)-Al(3)-N(3)	158.56(16)
C(59)-Al(3)-N(3)	98.0(2)	O(5)-Al(3)-Al(2)	117.61(12)
O(6)-Al(3)-Al(2)	39.38(10)	O(4)-Al(3)-Al(2)	37.45(10)
C(59)-Al(3)-Al(2)	108.00(17)	N(3)-Al(3)-Al(2)	127.85(14)
C(1)-O(1)-Al(1)	136.8(3)	C(18)-O(2)-Al(1)	129.0(3)
C(18)-O(2)-Al(1)#1	119.7(2)	Al(1)-O(2)-Al(1)#1	103.04(14)
C(21)-O(3)-Al(2)	137.1(3)	C(38)-O(4)-Al(2)	130.0(3)
C(38)-O(4)-Al(3)	119.5(3)	Al(2)-O(4)-Al(3)	103.63(15)
C(41)-O(5)-Al(3)	136.9(3)	C(58)-O(6)-Al(3)	130.0(3)
C(58)-O(6)-Al(2)	119.9(3)	Al(3)-O(6)-Al(2)	103.15(15)
C(15)-N(1)-C(16)	116.5(4)	C(15)-N(1)-Al(1)	125.9(3)
C(16)-N(1)-Al(1)	117.6(3)	C(35)-N(2)-C(36)	117.0(4)
C(35)-N(2)-Al(2)	125.5(3)	C(36)-N(2)-Al(2)	117.4(3)

C(55)-N(3)-C(56)	117.0(4)	C(55)-N(3)-Al(3)	125.6(3)
C(56)-N(3)-Al(3)	117.4(3)	O(1)-C(1)-C(2)	120.8(4)
O(1)-C(1)-C(6)	121.1(4)	C(2)-C(1)-C(6)	118.1(4)
C(3)-C(2)-C(1)	121.0(4)	C(3)-C(2)-C(15)	117.6(4)
C(1)-C(2)-C(15)	121.3(4)	C(4)-C(3)-C(2)	121.9(4)
C(4)-C(3)-H(3)	119.0	C(2)-C(3)-H(3)	119.0
C(3)-C(4)-C(5)	116.3(4)	C(3)-C(4)-C(11)	121.6(4)
C(5)-C(4)-C(11)	122.1(4)	C(6)-C(5)-C(4)	124.8(4)
C(6)-C(5)-H(5)	117.6	C(4)-C(5)-H(5)	117.6
C(5)-C(6)-C(1)	117.9(4)	C(5)-C(6)-C(7)	121.4(4)
C(1)-C(6)-C(7)	120.7(4)	C(6)-C(7)-C(8)	112.3(4)
C(6)-C(7)-C(9)	109.4(4)	C(8)-C(7)-C(9)	107.6(4)
C(6)-C(7)-C(10)	110.2(4)	C(8)-C(7)-C(10)	106.7(4)
C(9)-C(7)-C(10)	110.5(4)	C(7)-C(8)-H(8A)	109.5
C(7)-C(8)-H(8B)	109.5	H(8A)-C(8)-H(8B)	109.5
C(7)-C(8)-H(8C)	109.5	H(8A)-C(8)-H(8C)	109.5
H(8B)-C(8)-H(8C)	109.5	C(7)-C(9)-H(9A)	109.5
C(7)-C(9)-H(9B)	109.5	H(9A)-C(9)-H(9B)	109.5
C(7)-C(9)-H(9C)	109.5	H(9A)-C(9)-H(9C)	109.5
H(9B)-C(9)-H(9C)	109.5	C(7)-C(10)-H(10A)	109.5
C(7)-C(10)-H(10B)	109.5	H(10A)-C(10)-H(10B)	109.5
C(7)-C(10)-H(10C)	109.5	H(10A)-C(10)-H(10C)	109.5
H(10B)-C(10)-H(10C)	109.5	C(12)-C(11)-C(13)	110.5(4)
C(12)-C(11)-C(14)	108.4(4)	C(13)-C(11)-C(14)	107.0(4)
C(12)-C(11)-C(4)	108.5(4)	C(13)-C(11)-C(4)	111.3(4)
C(14)-C(11)-C(4)	111.1(4)	C(11)-C(12)-H(12A)	109.5
C(11)-C(12)-H(12B)	109.5	H(12A)-C(12)-H(12B)	109.5
C(11)-C(12)-H(12C)	109.5	H(12A)-C(12)-H(12C)	109.5
H(12B)-C(12)-H(12C)	109.5	C(11)-C(13)-H(13A)	109.5
C(11)-C(13)-H(13B)	109.5	H(13A)-C(13)-H(13B)	109.5
C(11)-C(13)-H(13C)	109.5	H(13A)-C(13)-H(13C)	109.5
H(13B)-C(13)-H(13C)	109.5	C(11)-C(14)-H(14A)	109.5
C(11)-C(14)-H(14B)	109.5	H(14A)-C(14)-H(14B)	109.5
C(11)-C(14)-H(14C)	109.5	H(14A)-C(14)-H(14C)	109.5

H(14B)-C(14)-H(14C)	109.5	N(1)-C(15)-C(2)	126.4(4)
N(1)-C(15)-H(15)	116.8	C(2)-C(15)-H(15)	116.8
N(1)-C(16)-C(17)	109.2(4)	N(1)-C(16)-H(16A)	109.8
C(17)-C(16)-H(16A)	109.8	N(1)-C(16)-H(16B)	109.8
C(17)-C(16)-H(16B)	109.8	H(16A)-C(16)-H(16B)	108.3
C(18)-C(17)-C(16)	112.4(4)	C(18)-C(17)-H(17A)	109.1
C(16)-C(17)-H(17A)	109.1	C(18)-C(17)-H(17B)	109.1
C(16)-C(17)-H(17B)	109.1	H(17A)-C(17)-H(17B)	107.9
O(2)-C(18)-C(17)	112.7(4)	O(2)-C(18)-H(18A)	109.1
C(17)-C(18)-H(18A)	109.1	O(2)-C(18)-H(18B)	109.1
C(17)-C(18)-H(18B)	109.1	H(18A)-C(18)-H(18B)	107.8
C(20)-C(19)-Al(1)	115.3(3)	C(20)-C(19)-H(19A)	108.4
Al(1)-C(19)-H(19A)	108.4	C(20)-C(19)-H(19B)	108.4
Al(1)-C(19)-H(19B)	108.4	H(19A)-C(19)-H(19B)	107.5
C(19)-C(20)-H(20A)	109.5	C(19)-C(20)-H(20B)	109.5
H(20A)-C(20)-H(20B)	109.5	C(19)-C(20)-H(20C)	109.5
H(20A)-C(20)-H(20C)	109.5	H(20B)-C(20)-H(20C)	109.5
O(3)-C(21)-C(26)	121.3(4)	O(3)-C(21)-C(22)	120.1(4)
C(26)-C(21)-C(22)	118.6(4)	C(23)-C(22)-C(21)	120.1(4)
C(23)-C(22)-C(35)	118.2(4)	C(21)-C(22)-C(35)	121.6(4)
C(24)-C(23)-C(22)	122.1(5)	C(24)-C(23)-H(23)	119.0
C(22)-C(23)-H(23)	119.0	C(23)-C(24)-C(25)	116.5(5)
C(23)-C(24)-C(31)	122.7(5)	C(25)-C(24)-C(31)	120.8(5)
C(26)-C(25)-C(24)	124.9(5)	C(26)-C(25)-H(25)	117.5
C(24)-C(25)-H(25)	117.5	C(25)-C(26)-C(21)	117.8(4)
C(25)-C(26)-C(27)	121.5(4)	C(21)-C(26)-C(27)	120.6(4)
C(26)-C(27)-C(28)	112.0(4)	C(26)-C(27)-C(29)	109.1(4)
C(28)-C(27)-C(29)	107.2(5)	C(26)-C(27)-C(30)	110.2(4)
C(28)-C(27)-C(30)	107.5(5)	C(29)-C(27)-C(30)	110.7(5)
C(27)-C(28)-H(28A)	109.5	C(27)-C(28)-H(28B)	109.5
H(28A)-C(28)-H(28B)	109.5	C(27)-C(28)-H(28C)	109.5
H(28A)-C(28)-H(28C)	109.5	H(28B)-C(28)-H(28C)	109.5
C(27)-C(29)-H(29A)	109.5	C(27)-C(29)-H(29B)	109.5
H(29A)-C(29)-H(29B)	109.5	C(27)-C(29)-H(29C)	109.5

H(29A)-C(29)-H(29C)	109.5	H(29B)-C(29)-H(29C)	109.5
C(27)-C(30)-H(30A)	109.5	C(27)-C(30)-H(30B)	109.5
H(30A)-C(30)-H(30B)	109.5	C(27)-C(30)-H(30C)	109.5
H(30A)-C(30)-H(30C)	109.5	H(30B)-C(30)-H(30C)	109.5
C(32)-C(31)-C(33)	128(4)	C(32)-C(31)-C(33A)	119(4)
C(33)-C(31)-C(33A)	12(6)	C(32)-C(31)-C(34A)	76.0(9)
C(33)-C(31)-C(34A)	113(4)	C(33A)-C(31)-C(34A)	120(4)
C(32)-C(31)-C(24)	109.4(6)	C(33)-C(31)-C(24)	111(4)
C(33A)-C(31)-C(24)	112(4)	C(34A)-C(31)-C(24)	115.7(8)
C(32)-C(31)-C(34)	106.6(9)	C(33)-C(31)-C(34)	91(3)
C(33A)-C(31)-C(34)	102(3)	C(34A)-C(31)-C(34)	30.7(8)
C(24)-C(31)-C(34)	107.0(7)	C(32)-C(31)-C(32A)	35.2(6)
C(33)-C(31)-C(32A)	102(3)	C(33A)-C(31)-C(32A)	91(3)
C(34A)-C(31)-C(32A)	108.7(9)	C(24)-C(31)-C(32A)	105.4(6)
C(34)-C(31)-C(32A)	137.3(8)	C(31)-C(32)-H(32A)	109.5
C(31)-C(32)-H(32B)	109.5	C(31)-C(32)-H(32C)	109.5
C(31)-C(33)-H(33A)	109.5	C(31)-C(33)-H(33B)	109.5
C(31)-C(33)-H(33C)	109.5	C(31)-C(34)-H(34A)	109.5
C(31)-C(34)-H(34B)	109.5	C(31)-C(34)-H(34C)	109.5
N(2)-C(35)-C(22)	126.5(4)	N(2)-C(35)-H(35)	116.8
C(22)-C(35)-H(35)	116.8	N(2)-C(36)-C(37)	109.0(4)
N(2)-C(36)-H(36A)	109.9	C(37)-C(36)-H(36A)	109.9
N(2)-C(36)-H(36B)	109.9	C(37)-C(36)-H(36B)	109.9
H(36A)-C(36)-H(36B)	108.3	C(38)-C(37)-C(36)	112.6(4)
C(38)-C(37)-H(37A)	109.1	C(36)-C(37)-H(37A)	109.1
C(38)-C(37)-H(37B)	109.1	C(36)-C(37)-H(37B)	109.1
H(37A)-C(37)-H(37B)	107.8	O(4)-C(38)-C(37)	113.1(4)
O(4)-C(38)-H(38A)	109.0	C(37)-C(38)-H(38A)	109.0
O(4)-C(38)-H(38B)	109.0	C(37)-C(38)-H(38B)	109.0
H(38A)-C(38)-H(38B)	107.8	C(40)-C(39)-Al(2)	120.8(4)
C(40)-C(39)-H(39A)	107.1	Al(2)-C(39)-H(39A)	107.1
C(40)-C(39)-H(39B)	107.1	Al(2)-C(39)-H(39B)	107.1
H(39A)-C(39)-H(39B)	106.8	C(39)-C(40)-H(40A)	109.5
C(39)-C(40)-H(40B)	109.5	H(40A)-C(40)-H(40B)	109.5

C(39)-C(40)-H(40C)	109.5	H(40A)-C(40)-H(40C)	109.5
H(40B)-C(40)-H(40C)	109.5	O(5)-C(41)-C(42)	120.6(4)
O(5)-C(41)-C(46)	121.1(4)	C(42)-C(41)-C(46)	118.2(4)
C(41)-C(42)-C(43)	121.0(4)	C(41)-C(42)-C(55)	121.3(4)
C(43)-C(42)-C(55)	117.5(4)	C(44)-C(43)-C(42)	121.7(4)
C(44)-C(43)-H(43)	119.1	C(42)-C(43)-H(43)	119.1
C(43)-C(44)-C(45)	116.0(5)	C(43)-C(44)-C(51)	122.6(5)
C(45)-C(44)-C(51)	121.4(4)	C(46)-C(45)-C(44)	124.8(5)
C(46)-C(45)-H(45)	117.6	C(44)-C(45)-H(45)	117.6
C(45)-C(46)-C(41)	118.2(4)	C(45)-C(46)-C(47)	120.9(4)
C(41)-C(46)-C(47)	120.9(4)	C(50)-C(47)-C(49)	110.8(4)
C(50)-C(47)-C(48)	107.2(5)	C(49)-C(47)-C(48)	107.6(4)
C(50)-C(47)-C(46)	110.0(4)	C(49)-C(47)-C(46)	109.0(4)
C(48)-C(47)-C(46)	112.2(4)	C(47)-C(48)-H(48A)	109.5
C(47)-C(48)-H(48B)	109.5	H(48A)-C(48)-H(48B)	109.5
C(47)-C(48)-H(48C)	109.5	H(48A)-C(48)-H(48C)	109.5
H(48B)-C(48)-H(48C)	109.5	C(47)-C(49)-H(49A)	109.5
C(47)-C(49)-H(49B)	109.5	H(49A)-C(49)-H(49B)	109.5
C(47)-C(49)-H(49C)	109.5	H(49A)-C(49)-H(49C)	109.5
H(49B)-C(49)-H(49C)	109.5	C(47)-C(50)-H(50A)	109.5
C(47)-C(50)-H(50B)	109.5	H(50A)-C(50)-H(50B)	109.5
C(47)-C(50)-H(50C)	109.5	H(50A)-C(50)-H(50C)	109.5
H(50B)-C(50)-H(50C)	109.5	C(53A)-C(51)-C(52)	127.9(16)
C(53A)-C(51)-C(53)	25.6(10)	C(52)-C(51)-C(53)	112.0(6)
C(53A)-C(51)-C(44)	115.1(15)	C(52)-C(51)-C(44)	110.2(5)
C(53)-C(51)-C(44)	112.4(5)	C(53A)-C(51)-C(54A)	114.0(13)
C(52)-C(51)-C(54A)	66.2(12)	C(53)-C(51)-C(54A)	130.6(11)
C(44)-C(51)-C(54A)	113.9(12)	C(53A)-C(51)-C(54)	79.3(11)
C(52)-C(51)-C(54)	108.6(6)	C(53)-C(51)-C(54)	103.8(5)
C(44)-C(51)-C(54)	109.6(5)	C(54A)-C(51)-C(54)	44.0(12)
C(53A)-C(51)-C(52A)	108.6(13)	C(52)-C(51)-C(52A)	37.8(11)
C(53)-C(51)-C(52A)	84.6(13)	C(44)-C(51)-C(52A)	99.4(14)
C(54A)-C(51)-C(52A)	103.8(12)	C(54)-C(51)-C(52A)	143.2(14)
C(51)-C(52)-H(52A)	109.5	C(51)-C(52)-H(52B)	109.5

C(51)-C(52)-H(52C)	109.5	C(51)-C(53)-H(53A)	109.5
C(51)-C(53)-H(53B)	109.5	C(51)-C(53)-H(53C)	109.5
C(51)-C(54)-H(54A)	109.5	C(51)-C(54)-H(54B)	109.5
C(51)-C(54)-H(54C)	109.5	N(3)-C(55)-C(42)	126.5(4)
N(3)-C(55)-H(55)	116.8	C(42)-C(55)-H(55)	116.8
N(3)-C(56)-C(57)	108.7(4)	N(3)-C(56)-H(56A)	110.0
C(57)-C(56)-H(56A)	110.0	N(3)-C(56)-H(56B)	110.0
C(57)-C(56)-H(56B)	110.0	H(56A)-C(56)-H(56B)	108.3
C(58)-C(57)-C(56)	113.6(4)	C(58)-C(57)-H(57A)	108.8
C(56)-C(57)-H(57A)	108.8	C(58)-C(57)-H(57B)	108.8
C(56)-C(57)-H(57B)	108.8	H(57A)-C(57)-H(57B)	107.7
O(6)-C(58)-C(57)	112.1(4)	O(6)-C(58)-H(58A)	109.2
C(57)-C(58)-H(58A)	109.2	O(6)-C(58)-H(58B)	109.2
C(57)-C(58)-H(58B)	109.2	H(58A)-C(58)-H(58B)	107.9
C(60)-C(59)-Al(3)	115.3(4)	C(60)-C(59)-H(59A)	108.5
Al(3)-C(59)-H(59A)	108.5	C(60)-C(59)-H(59B)	108.5
Al(3)-C(59)-H(59B)	108.5	H(59A)-C(59)-H(59B)	107.5
C(59)-C(60)-H(60A)	109.5	C(59)-C(60)-H(60B)	109.5
H(60A)-C(60)-H(60B)	109.5	C(59)-C(60)-H(60C)	109.5
H(60A)-C(60)-H(60C)	109.5	H(60B)-C(60)-H(60C)	109.5
C(31)-C(32A)-H(32D)	109.5	C(31)-C(32A)-H(32E)	109.5
H(32D)-C(32A)-H(32E)	109.5	C(31)-C(32A)-H(32F)	109.5
H(32D)-C(32A)-H(32F)	109.5	H(32E)-C(32A)-H(32F)	109.5
C(31)-C(33A)-H(33D)	109.5	C(31)-C(33A)-H(33E)	109.5
H(33D)-C(33A)-H(33E)	109.5	C(31)-C(33A)-H(33F)	109.5
H(33D)-C(33A)-H(33F)	109.5	H(33E)-C(33A)-H(33F)	109.5
C(31)-C(34A)-H(34D)	109.5	C(31)-C(34A)-H(34E)	109.5
H(34D)-C(34A)-H(34E)	109.5	C(31)-C(34A)-H(34F)	109.5
H(34D)-C(34A)-H(34F)	109.5	H(34E)-C(34A)-H(34F)	109.5
C(51)-C(52A)-H(52D)	109.5	C(51)-C(52A)-H(52E)	109.5
H(52D)-C(52A)-H(52E)	109.5	C(51)-C(52A)-H(52F)	109.5
H(52D)-C(52A)-H(52F)	109.5	H(52E)-C(52A)-H(52F)	109.5
C(51)-C(53A)-H(53D)	109.5	C(51)-C(53A)-H(53E)	109.5
H(53D)-C(53A)-H(53E)	109.5	C(51)-C(53A)-H(53F)	109.5

H(53D)-C(53A)-H(53F)	109.5	H(53E)-C(53A)-H(53F)	109.5
C(51)-C(54A)-H(54D)	109.5	C(51)-C(54A)-H(54E)	109.5
H(54D)-C(54A)-H(54E)	109.5	C(51)-C(54A)-H(54F)	109.5
H(54D)-C(54A)-H(54F)	109.5	H(54E)-C(54A)-H(54F)	109.5

Table B-17. Crystal Data and Structure Refinement for Complex **V2a**.

Identification code	Complex **V2a**	
Empirical formula	C46 H72 Al2 N2 O2	
Formula weight	739.02	
Temperature	110(2) K	
Wavelength	1.54178 Å	
Crystal system	Orthorhombic	
Space group	P4/ncc	
Unit cell dimensions	a = 23.795(3) Å	α= 90°.
	b = 23.795(3) Å	β= 90°.
	c = 18.707(3) Å	γ = 90°.
Volume	10592(2) $Å^3$	
Z	8	
Density (calculated)	0.927 Mg/m^3	
Absorption coefficient	0.723 mm^{-1}	
F(000)	3232	
Crystal size	0.18 x 0.18 x 0.16 mm^3	
Theta range for data collection	2.63 to 60.27°.	
Index ranges	-25<=h<=26, -26<=k<=25, -20<=l<=21	
Reflections collected	79230	
Independent reflections	3958 [R(int) = 0.1174]	
Completeness to theta = 60.27°	99.5 %	
Absorption correction	Semi-empirical from equivalents	
Max. and min. transmission	0.8931 and 0.8808	
Refinement method	Full-matrix least-squares on F^2	
Data / restraints / parameters	3958 / 0 / 257	
Goodness-of-fit on F^2	1.104	
Final R indices [I>2sigma(I)]	R1 = 0.0633, wR2 = 0.1578	
R indices (all data)	R1 = 0.0927, wR2 = 0.1712	
Largest diff. peak and hole	0.405 and -0.237 $e.Å^{-3}$	

Table B-18. Bond Lengths [Å] and Angles [°] for Complex **V2a**.

Al(1)-O(1)	1.811(2)	Al(1)-O(2)#1	1.873(2)
Al(1)-O(2)	1.899(2)	Al(1)-C(22)	1.963(3)
Al(1)-N(1)	2.011(3)	Al(1)-Al(1)#1	2.9650(18)
C(1)-O(1)	1.331(4)	C(1)-C(2)	1.416(4)
C(1)-C(6)	1.429(4)	C(2)-C(3)	1.408(4)
C(2)-C(15)	1.436(4)	C(3)-C(4)	1.382(5)
C(4)-C(5)	1.405(5)	C(4)-C(11)	1.533(5)
C(5)-C(6)	1.380(4)	C(6)-C(7)	1.534(5)
C(7)-C(8)	1.527(5)	C(7)-C(10)	1.535(6)
C(7)-C(9)	1.543(5)	C(11)-C(12)	1.502(6)
C(11)-C(13)	1.504(5)	C(11)-C(14)	1.525(6)
C(15)-N(1)	1.288(4)	C(16)-N(1)	1.476(4)
C(16)-C(17)	1.497(5)	C(16)-C(21)	1.528(4)
C(17)-O(2)	1.416(4)	C(17)-C(18)	1.504(5)
C(18)-C(19)	1.515(5)	C(19)-C(20)	1.490(5)
C(20)-C(21)	1.534(5)	C(22)-C(23)	1.542(5)
O(2)-Al(1)#1	1.873(2)		
O(1)-Al(1)-O(2)#1	94.78(10)	O(1)-Al(1)-O(2)	134.83(11)
O(2)#1-Al(1)-O(2)	75.30(10)	O(1)-Al(1)-C(22)	111.65(13)
O(2)#1-Al(1)-C(22)	106.84(12)	O(2)-Al(1)-C(22)	113.40(13)
O(1)-Al(1)-N(1)	88.31(10)	O(2)#1-Al(1)-N(1)	147.29(11)
O(2)-Al(1)-N(1)	79.52(10)	C(22)-Al(1)-N(1)	102.13(13)
O(1)-Al(1)-Al(1)#1	114.40(7)	O(2)#1-Al(1)-Al(1)#1	38.50(7)
O(2)-Al(1)-Al(1)#1	37.87(6)	C(22)-Al(1)-Al(1)#1	122.58(10)
N(1)-Al(1)-Al(1)#1	111.50(9)	O(1)-C(1)-C(2)	121.4(3)
O(1)-C(1)-C(6)	120.9(3)	C(2)-C(1)-C(6)	117.7(3)
C(3)-C(2)-C(1)	121.1(3)	C(3)-C(2)-C(15)	117.2(3)
C(1)-C(2)-C(15)	121.7(3)	C(4)-C(3)-C(2)	121.9(3)
C(3)-C(4)-C(5)	115.6(3)	C(3)-C(4)-C(11)	123.2(3)
C(5)-C(4)-C(11)	121.2(3)	C(6)-C(5)-C(4)	125.6(3)
C(5)-C(6)-C(1)	117.9(3)	C(5)-C(6)-C(7)	120.6(3)
C(1)-C(6)-C(7)	121.4(3)	C(8)-C(7)-C(6)	112.7(3)

C(8)-C(7)-C(10)	108.0(3)	C(6)-C(7)-C(10)	108.7(3)
C(8)-C(7)-C(9)	106.0(3)	C(6)-C(7)-C(9)	109.9(3)
C(10)-C(7)-C(9)	111.6(3)	C(12)-C(11)-C(13)	109.3(4)
C(12)-C(11)-C(14)	109.2(4)	C(13)-C(11)-C(14)	107.4(4)
C(12)-C(11)-C(4)	109.1(3)	C(13)-C(11)-C(4)	112.0(3)
C(14)-C(11)-C(4)	109.8(3)	N(1)-C(15)-C(2)	124.0(3)
N(1)-C(16)-C(17)	104.3(3)	N(1)-C(16)-C(21)	118.8(3)
C(17)-C(16)-C(21)	111.9(3)	O(2)-C(17)-C(16)	108.5(3)
O(2)-C(17)-C(18)	116.0(3)	C(16)-C(17)-C(18)	111.2(3)
C(17)-C(18)-C(19)	110.6(3)	C(20)-C(19)-C(18)	114.6(3)
C(19)-C(20)-C(21)	114.4(3)	C(16)-C(21)-C(20)	108.1(3)
C(23)-C(22)-Al(1)	119.5(2)	C(15)-N(1)-C(16)	123.6(3)
C(15)-N(1)-Al(1)	128.0(2)	C(16)-N(1)-Al(1)	108.0(2)
C(1)-O(1)-Al(1)	134.05(19)	C(17)-O(2)-Al(1)#1	132.8(2)
C(17)-O(2)-Al(1)	118.58(18)	Al(1)#1-O(2)-Al(1)	103.63(10)

Table B-19. Crystal Data and Structure Refinement for Complex **V3b**.

Identification code	Complex **V3b**	
Empirical formula	C42 H48 Al2 N2 O8	
Formula weight	762.78	
Temperature	110(2) K	
Wavelength	1.54178 Å	
Crystal system	Monoclinic	
Space group	P2(1)/c	
Unit cell dimensions	a = 20.036(2) Å	α= 90°.
	b = 13.6282(14) Å	β= 96.586(6)°.
	c = 17.6152(19) Å	γ = 90°.
Volume	4778.2(9) $Å^3$	
Z	4	
Density (calculated)	1.060 Mg/m^3	
Absorption coefficient	0.923 mm^{-1}	
F(000)	1616	
Crystal size	0.18 x 0.16 x 0.15 mm^3	
Theta range for data collection	2.22 to 60.14°.	
Index ranges	-22<=h<=22, -14<=k<=15, -19<=l<=19	
Reflections collected	37179	
Independent reflections	7055 [R(int) = 0.0390]	
Completeness to theta = 60.14°	99.1 %	
Absorption correction	Semi-empirical from equivalents	
Max. and min. transmission	0.8740 and 0.8515	
Refinement method	Full-matrix least-squares on F^2	
Data / restraints / parameters	7055 / 6 / 501	
Goodness-of-fit on F^2	1.128	
Final R indices [I>2sigma(I)]	R1 = 0.0964, wR2 = 0.2061	
R indices (all data)	R1 = 0.1061, wR2 = 0.2099	
Largest diff. peak and hole	0.657 and -0.393 $e.Å^{-3}$	

Table B-20. Bond Lengths [Å] and Angles [°] for Complex **V3b**.

Al(1)-O(8)	1.733(3)	Al(1)-O(1)	1.778(3)
Al(1)-O(6)	1.850(3)	Al(1)-O(3)	1.899(3)
Al(1)-N(1)	1.978(4)	Al(2)-O(7)	1.730(4)
Al(2)-O(4)	1.779(4)	Al(2)-O(3)	1.858(3)
Al(2)-O(6)	1.871(3)	Al(2)-N(2)	1.989(4)
C(1)-O(1)	1.316(6)	C(1)-C(2)	1.405(7)
C(1)-C(6)	1.429(7)	C(2)-C(3)	1.396(7)
C(2)-C(8)	1.451(7)	C(3)-C(4)	1.409(8)
C(4)-C(5)	1.383(9)	C(5)-C(6)	1.384(8)
C(6)-O(2)	1.367(7)	C(7)-O(2)	1.433(6)
C(8)-N(1)	1.280(6)	C(9)-N(1)	1.464(6)
C(9)-C(14)	1.519(7)	C(9)-C(10)	1.527(6)
C(10)-O(3)	1.433(5)	C(10)-C(11)	1.513(7)
C(11)-C(12)	1.539(7)	C(12)-C(13)	1.551(7)
C(13)-C(14)	1.542(8)	C(15)-O(4)	1.321(6)
C(15)-C(16)	1.400(7)	C(15)-C(20)	1.423(7)
C(16)-C(17)	1.428(7)	C(16)-C(22)	1.447(7)
C(17)-C(18)	1.339(8)	C(18)-C(19)	1.393(8)
C(19)-C(20)	1.385(8)	C(20)-O(5)	1.366(7)
C(21)-O(5)	1.444(7)	C(22)-N(2)	1.291(6)
C(23)-N(2)	1.480(6)	C(23)-C(28)	1.506(7)
C(23)-C(24)	1.538(7)	C(24)-O(6)	1.424(6)
C(24)-C(25)	1.504(7)	C(25)-C(26)	1.519(7)
C(26)-C(27)	1.521(7)	C(27)-C(28)	1.525(7)
C(29)-O(7)	1.370(6)	C(29)-C(30)	1.529(8)
C(30)-C(31)	1.340(10)	C(30)-C(35)	1.360(9)
C(31)-C(32)	1.339(11)	C(32)-C(33)	1.371(14)
C(33)-C(34)	1.412(14)	C(34)-C(35)	1.413(11)
C(36)-O(8)	1.420(7)	C(36)-C(37)	1.510(8)
C(37)-C(38)	1.338(9)	C(37)-C(42)	1.441(9)
C(38)-C(39)	1.360(9)	C(39)-C(40)	1.352(12)
C(40)-C(41)	1.319(12)	C(41)-C(42)	1.351(11)

		O(8)-Al(1)-O(1)	108.04(18)
O(8)-Al(1)-O(6)	109.35(17)	O(1)-Al(1)-O(6)	92.39(15)
O(8)-Al(1)-O(3)	105.77(16)	O(1)-Al(1)-O(3)	146.19(17)
O(6)-Al(1)-O(3)	76.66(14)	O(8)-Al(1)-N(1)	102.53(17)
O(1)-Al(1)-N(1)	90.26(16)	O(6)-Al(1)-N(1)	145.38(16)
O(3)-Al(1)-N(1)	82.12(15)	O(7)-Al(2)-O(4)	112.61(18)
O(7)-Al(2)-O(3)	108.10(16)	O(4)-Al(2)-O(3)	91.90(15)
O(7)-Al(2)-O(6)	108.36(17)	O(4)-Al(2)-O(6)	138.98(18)
O(3)-Al(2)-O(6)	77.15(14)	O(7)-Al(2)-N(2)	99.53(16)
O(4)-Al(2)-N(2)	89.95(16)	O(3)-Al(2)-N(2)	149.12(16)
O(6)-Al(2)-N(2)	81.34(15)	O(1)-C(1)-C(2)	123.6(5)
O(1)-C(1)-C(6)	117.9(5)	C(2)-C(1)-C(6)	118.5(5)
C(3)-C(2)-C(1)	120.9(5)	C(3)-C(2)-C(8)	118.7(5)
C(1)-C(2)-C(8)	120.4(4)	C(2)-C(3)-C(4)	119.9(5)
C(5)-C(4)-C(3)	119.3(5)	C(4)-C(5)-C(6)	122.0(6)
O(2)-C(6)-C(5)	126.0(5)	O(2)-C(6)-C(1)	114.6(5)
C(5)-C(6)-C(1)	119.5(5)	N(1)-C(8)-C(2)	124.2(5)
N(1)-C(9)-C(14)	118.5(4)	N(1)-C(9)-C(10)	104.4(4)
C(14)-C(9)-C(10)	110.9(4)	O(3)-C(10)-C(11)	112.8(4)
O(3)-C(10)-C(9)	106.6(4)	C(11)-C(10)-C(9)	110.9(4)
C(10)-C(11)-C(12)	108.4(4)	C(11)-C(12)-C(13)	111.0(4)
C(14)-C(13)-C(12)	111.0(5)	C(9)-C(14)-C(13)	108.4(4)
O(4)-C(15)-C(16)	124.2(5)	O(4)-C(15)-C(20)	117.6(4)
C(16)-C(15)-C(20)	118.1(5)	C(15)-C(16)-C(17)	119.9(5)
C(15)-C(16)-C(22)	121.1(4)	C(17)-C(16)-C(22)	119.0(5)
C(18)-C(17)-C(16)	120.1(5)	C(17)-C(18)-C(19)	121.7(5)
C(20)-C(19)-C(18)	119.7(5)	O(5)-C(20)-C(19)	126.0(5)
O(5)-C(20)-C(15)	113.5(5)	C(19)-C(20)-C(15)	120.5(5)
N(2)-C(22)-C(16)	122.7(4)	N(2)-C(23)-C(28)	120.0(4)
N(2)-C(23)-C(24)	103.6(4)	C(28)-C(23)-C(24)	111.6(4)
O(6)-C(24)-C(25)	114.3(4)	O(6)-C(24)-C(23)	106.1(4)
C(25)-C(24)-C(23)	109.6(4)	C(24)-C(25)-C(26)	109.4(5)
C(25)-C(26)-C(27)	111.8(4)	C(26)-C(27)-C(28)	112.4(4)
C(23)-C(28)-C(27)	108.6(4)	O(7)-C(29)-C(30)	110.2(4)

C(31)-C(30)-C(35)	118.6(6)	C(31)-C(30)-C(29)	121.5(6)
C(35)-C(30)-C(29)	119.9(6)	C(32)-C(31)-C(30)	123.6(8)
C(31)-C(32)-C(33)	119.4(9)	C(32)-C(33)-C(34)	120.4(8)
C(33)-C(34)-C(35)	116.3(7)	C(30)-C(35)-C(34)	121.6(8)
O(8)-C(36)-C(37)	111.8(5)	C(38)-C(37)-C(42)	116.8(6)
C(38)-C(37)-C(36)	123.9(6)	C(42)-C(37)-C(36)	119.2(6)
C(37)-C(38)-C(39)	121.9(7)	C(40)-C(39)-C(38)	119.7(7)
C(41)-C(40)-C(39)	121.3(7)	C(40)-C(41)-C(42)	120.6(8)
C(41)-C(42)-C(37)	119.6(7)	C(8)-N(1)-C(9)	123.7(4)
C(8)-N(1)-Al(1)	127.7(3)	C(9)-N(1)-Al(1)	108.5(3)
C(22)-N(2)-C(23)	123.2(4)	C(22)-N(2)-Al(2)	128.3(3)
C(23)-N(2)-Al(2)	108.5(3)	C(1)-O(1)-Al(1)	133.7(3)
C(6)-O(2)-C(7)	118.4(4)	C(10)-O(3)-Al(2)	129.8(3)
C(10)-O(3)-Al(1)	116.4(3)	Al(2)-O(3)-Al(1)	102.04(15)
C(15)-O(4)-Al(2)	132.2(3)	C(20)-O(5)-C(21)	115.5(5)
C(24)-O(6)-Al(1)	130.6(3)	C(24)-O(6)-Al(2)	118.9(3)
Al(1)-O(6)-Al(2)	103.42(15)	C(29)-O(7)-Al(2)	127.8(3)
C(36)-O(8)-Al(1)	121.1(3)		

Table B-21. Crystal Data and Structure Refinement for Complex **V2d**.

Identification code	Complex **V2d**	
Empirical formula	C44 H72 Al2 N2 O4 Si2	
Formula weight	803.18	
Temperature	110(2) K	
Wavelength	1.54178 Å	
Crystal system	Triclinic	
Space group	P_-1	
Unit cell dimensions	a = 9.5815(12) Å	α= 89.262(9)°.
	b = 13.506(2) Å	β= 86.668(9)°.
	c = 18.158(3) Å	γ = 75.039(9)°.
Volume	2266.4(6) $Å^3$	
Z	2	
Density (calculated)	1.177 Mg/m^3	
Absorption coefficient	1.407 mm^{-1}	
F(000)	872	
Crystal size	0.18 x 0.15 x 0.15 mm^3	
Theta range for data collection	2.44 to 60.23°.	
Index ranges	-10<=h<=10, -15<=k<=15, -19<=l<=19	
Reflections collected	15570	
Independent reflections	6277 [R(int) = 0.0274]	
Completeness to theta = ACTA 50°	ACTA 50 %	
Absorption correction	Semi-empirical from equivalents	
Max. and min. transmission	0.8167 and 0.7858	
Refinement method	Full-matrix least-squares on F^2	
Data / restraints / parameters	6277 / 0 / 513	
Goodness-of-fit on F^2	1.045	
Final R indices [I>2sigma(I)]	R1 = 0.0369, wR2 = 0.0962	
R indices (all data)	R1 = 0.0435, wR2 = 0.1052	
Largest diff. peak and hole	0.441 and -0.287 $e.Å^{-3}$	

Table B-22. Bond Lengths [Å] and Angles [°] for Complex **V2d**.

Al(1)-O(1)	1.8142(15)	Al(1)-O(4)	1.8716(15)
Al(1)-O(2)	1.8959(15)	Al(1)-C(21)	1.977(2)
Al(1)-N(1)	2.0241(18)	Al(2)-O(3)	1.8108(16)
Al(2)-O(2)	1.8828(15)	Al(2)-O(4)	1.8914(15)
Al(2)-C(43)	1.983(2)	Al(2)-N(2)	2.0224(18)
C(1)-O(1)	1.342(3)	C(1)-C(2)	1.420(3)
C(1)-C(6)	1.425(3)	C(2)-C(3)	1.406(3)
C(2)-C(14)	1.441(3)	C(3)-C(4)	1.378(3)
C(4)-C(5)	1.398(3)	C(4)-C(7)	1.517(3)
C(5)-C(6)	1.394(3)	C(6)-Si(1)	1.884(2)
C(8)-Si(1)	1.864(2)	C(9)-Si(1)	1.873(2)
C(10)-C(11)	1.532(3)	C(10)-C(13)	1.534(3)
C(10)-C(12)	1.539(3)	C(10)-Si(1)	1.915(2)
C(14)-N(1)	1.282(3)	C(15)-N(1)	1.466(3)
C(15)-C(16)	1.521(3)	C(15)-C(20)	1.524(3)
C(16)-O(2)	1.427(2)	C(16)-C(17)	1.506(3)
C(17)-C(18)	1.536(3)	C(18)-C(19)	1.530(3)
C(19)-C(20)	1.527(3)	C(21)-C(22)	1.533(3)
C(23)-O(3)	1.337(3)	C(23)-C(28)	1.420(3)
C(23)-C(24)	1.428(3)	C(24)-C(25)	1.397(3)
C(24)-C(36)	1.444(3)	C(25)-C(26)	1.378(3)
C(26)-C(27)	1.402(3)	C(26)-C(29)	1.507(3)
C(27)-C(28)	1.394(3)	C(28)-Si(2)	1.890(2)
C(30)-Si(2)	1.860(2)	C(31)-Si(2)	1.877(2)
C(32)-C(35)	1.524(4)	C(32)-C(33)	1.528(3)
C(32)-C(34)	1.532(4)	C(32)-Si(2)	1.903(2)
C(36)-N(2)	1.277(3)	C(37)-N(2)	1.470(3)
C(37)-C(42)	1.520(3)	C(37)-C(38)	1.527(3)
C(38)-O(4)	1.428(2)	C(38)-C(39)	1.507(3)
C(39)-C(40)	1.532(3)	C(40)-C(41)	1.530(3)
C(41)-C(42)	1.535(3)	C(43)-C(44)	1.540(3)
		O(1)-Al(1)-O(4)	97.19(7)

O(1)-Al(1)-O(2)	134.10(7)	O(4)-Al(1)-O(2)	74.61(6)
O(1)-Al(1)-C(21)	110.56(8)	O(4)-Al(1)-C(21)	107.09(8)
O(2)-Al(1)-C(21)	115.03(8)	O(1)-Al(1)-N(1)	88.93(7)
O(4)-Al(1)-N(1)	149.03(7)	O(2)-Al(1)-N(1)	79.36(7)
C(21)-Al(1)-N(1)	98.92(8)	O(3)-Al(2)-O(2)	98.03(7)
O(3)-Al(2)-O(4)	131.20(7)	O(2)-Al(2)-O(4)	74.46(6)
O(3)-Al(2)-C(43)	115.03(9)	O(2)-Al(2)-C(43)	102.94(8)
O(4)-Al(2)-C(43)	113.62(9)	O(3)-Al(2)-N(2)	89.54(7)
O(2)-Al(2)-N(2)	150.82(7)	O(4)-Al(2)-N(2)	79.36(7)
C(43)-Al(2)-N(2)	99.15(8)	O(1)-C(1)-C(2)	121.89(18)
O(1)-C(1)-C(6)	119.57(19)	C(2)-C(1)-C(6)	118.53(18)
C(3)-C(2)-C(1)	120.50(19)	C(3)-C(2)-C(14)	117.14(19)
C(1)-C(2)-C(14)	122.37(19)	C(4)-C(3)-C(2)	121.8(2)
C(3)-C(4)-C(5)	116.83(19)	C(3)-C(4)-C(7)	122.4(2)
C(5)-C(4)-C(7)	120.8(2)	C(6)-C(5)-C(4)	124.7(2)
C(5)-C(6)-C(1)	117.62(19)	C(5)-C(6)-Si(1)	121.76(16)
C(1)-C(6)-Si(1)	120.60(16)	C(11)-C(10)-C(13)	109.8(2)
C(11)-C(10)-C(12)	107.6(2)	C(13)-C(10)-C(12)	107.3(2)
C(11)-C(10)-Si(1)	113.74(17)	C(13)-C(10)-Si(1)	112.01(16)
C(12)-C(10)-Si(1)	106.02(15)	N(1)-C(14)-C(2)	123.3(2)
N(1)-C(15)-C(16)	104.28(16)	N(1)-C(15)-C(20)	120.34(18)
C(16)-C(15)-C(20)	110.29(18)	O(2)-C(16)-C(17)	114.40(18)
O(2)-C(16)-C(15)	107.63(17)	C(17)-C(16)-C(15)	109.83(18)
C(16)-C(17)-C(18)	109.45(18)	C(19)-C(18)-C(17)	112.38(18)
C(20)-C(19)-C(18)	112.95(18)	C(15)-C(20)-C(19)	108.70(17)
C(22)-C(21)-Al(1)	112.45(15)	O(3)-C(23)-C(28)	120.32(18)
O(3)-C(23)-C(24)	121.84(19)	C(28)-C(23)-C(24)	117.83(19)
C(25)-C(24)-C(23)	120.42(19)	C(25)-C(24)-C(36)	117.09(19)
C(23)-C(24)-C(36)	122.42(19)	C(26)-C(25)-C(24)	122.8(2)
C(25)-C(26)-C(27)	115.8(2)	C(25)-C(26)-C(29)	123.2(2)
C(27)-C(26)-C(29)	121.0(2)	C(28)-C(27)-C(26)	124.7(2)
C(27)-C(28)-C(23)	118.28(19)	C(27)-C(28)-Si(2)	116.40(16)
C(23)-C(28)-Si(2)	125.29(16)	C(35)-C(32)-C(33)	108.6(2)
C(35)-C(32)-C(34)	109.6(2)	C(33)-C(32)-C(34)	108.1(2)

C(35)-C(32)-Si(2)	110.86(17)	C(33)-C(32)-Si(2)	110.22(17)
C(34)-C(32)-Si(2)	109.38(17)	N(2)-C(36)-C(24)	123.93(19)
N(2)-C(37)-C(42)	120.00(18)	N(2)-C(37)-C(38)	103.21(16)
C(42)-C(37)-C(38)	110.26(17)	O(4)-C(38)-C(39)	114.12(18)
O(4)-C(38)-C(37)	107.42(17)	C(39)-C(38)-C(37)	110.02(18)
C(38)-C(39)-C(40)	108.82(19)	C(41)-C(40)-C(39)	111.94(18)
C(40)-C(41)-C(42)	112.44(18)	C(37)-C(42)-C(41)	108.39(18)
C(44)-C(43)-Al(2)	115.22(15)	C(14)-N(1)-C(15)	122.62(18)
C(14)-N(1)-Al(1)	128.36(15)	C(15)-N(1)-Al(1)	108.51(13)
C(36)-N(2)-C(37)	123.70(18)	C(36)-N(2)-Al(2)	127.83(15)
C(37)-N(2)-Al(2)	108.16(13)	C(1)-O(1)-Al(1)	133.19(13)
C(16)-O(2)-Al(2)	134.98(13)	C(16)-O(2)-Al(1)	119.34(12)
Al(2)-O(2)-Al(1)	105.15(7)	C(23)-O(3)-Al(2)	133.68(13)
C(38)-O(4)-Al(1)	134.95(13)	C(38)-O(4)-Al(2)	119.16(12)
Al(1)-O(4)-Al(2)	105.78(7)	C(8)-Si(1)-C(9)	111.91(11)
C(8)-Si(1)-C(6)	107.99(10)	C(9)-Si(1)-C(6)	107.68(10)
C(8)-Si(1)-C(10)	107.17(11)	C(9)-Si(1)-C(10)	108.28(11)
C(6)-Si(1)-C(10)	113.88(10)	C(30)-Si(2)-C(31)	106.27(11)
C(30)-Si(2)-C(28)	113.13(10)	C(31)-Si(2)-C(28)	108.48(10)
C(30)-Si(2)-C(32)	110.50(11)	C(31)-Si(2)-C(32)	108.19(11)
C(28)-Si(2)-C(32)	110.06(10)		

Table B-23. Crystal Data and Structure Refinement for Complex **V3e**.

Identification code	Complex **V3e**	
Empirical formula	C132 H124 Al4 B2 F48 N4 O10	
Formula weight	2967.89	
Temperature	110(2) K	
Wavelength	1.54178 Å	
Crystal system	Triclinic	
Space group	P_-1	
Unit cell dimensions	a = 16.202(6) Å	α= 74.59(2)°.
	b = 17.644(7) Å	β= 66.12(2)°.
	c = 18.126(6) Å	γ = 75.58(2)°.
Volume	4509(3) $Å^3$	
Z	1	
Density (calculated)	1.093 Mg/m^3	
Absorption coefficient	1.077 mm^{-1}	
F(000)	1518	
Crystal size	0.20 x 0.20 x 0.20 mm^3	
Theta range for data collection	2.63 to 61.64°.	
Index ranges	-18<=h<=17, -19<=k<=19, -20<=l<=20	
Reflections collected	34543	
Independent reflections	12628 [R(int) = 0.1016]	
Completeness to theta = ACTA 50°	ACTA 50 %	
Absorption correction	Semi-empirical from equivalents	
Max. and min. transmission	0.8135 and 0.8135	
Refinement method	Full-matrix least-squares on F^2	
Data / restraints / parameters	12628 / 42 / 913	
Goodness-of-fit on F^2	0.916	
Final R indices [I>2sigma(I)]	R1 = 0.1010, wR2 = 0.2435	
R indices (all data)	R1 = 0.1486, wR2 = 0.2762	
Largest diff. peak and hole	0.643 and -0.700 $e.Å^{-3}$	

Table B-24. Bond Lengths [Å] and Angles [°] for Complex **V3e**.

Al(1)-O(1)	1.779(4)	Al(1)-O(5)#1	1.810(4)
Al(1)-O(4)	1.862(3)	Al(1)-O(2)	1.873(4)
Al(1)-N(1)	1.944(4)	Al(2)-O(3)	1.765(4)
Al(2)-O(5)	1.817(4)	Al(2)-O(2)	1.832(3)
Al(2)-O(4)	1.876(4)	Al(2)-N(2)	1.959(4)
B(1)-C(35)	1.606(9)	B(1)-C(43)	1.637(7)
B(1)-C(51)	1.655(9)	B(1)-C(59)	1.658(7)
C(1)-O(1)	1.340(6)	C(1)-C(6)	1.414(7)
C(1)-C(2)	1.431(7)	C(2)-C(3)	1.424(8)
C(2)-C(15)	1.458(7)	C(3)-C(4)	1.372(8)
C(4)-C(5)	1.426(8)	C(4)-C(11)	1.520(9)
C(5)-C(6)	1.379(8)	C(6)-C(7)	1.562(7)
C(7)-C(9)	1.511(8)	C(7)-C(10)	1.538(8)
C(7)-C(8)	1.549(8)	C(11)-C(13)	1.505(9)
C(11)-C(14)	1.540(11)	C(11)-C(12)	1.541(10)
C(15)-N(1)	1.258(7)	C(16)-N(1)	1.478(6)
C(16)-C(17)	1.493(8)	C(17)-O(2)	1.467(6)
C(18)-O(3)	1.317(6)	C(18)-C(19)	1.426(8)
C(18)-C(23)	1.452(8)	C(19)-C(20)	1.417(9)
C(19)-C(32)	1.441(9)	C(20)-C(21)	1.362(10)
C(21)-C(22)	1.424(10)	C(21)-C(28)	1.523(9)
C(22)-C(23)	1.344(8)	C(23)-C(24)	1.563(8)
C(24)-C(26)	1.526(9)	C(24)-C(27)	1.532(8)
C(24)-C(25)	1.546(9)	C(28)-C(29)	1.520(11)
C(28)-C(31)	1.562(12)	C(28)-C(30)	1.570(11)
C(32)-N(2)	1.271(7)	C(33)-N(2)	1.444(7)
C(33)-C(34)	1.508(8)	C(34)-O(4)	1.436(5)
C(35)-C(40)	1.414(8)	C(35)-C(36)	1.423(8)
C(36)-C(37)	1.375(8)	C(37)-C(38)	1.396(8)
C(37)-C(42)	1.500(9)	C(38)-C(39)	1.367(8)
C(39)-C(40)	1.407(8)	C(39)-C(41)	1.467(9)
C(41)-F(3)	1.272(9)	C(41)-F(2)	1.290(11)

C(41)-F(1)	1.335(11)	C(42)-F(5)	1.325(7)
C(42)-F(4)	1.346(7)	C(42)-F(6)	1.353(7)
C(43)-C(48)	1.374(8)	C(43)-C(44)	1.417(7)
C(44)-C(45)	1.367(8)	C(45)-C(46)	1.364(9)
C(45)-C(50)	1.520(10)	C(46)-C(47)	1.390(8)
C(47)-C(48)	1.418(8)	C(47)-C(49)	1.463(9)
C(49)-F(9)	1.296(8)	C(49)-F(8)	1.333(8)
C(49)-F(7)	1.349(9)	C(50)-F(10)	1.322(10)
C(50)-F(11)	1.332(16)	C(50)-F(12)	1.346(12)
C(51)-C(52)	1.406(8)	C(51)-C(56)	1.412(9)
C(52)-C(53)	1.379(8)	C(53)-C(54)	1.353(9)
C(53)-C(58)	1.483(9)	C(54)-C(55)	1.405(10)
C(55)-C(56)	1.396(9)	C(55)-C(57)	1.485(10)
C(57)-F(13)	1.333(8)	C(57)-F(15)	1.357(7)
C(57)-F(14)	1.360(9)	C(58)-F(16)	1.285(7)
C(58)-F(17)	1.316(8)	C(58)-F(18)	1.352(9)
C(59)-C(60)	1.357(8)	C(59)-C(64)	1.414(7)
C(60)-C(61)	1.416(7)	C(61)-C(62)	1.389(8)
C(61)-C(66)	1.501(10)	C(62)-C(63)	1.353(8)
C(63)-C(64)	1.400(7)	C(63)-C(65)	1.517(7)
C(65)-F(20)	1.324(7)	C(65)-F(19)	1.332(6)
C(65)-F(21)	1.352(6)	C(66)-F(23)	1.271(8)
C(66)-F(22)	1.293(8)	C(66)-F(24)	1.375(10)
O(5)-Al(1)#1	1.811(4)		
O(1)-Al(1)-O(5)#1	103.25(17)	O(1)-Al(1)-O(4)	96.97(16)
O(5)#1-Al(1)-O(4)	103.84(17)	O(1)-Al(1)-O(2)	152.03(17)
O(5)#1-Al(1)-O(2)	104.72(16)	O(4)-Al(1)-O(2)	76.15(15)
O(1)-Al(1)-N(1)	92.06(18)	O(5)#1-Al(1)-N(1)	101.79(17)
O(4)-Al(1)-N(1)	150.00(19)	O(2)-Al(1)-N(1)	82.50(17)
O(3)-Al(2)-O(5)	105.53(18)	O(3)-Al(2)-O(2)	97.18(17)
O(5)-Al(2)-O(2)	103.10(16)	O(3)-Al(2)-O(4)	151.12(18)
O(5)-Al(2)-O(4)	103.34(17)	O(2)-Al(2)-O(4)	76.79(15)
O(3)-Al(2)-N(2)	91.67(19)	O(5)-Al(2)-N(2)	101.70(17)
O(2)-Al(2)-N(2)	150.29(19)	O(4)-Al(2)-N(2)	81.80(17)

C(35)-B(1)-C(43)	102.8(4)	C(35)-B(1)-C(51)	115.1(5)
C(43)-B(1)-C(51)	111.8(5)	C(35)-B(1)-C(59)	113.4(5)
C(43)-B(1)-C(59)	110.1(4)	C(51)-B(1)-C(59)	103.9(4)
O(1)-C(1)-C(6)	121.1(4)	O(1)-C(1)-C(2)	121.2(5)
C(6)-C(1)-C(2)	117.7(5)	C(3)-C(2)-C(1)	121.1(5)
C(3)-C(2)-C(15)	118.2(5)	C(1)-C(2)-C(15)	120.6(5)
C(4)-C(3)-C(2)	121.1(5)	C(3)-C(4)-C(5)	116.3(5)
C(3)-C(4)-C(11)	124.3(5)	C(5)-C(4)-C(11)	119.4(5)
C(6)-C(5)-C(4)	125.0(5)	C(5)-C(6)-C(1)	118.6(5)
C(5)-C(6)-C(7)	120.9(5)	C(1)-C(6)-C(7)	120.4(5)
C(9)-C(7)-C(10)	110.7(5)	C(9)-C(7)-C(8)	107.1(4)
C(10)-C(7)-C(8)	107.7(5)	C(9)-C(7)-C(6)	110.2(5)
C(10)-C(7)-C(6)	110.4(4)	C(8)-C(7)-C(6)	110.7(5)
C(13)-C(11)-C(4)	110.6(5)	C(13)-C(11)-C(14)	108.9(7)
C(4)-C(11)-C(14)	110.2(5)	C(13)-C(11)-C(12)	108.4(6)
C(4)-C(11)-C(12)	109.5(6)	C(14)-C(11)-C(12)	109.3(7)
N(1)-C(15)-C(2)	125.4(5)	N(1)-C(16)-C(17)	107.4(4)
O(2)-C(17)-C(16)	106.2(4)	O(3)-C(18)-C(19)	122.3(5)
O(3)-C(18)-C(23)	121.3(5)	C(19)-C(18)-C(23)	116.4(5)
C(20)-C(19)-C(18)	121.3(6)	C(20)-C(19)-C(32)	118.1(5)
C(18)-C(19)-C(32)	120.5(5)	C(21)-C(20)-C(19)	122.2(6)
C(20)-C(21)-C(22)	115.1(6)	C(20)-C(21)-C(28)	123.5(7)
C(22)-C(21)-C(28)	121.3(7)	C(23)-C(22)-C(21)	126.6(7)
C(22)-C(23)-C(18)	118.2(6)	C(22)-C(23)-C(24)	122.4(5)
C(18)-C(23)-C(24)	119.3(5)	C(26)-C(24)-C(27)	111.3(5)
C(26)-C(24)-C(25)	107.4(5)	C(27)-C(24)-C(25)	108.3(5)
C(26)-C(24)-C(23)	108.5(5)	C(27)-C(24)-C(23)	110.8(5)
C(25)-C(24)-C(23)	110.6(5)	C(21)-C(28)-C(29)	109.4(6)
C(21)-C(28)-C(31)	111.9(7)	C(29)-C(28)-C(31)	108.9(6)
C(21)-C(28)-C(30)	108.7(6)	C(29)-C(28)-C(30)	108.2(7)
C(31)-C(28)-C(30)	109.7(7)	N(2)-C(32)-C(19)	125.2(5)
N(2)-C(33)-C(34)	108.1(4)	O(4)-C(34)-C(33)	106.9(4)
C(40)-C(35)-C(36)	113.4(5)	C(40)-C(35)-B(1)	121.5(5)
C(36)-C(35)-B(1)	124.6(5)	C(37)-C(36)-C(35)	123.9(5)

C(36)-C(37)-C(38)	119.8(5)	C(36)-C(37)-C(42)	121.6(5)
C(38)-C(37)-C(42)	118.5(6)	C(39)-C(38)-C(37)	119.6(5)
C(38)-C(39)-C(40)	119.9(5)	C(38)-C(39)-C(41)	120.2(7)
C(40)-C(39)-C(41)	119.8(7)	C(39)-C(40)-C(35)	123.2(5)
F(3)-C(41)-F(2)	106.3(8)	F(3)-C(41)-F(1)	102.5(9)
F(2)-C(41)-F(1)	102.8(7)	F(3)-C(41)-C(39)	115.2(7)
F(2)-C(41)-C(39)	115.0(8)	F(1)-C(41)-C(39)	113.6(7)
F(5)-C(42)-F(4)	106.9(5)	F(5)-C(42)-F(6)	105.9(5)
F(4)-C(42)-F(6)	106.9(5)	F(5)-C(42)-C(37)	112.2(5)
F(4)-C(42)-C(37)	112.2(5)	F(6)-C(42)-C(37)	112.4(5)
C(48)-C(43)-C(44)	116.4(5)	C(48)-C(43)-B(1)	121.8(5)
C(44)-C(43)-B(1)	121.3(5)	C(45)-C(44)-C(43)	120.8(5)
C(46)-C(45)-C(44)	123.0(6)	C(46)-C(45)-C(50)	118.0(5)
C(44)-C(45)-C(50)	119.0(6)	C(45)-C(46)-C(47)	118.3(5)
C(46)-C(47)-C(48)	119.1(5)	C(46)-C(47)-C(49)	121.1(5)
C(48)-C(47)-C(49)	119.7(5)	C(43)-C(48)-C(47)	122.5(5)
F(9)-C(49)-F(8)	108.8(7)	F(9)-C(49)-F(7)	103.4(6)
F(8)-C(49)-F(7)	99.1(6)	F(9)-C(49)-C(47)	115.6(6)
F(8)-C(49)-C(47)	115.0(5)	F(7)-C(49)-C(47)	113.1(7)
F(10)-C(50)-F(11)	107.5(8)	F(10)-C(50)-F(12)	104.2(10)
F(11)-C(50)-F(12)	106.4(8)	F(10)-C(50)-C(45)	114.0(8)
F(11)-C(50)-C(45)	113.6(11)	F(12)-C(50)-C(45)	110.4(8)
C(52)-C(51)-C(56)	115.7(5)	C(52)-C(51)-B(1)	125.5(6)
C(56)-C(51)-B(1)	118.7(5)	C(53)-C(52)-C(51)	121.6(6)
C(54)-C(53)-C(52)	121.9(6)	C(54)-C(53)-C(58)	119.2(6)
C(52)-C(53)-C(58)	118.8(7)	C(53)-C(54)-C(55)	119.3(6)
C(56)-C(55)-C(54)	119.0(6)	C(56)-C(55)-C(57)	120.7(7)
C(54)-C(55)-C(57)	120.1(7)	C(55)-C(56)-C(51)	122.4(6)
F(13)-C(57)-F(15)	105.8(6)	F(13)-C(57)-F(14)	104.1(6)
F(15)-C(57)-F(14)	105.8(6)	F(13)-C(57)-C(55)	115.9(7)
F(15)-C(57)-C(55)	111.2(6)	F(14)-C(57)-C(55)	113.3(6)
F(16)-C(58)-F(17)	106.5(6)	F(16)-C(58)-F(18)	104.5(7)
F(17)-C(58)-F(18)	101.6(6)	F(16)-C(58)-C(53)	114.1(5)
F(17)-C(58)-C(53)	114.3(7)	F(18)-C(58)-C(53)	114.6(5)

C(60)-C(59)-C(64)	114.9(5)	C(60)-C(59)-B(1)	121.5(4)
C(64)-C(59)-B(1)	123.2(5)	C(59)-C(60)-C(61)	123.2(5)
C(62)-C(61)-C(60)	120.1(5)	C(62)-C(61)-C(66)	120.4(5)
C(60)-C(61)-C(66)	119.4(5)	C(63)-C(62)-C(61)	118.2(5)
C(62)-C(63)-C(64)	120.9(5)	C(62)-C(63)-C(65)	119.1(4)
C(64)-C(63)-C(65)	120.0(5)	C(63)-C(64)-C(59)	122.5(5)
F(20)-C(65)-F(19)	106.2(5)	F(20)-C(65)-F(21)	105.9(4)
F(19)-C(65)-F(21)	105.8(4)	F(20)-C(65)-C(63)	113.9(4)
F(19)-C(65)-C(63)	112.4(5)	F(21)-C(65)-C(63)	112.0(5)
F(23)-C(66)-F(22)	109.2(7)	F(23)-C(66)-F(24)	104.0(9)
F(22)-C(66)-F(24)	104.6(6)	F(23)-C(66)-C(61)	115.0(6)
F(22)-C(66)-C(61)	112.6(7)	F(24)-C(66)-C(61)	110.6(6)
C(15)-N(1)-C(16)	121.7(4)	C(15)-N(1)-Al(1)	126.9(3)
C(16)-N(1)-Al(1)	111.2(3)	C(32)-N(2)-C(33)	121.7(5)
C(32)-N(2)-Al(2)	125.9(4)	C(33)-N(2)-Al(2)	112.3(3)
C(1)-O(1)-Al(1)	132.3(3)	C(17)-O(2)-Al(2)	131.0(3)
C(17)-O(2)-Al(1)	118.0(3)	Al(2)-O(2)-Al(1)	103.98(15)
C(18)-O(3)-Al(2)	131.5(3)	C(34)-O(4)-Al(1)	131.2(3)
C(34)-O(4)-Al(2)	118.9(3)	Al(1)-O(4)-Al(2)	102.74(15)
Al(1)#1-O(5)-Al(2)	139.3(2)		

Table B-25. Crystal Data and Structure Refinement for Complex **V4e**.

Identification code	Complex **V4e**	
Empirical formula	C150 H145 Al4 B2 Cl18 F48 N4 O18	
Formula weight	3971.34	
Temperature	110(2) K	
Wavelength	1.54178 Å	
Crystal system	Monoclinic	
Space group	P21/c	
Unit cell dimensions	a = 29.458(2) Å	α= 90°.
	b = 20.3463(15) Å	β= 102.383(4)°.
	c = 30.256(2) Å	γ = 90°.
Volume	17712(2) $Å^3$	
Z	4	
Density (calculated)	1.489 Mg/m^3	
Absorption coefficient	3.725 mm^{-1}	
F(000)	8068	
Crystal size	0.12 x 0.11 x 0.10 mm^3	
Theta range for data collection	2.64 to 60.90°.	
Index ranges	-31<=h<=33, -23<=k<=23, -33<=l<=34	
Reflections collected	129138	
Independent reflections	26167 [R(int) = 0.0959]	
Completeness to theta = 60.90°	96.9 %	
Absorption correction	Semi-empirical from equivalents	
Max. and min. transmission	0.7071 and 0.6635	
Refinement method	Full-matrix least-squares on F^2	
Data / restraints / parameters	26167 / 1005 / 2194	
Goodness-of-fit on F^2	3.754	
Final R indices [I>2sigma(I)]	R1 = 0.1655, wR2 = 0.3270	
R indices (all data)	R1 = 0.2258, wR2 = 0.3404	
Largest diff. peak and hole	2.367 and -1.045 $e.Å^{-3}$	

Table B-26. Bond Lengths [Å] and Angles [°] for Complex **V4e**.

Al(1)-O(1)	1.756(7)	Al(1)-O(9)	1.805(6)
Al(1)-O(4)	1.839(6)	Al(1)-O(2)	1.886(6)
Al(1)-N(1)	1.948(8)	Al(1)-Al(2)	2.901(4)
Al(2)-O(3)	1.753(6)	Al(2)-O(2)	1.813(6)
Al(2)-O(10)	1.817(6)	Al(2)-O(4)	1.877(6)
Al(2)-N(2)	1.943(8)	Al(3)-O(5)	1.758(7)
Al(3)-O(9)	1.809(6)	Al(3)-O(8)	1.845(7)
Al(3)-O(6)	1.886(6)	Al(3)-N(3)	1.931(8)
Al(3)-Al(4)	2.905(4)	Al(4)-O(7)	1.766(6)
Al(4)-O(10)	1.786(6)	Al(4)-O(6)	1.826(6)
Al(4)-O(8)	1.866(7)	Al(4)-N(4)	1.938(9)
B(1)-C(77)	1.599(14)	B(1)-C(93)	1.617(15)
B(1)-C(69)	1.646(15)	B(1)-C(85)	1.663(16)
B(2)-C(101)	1.60(2)	B(2)-C(125)	1.646(17)
B(2)-C(109)	1.66(2)	B(2)-C(117)	1.656(17)
C(1)-O(1)	1.371(10)	C(1)-C(2)	1.398(14)
C(1)-C(6)	1.428(14)	C(2)-C(15)	1.431(15)
C(2)-C(3)	1.430(14)	C(3)-C(4)	1.317(16)
C(4)-C(5)	1.406(17)	C(4)-C(11)	1.554(15)
C(5)-C(6)	1.420(14)	C(6)-C(7)	1.471(15)
C(7)-C(9)	1.519(15)	C(7)-C(8)	1.534(15)
C(7)-C(10)	1.571(14)	C(11)-C(12)	1.500(13)
C(11)-C(14)	1.517(13)	C(11)-C(13)	1.548(14)
C(15)-N(1)	1.318(12)	C(16)-N(1)	1.459(12)
C(16)-C(17)	1.525(13)	C(17)-O(2)	1.435(11)
C(18)-O(3)	1.352(11)	C(18)-C(23)	1.382(11)
C(18)-C(19)	1.428(13)	C(19)-C(20)	1.398(12)
C(19)-C(32)	1.449(13)	C(20)-C(21)	1.367(13)
C(21)-C(22)	1.333(12)	C(21)-C(28)	1.511(13)
C(22)-C(23)	1.430(12)	C(23)-C(24)	1.551(12)
C(24)-C(27)	1.537(17)	C(24)-C(26)	1.540(17)
C(24)-C(25)	1.603(15)	C(28)-C(31)	1.503(14)

C(28)-C(29)	1.543(14)	C(28)-C(30)	1.577(13)
C(32)-N(2)	1.302(11)	C(33)-N(2)	1.472(11)
C(33)-C(34)	1.504(12)	C(34)-O(4)	1.401(11)
C(35)-O(5)	1.354(11)	C(35)-C(40)	1.393(13)
C(35)-C(36)	1.437(13)	C(36)-C(37)	1.401(12)
C(36)-C(49)	1.431(14)	C(40)-C(39)	1.386(13)
C(40)-C(41)	1.522(14)	C(41)-C(44)	1.526(15)
C(41)-C(42)	1.540(14)	C(41)-C(43)	1.568(16)
C(49)-N(3)	1.303(12)	C(50)-C(51)	1.429(12)
C(50)-N(3)	1.474(17)	C(51)-O(6)	1.405(15)
C(50A)-C(51A)	1.414(12)	C(50A)-N(3)	1.472(17)
C(51A)-O(6)	1.399(16)	C(52)-O(7)	1.330(10)
C(52)-C(53)	1.407(13)	C(52)-C(57)	1.423(13)
C(53)-C(54)	1.420(13)	C(53)-C(66)	1.443(14)
C(54)-C(55)	1.330(15)	C(55)-C(56)	1.370(15)
C(55)-C(62)	1.577(17)	C(56)-C(57)	1.407(14)
C(57)-C(58)	1.516(14)	C(58)-C(59)	1.522(14)
C(58)-C(61)	1.522(15)	C(58)-C(60)	1.581(14)
C(62)-C(63)	1.45(2)	C(62)-C(65)	1.54(2)
C(62)-C(64)	1.63(2)	C(66)-N(4)	1.272(12)
C(67)-N(4)	1.468(12)	C(67)-C(68)	1.547(13)
C(68)-O(8)	1.429(12)	C(69)-C(70)	1.411(13)
C(69)-C(74)	1.409(13)	C(70)-C(71)	1.348(13)
C(71)-C(72)	1.388(14)	C(71)-C(75)	1.505(15)
C(72)-C(73)	1.372(15)	C(73)-C(74)	1.369(14)
C(73)-C(76)	1.469(17)	C(75)-F(5A)	1.308(17)
C(75)-F(5)	1.312(11)	C(75)-F(6)	1.320(11)
C(75)-F(6A)	1.327(17)	C(75)-F(4)	1.330(11)
C(75)-F(4A)	1.340(17)	C(76)-F(2)	1.305(17)
C(76)-F(3)	1.29(2)	C(76)-F(1)	1.37(2)
C(77)-C(78)	1.422(13)	C(77)-C(82)	1.423(13)
C(78)-C(79)	1.316(13)	C(79)-C(80)	1.457(15)
C(79)-C(83)	1.469(16)	C(80)-C(81)	1.384(14)
C(81)-C(82)	1.364(13)	C(81)-C(84)	1.517(15)

C(83)-F(9)	1.305(11)	C(83)-F(7A)	1.320(17)
C(83)-F(9A)	1.316(16)	C(83)-F(8)	1.336(11)
C(83)-F(8A)	1.320(17)	C(83)-F(7)	1.334(12)
C(84)-F(10)	1.329(13)	C(84)-F(12)	1.317(13)
C(84)-F(11)	1.341(12)	C(85)-C(86)	1.403(13)
C(85)-C(90)	1.437(13)	C(86)-C(87)	1.379(13)
C(87)-C(88)	1.390(13)	C(87)-C(91)	1.510(14)
C(88)-C(89)	1.369(14)	C(89)-C(90)	1.370(14)
C(89)-C(92)	1.483(15)	C(91)-F(13)	1.335(11)
C(91)-F(14)	1.329(11)	C(91)-F(15)	1.369(12)
C(92)-F(16)	1.324(13)	C(92)-F(17)	1.348(15)
C(92)-F(18)	1.365(14)	C(93)-C(98)	1.401(13)
C(93)-C(94)	1.431(13)	C(94)-C(95)	1.337(14)
C(95)-C(96)	1.363(15)	C(95)-C(99)	1.559(17)
C(96)-C(97)	1.355(15)	C(97)-C(98)	1.413(14)
C(97)-C(100)	1.484(16)	C(99)-F(21A)	1.272(15)
C(99)-F(21)	1.296(11)	C(99)-F(19A)	1.299(15)
C(99)-F(19)	1.309(12)	C(99)-F(20A)	1.317(15)
C(99)-F(20)	1.344(12)	C(100)-F(23)	1.299(14)
C(100)-F(22)	1.349(13)	C(100)-F(24)	1.337(15)
C(101)-C(106)	1.453(19)	C(101)-C(102)	1.45(2)
C(102)-C(103)	1.40(2)	C(103)-C(104)	1.47(2)
C(103)-C(107)	1.61(2)	C(104)-C(105)	1.41(2)
C(105)-C(106)	1.316(18)	C(105)-C(108)	1.567(19)
C(107)-F(29)	1.19(2)	C(107)-F(28)	1.36(2)
C(107)-F(30)	1.43(2)	C(108)-F(25)	1.291(19)
C(108)-F(26)	1.270(18)	C(108)-F(27)	1.38(2)
C(109)-C(110)	1.365(18)	C(109)-C(114)	1.426(18)
C(110)-C(111)	1.38(2)	C(111)-C(112)	1.34(2)
C(111)-C(115)	1.49(3)	C(112)-C(113)	1.39(2)
C(113)-C(114)	1.375(18)	C(113)-C(116)	1.51(2)
C(115)-F(33)	1.28(2)	C(115)-F(32)	1.27(2)
C(115)-F(31)	1.32(2)	C(116)-F(35)	1.254(19)
C(116)-F(36)	1.274(19)	C(116)-F(34)	1.37(2)

C(117)-C(118)	1.395(15)	C(117)-C(122)	1.390(16)
C(118)-C(119)	1.368(15)	C(119)-C(120)	1.433(18)
C(119)-C(123)	1.488(18)	C(120)-C(121)	1.360(17)
C(121)-C(122)	1.387(15)	C(121)-C(124)	1.49(2)
C(123)-F(38)	1.304(18)	C(123)-F(39)	1.283(16)
C(123)-F(37)	1.38(2)	C(124)-F(42)	1.086(17)
C(124)-F(41)	1.42(2)	C(124)-F(40)	1.43(2)
C(125)-C(130)	1.409(14)	C(125)-C(126)	1.428(15)
C(126)-C(127)	1.391(14)	C(127)-C(128)	1.396(14)
C(127)-C(131)	1.499(15)	C(128)-C(129)	1.382(15)
C(129)-C(130)	1.359(14)	C(129)-C(132)	1.494(15)
C(131)-F(44)	1.339(12)	C(131)-F(43)	1.325(12)
C(131)-F(45)	1.329(13)	C(132)-F(48)	1.292(14)
C(132)-F(47)	1.319(13)	C(132)-F(46)	1.385(14)
C(133)-O(11)	1.090(18)	C(133)-O(12)	1.31(2)
C(133)-C(134)	1.56(2)	C(134)-O(14)	1.414(19)
C(134)-C(137)	1.44(2)	C(135)-O(13A)	1.138(15)
C(135)-O(13)	1.131(14)	C(135)-O(14)	1.32(2)
C(135)-C(136)	1.566(17)	C(136)-O(12)	1.324(14)
C(136)-C(138)	1.51(2)	C(139)-O(17)	1.15(2)
C(139)-O(15)	1.28(2)	C(139)-C(140)	1.47(2)
C(139)-C(240)	1.49(2)	C(140)-O(16)	1.44(2)
C(140)-C(143)	1.561(16)	C(141)-O(18)	1.136(12)
C(141)-O(16)	1.30(2)	C(141)-C(142)	1.452(18)
C(240)-C(243)	1.555(17)	C(240)-O(16)	1.47(3)
C(241)-O(18A)	1.110(15)	C(241)-O(16)	1.31(2)
C(241)-C(142)	1.441(18)	C(142)-O(15)	1.442(18)
C(142)-C(144)	1.472(15)	C(150)-Cl(2)	1.757(15)
C(150)-Cl(1)	1.781(16)	C(150)-Cl(3A)	1.788(17)
C(150)-Cl(3)	1.819(17)	C(151)-Cl(6)	1.665(12)
C(151)-Cl(4)	1.755(11)	C(151)-Cl(5)	1.776(12)
C(152)-Cl(7A)	1.658(19)	C(152)-Cl(9)	1.607(17)
C(152)-Cl(8)	1.654(16)	C(152)-Cl(7)	1.827(17)
C(152)-Cl(8A)	1.785(19)	C(152)-Cl(9A)	1.82(2)

C(153)-Cl(12)	1.713(15)	C(153)-Cl(11)	1.719(14)
C(153)-Cl(10)	1.726(14)	C(153)-Cl(22)	1.756(17)
C(154)-Cl(13)	1.786(18)	C(154)-Cl(14)	1.792(19)
C(154)-Cl(25)	1.81(2)	C(154)-Cl(23)	1.822(19)
C(154)-Cl(15)	1.842(19)	C(154)-Cl(24)	1.853(19)
C(155)-Cl(17)	1.725(18)	C(155)-Cl(18)	1.727(18)
C(155)-Cl(16)	1.755(18)	C(255)-Cl(28)	1.718(18)
C(255)-Cl(27)	1.732(18)	C(255)-Cl(26)	1.741(19)
C(38)-C(37)	1.347(14)	C(38)-C(39)	1.397(14)
C(38)-C(45)	1.536(15)	C(45)-C(47)	1.45(2)
C(45)-C(46)	1.52(2)	C(45)-C(48)	1.63(2)
		O(1)-Al(1)-O(9)	104.6(3)
O(1)-Al(1)-O(4)	96.7(3)	O(9)-Al(1)-O(4)	105.2(3)
O(1)-Al(1)-O(2)	151.4(3)	O(9)-Al(1)-O(2)	103.9(3)
O(4)-Al(1)-O(2)	76.5(3)	O(1)-Al(1)-N(1)	92.4(3)
O(9)-Al(1)-N(1)	100.3(3)	O(4)-Al(1)-N(1)	149.7(3)
O(2)-Al(1)-N(1)	81.7(3)	O(1)-Al(1)-Al(2)	128.7(2)
O(9)-Al(1)-Al(2)	110.7(2)	O(4)-Al(1)-Al(2)	39.1(2)
O(2)-Al(1)-Al(2)	37.4(2)	N(1)-Al(1)-Al(2)	115.6(3)
O(3)-Al(2)-O(2)	97.1(3)	O(3)-Al(2)-O(10)	105.1(3)
O(2)-Al(2)-O(10)	102.8(3)	O(3)-Al(2)-O(4)	149.9(3)
O(2)-Al(2)-O(4)	77.3(3)	O(10)-Al(2)-O(4)	104.9(3)
O(3)-Al(2)-N(2)	92.2(3)	O(2)-Al(2)-N(2)	152.8(3)
O(10)-Al(2)-N(2)	99.3(3)	O(4)-Al(2)-N(2)	81.8(3)
O(3)-Al(2)-Al(1)	128.4(2)	O(2)-Al(2)-Al(1)	39.2(2)
O(10)-Al(2)-Al(1)	110.0(2)	O(4)-Al(2)-Al(1)	38.2(2)
N(2)-Al(2)-Al(1)	117.3(2)	O(5)-Al(3)-O(9)	102.3(3)
O(5)-Al(3)-O(8)	96.9(3)	O(9)-Al(3)-O(8)	107.8(3)
O(5)-Al(3)-O(6)	156.8(3)	O(9)-Al(3)-O(6)	100.9(3)
O(8)-Al(3)-O(6)	76.5(3)	O(5)-Al(3)-N(3)	92.4(3)
O(9)-Al(3)-N(3)	104.8(4)	O(8)-Al(3)-N(3)	143.2(3)
O(6)-Al(3)-N(3)	81.1(3)	O(5)-Al(3)-Al(4)	131.0(2)
O(9)-Al(3)-Al(4)	109.8(2)	O(8)-Al(3)-Al(4)	38.7(2)
O(6)-Al(3)-Al(4)	37.8(2)	N(3)-Al(3)-Al(4)	113.0(3)

O(7)-Al(4)-O(10)	105.2(3)	O(7)-Al(4)-O(6)	95.5(3)
O(10)-Al(4)-O(6)	104.6(3)	O(7)-Al(4)-O(8)	149.5(3)
O(10)-Al(4)-O(8)	105.3(3)	O(6)-Al(4)-O(8)	77.4(3)
O(7)-Al(4)-N(4)	91.6(3)	O(10)-Al(4)-N(4)	99.9(3)
O(6)-Al(4)-N(4)	151.7(3)	O(8)-Al(4)-N(4)	82.6(3)
O(7)-Al(4)-Al(3)	127.2(2)	O(10)-Al(4)-Al(3)	110.9(2)
O(6)-Al(4)-Al(3)	39.3(2)	O(8)-Al(4)-Al(3)	38.2(2)
N(4)-Al(4)-Al(3)	117.7(3)	C(77)-B(1)-C(93)	104.5(8)
C(77)-B(1)-C(69)	113.1(8)	C(93)-B(1)-C(69)	111.5(8)
C(77)-B(1)-C(85)	113.7(8)	C(93)-B(1)-C(85)	109.7(8)
C(69)-B(1)-C(85)	104.5(8)	C(101)-B(2)-C(125)	111.4(10)
C(101)-B(2)-C(109)	111.1(11)	C(125)-B(2)-C(109)	103.9(11)
C(101)-B(2)-C(117)	105.1(11)	C(125)-B(2)-C(117)	114.3(10)
C(109)-B(2)-C(117)	111.2(10)	O(1)-C(1)-C(2)	119.2(9)
O(1)-C(1)-C(6)	118.4(9)	C(2)-C(1)-C(6)	122.3(9)
C(1)-C(2)-C(15)	125.4(9)	C(1)-C(2)-C(3)	118.2(11)
C(15)-C(2)-C(3)	116.3(10)	C(4)-C(3)-C(2)	122.6(12)
C(3)-C(4)-C(5)	118.0(10)	C(3)-C(4)-C(11)	122.1(12)
C(5)-C(4)-C(11)	119.8(11)	C(4)-C(5)-C(6)	125.1(11)
C(1)-C(6)-C(5)	113.6(10)	C(1)-C(6)-C(7)	123.7(9)
C(5)-C(6)-C(7)	122.7(10)	C(6)-C(7)-C(9)	112.8(10)
C(6)-C(7)-C(8)	114.0(9)	C(9)-C(7)-C(8)	107.0(9)
C(6)-C(7)-C(10)	109.1(9)	C(9)-C(7)-C(10)	108.2(9)
C(8)-C(7)-C(10)	105.4(9)	C(12)-C(11)-C(14)	110.1(10)
C(12)-C(11)-C(13)	112.9(11)	C(14)-C(11)-C(13)	105.5(12)
C(12)-C(11)-C(4)	107.3(11)	C(14)-C(11)-C(4)	110.7(9)
C(13)-C(11)-C(4)	110.4(11)	N(1)-C(15)-C(2)	121.9(10)
N(1)-C(16)-C(17)	105.4(8)	O(2)-C(17)-C(16)	107.1(7)
O(3)-C(18)-C(23)	120.8(9)	O(3)-C(18)-C(19)	120.1(8)
C(23)-C(18)-C(19)	119.0(9)	C(20)-C(19)-C(18)	121.0(9)
C(20)-C(19)-C(32)	117.4(9)	C(18)-C(19)-C(32)	121.6(8)
C(21)-C(20)-C(19)	121.4(10)	C(22)-C(21)-C(20)	115.1(9)
C(22)-C(21)-C(28)	121.4(9)	C(20)-C(21)-C(28)	123.5(9)
C(21)-C(22)-C(23)	129.2(9)	C(18)-C(23)-C(22)	114.2(8)

C(18)-C(23)-C(24)	121.0(8)	C(22)-C(23)-C(24)	124.7(8)
C(27)-C(24)-C(23)	109.1(10)	C(27)-C(24)-C(26)	111.2(9)
C(23)-C(24)-C(26)	110.1(9)	C(27)-C(24)-C(25)	107.9(10)
C(23)-C(24)-C(25)	114.7(8)	C(26)-C(24)-C(25)	103.7(11)
C(31)-C(28)-C(21)	112.6(8)	C(31)-C(28)-C(29)	108.7(9)
C(21)-C(28)-C(29)	111.2(8)	C(31)-C(28)-C(30)	107.4(9)
C(21)-C(28)-C(30)	107.8(8)	C(29)-C(28)-C(30)	109.1(8)
N(2)-C(32)-C(19)	124.5(9)	N(2)-C(33)-C(34)	106.1(7)
O(4)-C(34)-C(33)	108.5(8)	O(5)-C(35)-C(40)	121.9(9)
O(5)-C(35)-C(36)	119.6(9)	C(40)-C(35)-C(36)	118.4(8)
C(37)-C(36)-C(35)	120.7(9)	C(37)-C(36)-C(49)	117.3(9)
C(35)-C(36)-C(49)	121.9(8)	C(39)-C(40)-C(35)	117.2(9)
C(39)-C(40)-C(41)	121.8(9)	C(35)-C(40)-C(41)	121.1(8)
C(40)-C(41)-C(44)	109.9(9)	C(40)-C(41)-C(42)	113.1(9)
C(44)-C(41)-C(42)	104.8(10)	C(40)-C(41)-C(43)	109.6(9)
C(44)-C(41)-C(43)	112.4(9)	C(42)-C(41)-C(43)	107.0(9)
N(3)-C(49)-C(36)	125.2(9)	C(51)-C(50)-N(3)	108.2(16)
O(6)-C(51)-C(50)	114.4(16)	C(51A)-C(50A)-N(3)	114.2(17)
O(6)-C(51A)-C(50A)	109.2(17)	O(7)-C(52)-C(53)	120.6(8)
O(7)-C(52)-C(57)	119.5(9)	C(53)-C(52)-C(57)	119.8(9)
C(52)-C(53)-C(54)	119.3(10)	C(52)-C(53)-C(66)	121.7(9)
C(54)-C(53)-C(66)	119.0(10)	C(55)-C(54)-C(53)	122.3(11)
C(54)-C(55)-C(56)	117.3(10)	C(54)-C(55)-C(62)	122.6(12)
C(56)-C(55)-C(62)	120.1(11)	C(55)-C(56)-C(57)	126.1(10)
C(56)-C(57)-C(52)	114.9(10)	C(56)-C(57)-C(58)	122.9(9)
C(52)-C(57)-C(58)	122.1(8)	C(57)-C(58)-C(59)	113.1(9)
C(57)-C(58)-C(61)	111.5(9)	C(59)-C(58)-C(61)	107.3(10)
C(57)-C(58)-C(60)	110.7(8)	C(59)-C(58)-C(60)	106.3(9)
C(61)-C(58)-C(60)	107.8(9)	C(63)-C(62)-C(65)	123.2(15)
C(63)-C(62)-C(55)	110.0(12)	C(65)-C(62)-C(55)	108.7(12)
C(63)-C(62)-C(64)	104.7(13)	C(65)-C(62)-C(64)	97.8(13)
C(55)-C(62)-C(64)	111.6(12)	N(4)-C(66)-C(53)	124.8(10)
N(4)-C(67)-C(68)	107.5(8)	O(8)-C(68)-C(67)	106.6(8)
C(70)-C(69)-C(74)	112.5(9)	C(70)-C(69)-B(1)	125.0(8)

C(74)-C(69)-B(1)	122.4(8)	C(71)-C(70)-C(69)	124.8(9)
C(70)-C(71)-C(72)	119.6(9)	C(70)-C(71)-C(75)	121.9(9)
C(72)-C(71)-C(75)	118.5(9)	C(73)-C(72)-C(71)	119.3(9)
C(74)-C(73)-C(72)	119.5(10)	C(74)-C(73)-C(76)	120.6(12)
C(72)-C(73)-C(76)	119.8(12)	C(73)-C(74)-C(69)	124.3(9)
F(5A)-C(75)-F(5)	35(2)	F(5A)-C(75)-F(6)	119(2)
F(5)-C(75)-F(6)	105.7(12)	F(5A)-C(75)-F(6A)	114(4)
F(5)-C(75)-F(6A)	87(3)	F(6)-C(75)-F(6A)	28(2)
F(5A)-C(75)-F(4)	69(2)	F(5)-C(75)-F(4)	103.9(11)
F(6)-C(75)-F(4)	107.6(10)	F(6A)-C(75)-F(4)	134(2)
F(5A)-C(75)-F(4A)	111(3)	F(5)-C(75)-F(4A)	139.8(18)
F(6)-C(75)-F(4A)	68.9(17)	F(6A)-C(75)-F(4A)	97(3)
F(4)-C(75)-F(4A)	47.1(16)	F(5A)-C(75)-C(71)	122(2)
F(5)-C(75)-C(71)	112.1(10)	F(6)-C(75)-C(71)	114.4(11)
F(6A)-C(75)-C(71)	104(3)	F(4)-C(75)-C(71)	112.3(9)
F(4A)-C(75)-C(71)	105.6(16)	F(2)-C(76)-F(3)	106.4(15)
F(2)-C(76)-F(1)	104.1(13)	F(3)-C(76)-F(1)	103.1(14)
F(2)-C(76)-C(73)	117.1(14)	F(3)-C(76)-C(73)	114.3(15)
F(1)-C(76)-C(73)	110.4(15)	C(78)-C(77)-C(82)	110.5(8)
C(78)-C(77)-B(1)	123.9(8)	C(82)-C(77)-B(1)	125.1(9)
C(79)-C(78)-C(77)	127.6(9)	C(78)-C(79)-C(80)	118.8(9)
C(78)-C(79)-C(83)	124.2(10)	C(80)-C(79)-C(83)	116.8(9)
C(81)-C(80)-C(79)	116.2(9)	C(80)-C(81)-C(82)	121.7(9)
C(80)-C(81)-C(84)	118.0(10)	C(82)-C(81)-C(84)	120.0(10)
C(81)-C(82)-C(77)	124.6(9)	F(9)-C(83)-F(7A)	119(3)
F(9)-C(83)-F(9A)	51.5(19)	F(7A)-C(83)-F(9A)	118(3)
F(9)-C(83)-F(8)	106.7(11)	F(7A)-C(83)-F(8)	28(2)
F(9A)-C(83)-F(8)	132.5(19)	F(9)-C(83)-F(8A)	46.4(17)
F(7A)-C(83)-F(8A)	89(3)	F(9A)-C(83)-F(8A)	96(3)
F(8)-C(83)-F(8A)	66.5(18)	F(9)-C(83)-F(7)	108.1(11)
F(7A)-C(83)-F(7)	75(2)	F(9A)-C(83)-F(7)	60.3(19)
F(8)-C(83)-F(7)	102.2(12)	F(8A)-C(83)-F(7)	137.8(18)
F(9)-C(83)-C(79)	116.5(10)	F(7A)-C(83)-C(79)	119(3)
F(9A)-C(83)-C(79)	116.3(18)	F(8)-C(83)-C(79)	111.2(10)

F(8A)-C(83)-C(79)	110.8(17)	F(7)-C(83)-C(79)	111.1(10)
F(10)-C(84)-F(12)	106.7(10)	F(10)-C(84)-F(11)	105.9(9)
F(12)-C(84)-F(11)	107.4(10)	F(10)-C(84)-C(81)	112.2(10)
F(12)-C(84)-C(81)	113.3(9)	F(11)-C(84)-C(81)	110.8(10)
C(86)-C(85)-C(90)	113.5(9)	C(86)-C(85)-B(1)	125.6(8)
C(90)-C(85)-B(1)	120.5(8)	C(87)-C(86)-C(85)	122.6(9)
C(86)-C(87)-C(88)	122.5(9)	C(86)-C(87)-C(91)	119.8(9)
C(88)-C(87)-C(91)	117.7(9)	C(89)-C(88)-C(87)	115.9(9)
C(88)-C(89)-C(90)	123.0(9)	C(88)-C(89)-C(92)	119.9(10)
C(90)-C(89)-C(92)	117.1(10)	C(89)-C(90)-C(85)	122.2(9)
F(13)-C(91)-F(14)	107.0(8)	F(13)-C(91)-F(15)	104.8(8)
F(14)-C(91)-F(15)	105.3(8)	F(13)-C(91)-C(87)	114.0(9)
F(14)-C(91)-C(87)	114.0(8)	F(15)-C(91)-C(87)	111.0(8)
F(16)-C(92)-F(17)	106.9(11)	F(16)-C(92)-F(18)	105.7(11)
F(17)-C(92)-F(18)	103.1(9)	F(16)-C(92)-C(89)	114.3(10)
F(17)-C(92)-C(89)	113.1(10)	F(18)-C(92)-C(89)	112.9(11)
C(98)-C(93)-C(94)	114.4(9)	C(98)-C(93)-B(1)	121.8(9)
C(94)-C(93)-B(1)	123.5(9)	C(95)-C(94)-C(93)	122.6(9)
C(94)-C(95)-C(96)	121.7(10)	C(94)-C(95)-C(99)	118.5(9)
C(96)-C(95)-C(99)	119.9(10)	C(97)-C(96)-C(95)	119.5(11)
C(96)-C(97)-C(98)	120.1(10)	C(96)-C(97)-C(100)	122.8(11)
C(98)-C(97)-C(100)	117.1(10)	C(93)-C(98)-C(97)	121.5(9)
F(21A)-C(99)-F(21)	129(2)	F(21A)-C(99)-F(19A)	111.0(16)
F(21)-C(99)-F(19A)	36.6(17)	F(21A)-C(99)-F(19)	62.4(17)
F(21)-C(99)-F(19)	108.7(11)	F(19A)-C(99)-F(19)	133.8(19)
F(21A)-C(99)-F(20A)	109.2(15)	F(21)-C(99)-F(20A)	71.6(17)
F(19A)-C(99)-F(20A)	107.8(15)	F(19)-C(99)-F(20A)	47.9(15)
F(21A)-C(99)-F(20)	43.2(18)	F(21)-C(99)-F(20)	106.6(11)
F(19A)-C(99)-F(20)	74.2(18)	F(19)-C(99)-F(20)	104.1(11)
F(20A)-C(99)-F(20)	144.3(19)	F(21A)-C(99)-C(95)	115.0(18)
F(21)-C(99)-C(95)	113.9(11)	F(19A)-C(99)-C(95)	110.3(17)
F(19)-C(99)-C(95)	113.3(11)	F(20A)-C(99)-C(95)	103.0(18)
F(20)-C(99)-C(95)	109.6(10)	F(23)-C(100)-F(22)	109.9(11)
F(23)-C(100)-F(24)	103.9(11)	F(22)-C(100)-F(24)	101.9(10)

F(23)-C(100)-C(97)	113.1(11)	F(22)-C(100)-C(97)	112.9(10)
F(24)-C(100)-C(97)	114.1(11)	C(106)-C(101)-C(102)	113.6(12)
C(106)-C(101)-B(2)	123.1(12)	C(102)-C(101)-B(2)	123.3(13)
C(103)-C(102)-C(101)	123.8(15)	C(102)-C(103)-C(104)	116.2(15)
C(102)-C(103)-C(107)	120.6(16)	C(104)-C(103)-C(107)	122.3(16)
C(105)-C(104)-C(103)	120.1(15)	C(106)-C(105)-C(104)	120.7(15)
C(106)-C(105)-C(108)	119.9(15)	C(104)-C(105)-C(108)	119.4(15)
C(105)-C(106)-C(101)	125.0(13)	F(29)-C(107)-F(28)	110(2)
F(29)-C(107)-F(30)	121(2)	F(28)-C(107)-F(30)	111.5(18)
F(29)-C(107)-C(103)	107.7(18)	F(28)-C(107)-C(103)	103.5(17)
F(30)-C(107)-C(103)	101.2(16)	F(25)-C(108)-F(26)	113.9(17)
F(25)-C(108)-F(27)	98.8(15)	F(26)-C(108)-F(27)	104.6(14)
F(25)-C(108)-C(105)	115.3(14)	F(26)-C(108)-C(105)	115.1(16)
F(27)-C(108)-C(105)	106.9(15)	C(110)-C(109)-C(114)	112.1(13)
C(110)-C(109)-B(2)	122.6(12)	C(114)-C(109)-B(2)	124.8(12)
C(109)-C(110)-C(111)	124.0(15)	C(112)-C(111)-C(110)	121.8(17)
C(112)-C(111)-C(115)	120.3(18)	C(110)-C(111)-C(115)	117.3(17)
C(111)-C(112)-C(113)	118.5(16)	C(114)-C(113)-C(112)	118.6(14)
C(114)-C(113)-C(116)	116.9(15)	C(112)-C(113)-C(116)	124.5(15)
C(113)-C(114)-C(109)	124.6(13)	F(33)-C(115)-F(32)	104(2)
F(33)-C(115)-F(31)	105(2)	F(32)-C(115)-F(31)	103.5(19)
F(33)-C(115)-C(111)	117(2)	F(32)-C(115)-C(111)	113(2)
F(31)-C(115)-C(111)	112.5(19)	F(35)-C(116)-F(36)	109.5(17)
F(35)-C(116)-F(34)	98.7(15)	F(36)-C(116)-F(34)	104.0(16)
F(35)-C(116)-C(113)	114.8(17)	F(36)-C(116)-C(113)	118.9(16)
F(34)-C(116)-C(113)	108.2(16)	C(118)-C(117)-C(122)	115.3(10)
C(118)-C(117)-B(2)	120.3(10)	C(122)-C(117)-B(2)	123.5(10)
C(119)-C(118)-C(117)	123.5(11)	C(118)-C(119)-C(120)	119.3(11)
C(118)-C(119)-C(123)	121.9(13)	C(120)-C(119)-C(123)	118.9(12)
C(121)-C(120)-C(119)	117.3(12)	C(120)-C(121)-C(122)	121.6(12)
C(120)-C(121)-C(124)	118.9(13)	C(122)-C(121)-C(124)	118.8(12)
C(121)-C(122)-C(117)	122.2(11)	F(38)-C(123)-F(39)	105.7(14)
F(38)-C(123)-F(37)	112.3(15)	F(39)-C(123)-F(37)	102.4(14)
F(38)-C(123)-C(119)	111.9(14)	F(39)-C(123)-C(119)	115.5(14)

F(37)-C(123)-C(119)	108.8(14)	F(42)-C(124)-F(41)	112.6(19)
F(42)-C(124)-F(40)	101.0(19)	F(41)-C(124)-F(40)	90.5(13)
F(42)-C(124)-C(121)	124.2(17)	F(41)-C(124)-C(121)	109.6(15)
F(40)-C(124)-C(121)	113.5(16)	C(130)-C(125)-C(126)	114.5(9)
C(130)-C(125)-B(2)	120.2(10)	C(126)-C(125)-B(2)	124.5(9)
C(127)-C(126)-C(125)	121.3(9)	C(128)-C(127)-C(126)	121.4(10)
C(128)-C(127)-C(131)	118.6(10)	C(126)-C(127)-C(131)	120.0(9)
C(129)-C(128)-C(127)	117.6(10)	C(130)-C(129)-C(128)	121.3(9)
C(130)-C(129)-C(132)	118.8(11)	C(128)-C(129)-C(132)	119.9(10)
C(129)-C(130)-C(125)	123.8(10)	F(44)-C(131)-F(43)	106.1(8)
F(44)-C(131)-F(45)	105.1(9)	F(43)-C(131)-F(45)	105.9(10)
F(44)-C(131)-C(127)	112.3(9)	F(43)-C(131)-C(127)	113.9(10)
F(45)-C(131)-C(127)	112.9(9)	F(48)-C(132)-F(47)	109.2(11)
F(48)-C(132)-F(46)	106.7(10)	F(47)-C(132)-F(46)	104.1(10)
F(48)-C(132)-C(129)	112.9(10)	F(47)-C(132)-C(129)	114.0(10)
F(46)-C(132)-C(129)	109.2(10)	O(11)-C(133)-O(12)	116.0(19)
O(11)-C(133)-C(134)	126(2)	O(12)-C(133)-C(134)	118.1(17)
O(14)-C(134)-C(137)	109.1(15)	O(14)-C(134)-C(133)	104.4(15)
C(137)-C(134)-C(133)	116.0(16)	O(13A)-C(135)-O(13)	54(2)
O(13A)-C(135)-O(14)	119(2)	O(13)-C(135)-O(14)	122.0(19)
O(13A)-C(135)-C(136)	123(2)	O(13)-C(135)-C(136)	123(2)
O(14)-C(135)-C(136)	107.3(17)	O(12)-C(136)-C(138)	110.4(15)
O(12)-C(136)-C(135)	109.2(14)	C(138)-C(136)-C(135)	108.4(16)
O(17)-C(139)-O(15)	119.9(19)	O(17)-C(139)-C(140)	129(2)
O(15)-C(139)-C(140)	106(2)	O(17)-C(139)-C(240)	118(2)
O(15)-C(139)-C(240)	120(2)	C(140)-C(139)-C(240)	39.5(19)
O(16)-C(140)-C(139)	113.4(19)	O(16)-C(140)-C(143)	98(2)
C(139)-C(140)-C(143)	104(2)	O(18)-C(141)-O(16)	120.1(19)
O(18)-C(141)-C(142)	128(2)	O(16)-C(141)-C(142)	111.4(14)
C(139)-C(240)-C(243)	116(3)	C(139)-C(240)-O(16)	111(2)
C(243)-C(240)-O(16)	125(3)	O(18A)-C(241)-O(16)	115(2)
O(18A)-C(241)-C(142)	131(3)	O(16)-C(241)-C(142)	111.8(16)
C(241)-C(142)-C(141)	11(2)	C(241)-C(142)-O(15)	122.6(15)
C(141)-C(142)-O(15)	119.6(14)	C(241)-C(142)-C(144)	120.2(14)

C(141)-C(142)-C(144)	117.9(14)	O(15)-C(142)-C(144)	113.5(14)
C(15)-N(1)-C(16)	120.9(8)	C(15)-N(1)-Al(1)	126.9(8)
C(16)-N(1)-Al(1)	112.2(5)	C(32)-N(2)-C(33)	121.9(8)
C(32)-N(2)-Al(2)	125.2(7)	C(33)-N(2)-Al(2)	112.7(6)
C(49)-N(3)-C(50A)	118.9(11)	C(49)-N(3)-C(50)	119.6(11)
C(50A)-N(3)-C(50)	29.3(10)	C(49)-N(3)-Al(3)	125.5(7)
C(50A)-N(3)-Al(3)	113.6(10)	C(50)-N(3)-Al(3)	113.0(9)
C(66)-N(4)-C(67)	121.6(9)	C(66)-N(4)-Al(4)	126.3(7)
C(67)-N(4)-Al(4)	112.1(6)	C(1)-O(1)-Al(1)	132.7(6)
C(17)-O(2)-Al(2)	132.4(5)	C(17)-O(2)-Al(1)	118.1(5)
Al(2)-O(2)-Al(1)	103.3(3)	C(18)-O(3)-Al(2)	131.6(6)
C(34)-O(4)-Al(1)	132.8(5)	C(34)-O(4)-Al(2)	118.8(5)
Al(1)-O(4)-Al(2)	102.7(3)	C(35)-O(5)-Al(3)	132.3(6)
C(51A)-O(6)-C(51)	21.8(14)	C(51A)-O(6)-Al(4)	124.7(11)
C(51)-O(6)-Al(4)	140.3(10)	C(51A)-O(6)-Al(3)	121.3(10)
C(51)-O(6)-Al(3)	115.3(10)	Al(4)-O(6)-Al(3)	103.0(3)
C(52)-O(7)-Al(4)	132.1(6)	C(68)-O(8)-Al(3)	133.0(5)
C(68)-O(8)-Al(4)	120.0(5)	Al(3)-O(8)-Al(4)	103.0(3)
Al(1)-O(9)-Al(3)	139.2(3)	Al(4)-O(10)-Al(2)	139.2(3)
C(133)-O(12)-C(136)	116.6(15)	C(135)-O(14)-C(134)	126.3(15)
C(139)-O(15)-C(142)	120.6(16)	C(141)-O(16)-C(241)	12(3)
C(141)-O(16)-C(140)	114.8(16)	C(241)-O(16)-C(140)	109.9(18)
C(141)-O(16)-C(240)	126(2)	C(241)-O(16)-C(240)	130.1(18)
C(140)-O(16)-C(240)	40.2(18)	Cl(2)-C(150)-Cl(1)	109.3(9)
Cl(2)-C(150)-Cl(3A)	120.5(10)	Cl(1)-C(150)-Cl(3A)	108.7(9)
Cl(2)-C(150)-Cl(3)	100.3(8)	Cl(1)-C(150)-Cl(3)	111.8(8)
Cl(3A)-C(150)-Cl(3)	22.1(4)	Cl(6)-C(151)-Cl(4)	113.2(8)
Cl(6)-C(151)-Cl(5)	110.8(8)	Cl(4)-C(151)-Cl(5)	108.5(7)
Cl(7A)-C(152)-Cl(9)	90.6(10)	Cl(7A)-C(152)-Cl(8)	115.9(11)
Cl(9)-C(152)-Cl(8)	119.8(11)	Cl(7A)-C(152)-Cl(7)	27.9(5)
Cl(9)-C(152)-Cl(7)	114.4(10)	Cl(8)-C(152)-Cl(7)	90.4(8)
Cl(7A)-C(152)-Cl(8A)	140.1(12)	Cl(9)-C(152)-Cl(8A)	114.2(10)
Cl(8)-C(152)-Cl(8A)	24.8(6)	Cl(7)-C(152)-Cl(8A)	113.2(10)
Cl(7A)-C(152)-Cl(9A)	114.0(11)	Cl(9)-C(152)-Cl(9A)	23.5(6)

Cl(8)-C(152)-Cl(9A)	104.9(10)	Cl(7)-C(152)-Cl(9A)	136.1(11)
Cl(8A)-C(152)-Cl(9A)	93.1(10)	Cl(12)-C(153)-Cl(11)	110.1(11)
Cl(12)-C(153)-Cl(10)	115.8(12)	Cl(11)-C(153)-Cl(10)	131.6(14)
Cl(12)-C(153)-Cl(22)	49.2(11)	Cl(11)-C(153)-Cl(22)	93.8(15)
Cl(10)-C(153)-Cl(22)	104.4(16)	Cl(13)-C(154)-Cl(14)	106.7(15)
Cl(13)-C(154)-Cl(25)	139(2)	Cl(14)-C(154)-Cl(25)	59.3(14)
Cl(13)-C(154)-Cl(23)	43.1(7)	Cl(14)-C(154)-Cl(23)	116.2(19)
Cl(25)-C(154)-Cl(23)	104.6(18)	Cl(13)-C(154)-Cl(15)	90.1(14)
Cl(14)-C(154)-Cl(15)	101.8(17)	Cl(25)-C(154)-Cl(15)	59.7(15)
Cl(23)-C(154)-Cl(15)	47.6(11)	Cl(13)-C(154)-Cl(24)	86.6(12)
Cl(14)-C(154)-Cl(24)	33.2(8)	Cl(25)-C(154)-Cl(24)	91.9(16)
Cl(23)-C(154)-Cl(24)	117.3(17)	Cl(15)-C(154)-Cl(24)	129(2)
Cl(17)-C(155)-Cl(18)	110.6(16)	Cl(17)-C(155)-Cl(16)	105.7(15)
Cl(18)-C(155)-Cl(16)	109.3(16)	Cl(28)-C(255)-Cl(27)	110.3(15)
Cl(28)-C(255)-Cl(26)	110.4(15)	Cl(27)-C(255)-Cl(26)	107.8(15)
C(37)-C(38)-C(39)	117.4(9)	C(37)-C(38)-C(45)	121.8(11)
C(39)-C(38)-C(45)	120.9(10)	C(40)-C(39)-C(38)	125.3(9)
C(38)-C(37)-C(36)	121.0(10)	C(47)-C(45)-C(38)	114.5(12)
C(47)-C(45)-C(46)	124.7(14)	C(38)-C(45)-C(46)	111.1(12)
C(47)-C(45)-C(48)	104.8(14)	C(38)-C(45)-C(48)	104.7(12)
C(46)-C(45)-C(48)	92.1(12)		

VITA

Osit Karroonnirun was born to Sumate and Wilawan Karroonnirun. He grew up in the southern part of Thailand in the city of Narathiwat. He later moved to Bangkok where he graduated from Mahidol Wittayanusorn High School in 1999. He attended Mahidol University in Bangkok and graduated with a B.S. in chemistry in March 2003. Osit began his graduate studies at Texas A&M University in September 2005 under the direction of Dr. Donald J. Darensbourg and received his Ph.D. degree in May 2011. Questions and comments may be directed to pope_chem1ok@hotmail.com or Texas A&M University, Department of Chemistry, MS 3255, College Station, TX 77842-3012.